Material Characterisation and Response Modelling of Recycled Concrete and Masonry in Pavements

by
Fabrice Barisanga

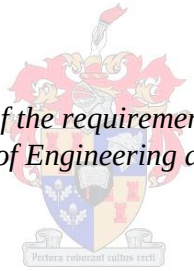

Thesis presented in fulfilment of the requirements for the degree of Master *of Engineering in the Faculty of Engineering at Stellenbosch University*

Supervisor: Ms Chantal Rudman
Co-supervisor: Prof Kim Jonathan Jenkins

April 2014

DECLARATION

By submitting this thesis electronically, I declare that the entirety of the work contained therein is my own, original work, that I am the sole author thereof (save to the extent explicitly otherwise stated), that reproduction and publication thereof by Stellenbosch University will not infringe any third party rights and that I have not previously in its entirety or in part submitted it for obtaining any qualification.

April 2014

ABSTRACT

The global quest for sustainability has intensified the requirement for waste recycling in a number of countries. Waste recycle includes Construction and Demolition Waste (CDW), which emanates from the demolition of buildings and other civil engineering structures. In Europe, the United States, China, and Australia, waste recycling has proven to be successful, both structurally and functionally. In particular, the consideration and /or use of CDW in pavement layers remain on the increase. However, in Southern Africa the use and/or application of CDW and its allied practice is limited; the abundant natural aggregates, the lack of knowledge and technical expertise besides the availability of suitable CDW remain the prominent reasons for its limited consideration.

In this research, recycled material infers to Construction and Demolition Waste pertaining to Recycled Concrete and Masonry (RCM). The quality and the type of RCM vary from region to region and as a result, quality control measures aimed at limiting the inconsistency are usually required.

Results revealed that secondary crushing influences the physical and mechanical behaviour of RCM aggregates; this information remains insightful in terms of material gradation, performance and viability. The compaction protocol followed and its findings revealed that the initial material grading lightly changed after compaction. However, the 10% FACT results showed that the RCM aggregates exhibit less degradation due to crushing when dry than when they are wet.

It is eminent that compaction and/or densification are a cheaper method to improve the pavement layer structural capacity. However, this is reliant on material characteristics, quality, and type. With this cognisance, an experimental program in line with RCM aimed at assessing the mechanical behaviour was developed. The experimental variables include mix composition, mixing and compaction moisture as well as degree of compaction and/or compactive effort.

In general, the laboratory evaluation and analysis of the results showed that the mix composition in addition to compaction moisture and the degree of compaction were influential to the obtained shear strength, resilient modulus and Poisson Ratio. Particularly, mix composition exhibited relatively higher influence on the resilient modulus while the compaction moisture effect on the Poisson Ratio dominated other investigated variables such as mix composition and the degree of compaction.

Shear strength and resilient response results show that RCM exhibits significant shear strength due to its cohesion, and satisfactory resilient modulus. Pavement analysis and design using multi-layer linear-elastic model and transfer functions in pavement layers where RCM is used also revealed that this material could perform satisfactorily. It was deduced that RCM is a viable material type to consider in the construction of pavement layers that carry low to moderate levels of traffic.

ABSTRAK

Die globale beweging na meer onderhoubare aktiwiteite het gelei tot die ’n toename in vereistes met betrekking tot herwinning van rommel. Rommelherwinning sluit materiaal van bouwerke en ander siviele strukture in. In Europa, Amerika, China en Australië het die herwinning van afval materiaal tot groot sukses gelei. Spesifiek die gebruik van geselekteerde bourommel in padlae bleik om toe te neem. In Suid -Afrika word die materiaal net in enkele geïsoleerde gevalle gebruik as gevolg van die onderbreking van tegniese kennis met betrekking tot die toeganklikheid en bruikbaarheid van die materiaal. Ook, tans geniet die gebruik van gebreekte klip voorrang omdat die verbruiker glo dat daar nog baie van hierdie materiaal beskikbaar is.

In hierdie navorsing verwys bourommel spesifiek na herwinde beton en boustene. Die “kwaliteit” van boustene in verskillende gebiede varieer en as ‘n gevolg moet kwaliteitskontroles toegepas word om hierdie te beperk.

Resultate in diè navorsing het gewys dat sekondêre klipbreking/vergruising die fisiese en meganiese gedrag van “bourommel aggregaat” beïnvloed. Die 10% FACT (Fynstof Aggregaat Breekwaarde) resultate het ook gewys dat geselekteerde bourommel minder degradasie ondervind as dit droog is in vergelyking met nat materiaal.

Goeie kompaksie van die tipe materiale word erken as een van die goedkoopste maniere om die gedrag daarvan in plaveisellae te verbeter. Dit is wel afhanklik van materiaal karakteristieke, kwaliteit en tipe materiaal. Hierdie faktore is ingesluit in die eksperimentele plan wat eienskappe soos mengsel komposisie, meng en kompaksie voginhoud sowel as graad van kompaksie insluit.

Die resultate van die laboratorium analise het gewys dat die mengkomposisie, vog tydens kompaksie en graad van kompaksie ’n invloed op die skuifsterkte, veerkragsmodulus en die Poisson verhouding het. Veral die mengkomposisie het ’n merkwaardige invloed op die veerkragmodulus gehad, terwyl die voginhoud tydens kompaksie die grootste invloed op die Poissonverhouding gehad het.

Die skuifsterkte (agv hoë kohesie) en veerkragsmodulus van geselekteerde bourommel dui aanvaarbare resultate vir die gebruik in paaie, spesifiek in padlae waar lae spanningsvlakke ondervind word,soos deur liniere elastiese berekeninge gewys is.

ACKNOWLEDGMENTS

My studies at Stellenbosch would not turn into success without the participation of different personalities. I would therefore, like to extend my gratitude to those who contributed in one way or another to make my endeavour a success:

- My study leader Ms Chantal Rudman and co- study leader Prof. Kim Jonathan Jenkins. I am thankful to Ms Rudman for her guidance, encouragement and financial support. All evenings and weekends you have sacrificed for this study despite other responsibilities that you had, are deeply acknowledged. My gratitude also goes to Prof Jenkins for introducing me to this wonderful University and accepting to take part in the guidance of this study
- Dr Elias Twagira Mathaniya for his valuable advice
- Prof Martin van de Ven for kindly providing documentation
- Alex Mbaraga Ndiku for his contribution to the success of this study
- The government of Rwanda for granting me a study loan
- The Laboratory technicians Colin Isaac and Gavin Williams and workshop personnel Dion Viljoen for their help and laboratory equipment maintenance
- My fellow students in the department of civil engineering for their encouragement
- The Civil Engineering academic personnel and staff for sharing knowledge and assistance during my time in Stellenbosch
- The Rwandan Student Association at Stellenbosch University for helping me in laboratory works and keeping alive the marvellous Rwandan culture while being far away from our home
- Rev. Jurie Goosen and his wife Maggie for their warm welcome and fellowship while in Stellenbosch. Your love and fellowship for foreigners is acknowledged
- My place of work IPRC- Kigali for facilitating my studies in different ways
- My Family for their love, support and prayers

To God who protects and guides, praise be to thee.

TABLE OF CONTENT

LIST OF FIGURES

Chapter 1

Chapter 2

Chapter 3

Chapter 4

Chapter 5

Chapter 6

Appendix A

Appendix B

Appendix C

Appendix D

Appendix E

LIST OF TABLES

Chapter 2

Chapter 3

Chapter 4

Chapter 5

Appendix F

LIST OF SYMBOL AND ABBREVIATIONS

SYMBOLS

ε	strain
σ	stress
σ_1	major principal stress
σ_3	minor principal stress
σ_d	deviator stress
σ_{df}	deviator stress at failure
C	cohesion
ϕ	friction angle
τ	shear stress
Θ	sum of principal stresses
Mr	resilient modulus
ν	Poisson Ratio

ABBREVIATIONS

AASTHO	American Association of State Highways and Transportation Officials
ARD	Apparent Relative density
BRD	Bulk Relative Density
CM	Compaction Moisture
DOC	Degree of Compaction
EMC	Equilibrium moisture content
GM	Grading Modulus
LVDT	Linear Variable Differential Transducer

M	Mix composition
OMC	Optimum Moisture Content
MDD	Maximum Dry Density
RCA	Recycled Concrete Aggregate
RCDW	Recycled Construction and Demolition Waste
RCM	Recycled Crushed and Masonry
SAPEM	South African Pavement Engineering Manual
TRH	Technical Recommendations for Highways
TMH	Technical Methods for Highways
ACV	Aggregate Crushing Value
AIV	Aggregate Impact Value
SAMDM	South African Mechanistic-empirical Design Method

CHAPTER 1

INTRODUCTION

1.1 BACKGROUND

An increasing need for sustainable development has made recycling a high requirement in many countries. Since the end of the Second World War, the recycling of concrete and masonry was introduced and have been used as unbound materials for pavements in several countries such as Netherlands, Germany, USA, Japan, Brazil, China, and Australia. The need for recycling in pavement engineering is due to the shortage of virgin materials and strict laws on opening new borrow pits and landfills.

In The Netherlands, recycling waste from concrete and masonry for use as unbound materials in the base course has become common practice since the late 1970s (Molenaar & Van Niekerk, 2002). The United States of America have been using Recycled Concrete and Masonry(RCM) in roads since 1987 (Environmental Council of Concrete Organizations, 1999). Australia started using RCM in roads since the late 1980s and Brazil has released the first standard regarding the use of recycled construction and demolished waste for pavements in 2004(Leite *et al.,* 2010).

While extensive research and usage of RCM materials within the pavement-engineering context has been in existence, several knowledge-gaps still prevail; this includes the comprehension of the material physical properties and mechanical performance. In this regard, researchers such as Barbudo *et al*. (2011) affirm that material variability and quality control plays a significant role in the contribution to performance.

In South Africa, recycling and reuse of demolished concrete and masonry remains limited. The abundance of high-quality virgin aggregates, cheap price for landfill and limited expertise have hindered the consideration of sustainability and the allied practices. Additionally, material recycling and comprehension of the material mechanical behaviour remain eminent factors of influence. In general, the present undeveloped demolished waste recycling system is attributable to the low disposal costs and lack of information on recycled materials performance (Gauteng Province, 2009). However, Paige-Green (2010), Suvash (2011) and Dix (2013) note that RCM materials are gradually gaining prominence as road and building materials.

In spite of the pavement materials situation in South Africa mentioned above, the government has established different policies for sustainable development. Namely, the South African Environmental and Resource Conservation Act of 2004 that limits the exploitation of new borrow pits for road construction and rehabilitation and the "National Environmental Management Waste Act, 2008 (Act No 59 of 2008)" that establishes the hierarchy of waste management (Republic of South Africa, 2010). The latter Act specifies that the waste disposal including demolished waste should be the last option and encourages re-use and recycling when waste avoidance is not possible.

The knowledge on performance of RCM and possible use in pavement is currently a concern for both researchers and practitioners. Although there are some attempts in studying the behaviour of RCM material, there is still a noticeable gap in knowledge and further information is required. Therefore, one aspect of concern at which this study will focus on is the RCM material properties and performance characterisation under traffic loading and climate conditions in the pavement layers.

1.1.1 What is Recycled Concrete and Masonry (RCM)?

There are different terminologies used to refer to recycled concrete and masonry and these depend on the country. In some studies, RCM is referred to as Recycled Crushed Aggregates (RCA) and in others; it is referred to as Recycled Construction and Demolition Waste (RCDW) or Recycled Debris (RD). The general composition may be the same but with probable different proportions depending on regions. In this study however, recycled materials are denoted as RCM.

The definition of recycled materials is mostly based on the type of aggregates and content, thus providing a universal definition could not be feasible. However, several researchers have attempted to establish a number of definitions. Bester *et al.* (2004) for instance, define RCM as aggregates obtained by the crushing of residual materials that remain from buildings or structures under construction, renovation and demolition. This definition includes the crushed haul-backs and overruns. Haul-back materials are the excess from produced concrete, which have not been delivered to consumers while overruns are excess concrete delivered to site. Moreover, Hansen (1992) has defined recycled concrete aggregates as materials obtained from the crushing of old concrete, which contains limited amount of brick and masonry. The same author has also defined recycled masonry as aggregates obtained from the crushing of masonry rubble. He indicated that masonry are materials resulting from the demolition of building and

other civil structures predominantly composed by ordinary concrete, clayey materials and concrete blocks. It can be seen from the definition of the latter author that a separation was made between concrete and masonry materials.

The different descriptions given to the recycled concrete and masonry correspond to the different regions where they are produced. The recycling method differs from one country to another and this influences the composition of recycled debris as well as mechanical performance. Barbudo *et al.* (2011) indicated that even though concrete is the main constituent of construction and demolished waste, the architecture of the region could influence the total composition depending on the preferences of construction materials of each region.

1.1.2 Benefit of recycling and reuse of concrete and masonry

Recycling and reuse of concrete and masonry in road domain has a number of advantages that can be summarised in the following aspects of sustainability:

- Reduce the opening of new quarries and the amount of waste reaching landfill sites
- Provide alternative materials for road building contractors hence saving natural resources
- Generate economical interest: research in the USA on recycled materials has revealed that the recycled materials are 30% cheaper than virgin aggregates (Brandon & Guthrie, 2006)

1.2 PROBLEM STATEMENT

Following practice and expertise from Europe, USA, Brazil, Australia, and Asia the use of RCM often offers structural viability besides sustainability within practice. In particular, the use of RCM as pavement layer materials provides feasible structural capacity to the road industry.

In South Africa, due to rapid urbanisation, millions of tons of construction and demolition waste are generated and significant percentages end up in landfills. Department of Environmental Affairs (2012) states that among 4,725,542 tonnes of construction and demolition waste that were generated in 2011, only 16% were recycled. However, this amount of generated construction and demolition waste could be exceeded since this report mentioned a general lack of accurate waste data reporting.

From the background information, South Africa is applying effort in sustainable development through the implementation of laws on waste management and the exploitation of new borrow pits for road construction materials.

The TRH 14(1985) and SAPEM (2013) provide the required properties for traditional South African unbound and cemented road building materials. In these manuals, the material properties are often cantered on the mineralogical composition of the parent rock and the physical-mechanical characteristics of the resulted materials. These physical-mechanical properties are determined through empirical testing methods. However, demolition materials are not established in South African guidelines for road construction materials TRH14 (1985) and are still not well understood in the current South African Pavement Engineering Manual SAPEM (2013). The reason being could be the lack of RCM properties and performance information. In light of this gap in performance information, the usage of the recycled concrete and masonry materials are quite often restricted.

RCM performance is characterised by aggregate strength and material mix composition resistance to the applied stresses. Particularly, the problem related to the performance of RCM materials emanates from their physical characteristics and composition. These govern the resistance of aggregates to wear and tear and the performance of the material under destructive factors such as traffic loading and climate stresses. However, these properties vary from one country to another depending on the architectural preferences and construction materials specifications that influence the quality and strength of demolition waste.

The empirical specifications which the South African pavement materials properties are mainly based on, seems to be favourable to natural aggregates in which inherent variability is minimum, but they limit the introduction of secondary materials characterised by high variability. In contrast, functional specifications that are based on the required material performance in pavement layers such as strength, stiffness and permanent deformation could open the usage of both natural and alternative materials. This will allow for the introduction of guidelines and/ or specifications on RCM. However, the constraint related to functional specifications is that they require good understanding and information of the mechanical performance of the material. Therefore, developing an understanding and providing performance information on properties and mechanical behaviour of granular materials could optimise the usage of the available material resources.

The key focus of this study is the assessment of RCM materials concerning the physical and mechanical characteristics, performance response based on their variability and the influence of the extrinsic factors such as climate and traffic stresses.

This study will endeavour to develop an understanding on the performance response of RCM influenced by materials characteristics, mix composition properties and extrinsic parameters through laboratory testing.

1.3 RESEARCH OBJECTIVES AND LIMITATIONS

The studies on the performance of construction and demolition waste have been carried out in various countries predominantly in developed countries. However, recycled materials have different characteristics depending on the different regions due to the quality and the construction practices such as the type of aggregates in concrete manufacturing or bricks manufacturing process etc. This variability affects the exhibited physico-chemical and mechanical behaviour in pavement layers. Therefore, it is important to carry out this study on locally available South African demolition materials.

The main objective of this study is to characterise the material properties and model the mechanical performance of recycled concrete and masonry materials. To achieve this main objective, the following objectives were developed:

- Laboratory assessment of the recycled aggregates physical-mechanical characteristics
- Conduct an experimental testing program to assess the influence of material properties such as mix characteristics and compaction on mechanical performance behaviour
- Understanding the mechanical performance response of RCM through fitting the Mohr-coulomb model for shear behaviour, Mr-Θ and Mr-Θ-σ_d/ σ_{df} models for resilient modulus, and "Exponential" ν-σ_d/σ_3 model and ν-σ_d/σ_3- σ_3 model for resilient Poisson Ratio.

This study used a blend of recycled concrete and clay bricks processed separately. A laboratory experimental program undertaken was limited to the material gradation, particles specific gravities, absorption, moisture-density, flakiness index and the 10% FACT tests for aggregates characterisation. While the mechanical behaviour evaluated through monotonic and resilient triaxial testing was limited to a number of factors such as two relative mixes of concrete to masonry, two degrees of compaction and two compaction moistures.

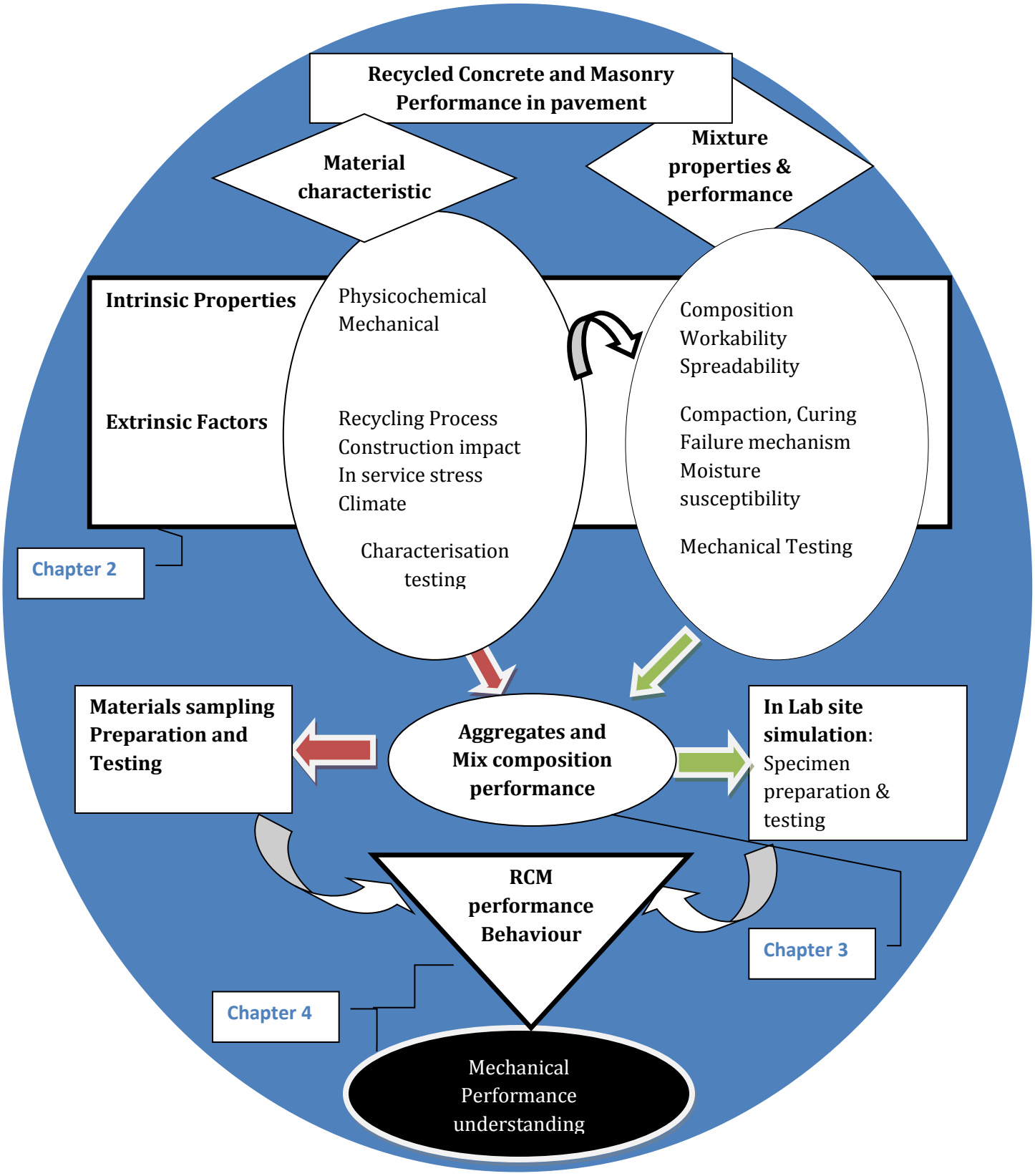

Figure 1- 1: RCM Performance Evaluation Layout

1.4 OUTLINE OF THE RESEARCH

Chapter 1: Introduction

Chapter 1 presents definitions and a brief history of the application of RCM in pavement domain. It provides the description of RCM, advantages of recycling as well as the motivation of this research.

Chapter 2: Literature survey on RCM materials in pavement

Chapter 2 provides an extensive literature study on the characteristics and performance of granular pavement materials in general and recycled concrete and masonry particularly. It outlines the recycling methods and the resulted aggregates characteristics. It also points out other predominant factors and their relation to the performance of the aforementioned materials under traffic and environmental stresses.

Chapter 3: Experimental Program

Chapter 3 describes the acquirement and characteristics of the RCM material used in this research and the experimental testing methodologies undertaken in order to assess the laboratory performance of RCM.

Chapter 4: Tests results and discussion

Chapter 4 presents the results of characterisation and performance tests and provides analytical discussions.

Chapter 5: Application of the results

Chapter 5 contains the practical application of the results obtained in this research.

Chapter 6: Synthesis

Chapter 6 provides the discussion on important findings of this research.

Chapter 7: Conclusion and Recommendations

Chapter 7 draws general conclusions from the findings of this research and give recommendations for further research.

CHAPTER 2

LITERATURE STUDY ON THE PROPERTIES AND THE PERFORMANCE RESPONSE OF RECYCLED CONCRETE AND MASONRY (RCM) IN PAVEMENTS

2.1 INTRODUCTION

The increasing emphasis on sustainability creates high demand on recycled concrete and masonry in cement concrete as aggregates and in pavement as unbound materials in both developed and developing countries. However, the final application of RCM in pavement layers is not the same for developed (industrialised) and developing countries due to different pavement design approaches as indicated in Figure 2-1.

The pavement is a multi-layered structure composed from the top by the surfacing that can be concrete slab or asphalt layer, and this is followed by the foundation system composed by the base, subbase, and subgrade layers.

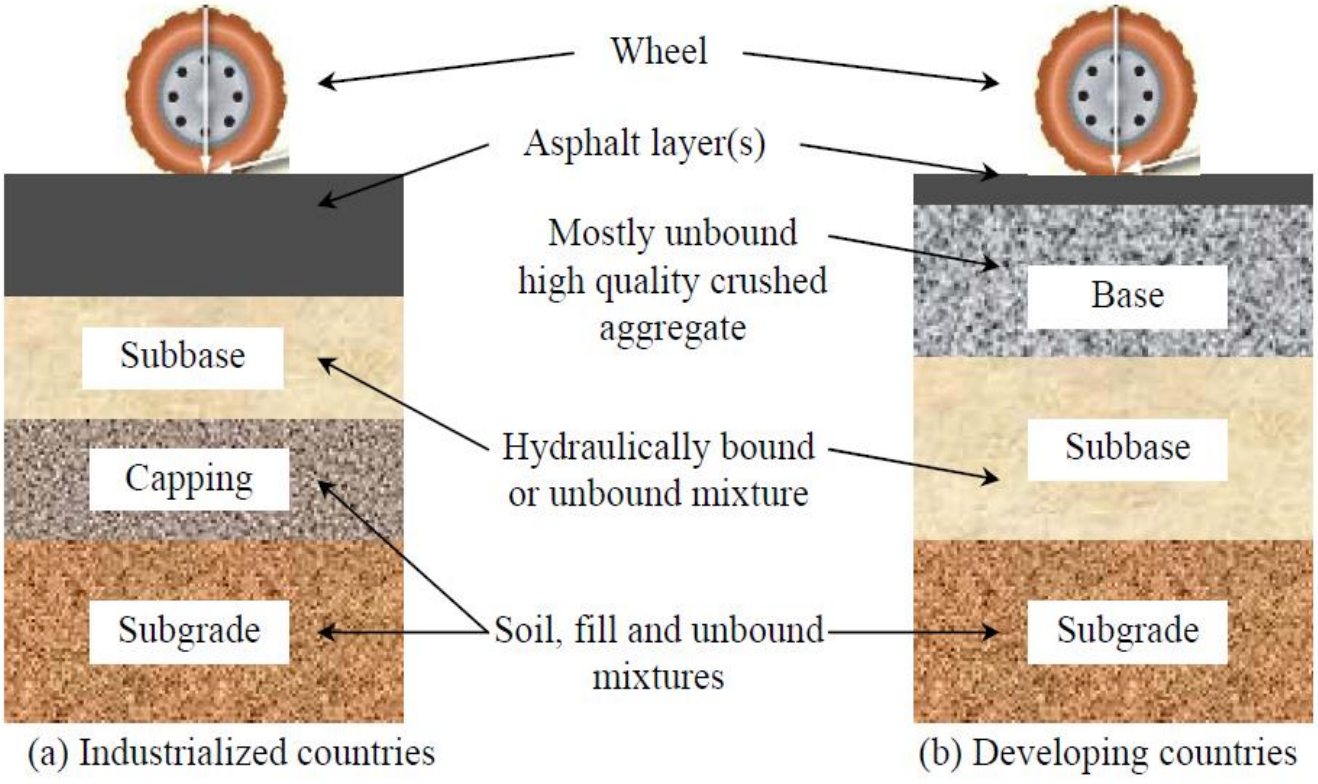

Figure 2- 1: Flexible Pavement Structures in Different Countries (Araya, 2011)

Depending on the design, especially the type and the thickness of the surface layer, the base and subbase layers can be constructed using good quality unbound materials such as natural crushed rock, and lightly or purely cemented materials. Recycled concrete and masonry used in road construction as unbound material should exhibit good performance. Good quality implies aggregates that are strong with denser packing, chemically resistant and non-susceptible to major change due to traffic and climate stresses. However, considering the physical and mechanical characteristics of these secondary materials, the choice of the application on a specific pavement layer should be based on the traffic stresses available in that layer depending on the designed pavement system.

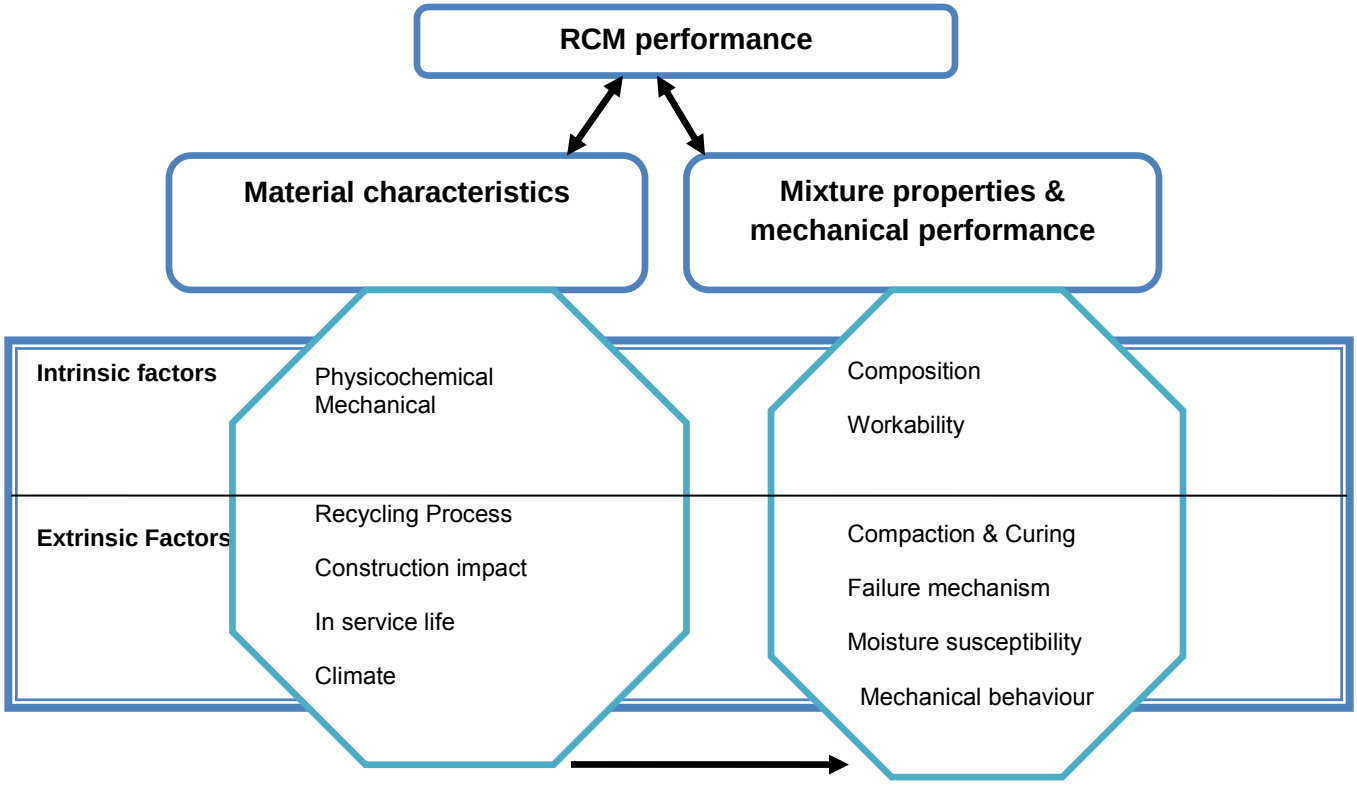

Figure 2- 2: Predominant Factors that Influence the Performance of RCM

To understand the performance response of RCM materials, it is important to evaluate their behaviour under different mechanisms. The aggregates relate to both recycled concrete and recycled masonry particles, and the blend or mix composition composition relates to the ratio of concrete to the masonry mixed using lubricant such as water.

Numerous parameters both intrinsic and extrinsic influence the performance of aggregates and mix composition. This chapter reviews the predominant factors on the strength of aggregates and mix composition performance as shown in Figure 2-2.

2.2 MATERIAL PROPERTIES

2.2.1 Background

Aggregates are exposed to a number of physical and chemical degrading factors during processing, transport, construction, and in service life. These factors cause aggregate mechanical deterioration (wear) and physico-chemical degradation in the overall aggregate life cycle. The strength of recycled aggregates is mainly governed by the mineralogical characteristics and the composition of the recycled rubbles. Understanding the material parameters as well as extrinsic factors such as recycling process, construction, traffic and climate stresses provides good indication in the development of an understanding on the RCM aggregates strength.

Several studies on the behaviour of various types of RCM aggregate indicated that the recycled concrete aggregates have higher strengths than masonry. This recycled concrete aggregates strength provides resistance to the disintegration or fragmentation than recycled masonry aggregates (Nataatmandja & Tan, 2001; Poon & Chan, 2005; Barbudo *et al*., 2011). According to the observed low resistance to disintegration of recycled masonry, Arulrajah *et al*. (2011) recommended that recycled masonry should be mixed with other durable aggregates such as crushed concrete or crushed rock to improve durability and in service performance in pavement.

This section critically reviews the physicochemical and strength properties of recycled aggregates from concrete and masonry in accordance with the influence of the extrinsic and intrinsic factors and the related affect on the material performance.

2.2.2 Impact of physicochemical characteristics

The physical characteristics, chemical composition and the inertness of the aggregates have a significant impact on their strength, durability and to the pavement performance. Dukatz (1989) has established a relationship between the aggregate properties and different pavement performance indicators. It can be seen in Table 2-1 that the aggregate shape and mechanical characteristics have a significant influence on permanent deformation. This table also indicates the important impact of aggregate chemical characteristics on moisture damage.

Since recycled aggregates are obtained from demolition waste, they are susceptible to contain impurities, which could adversely affect the material performance. These contaminants are asphalt, chlorides, cladding, soil, paper, gypsum, wood, steel reinforcement, etc. Therefore, depending on the properties of recycled aggregates and contaminants content, these materials may exhibit less mechanical performance than required.

Table 2- 1: Impact of aggregate properties on the pavement performance (Dukatz, 1989)

Property	Permanent Deformation	Fatigue	Low Temperature Cracking	Moisture damage
Physical				
Shape	5	4	3	2
Surface	3	1	3	4
Absorption	3	3	1	4
Specific gravity	3	3	3	1
Morphology	3	4	3	4
Gradation	5	4	3	4
Chemical				
Composition	3	3	2	5
Solubility	3	3	1	5
Surface charge	1	2	2	5
Mechanical				
Strength	3	4	2	1
Durability	5	5	2	1
Toughness	5	5	2	1
Hardness	3	5	1	1

Note: 5 denotes significant influence and 1 denotes minor influence

2.2.2.1 Effects of physicochemical characteristics on RCM Performance

Aggregates during construction and in service are subjected to possible weathering. Weinert (1980) divided weathering into two main parts namely disintegration and decomposition. The disintegration is defined as the “physical breakdown” without alteration of minerals whereas decomposition is defined as “chemical decomposition” or alteration of minerals. Therefore, the study of the physicochemical behaviour of aggregates provides information on their durability characteristics and on long-term performance in pavement layers.

2.2.2.1.1 Effect of Physical properties on aggregates performance

Aggregates in their life cycle are subjected to various detrimental aspects: attrition during handling and construction, degradation during construction and in-service life as well as environmental degradation due to wet and drying cycles. The aggregates physical characteristics that affect the resistance to these detrimental factors are predominantly the particle shape, texture, and the gradation.

a. Shape, texture and inertness

The production of recycled aggregates requires crushing of demolished rubbles. The processing methods have a significant influence on the aggregate physical characteristics such as gradation, aggregate shape and texture. These physical properties exhibit a major influence on aggregate particles behaviour during their lifecycle and affect the performance of pavement layers in which they are used.

The aggregate shape is qualified to be cubical, flat or/and elongated as it can be seen in Figure 2-3. For natural aggregates, flat particles are produced when the crushed parent rock is stratified and the crushing is along stratification. Nevertheless, because RCM is not very stratified, flat particles originate much from soft constituents such as ceramic (van Niekerk, 2002).

The recycled material contains flaky aggregates especially when it has a significant amount of soft materials such as masonry or mortar. High content of flaky aggregates in the material increases the proneness to crushing and results in less workable material during compaction. The flakiness is defined as a mass of flaky particles contained in a mass of sample expressed as a percentage. The flakiness index provides trend of the aggregate shape but it does not fully describe the particle shape (Van Niekerk & Huurman, 1995).

Aggregates shape is also characterised by angularity, which is the extent at which the aggregates differs from smooth to rounded sphere (van Niekerk, 2002). Based on this distinction, aggregates are classified as angular and round.

The texture of the aggregate is the physical characteristic of its surface. The texture distinguishes smooth from rough aggregates, this affects the workability during compaction and aggregates interlock for the compacted mix composition. The interlock between particles influences significantly the failure behaviour of the material by influencing the apparent friction angle of the material.

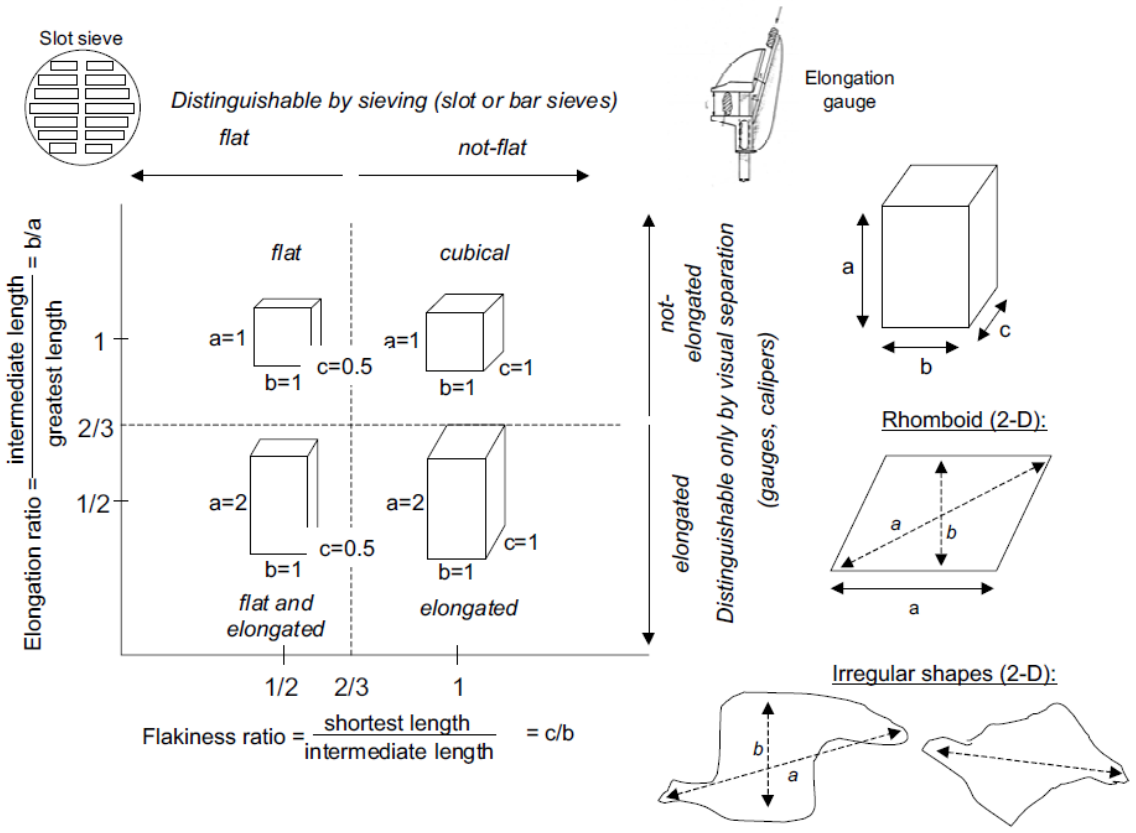

Figure 2- 3: Flatness, Elongation and Cubicity of Particles (van Niekerk, 2002)

The inertness characterises the mechanical strength of aggregates and this affects the durability and long-term performance. The specific gravity, which is an indication of the aggregate inertness, provides a trend on the mineralogy of the aggregates and their porosity. The AASTHO T 85(1999) standard defines the apparent specific gravity (apparent relative density) of the aggregate as “the ratio of the weight in air of a unit volume of the impermeable portion of aggregate (does not include the permeable pores in aggregate) to the weight in air of an equal volume of gas-free distilled water at the stated temperature”. The same standard indicates that the bulk specific gravity is “the ratio of the weight in air of a unit volume of aggregate at a stated temperature to the weight in air of an equal volume of gas-free distilled water at the stated temperature”. Figure 2-4 illustrates the aggregate characteristics during evaluation of specific gravities.

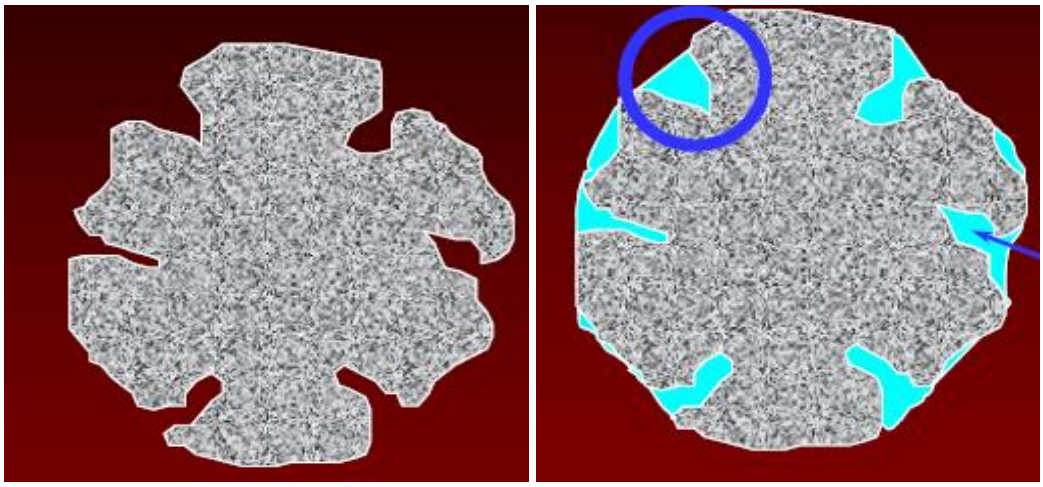

Figure 2- 4: Apparent Specific Gravity (left), Bulk Specific Gravity (Right)

For asphalt concrete mix compositions and unbound aggregate base material, angular and cubical are preferred in order to provide aggregate interlock that increases the shear strength of the mix composition (Barksdale, 1991).

Nataatmandja & Tan (2001) have observed an increase in degradation of Recycled Crushed Concrete (RCC) aggregates due to the high flakiness index during a study that they conducted on four recycled crushed concrete materials obtained from concrete rubbles of different compressive strength. They concluded that the concrete compressive strength and the flakiness index affect the degradation of "well-graded" and well-compacted" RCC road aggregates. However, the flakiness index exhibited a more pronounced effect than the compressive strength of the parent concrete rubble. Furthermore, Van Niekerk, (2002) in his extensive research on the mechanical behaviour of recycled aggregates has found more aggregates that are flat in masonry rather than in concrete. These flat particles lead to low resistance to the fragmentation of recycled masonry aggregates than the recycled concrete.

Park (2003) found that the recycled concrete aggregates were more angular and with a rough surface texture compared to gravel (round and smooth) but less angular to natural crushed stones. In light of this, he noticed a decrease in the elastoplastic index of the recycled aggregates compared to the crushed stone aggregates but with higher elastoplastic index compared to natural gravel. The decrease in elastoplastic index is an indication of the aggregates deterioration caused by aggregates breakdown.

Hamzah *et al.* (2010) carried out 3 tests; ACV, AIV and 10% fines on cubical and normal aggregates. They have observed higher toughness of cubical aggregates than normal. This toughness was attributed to aggregates geometrical shape.

Cho *et al.* (2006) characterised particle shape based on sphericity and roundness as presented in Figure 2-5. The sphericity of particles is defined as the diameter of the largest inscribed sphere relative to the diameter of the smallest circumscribed sphere. Roundness is the average radius of curvature of surface features relative to the radius of the maximum sphere that can be inscribed in the particle. They have found that as the roundness and sphericity decrease, the maximum void ratio (e_{max}), the minimum void ratio (e_{min}) and the void ratio difference (I_e) increase. This increase in void ratios has an influence on the packing of aggregates and affects the proneness to higher particle degradation.

The aggregate specific gravity and water absorption provide a trend of the resistance to degradation and long-term performance. While assessing the characteristics of recycled aggregates, Van Niekerk (2002) has found that recycled concrete aggregates manifest higher specific gravity compared to recycled masonry. He indicated accordingly that recycled aggregates resist more than recycled masonry to degradation/fragmentation. There is a relationship between aggregate specific gravity and water absorption because aggregate with high specific gravity manifest low water absorption. Natural aggregates have lower water absorption than that of recycled concrete due to the soft attached mortar, and the recycled masonry manifest higher water absorption due to higher porosity. Even though water absorption is not a direct measure of aggregate durability, it can be a screening indication to assess aggregate durability. Subsequently, Williamson (2005) indicates that because the aggregates with high specific gravity have a low absorption, these aggregates manifest in terms of durability a resistance to abrasion and dimensional changes. This durability characteristic indicates a good performing pavement material.

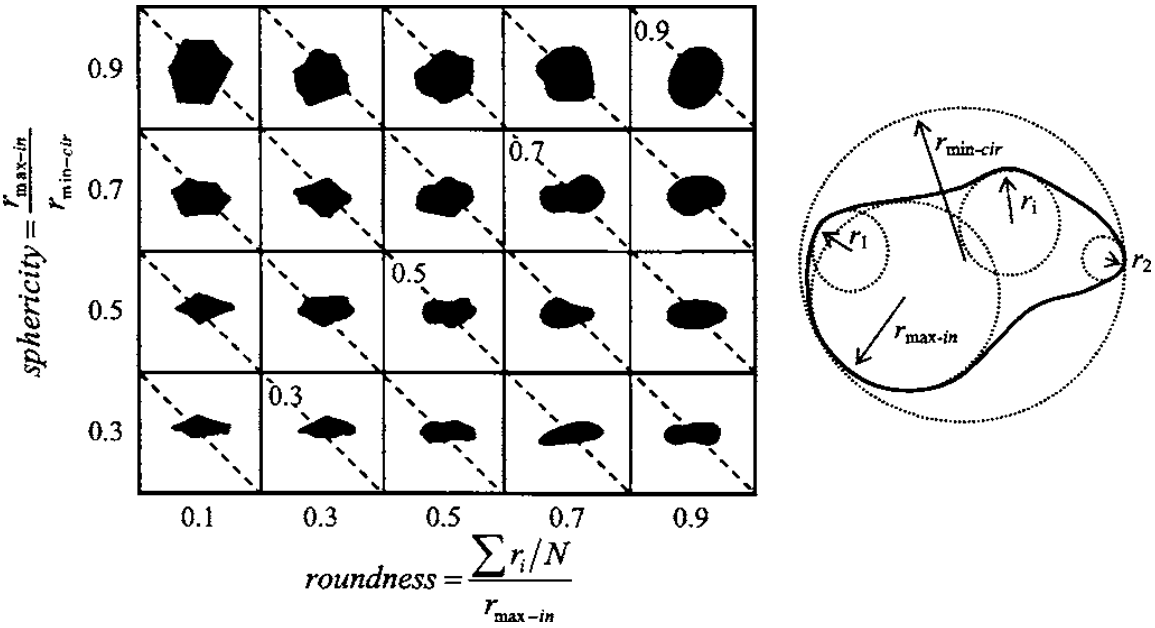

Figure 2- 5: Aggregate Particle Shape (Cho *et al.*, 2006)

b. Grading

The grading of granular materials is generally determined through a material sieve analysis. The grading curve obtained gives the relative proportions of the different grain sizes within a mass of material. The grading of the granular material is generally qualified to be well graded or poorly graded (Sivakugan, 2000). These characteristics can be evaluated through the coefficient of uniformity (c_u). The C_u provides good information on the skeleton of granular material as presented in Figure 2-7.

$$C_u = \frac{D60}{D10} \qquad \text{(Equation 1)}$$

Where, C_u is the coefficient of uniformity, D_{60} represents the sieve opening size (mm) through which 60% of the aggregate passes, and D_{10} is the sieve opening size (mm) through which 10% of the material passes.

Granular material is qualified as a well-graded material if there is a good distribution of sizes in a wide range with the smaller grains filling the voids created by the larger grains and producing a dense packing. This is expressed by a smooth and concave curve “A” obtained through sieve analysis as indicated in Figure 2-6.

Poorly graded granular soils can be divided, as shown in Figure 2-6, into uniform soils (C) with grain of same size and gap-graded soil (B) characterised by smaller and larger grains but without intermediate grain size.

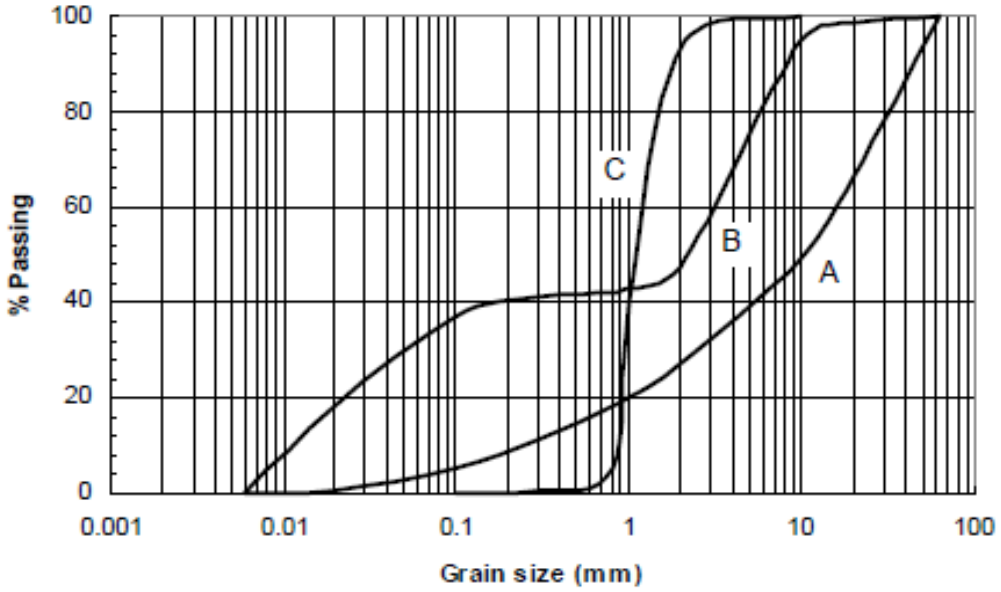

Figure 2- 6: Different Types of Grading (Sivakugan, 2000)

In South Africa, the grading characteristic for soils and gravel can also be assessed according to the Grading Modulus (GM). It is calculated using the equation below:

$$GM = \frac{300 - [P2.00mm + P\ 0.425 + P0.075]}{100} \qquad \text{(Equation 2)}$$

Where, P indicates the percentage passing on the indicated sieve size.

A material with a grading modulus greater than 2 indicates a coarsely graded material, which is of a relative good quality while material with a grading modulus less than 2 is finer grained material with poorer road building quality (SAPEM, 2013).

To assess the effect of gradation on the material performance, it is important to understand the behaviour of unbound granular materials in their natural state. Unbound granular materials build an aggregates skeleton that can resist external applied forces by distributing these forces through particle connections points. Bjarnason *et al.*(2000) study on four different aggregates with four different grain size distributions (Fraction 8-16mm, gap graded, Fuller curve, and dense graded curve), have found more fragmentation occurring in single fraction (8-16mm)

than in denser materials. They concluded that the stresses are lower at connection points for dense graded material than in single fraction or gap-graded materials.

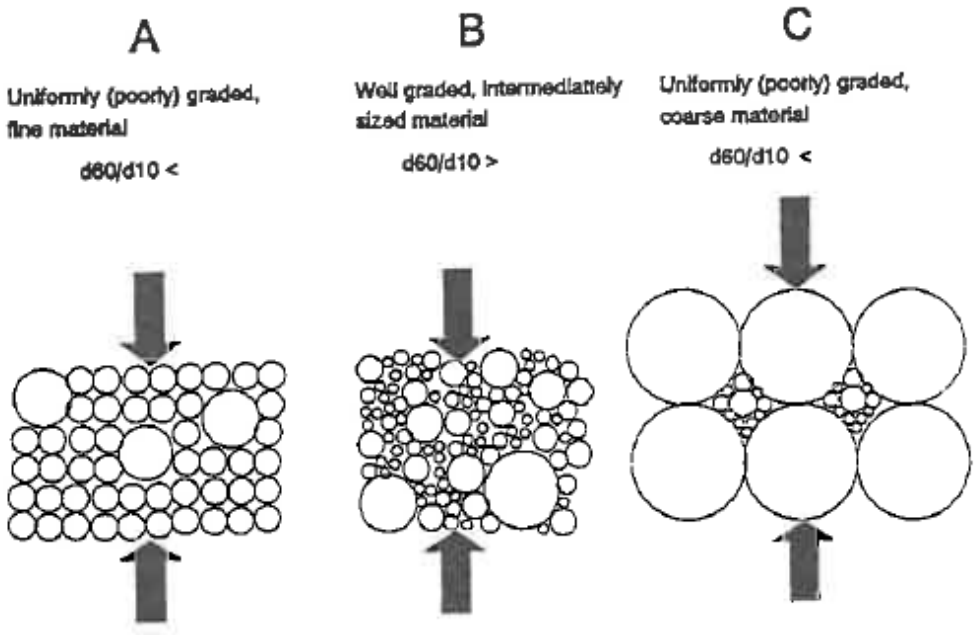

Figure 2- 7: Skeleton of Poorly- Graded and Well-Graded Materials (Van Niekerk & Huurman, 1995)

Molenaar & van Niekerk (2002) have researched the effects of composition, gradation, and degree of compaction on mechanical characteristics of recycled unbound materials. To investigate the impact of grading, they used six different gradations in accordance to the Dutch standard for base courses (upper limit, continuous, uniform, lower limit, average of upper and lower limits, and Fuller). They found better mechanical performance for balanced or denser grading materials than that of uniform or gap graded materials. The denser grading (average limit, continuous, Fuller) has sufficient fines that mobilise the friction between particles. It also has coarse particles skeleton providing a matrix structure. These characteristics increase the friction with a reasonable cohesion providing higher stiffness.

2.2.2.1.2 Effects of chemical properties

The chemical properties of an aggregate identify the chemical composition and/or indicate the transformation that an aggregate can undergo due to chemical action (Roberts *et al.*, 1996). Recycled concrete and masonry are materials obtained from the processing of demolished building, concrete pavement, and other civil structures. Demolition waste is composed of various materials such as concrete, clay or/and concrete bricks and contaminants like gypsum,

paper, asphalt, and tiles. However, the fine aggregates namely clay particles play a predominant influence on the material chemical behaviour.

Chemical properties of the aggregates influence the chemical composition or mineralogical composition, solubility, and surface charges (Dukartz, 1989). The information on these parameters will lead to a good understanding of the performance of RCM especially on moisture damage, stability, and self-cementing. Mitchell (1993) indicated that the mineralogy of the material is of significant importance in developing an understanding on material geotechnical behaviour even if it is not appropriate for a geotechnical investigation.

The chemical composition of RCM depends on the regions. Vegas *et al*. (2008) identified in Basque (Spain) that the Construction and Demolition Waste (CDW) are mainly composed by calcite ($CaCO_3$), quartz (SiO_2) from concrete, and feldspars ($(K,Na)AlSi_3O_8$) and muscovite($KAl_2(Si_3Al)O_{10}(OH)_2$) from ceramic materials. They also found gypsum ($CaSO_4.2H_2O$) in concrete and mixed rubbles. Meanwhile, Weinert (1980) in categorising decomposing minerals for crystalline rock has indicated that except for quartz, other minerals such as feldspars, micas (muscovite, or biotite), pyroxene, amphibole and olivine are highly likely to decompose and give rise to secondarily clay minerals such as kaolinite or montmorillonite. These clay minerals are subject to volume change upon wetting and drying cycles and this reduces the stability of the pavement layer in which these minerals are generated. The same author also mentioned that although other minerals such as calcite, dolomite, gypsum sulphate salt, rock salt and clay are stable and do not decompose because these are final products of some weathering process, they do dissolve in water. The material dissolution in water affects also its stability in pavement. The decomposition of feldspar is shown in the chemical reaction below as given in Weinert (1980):

$$K_2Al_2O_3.6H_2O + CO_2 + nH_2O \rightarrow K_2CO_3 + Al_2O_3.2SiO_2.2H_2O + 4SiO_2.nH_2O \quad \text{(Equation 3)}$$

(Orthoclase) (Alkaline carbonate) (Kaolinite) (Hydrated silicate)

The tendency of the aggregate to be dissolved into liquid is defined as *solubility* (Barksdale, 1991). The most soluble salts present in CDW are calcium ions and sulphates from gypsum (Vegas *et al*., 2008). These salts are the basic cause of solubility of CDW that can result in aqueous dissolutions leading to the loss of resistance. This loss of stability is caused by volumetric expansion due to crystallisation of calcium sulphates or its anhydride form.

It can be seen from the above section that the mineralogical composition of the material affects its decomposition and solubility, which could potentially lead to poor material performance. It is also evident that some materials attract more water than others do and this leads to a weaker structure. Therefore, a good understanding of the material performance behaviour of RCM requires the assessment of RCM composition, solubility behaviour, as well as the climate at which the material will be exposed.

The chemical composition and moisture, not only have a negative impact on the performance of cementitious materials, but also the residual cement present in RCM contribute when hydrated further to the increase in stiffness of the material with time due to pozzolanic reactions. This phenomenon is termed "self-cementing" (Molenaar & van Niekerk, 2002; FHWA, 2004; Blankenagel & Guthrie, 2007; Marradi & Lancieri, 2008; Paige-Green, 2010; Vegas *et al.*, 2010). The increase in stiffness resulting from self-cementing enhances the long-term material performance in the pavement.

The hydration is the formation of new a compound from interaction of water and cementitious material and this reaction is a dissolution-precipitation process (Scrivenet & Nonat, 2011). Portland cement that contains calcium-alluminates and calcium- silicates when hydrated, these constituents generate cementing materials named cement gels such as calcium-silicate-hydrate, calcium-aluminate-hydrate with an excess of calcium hydrate. The equations below given by the latter authors shows the reactions of the most well-known cement reactive phases which are the calcium-silicate phases: reactions of the tricalcium silicate Ca_3SiO_5 (≡ C_3S) and dicalicium silicate Ca_2SiO_4 (≡ C_2S) with water.

$$2C_3S + 6H_2O \rightarrow C_3S_2H_3 + 3CH \quad \text{(Equation 4)}$$

Tricalicium silicate Tricalicium silicate Hydrate Calcium Hydrate

$$C_2S + 4H_2O \rightarrow C_3S_2H_3 + CH \quad \text{(Equation 5)}$$

Dicalicium silicate Dicalicium silicate Hydrate Calcium Hydrate

Jenkins (2013) has indicated that when these cement gels crystallise or set into an interlocking matrix, they cause a hardening of the soil-cement mix composition. Furthermore, Little *et al.* (2001) indicated that these chemical compounds highly reduce the permeability of the material that results in high durability and resistance with good performance over time. On the other hand, Paige-Green (2010) indicated that the higher self-cementing is likely to happen for a

denser material with a greater percentage of fines from cementing agent and for high material pH.

Briefly, it can be seen from RCM's physical and chemical characteristics that even though it contains clay bricks, mortar and deleterious components that require high compaction moisture especially at high masonry content in the mix composition, it exhibits limited moisture damage. It can also be observed that the RCM chemical composition can probably improve long-term performance though the self- cementing phenomenon. However, care should be taken during processing in order to remove soluble salt such as gypsum sulphates that can cause dissolution and lead to low material performance.

2.2.2.2 Effect of aggregates mechanical properties on RCM performance

The mechanical properties of a material are the response behaviour to the applied forces influenced by its physical properties (Barksdale, 1991). This author pointed out and defined the predominant aggregate mechanical properties, which are strength, stiffness, wear resistance, and resistance to degradation.

The particle strength can be defined as the magnitude of the applied compressive and/or tensile stresses that an individual aggregate particle can withstand before failure. The stiffness is defined as the resistance of an aggregate particle to deformation.

The resistance to wear is defined as the resistance of the aggregate surface to polishing due to rubbing and friction. The external applied forces such as vehicle or foot traffic produce this.

The resistance to degradation is the resistance of the aggregate to the breakdown into smaller pieces. The applied forces such as mixer blades, compaction, heavy wheel loads, and grinding action generate this break down.

For maximum stability to unbound materials, mechanical aggregate properties are essential; these properties are influenced by particle physical characteristics as the definition above indicates. Therefore, for good performance, unbound materials require coarse and angular aggregates to provide interparticle friction, sufficient fines to produce dense material and also hard and durable aggregates are required in order resist breakdown during handling, compaction, and in service stresses. Several researchers have attempted to assess RCM's aggregates mechanical properties:

Poon & Chan (2005) have identified a higher ten percent fines value for recycled concrete than recycled masonry. The ten percent fines values decreased as the masonry content increased. High value of ten percent fines is an indication of good resistance of the material to crushing.

Barbudo *et al.* (2011) have found an increase of the Los Angeles abrasion as the masonry content increases during the assessment of the impact of the masonry (ceramic) on the Los Angeles index. The increase in Los Angeles index indicates aggregates poor resistance to abrasion and impact. Sanchez de Juan & Gutierrez (2008) have carried out research on the influence of the attached mortar on the properties of recycled aggregate. They have found that the resistance to abrasion was reduced by the attached mortar on the aggregates because this soft mortar is powdered during the Los Angeles test.

Comparing the mechanical properties of recycled aggregates and the strength of the parent concrete, Van Niekerk (2002) indicated that good quality aggregates could not be expected from a weak reclaimed concrete. However, this should not be a definitive indication of getting good recycled aggregates from high strength reclaimed concrete. The reason for this is that high strength concrete can be obtained from the poor aggregates but with good water-cement ratio as indicated by Barksdale (1991). In addition, Sanchez de Juan & Gutierrez (2008) investigated the relationship between the recycled concrete aggregates quality and the compressive strength of the original concrete and were not able to explain a clear relation between these parameters. These research findings show that high concrete strength could not always result in good recycled aggregates.

It can be observed from the above-mentioned literature that the strength of the aggregate plays a key role in its resistance to fragmentation due to traffic wear, particles abrasion, and stress degrading impact. It is also mentioned that soft aggregates such as mortar or masonry exhibit high degradation. Therefore, to provide good material performance, the choice of aggregate blend based on the intended application and the individual aggregate strength is of significant importance.

2.2.3 Masonry and recycled masonry characteristics

The properties of recycled clay bricks in contrast to recycled concrete depends predominantly on to the brick quality, which is a result of various factors. The physical and mechanical properties of clay bricks depend on the physical, chemical and mineralogical characteristics of the raw materials and the method of production such as firing temperature, time and methods

(Cultrone *et a*l., 2004; Karaman *et al*., 2005). Bricks require an appropriate study in order to understand the behaviour of recycled clay bricks.

Karaman *et al.* (2005) indicated that for clay bricks in Turkey, the density, water absorption and the compressive strength of clay bricks depend on the firing temperature. Firing bricks between 700°C to 1100°C has resulted in a "sharp" increase in compressive strength, density and decrease of pores and hence a decrease of water absorption especially at temperature higher than 1000°C. This was attributed to vitrification in clay minerals. On the other hand, it was observed that the compressive strength and density also depend on the mineralogical characteristics of the raw materials (Cultrone *et al.*, 2004; Weng *et al.*, 2003). These authors have observed high vitrification in non-calcareous clay bricks when compared to calcareous clay bricks when fired at the same temperature. This significantly reduces the pores in the fired bricks, which in return increases the density, the compressive strength and reduces the water absorption. In addition, they observed that non-calcareous clay bricks presented good quality and durability characteristics at firing temperature ≥ 1000°C. The same characteristics were achievable by calcareous clay bricks but at a higher firing temperature. In other words, calcareous bricks required more energy than non-calcareous to attain similar characteristics.

The literature reviewed has shown that fired clay brick characteristics depend on various factors. The most influential factors that the author recorded were the raw material and production method. The primary constituent of clay bricks is the clay which intrinsic mineralogy depends on the region. However, due to the increase in scarcity of raw material (clay) and the need for energy saving, brick production uses clay with different additives and the production approaches in different countries have been accordingly upgraded. Since 1979, South Africa started adding sludge to clay in order to replace the traditional method of clay masonry production from purely clay (Slim & Wakefield, 1991). In China, the introduction of sludge as well as fly ash in the clay bricks production is also gaining popularity (Weng *et al.*, 2003, Lingling *et al.*, 2004). The variation in raw materials constituents changes the required firing temperature for bricks vitrification. For example in South Africa, the firing temperature varies between 1000°C to 1200°C depending on the raw materials (Clay Brick Association, 2002).

In conclusion, the change in constituents and production methods such as furnace temperature plays a key role in increasing the compressive strength and especially reducing the porosity of the clay bricks, which in return enhances the physical and mechanical properties of recycled masonry in the mix. In addition, since different additives and firing procedures are used in

different regions, this justifies the variability that occurs in clay bricks as well as in recycled clay bricks.

2.2.4 Impact of recycling process on RCM material properties

Recycled concrete and masonry are produced when buildings and others structures such as roads and bridges are under construction, renovation or demolition. This practice generates a large variety of materials in terms of size and composition. The processing of these materials has the benefit of reducing the materials into the desirable size. It also has the role of separating constituents and removing the contaminants that can make the materials unsuitable for a specific usage or the environment.

To achieve a target usage, different processing methods are required. Xing (2004) indicated that the quality of recycled material depends on the number of process steps and initial quality of demolished waste. The processing of demolition waste comprises of separation, crushing and sizing. These processing steps play an important role in the achievable compositional quality of the material, which results in good aggregates physico-mechanical characteristics. These characteristics provide better material performance during in-service life as indicated in previous sections of this research.

Separation

The aim of separation is to remove undesirable components such as wood, steel, plastic as well as other environmental or material contaminants. Separation is also required to distinguish concrete from masonry (Xing, 2004).

There exist different separation techniques, which are mainly based on:

- size
- shape
- magnetism
- density
- electrical conductivity
- surface wettability; and
- colour.

The initial separation methods and the products are presented in Figure 2-8 while the separation techniques are summarised in Table 2-2.

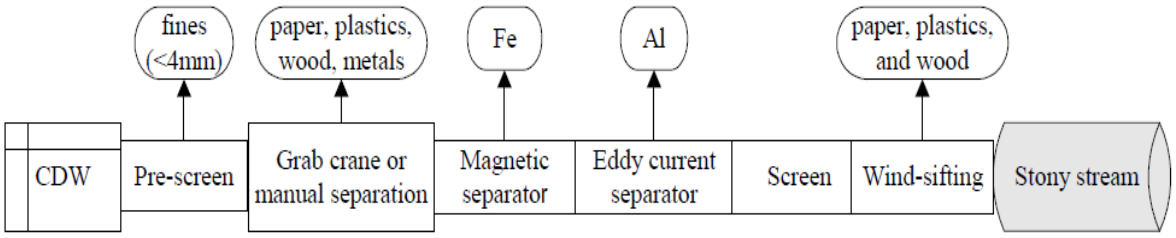

Figure 2- 8: Initial Separation for the Removal of Contaminants (Xing, 2004)

A number of methods exist that can separate mixed constituents of concrete and masonry. Since the basic difference between concrete and masonry are density, colour and Fe_2O_3 content, the separation is based on these aspects. Dry techniques such as the magnetic method based on Fe_2O_3, wet techniques such as the jigging separation method for coarse(>3mm) and spiral separation for fines(<3mm) based on density and the colour separation can be effectively used to separate concrete materials from masonry contained in mixed crushed rubbles (Xing, 2004)

The crushing and treatment methods for CDW depend on the type of demolition material and the required products as presented in Figure 2-8 and Figure 2-9. These techniques however are not all adequate for the large industry of recycled aggregates. For example, colour separation even though effective, is not economically sound for large quantities of recycled materials due to high process costs (Xing, 2004).

Separation has the benefit of isolating concrete and masonry constituents respectively. This is important in assisting in controlling the blending of these two types of demolition waste for a specific use. As mentioned previously, the role of separation is primarily to remove contaminants such as gypsum sulphates and other soluble salts. These chemical contaminants affect the material performance by causing the dissolution in water that reduces the material stability. Therefore, pre-screening and other methods of separation are very important in order to produce good RCM materials that perform well in pavement layers.

Table 2- 2: Separation Methods for Concrete and Demolition Waste (Xing, 2004)

Technique	Type	Input of material	Feed properties	Parameters
Aquamator system	wet	containing lighter and heavier materials	weight/density	water flow speed
Coal-spiral	wet	materials with different densities (<3mm)	density	water speed, amount of feed
Colour separation	dry	materials with different colours	colour	
Eddy current sep.	dry	non-magnetic metals	non-magnetic metal	electric current
Fluidised bed sep. (with water)	wet	materials with different densities	density	particle size and density, water supply
Fluidised bed sep. (with sand)	dry	materials with different densities	density	particle size and density, air flow speed
Grab crane	dry	large and light material	particle size	particle size
Hand-sorting	dry	large and light material	particle size	particle size
Humphrey spiral	wet	materials with different densities (<3mm)	density	particle density, amount of feed, water supply
Jigging	wet	materials with different densities (>3mm)	density	particle size, speed and frequency of water flow
Magnetic sep.	dry	containing ferrous metals or iron oxide	magnetic susceptibility	electric current
Screen	dry/wet	material with different particle sizes	particle size	the size of material to be removed
Thermal method	dry		thermal property (shrinkage)	temperature and time
Wind-sifting	dry	light material	weight	wind strength

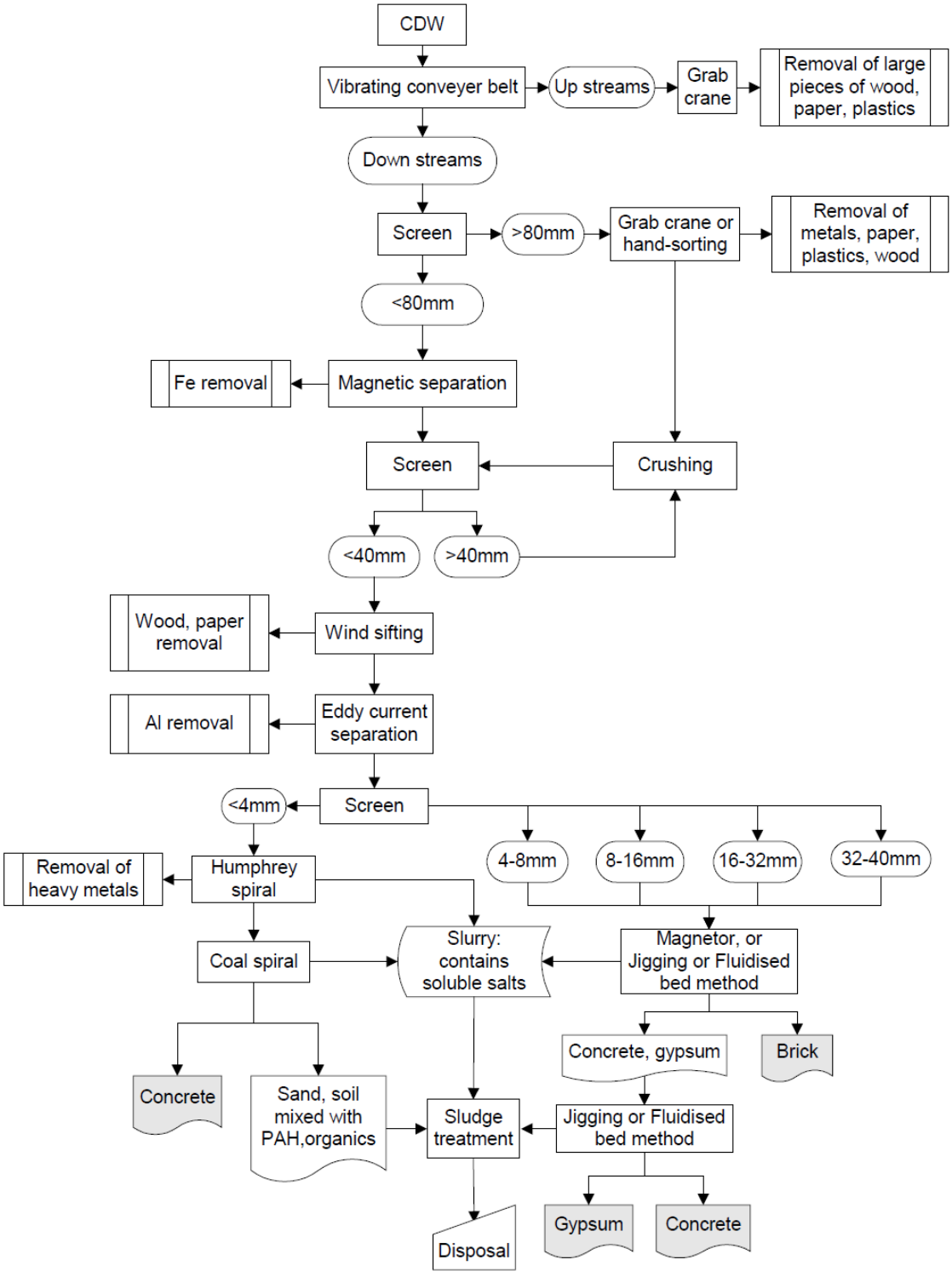

Figure 2- 9: Concrete and Demolition Waste Treatment Flowchart (Xing, 2004)

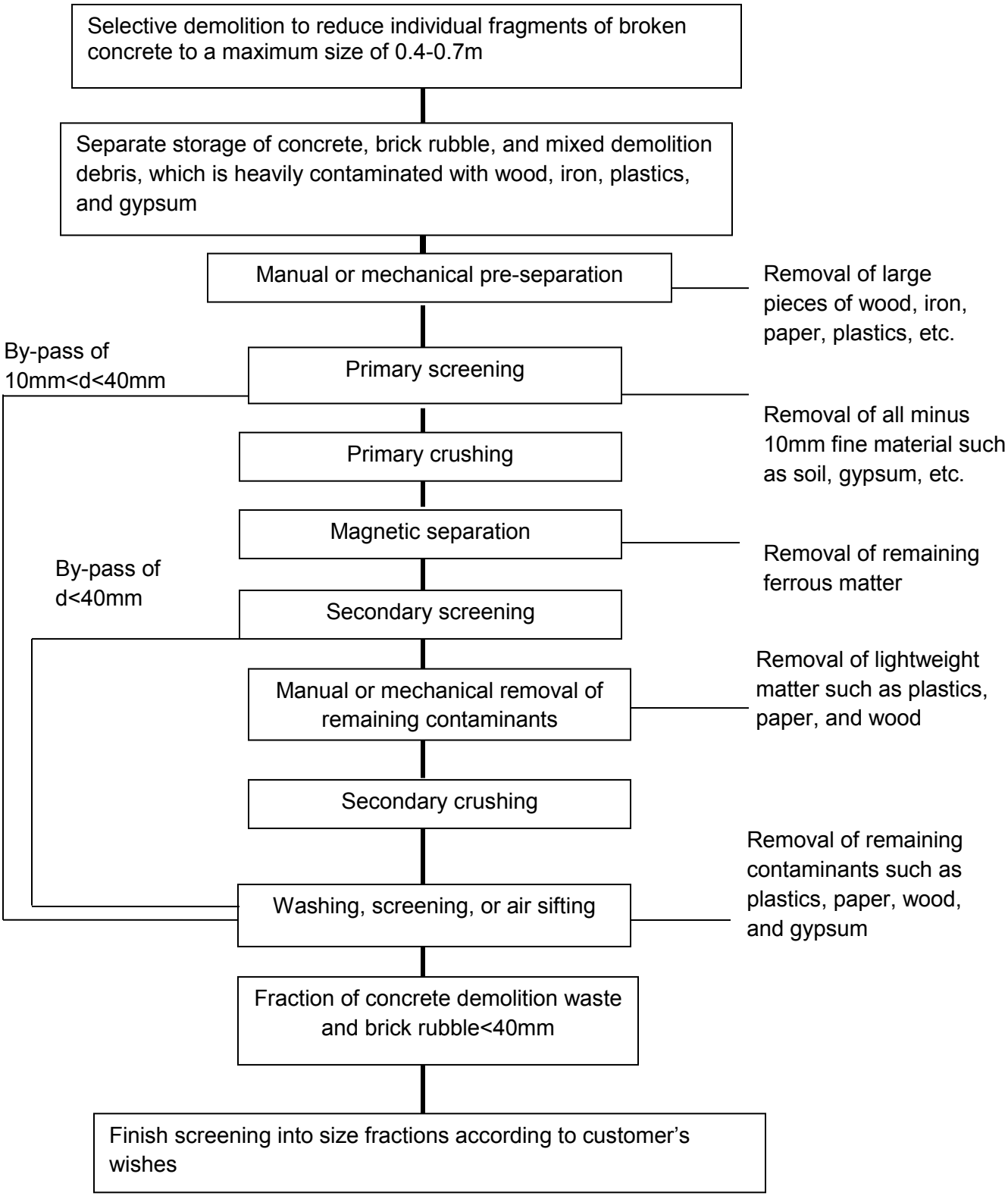

Figure 2- 10: Processing of Construction and Demolition Waste (Hansen, 1992)

Crushing and sizing

The materials from demolition rubbles have different sizes. At the crushing plant, large pieces are crushed and sieved to usable sizes. This operation is an iterative process as can be seen in Figure 2-9 and Figure 2-10. The crushing operation uses different types of crushers and crushing stages. The main types of crushers that are commonly used by recycling plants are compression crushers (jaw crusher and cone crusher) and impact crushers. The crushing methodologies of these crushers are illustrated in Figure 2-12 through Figure 2-15.

Figure 2-11 shows a brief procedure of crushing using a jaw crusher, and screening of concrete pavement rubble.

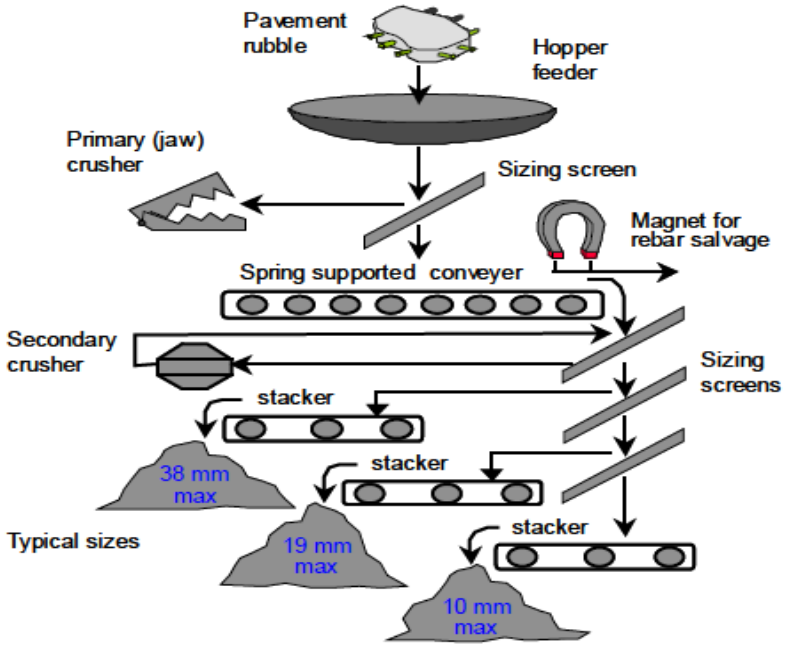

Figure 2- 11: Crushing and Sizing (Hoerner *et al*., 2001 cited in MDOT, 2011)

The jaw crusher is a type of crusher that uses a set of steel plate, i.e jaw to compress material fragments against a stationary plate within the crusher housing and the crushed materials flow at the bottom of the crusher by gravity. Aggregate sizes are controlled by varying the jaw opening.

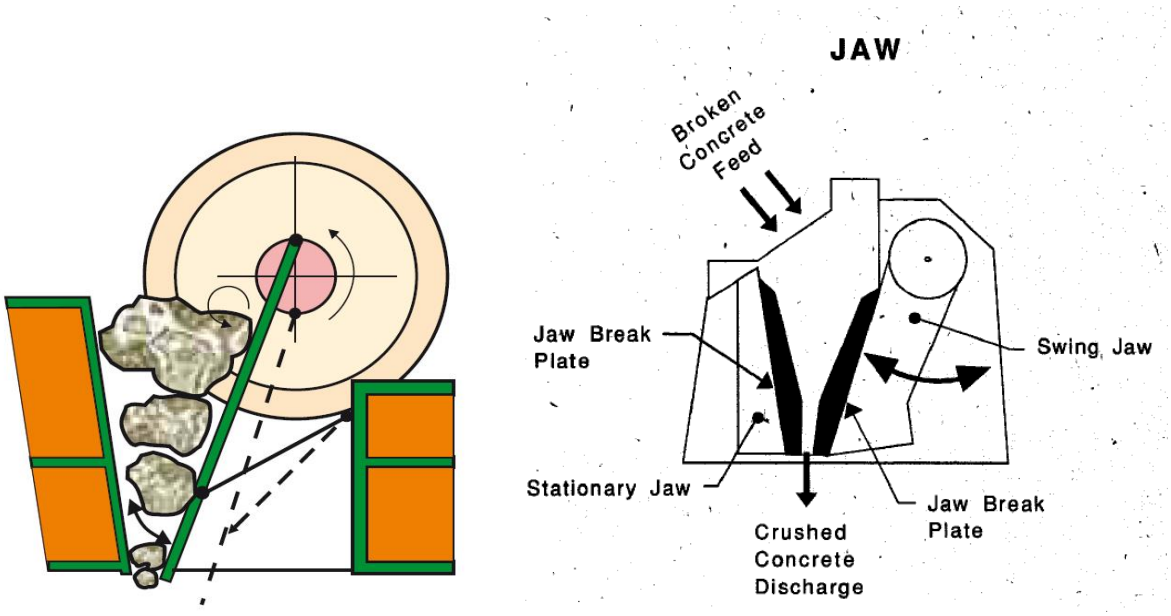

Figure 2- 12 : Jaw Crusher (Metso Minerals Handbook, 2007; Environmental Council of Concrete Organizations, 1999)

Cone crushing is a method that uses an eccentric rotating cone to trap and crush materials against the inner walls of the crusher. The small size crushed materials are collected at the bottom of the crusher.

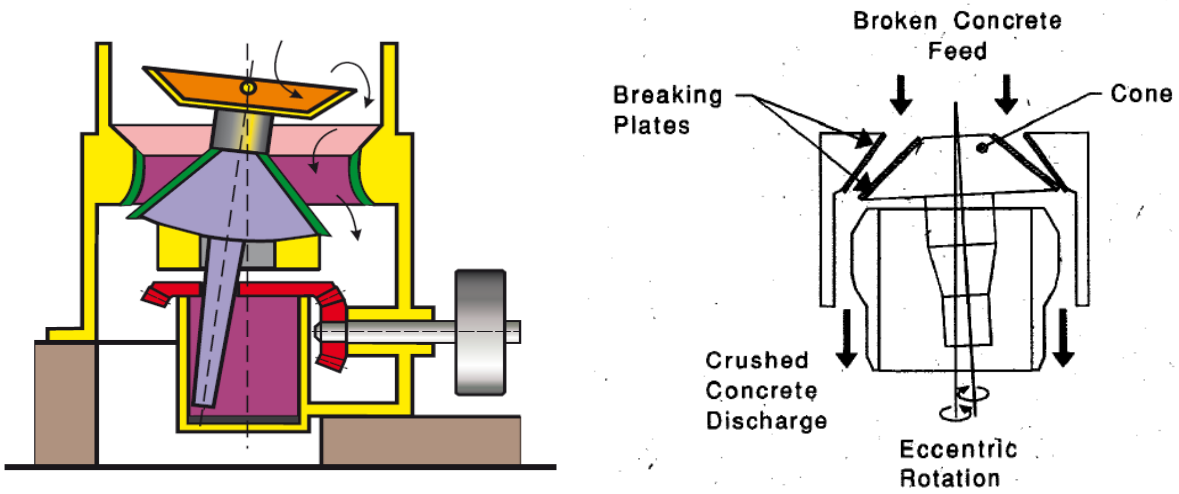

Figure 2- 13: Cone Crusher (Metso Minerals Handbook, 2007; Environmental Council of Concrete Organizations, 1999)

Impact crushers are type of crushers that break materials by impacting the material on the break plates mounted inside the crusher.

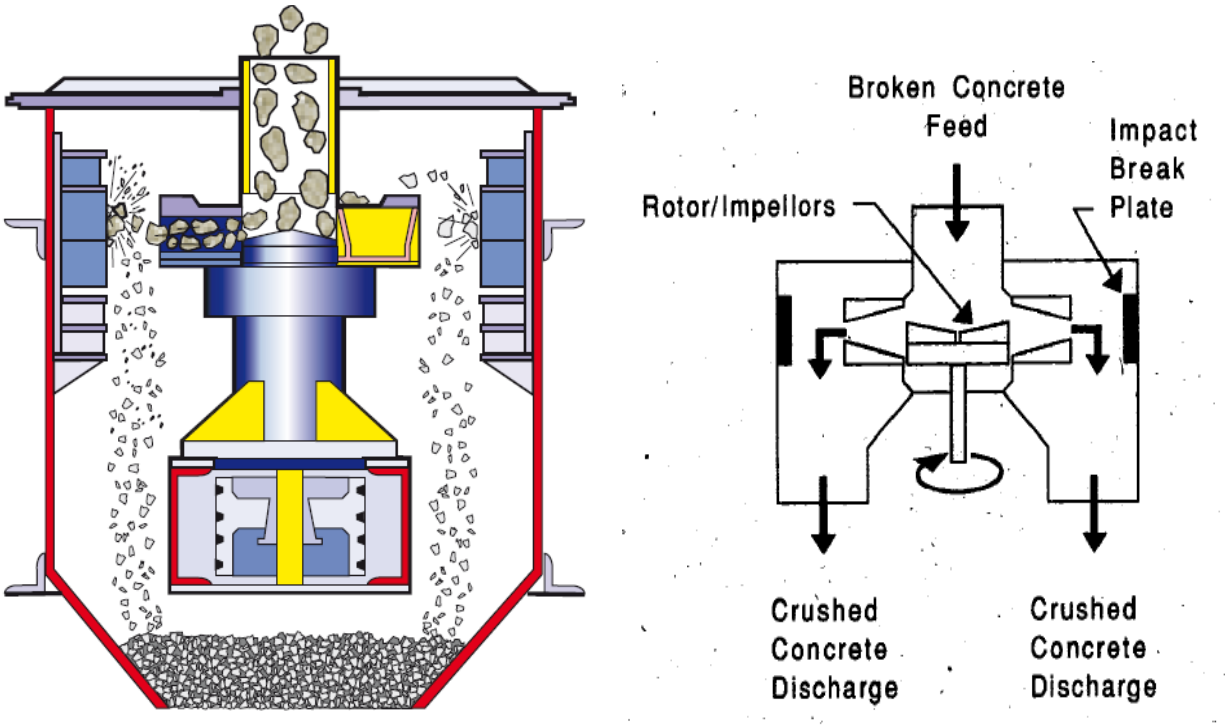

Figure 2- 14 : Impact crusher (Metso Minerals Handbook, 2007; Environmental Council of Concrete Organizations, 1999)

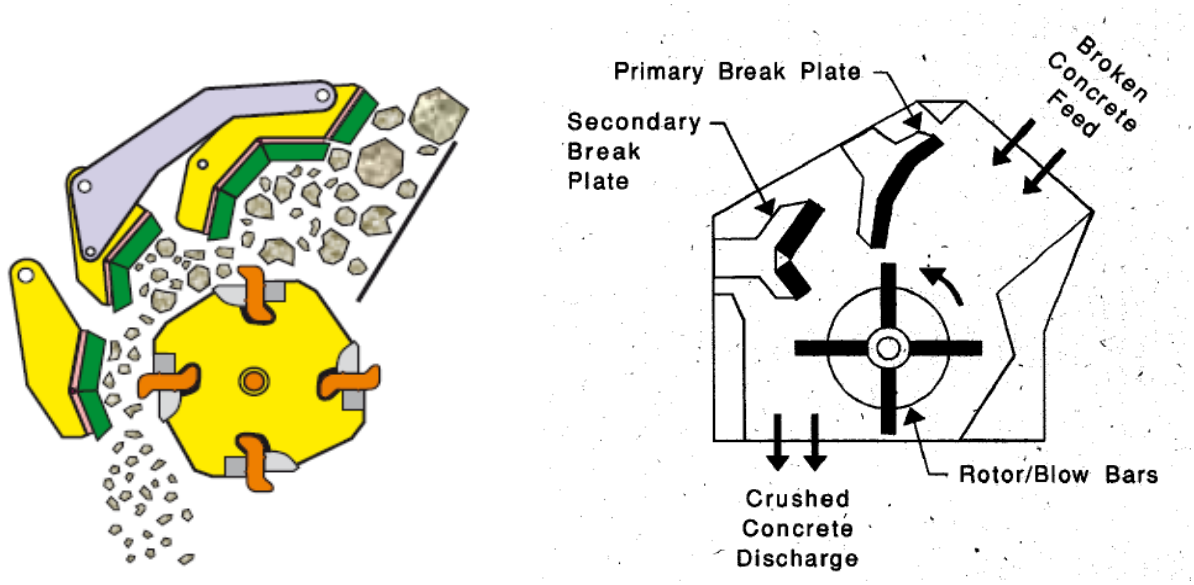

Figure 2- 15: Impact crusher (Metso Minerals Handbook, 2007; Environmental Council of Concrete Organizations, 1999)

The physical characteristics have a significant influence on material performance and durability as discussed in previous sections of this study. Several studies have been carried out on the

influence of crusher type and crushing stages on aggregates physical characteristics such as shape and gradation. In these investigations, it was observed that the process of double crushing is beneficial due to second stage producing rounder and less sharp particles, and generates fines.

Van Niekerk (2002) has found that the jaw crusher produces more flat particles than that of the impact crusher. However, Barksdale (1991) indicated that although the impact crusher produces more cubical particles than that of the compression crusher, the most important factor deciding the shape of the crushed particles is the *reduction ratio* rather than crusher type. The reduction ratio is "the ratio of the size of the piece of rock from which it was broken to the size of the given particles" (Shergold, 1959 cited in Barksdale, 1991). In other words, the size of the material fed to the crusher and the crusher setting according to the desired size of the discharge influences the shape of the produced aggregates.

Hansen (1992) studied the influence of crusher type on the obtained grading. He observed that the impact crusher produced a better grading than of the jaw crusher because the latter generates a coarser grading with fewer fines. However, Barksdale (1991) argued that the jaw crusher could also generate a good grading with sufficient fines if it operates at a low "reduction ratio".

It can be deduced that despite the type of crusher, a good material grading with cubical particles can be obtained by secondary crushing. Therefore, it is advisable to apply at least two stages of crushing in order to reduce flakier particles and generate fines.

2.2.5 Impact of construction and in service traffic characteristics on aggregates properties

The loading caused by construction vehicles and machines as in-service pavement usage has a major influence on the aggregates durability and performance behaviour. When aggregates are exposed to traffic, they are subjected to wear and tear, and degradation resulting in crushing of the aggregates.

The aggregate wearing is its polishing due to rubbing or abrasion and friction produced by external forces such as wheel loads. This phenomenon is a result of construction vehicles and machines when the pavement layer is still under construction or traffic loading during in service life for pavement surface layer. The polished or abraded materials are brushed away and they are no longer contributing to the pavement system (Barksdale, 1991). Since the rate of polishing

primarily depends on the strength of the aggregate, the RCM aggregates are highly susceptible to polishing compared to that of natural aggregates.

The external forces resulting from compaction or heavy wheel loads on the other hand, cause the breakdown of the aggregates into small pieces and the phenomenon is called degradation. It consists of deflection and rebound of pavement layers system when subjected to dynamic loading, which is also transmitted to the aggregate particles in the system. When this movement is pronounced, the edges of the aggregate can be crushed and this results in general degradation of the aggregates. The crushed particles that emanate from aggregates degradation remain and contribute to the performance of the pavement system and this makes the difference with the particles resulted from polishing that are brushed aside (Barksdale, 1991).

The degradation of aggregates results in the modification of the original grading. This when pronounced, it decreases the density of the layer and therefore results into consolidation thus rutting in unbound pavement layers. Rutting is more detrimental to pavement performance when it occurs during pavement service life. Achieving a denser packing is very important during compaction of RCM in order to prevent high deformation caused by crushing during the service life. Therefore, it is important to adjust the compaction method so that the particle crushing happens during construction and not during the pavement service life (Leite *et al*., 2011).

The wearing and the degradation are more severe when heavy steel tyred vehicles i.e steel drum compactors or heavily loaded axles move over the aggregates. The crushing is also caused by the impact due to the jumping of steel tyred compactor machines from one particle to another. Consequently, Aurstad & Uthus (2000) argued that it is not preferable to use heavy compaction machines since RCM aggregates are weaker and porous and thus susceptible to crushing. They also advised to compact at higher moisture content in order to minimise the risk for crushing.

Furthermore, it is of great importance to know the final application of RCM materials in different pavement layers for various road types. This provides information on whether these materials will be exposed to intense traffic stresses or to less intense stresses. Leek (2008) during the construction of a trial road section in Western Australia using recycled constituents as base material has found that the recycled materials can be safely used as base for low volume roads or high volume roads with minor truck traffic. RCM materials can also be successfully applied in the subbase of heavily trafficked roads but care should be taken when considered for base

layers in heavily trafficked applications. This low performance of RCM materials in the above mentioned pavement layers may be due to the Australian pavement structure where the surfacing is composed of a thin layer compared to thick surfacing layers used in European countries.

2.2.6 Influence of climate

The environment in which the pavement is exposed influences the performance of the materials. Weinert (1980) indicated that the rate of weathering, in particular decomposition (chemical weathering) is highly influenced by the climate to which the materials are exposed. However, the environment is a parameter that has to be accepted as it is, therefore the design and the construction shall be adapted to it.

The literature highlights the impact of climate on the quality of road building materials and performance in pavement. Weinert (1980) argued that the climate impact is more pronounced in large countries such as South Africa where there is great climate variation. This climate impact is manifested in different durability behavioural aspects observed in the weathered basic igneous materials that were used in base layer and other layers in pavement in different parts of South Africa. For example, severe low performance was observed for dolerite by which the road only lasted few years and in some case only months. When these failed materials were compared with the materials from the same borrow pit, they showed severe deterioration in quality and condition (Clauss, 1967 cited in Weinert 1980). Furthermore, the moisture movement and its corresponding influence in pavement layers has been studied and mentioned by Emery (1992) and (Jenkins, 2013).

Figure 2-16 and Figure 2-17 indicate how the moisture movement in pavement layers is not a simple phenomenon and indicates the paramount role of good drainage, road geometry and the pavement structure in order to deal with this problem.

Weinert (1980) has investigated the influence of climate on the performance of weathered basic igneous rock but in a different approach than with the previous research studies (Lang rain factor, Martonne's Aridity index). These later climatic indices were based on the annual rainfall but the Weinert climatic index is based on the seasonal variation of rainfall, i.e rainfall during warm or cold season or throughout the year, in combination with the potential evaporation.

Weinert (1980) extended his investigation to include the warmest month (January) and coldest month (July) in the Cape Peninsula region. The month of January, is dry in winter rainfall areas

and consequently high evaporation (E_j) and low precipitation (P_j) while the month of July is the coldest month and consequently the evaporation is low with high precipitation. He found the investigation based on January (winter rainfall areas) to agree satisfactorily with the performance and weathering boundary in summer rainfall areas.

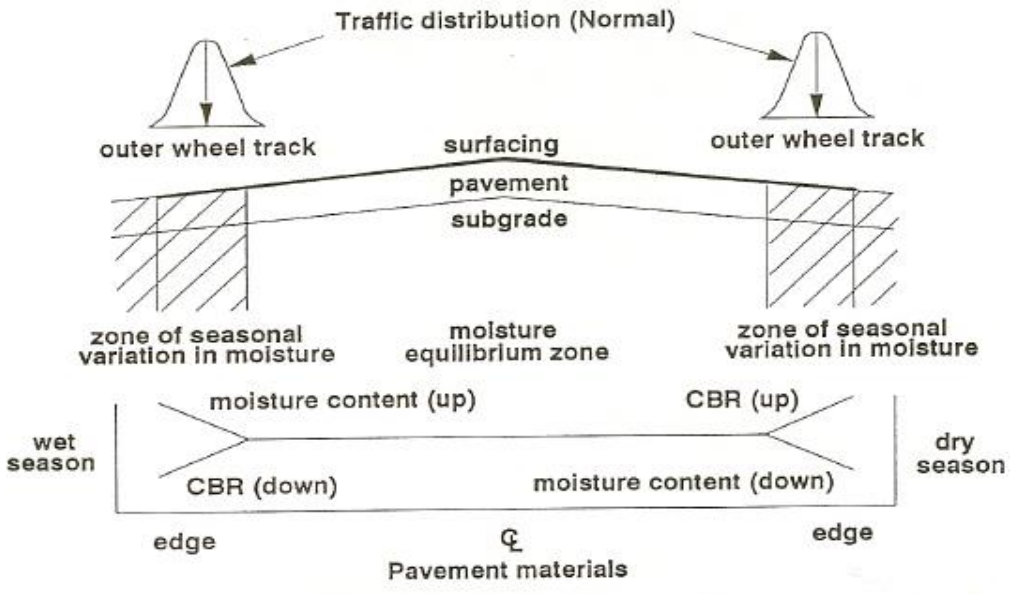

Figure 2- 16: Moisture Variation and Impact on the Material (Emery, 1992 cited in TRH4)

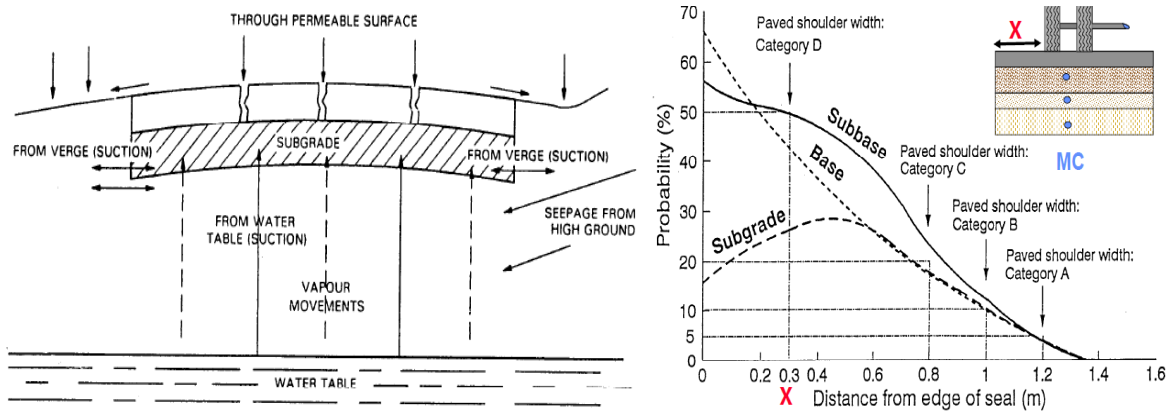

Figure 2- 17: Moisture Movement in Pavement Layers (Jenkins, 2013)

However, not only moisture has been found to have an impact on the weathering of the material, but also temperature influence on the rate of chemical degradation. Glasstone (1956) indicates that the water reactivity increases with temperature. He found in South Africa that an increase in 10^0C usually doubles the speed of chemical reaction.

Weinert (1980) has developed a climatic index namely *N-value* which is an expression of 12 times the computed evaporation of the warmest month, mostly January in South Africa, divided by the total annual rainfall. This N-value index can be used to describe the different climatic environments in which rock weathering might exhibit different performance in roads.

$$N = \frac{12Ej}{Pa} \qquad \text{(Equation 6)}$$

Where P_a is the total annual rainfall and Ej, the evaporation during the month of January.

The climatic indices N equal to 1; 2; 5 and; 10, are important for road engineering.

However, due to the wide area covered by Weinert regions (Figure 2-18) compared to Thornthwaite's (Figure 2-19) in climate classifications, Paige-Green (2010b) indicated that Thornthwaite's Moisture Index realistically covers the climatic condition in South Africa.

Thornthwaite (1948) observed that climatic elements were dictated by meteorological observations such as precipitation, pressure, humidity and wind velocity. However, he argued that among meteorological observations, one important aspect that was missing is the evaporation from the soil combined with the transpiration from plants. He concluded that the most important factors for climate are the precipitation and the evapotranspiration. He identified that potential evapotranspiration is more realistic than actual evapotranspiration since the earlier represents the evapotranspiration that will take place in ideal conditions of soil and vegetation. However, he indicated that the measurement of this climatic factor is difficult. Therefore, he used Indices of Humidity (I_h) and Aridity (I_d) to describe the evapotranspiration in terms of water surplus or deficit.

The Thornthwaite's Climatic Index is calculated as follow:

$$PE = 16\, N_m \left(\frac{10\,\overline{Tm}}{I}\right)^a \qquad \text{(Equation 7)}$$

Where m is the months 1,2,….12 and N is the monthly adjustment factor related to daylight hours, T_m is the monthly mean temperature(^{0}C), and I is the heat index for the year. I is given by : $I = \Sigma i_m = \Sigma\left(\frac{\overline{Tm}}{5}\right)^{1.5}$

Then climatic index is given by: $I_m = \frac{(100s - 60d)}{PE}$ (Equation 8)

Where, *s* is the maximum moisture surplus, *d* is the moisture deficit, and PET is the potential evapotranspiration.

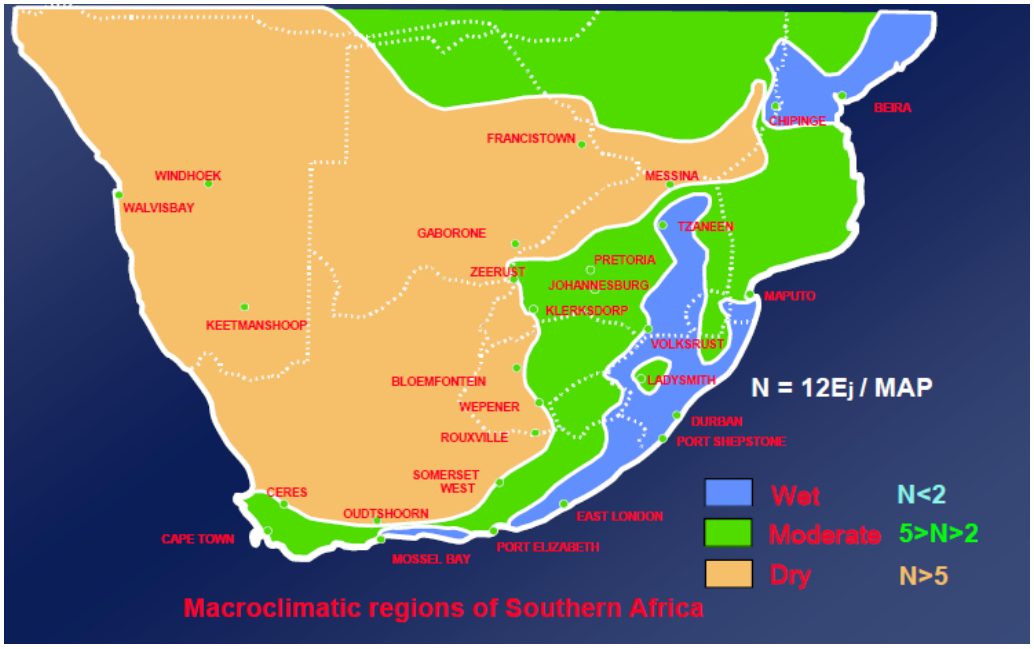

Figure 2- 18: Modified Climatic Regions of Southern Africa by Weinert (Jenkins, 2010)

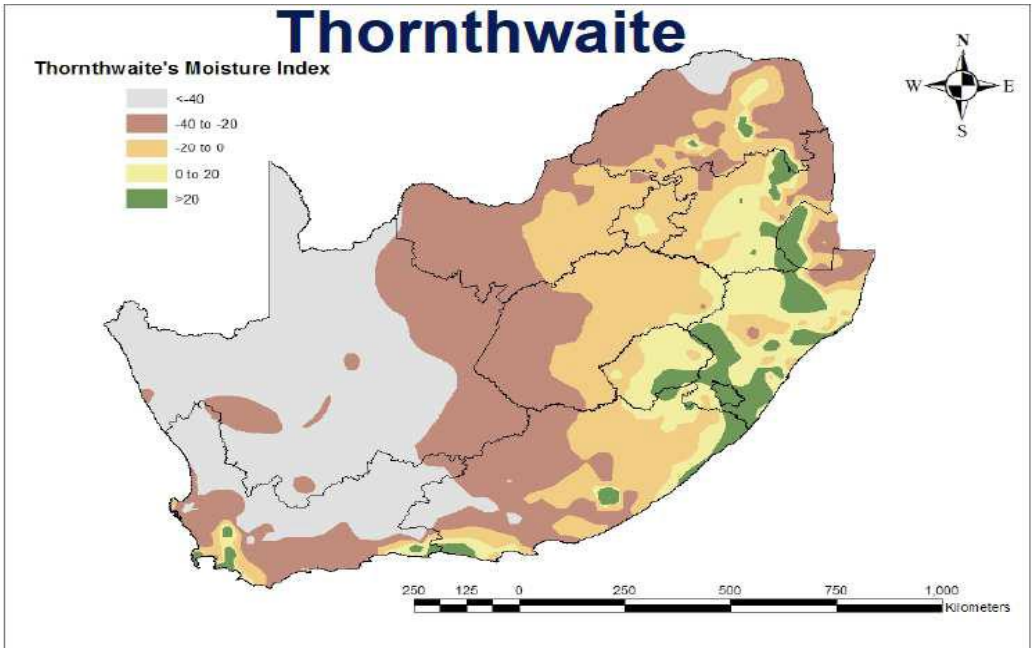

Figure 2- 19: Climatic Regions of South Africa by Thornthwaite (Paige-Green, 2010b)

Table 2- 3: Thornthwaite Moisture Index Interpretation (Paige-Green, 2010b)

Index range	Climatic region	
< -40	Arid	Dry
-40 to -20	Semi-arid	
-20 to 0	Dry sub-humid	Moderate
0 to 20	Moist sub-humid	
>20	humid	Wet

These various climate indices have been used by Emery (1988) to characterise the moisture content in untreated pavement layers in Southern Africa. He established the ratio of the pavement Equilibrium Moisture Content to the AASTHO Optimum Moisture Content (EMC/OMC_m) for different climatic regions of South Africa.

Table 2- 4: Equilibrium to Optimum Moisture Content ratios in Pavement Layers (Emery, 1988)

Climatic area	Base (EMC/OMC_m)			Subbase (EMC/OMC_m)			Subgrade (EMC/OMC_m)		
	Mean	s.d	n	Mean	s.d	n	Mean	s.d	n
Arid	0.53	0.24	26	0.70	0.26	19	0.71	0.34	131
Cape (Winter rain)	0.63	0.16	16	0.78	0.28	17	0.75	0.45	81
Transvaal(I_m<o)	-	-	-	-	-	-	0.94	0.29	894
Cape(all year rain)	0.57	0.17	19	0.83	0.28	20	0.98	0.31	98
Transvaal (I_m)>=0)	-	-	-	-	-	-	0.96	0.29	178
Natal (I_m>0)	-	-	-	-	-	-	1.05	0.34	52
Weighted mean	0.58	-		0.75			0.92		

2.2.7 Material characterisation testing

2.2.6.1 Introduction

The characterisation testing of aggregates consists of the assessment of the physical properties and mechanical characteristics of particles. The results from this characterisation testing provide a trend in the material mechanical performance in pavement layers.

The choice of appropriate tests is a key parameter in successful evaluation of material performance. Dependent on the material type; some tests can manifest severe results that are not comparable to the real situation or even not applicable at all. This can cause a misinterpretation of results, which sometimes leads to rejection of materials while they can perform well in a pavement.

This section presents various tests that can be used to characterise recycled concrete and masonry properties and mechanical performance.

2.2.6.2 Conventional characterisation tests

2.2.6.2.1 Physical tests

Physical characteristics of the aggregates are evaluated through various tests. The flakiness index test is used to assess the amount of flakier particles in an aggregates sample. This is a prime indication of the resistance of the aggregates to crushing and the probable material performance. Aggregates specific gravity and water absorption tests characterise the aggregate relative and bulk densities. These tests provide information on the strength and porosity of the aggregate. In addition, the sieve analysis test has the main objective of assessing the particle size distribution in the material. The particle size distribution obtained during sieve analysis test provides information on the skeleton of the material. The skeleton of the material is used to explain various material mechanical properties and performance such as achievable density, shear strength and deformation.

2.2.6.2.2 Mechanical tests

Material moisture-density test

The aim of the proctor test is to evaluate the relationship between the density and the change of moisture content during compaction using a standard compaction method. There is a clear relationship between density and material performance.

The Modified AASHTO compaction test consists of compacting material into five layers in 152mm x152mm cylindrical mould with 127 mm effective. Each layer receives 55 blows by a 4.536 kg hammer dropping at a height of 457.2 mm.

Aggregate crushing test/ 10% fines aggregates crushing test

The aggregate crushing test is a test that provides the percentage known as the *Aggregate Crushing Value* (ACV). This crushing test simply yields the percentage of fines passing the 2.36 mm sieve during crushing process after applying a gradually increased force up to 400kN over 10 minutes. It is carried out on a material sample of passing the 13.2 mm and retained to the 9.5 mm sieves. However this test was amended by Shergold & Hosking (1959) to determine at which force 10% fines passing 2.36mm sieve is produced and the test was named 10% Fines Aggregate Crushing Test (10% FACT). This allows varying the applied load while the

percentage of fine remains constant. Nevertheless, these two tests use the same apparatus (Figure 2-20) and sample preparation.

During the 10% FACT, the variation of the load depends on the condition of the sample to produce 10% fines passing the 2.36 mm sieve and the required force is measured and used for interpretation. The 10% FACT is always done for both air-dried sample and a 24 hours water soaked sample. This provides information on the degree of disintegration and especially the resistance of the material to construction operation particularly rolling.

Figure 2- 20: Crushing tests apparatus

2.3 MATERIAL MIX COMPOSITION PROPERTIES AND MECHANICAL PERFORMANCE

2.3.1 Introduction

The performance behaviour of recycled materials has a significant effect on the pavement life in which they are used. The aggregate particles must be durable in order to resist different types of stresses applied to them. In addition, the mix composition properties must be well designed for stability in order to enhance good performance to the entire material system. The mix composition should be analysed regarding all parameters and factors such as composition, workability during mixing and laying down, compaction, traffic loading, curing, and moisture susceptibility that affect it on the full phase of application.

However, it is not easy to separate the aggregates characteristics from mixture properties and performance because the aggregate characteristics affect the material mixture properties such as density and workability. They affect also the material performance such as the failure and deformation response as it is presented in Figure 2-21.

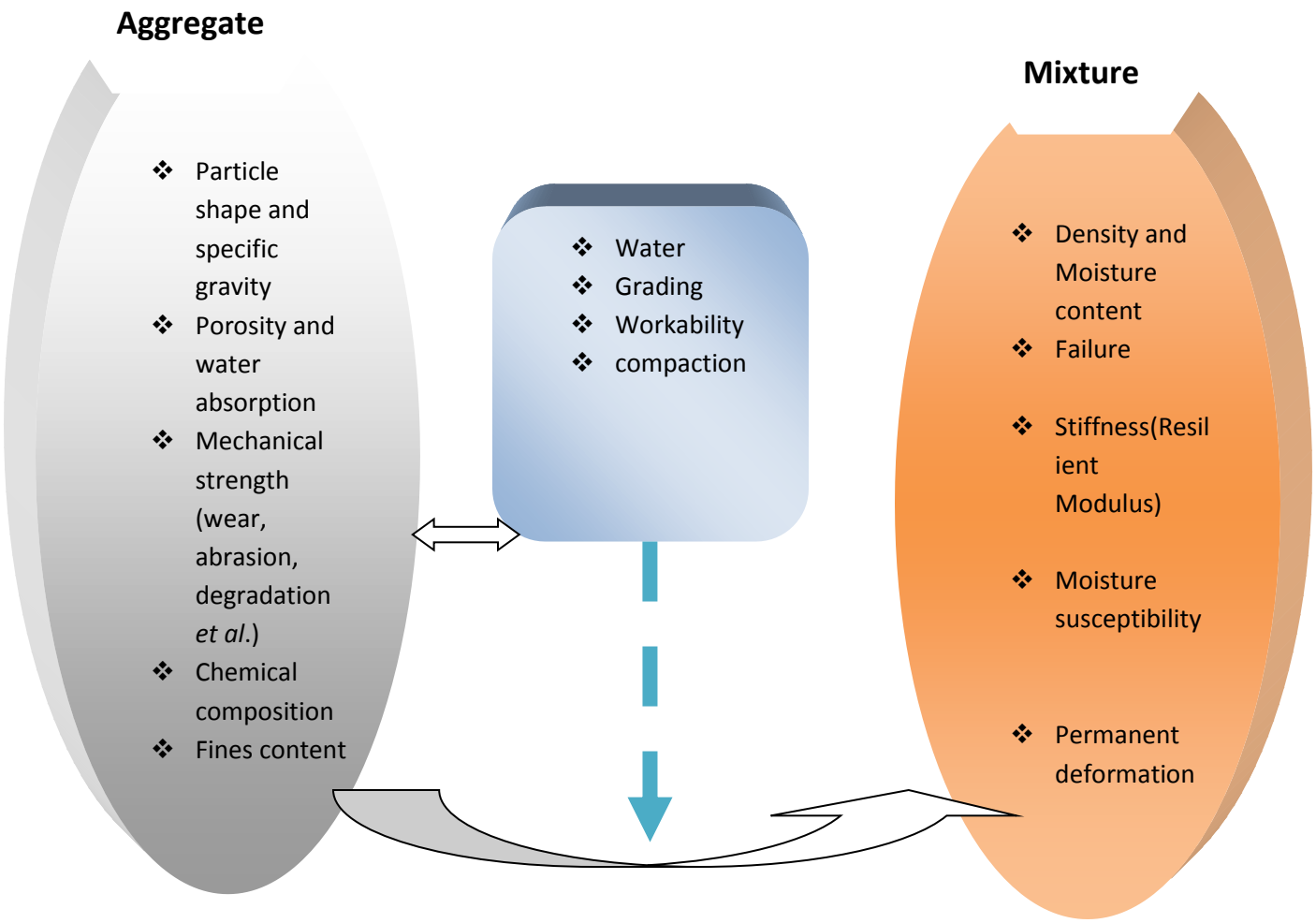

Figure 2- 21: Interaction of Parameters on the Performance Response of RCM

This section discusses the mix composition properties, loading characteristics, and their relation to the mechanical performance of RCM materials.

2.3.2 Effect of composition on the mix composition mechanical performance

The composition of RCM relates to the proportion of concrete aggregates content to masonry aggregates. The impact of composition on RCM mix composition performance is mainly governed by the physicochemical and mechanical characteristics of aggregate particles. Section

2.2.2 of this study indicates various aggregates characteristics depending on whether they are from recycled concrete or masonry. It indicates also that recycled concrete aggregates are characterised by cubical and denser aggregates, less water absorption, higher resistance to wear and degradation in comparison with recycled masonry aggregates. These aggregate properties influence the achievable mixture density, the resilient response and the resistance to permanent deformation. Moreover, the self-cementing characteristic of RCM has an influence on the performance response.

Several studies have been carried out to assess the impact of composition on the performance and durability of recycled materials; Poon & Chan (2005) noted high achievable densities for mix composition containing higher concrete aggregates compared to masonry aggregates. However, mix composition with fines from masonry exhibited less moisture susceptibility. Nataatmadja & Tan (2001) found higher degradation under repeated loading for recycled materials containing traces of bricks compared to other recycled materials containing only concrete.

Van Nierkerk (2002) reported that composition affects the mechanical performance such as resilient modulus and Poisson Ratio. Material containing higher percentage of recycled concrete than masonry exhibited high resilient modulus and low Poisson Ratio. He indicated that the bonds developed in the material containing high concrete enhance the resilient modulus and reduce the Poisson Ratio. The author argued that when the material is tested in “mild” stress regime where there is low risk of bond breakage, the friction between particles is mobilised hence the strength and the stiffness increase. The bonds also take up to an extent, the tensile stress generated during particle rearrangement that can develop in the material and pull apart particles causing material resilient dilation behaviour. This dilation results in a high material Poisson Ratio.

During the assessment of the resilient modulus and the permanent deformation behaviour of Recycled Construction and Demolition Waste (RCDW), Leite *et al.* (2010) have observed an increase in resilient modulus and reduction in permanent deformation according to the increase of the concrete content in the mix composition and the increase of the compaction effort. They concluded that composition and the degree of compaction are the predominant factors for the performance of RCDW.

The current findings by Azam & Cameron (2013) has shown that increasing the recycled masonry content in the mix by 20% decreased 7 to 33% to the resilient modulus and increased 57 to 83% to the permanent strains depending on the type of recycled concrete.

The ratio of recycled concrete to recycled masonry however does not have a significant effect on the mechanical performance compared to cement content when these materials are stabilised with cement (Wilson, 2007; Xuan *et al*., 2011).

2.3.3 Influence of workability on the RCM performance behaviour

The workability of the material is defined as "the timescale between the mixing of component and need for final compaction, or any specific laying/curing requirements, such as minimum temperature" (Wilson, 2007). The definition of the workability clearly indicates how it affects the compaction effectiveness, which leads to denser mix composition that characterises good pavement material.

The workability depends on the material physical characteristics, which in return influences the amount of water to be added during compaction. Arulrajah *et al.* (2011) indicated that the less elongated aggregates in a material the more workable it is during compaction. Furthermore, the material that has a packing with little or no fines was found to be very difficult to handle during construction due to its non-cohesive nature (Yoder and Witczak, 1975 cited in Siswosoebrotho *et al*., 2005). Xuan *et al.* (2011) indicated that the mix composition with higher recycled masonry content, which is characterised by elongated aggregates, is less workable during compaction. In light of this behaviour, they recommended to add more water in order to improve its workability.

2.3.4 Role of compaction on mix composition mechanical performance

The compaction can be defined as the densification of the material by the reduction of voids that diminishes the compressibility, enhance the rigidity and thus improves the strength of the soil (Rodriguez del Castillo & Sowers, 1988). According to this definition, the compaction has a significant importance on the performance of the material in the pavement layers because it improves the material engineering properties and provides structural stability to the pavement layers. Poorly compacted material results in a less dense, and permeable pavement layers with substandard mechanical performance and high moisture susceptibility.

The material at initial stage during mixing is in a conglomerate state, the compaction has the benefit of squeezing air out from aggregates, and reduces the voids. This increases the number

of particle contact and therefore enhances the packing of the aggregates skeleton, which increases the strength of the material. Since compaction strengthen the material and stronger material exhibits higher performance during service life, therefore compaction is a key parameter for ensuring material good mechanical performance.

The degree of densification however, has a direct relationship with the grading of the mix composition as discussed in Section 2.2.2.1.1 of this study. It is indicated that a well graded material produces a denser mix composition than an uniform graded material because the voids between the coarser particles are filled with fine particles. In contrast, when the material has a higher fine content, it can be detrimental to its performance because there will be less or no contact of coarse particles in order to build strong aggregate skeleton. Consequently, the loading carried by the fine fractions will increase. Not only the amount of fines has an influence on the achieved degree of compaction, but also the quality plays a major role on the obtained material densities and stiffness. This is because when the material has higher actives (plastic) fines, they will increase the moisture demand and this reduces the achievable density. On the other hand, when denser material contains the fines from an active cementing agent, this can contribute to enhance the material stiffness as mentioned in Section 2.2.2.1.2 of this study.

Compaction energy in isolation does not influence the mechanical performance of the material, but additionally the compaction moisture also influences the material bearing capacity. Kelfkens (2008) indicated that the moisture has a significant impact on the quality and the level of compaction because it has the role of a lubricant to allow the particles to slide past each other in order to achieve the desired density. He indicated that when little moisture is available, less lubrication is provided and hence yields inadequate compaction. On the other hand, when too much water is used during compaction, the water-filled voids are left in the material after compaction and this reduces the bearing capacity of the compacted material.

Leite *et al.* (2010) during the assessment of the resilient modulus and permanent deformation of material samples have found an increase in resilient modulus and a decrease in permanent deformation when the material sample is compacted with modified proctor compaction effort (higher compaction) compared to intermediate proctor compaction.

Van Niekerk (2002) observed an increase by 50% to 150% for the cohesion and the friction angle from 39^0 to 46^0 as the degree of compaction increased from 97% to 105%. The increase of the composition from 50/50 to 80/20 relative ratio of concrete to masonry has increased the cohesion by approximately 35% for the specimen tested after four days. He has also obtained

higher friction angle and moderate cohesion for balanced grading or a well graded grading than coarser or finer grading. He also assessed the impact of the above-mentioned composition, degree of compaction and grading on the resilient modulus and permanent deformation. He found that the resilient modulus increased as the degree of compaction, and the concrete content increased. In contrast to the shear parameters, the resilient modulus results showed that a fine grading mix composition exhibited higher values than a balanced grading followed by the coarse grading. Furthermore, for the permanent deformation, he observed a decrease in permanent deformation as the degree of compaction increased from 97% to 105%. A noticeable impact of grading on the permanent deformation was also observed. The balanced grading performed better than the other mentioned grading. In addition, composition also showed an effect on the permanent deformation but its influence was less than the other factors previously mentioned. Therefore, according to his findings he concluded that compaction had the major impact on the mechanical performance more than material composition, curing. However, it should be considered that compaction is the cheapest option and easier to control.

However, Xuan *et al.* (2011) have argued that albeit compaction is the cheapest technique to increase the material strength, it is not efficient to enhance elastic strain and improve flexural rigidity. The authors argued that as the aggregate affect the skeleton deformation and the recycled concrete aggregates exhibit high elastic modulus than that of recycled masonry aggregates; therefore, the composition affects the deformation characteristics.

The impact of compaction level or the degree of compaction on the Poisson Ratio presents uncertainty and disagreement in various studies. As reported by Lekarp *et al*. (2000) some studies indicated a small influence and inconsistency variation of Poisson Ratio with the increase in density and others reported a slight decrease as the density increases.

2.3.5 Influence of curing

The curing process allows for the homogenising of water in the materials and to dry back from the compaction moisture. This is an important factor for the strength gain, and subsequently for good material performance in a pavement. The literature indicates that the premature failure of material is caused by early traffic before sufficient strength gain has been achieved. Theyse (2007) indicated that granular materials should be allowed to dry back from compaction moisture before constructing a new layer above it. He pointed out that a minimum of 50% of saturation will optimise the performance of these materials. However, laboratory curing should simulate the field conditions and its practicality should be well assessed.

RCM material or other materials containing residual cement could lead to the probable development of bonding due to hydration of residual cement when allowed to cure under favourable conditions and for sufficient time. Sufficient moisture in the material, the availability of residual cement and time allow the pozzolanic reactions to develop, which produce a cement gel that crystallises in the matrix of the aggregate and thus leading to an increase in the material stiffness. Wilson (2007) indicated that the rate of strength gain and the performance of the hydraulically bound materials are highly dependent on time, curing conditions, and composition. Moreover, to assess the influence of self-cementing of RCM material on mechanical performance of recycled materials, Molenaar & van Niekerk(2002) have cured specimens for intervals of time of 4, 14, 28, and 90 days respectively. The influence of self-cementing was well observed from 14 days upwards. However, they indicated that the European specification for triaxial testing of unbound base material specifies 4 to 7 days curing. It is believed that the bonds for these materials start to develop after 4 days.

Unfortunately, many uncertainties exist on the bond development or strength gain for hydraulically bound material ranging from pavement where no increase in stiffness could be identified to pavements with significant increase in stiffness (Van Niekerk, 2002).

2.3.6 Mechanical performance behaviour

During the service life of a pavement, an element of the pavement structure is subjected to the loading pulses of the moving wheel and these pulses consist of vertical, horizontal, and shear stresses. As illustrated in Figure 2-22, for unbound layers, as the load passes, it creates horizontal and vertical positive stresses and the double shear stress. The latter causes a rotation of the principle stress axes. The resulted response to the applied load, which is the deformation, is characterised by a recoverable (resilient) deformation and a residual (permanent) deformation (Lekarp *et al*., 2000). However, these stresses are pronounced when unbound granular materials are under a thin surfacing or in direct contact with loading such as during construction. This deformation characteristic is presented in Figure 2-23.

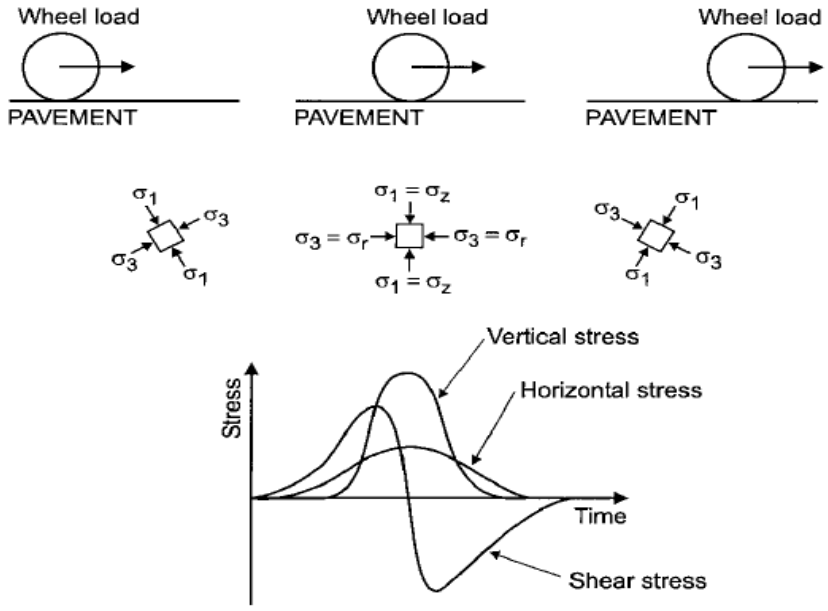

Figure 2- 22: Stresses under a Moving Wheel Load (Lekarp *et al*., 2000)

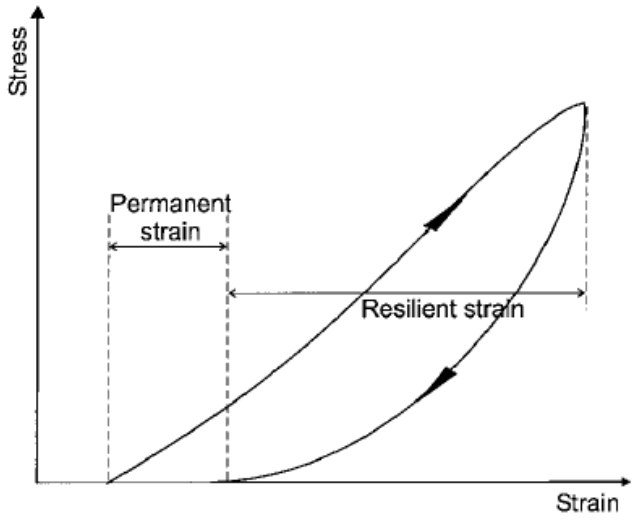

Figure 2- 23: Stress- Strain Behaviour in Granular Materials for One Load Cycle (Lekarp *et al*., 2000)

When shear stresses are experienced in granular material particles, they initially develop a resistance to volume change, followed by sliding of particles against each other. For dense material this sliding is followed by roll up and over of particles to each other and that leads to an increase of volume in the whole particles system. On the other hand, loose material particles experience a roll down leading to a decrease in volume. This volume change is known as dilatancy. The increase in stresses at high degree finally causes the crushing of particles. The

crushed small particles produce a rearrangement of the assembly that increases the frictional resistance. The rearrangement of particles increases the density of the material because the produced small particles fill the voids between the large particles, which in return increases the particle interlock (Noava- Martinez, 2003).

The deformation of granular layer in other words, results into three main mechanisms namely consolidation, distortion and attrition. The consolidation (dilation) is defined as the change in particle shape and compressibility. Distortion is a mechanism characterised by particles bending, and rolling whereas attrition is a mechanism of particles crushing and breakdown due to the applied wheel load (Lekarp *et al*., 2000). These authors indicated that the combination of these three mechanisms, on macroscopic level, produce deformation that may be volumetric, shear, or simply a combination of two. They reported that it is not easy to separate induced shear strain due to the distortional movement of particles, and volumetric strain caused by consolidation and attrition. This is because the shear strain is usually associated with volumetric strain for granular material.

In order to understand the performance behaviour of RCM material, it is important to assess its failure and deformation characteristics. This study focuses on the shear strength and the resilient response.

2.3.6.1 Shear strength

The shear strength is a mechanical property of the material and is expressed in terms of shear properties (C, ϕ). These properties are used to characterise numerous materials for design and performance analysis. They are tested using various methods such as direct shear or triaxial monotonic test. In pavement engineering however, triaxial monotonic test is usually used to assess the shear strength of granular materials. Different theories describe the shear strength of material, but the Mohr-Coulomb theory is commonly used to portray approximately the shear strength of granular material. As presented in Figure 2-24, this theory results in a well-known Mohr-Coulomb circle corresponding to the state of stress in the specimen. The maximum shear is plotted against the average of the major normal principal stress to the minor normal principal stress. The Mohr-Coulomb failure envelope is the tangent line to the circles and this is an approximate shear failure behaviour of granular materials.

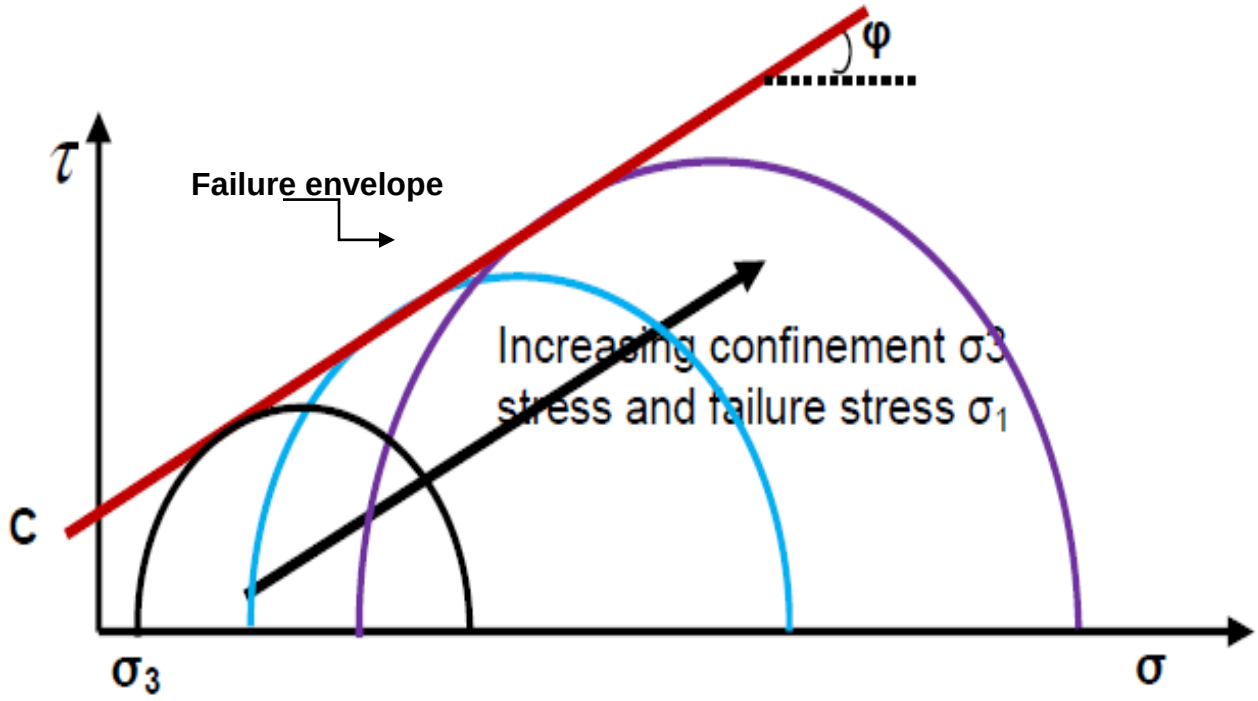

Figure 2- 24: Mohr-Coulomb Failure Envelope (Twagira, 2010)

2.3.6.2 Resilient response

The resilient behaviour of unbound materials is also a key parameter in the analysis and the design of the pavement. Resilient modulus is defined as a material mechanical property that indicates its stress –strain behaviour under dynamic loading and specific physical conditions (Khogali & Zeghal, 2000).

The resilient modulus of the material is affected by several factors such as stress , the density, aggregates physical properties (shape, grading, fines etc.), moisture content, stress history, number of load cycles, composition(aggregate types), loading duration, frequency, and load sequence. Lekarp *et al.* (2000) during an extensive literature research on the resilient response behaviour of unbound aggregates found that the most important factor on the resilient modulus is the stress level. Some of these factors for instance, have been mentioned in the previous sections of this study.

The impact of stress history however, can be almost eliminated when the specimen is conditioned at 1000 load repetitions before resilient test (Allen, 1974). Moreover, Houston *et al.* (1993) argued that among the objectives of specimen preconditioning during triaxial testing is to eliminate the non-recoverable (plastic) strains that are prone to occur so that the measured strains can be elastic strains. The European Standard EN 13286-7 also stipulates that the

importance of specimen conditioning prior to testing is to prevent the permanent deformation that may rise during the first load cycles of the testing and to eliminate the influence of the number of the load cycles on the measured resilient modulus. It is assumed that testing the specimen in its elastic zone; the resilient modulus is not affected by the stress history of the material.

2.3.6.2.1 Modelling of Mechanical behaviour

Shear failure behaviour

The pavement granular materials fail predominantly due to shear stresses as discussed in Section 2.3.6.1 .The shear stress that these materials can withstand depends on the magnitude of the applied normal stress at failure (σ_{Nf}). This stress dependency is modelled by the linear failure model developed by Mohr and Coulomb and named Mohr-Coulomb failure condition model.

$$\tau_f = C + \sigma_{Nf}.\tan\phi \qquad \text{(Equation 9)}$$

Where:

τ_f= shear stress at failure

C= cohesion

σ_{Nf}.= normal stress at failure

ϕ= angle of internal friction

This model can also be expressed in principal stresses as follows:

$$\sigma_{1,f} = \frac{(1+\sin\phi)\sigma_{3,f} + 2C\cos\phi}{(1-\sin\phi)} \qquad \text{(Equation 10)}$$

In which:

$\sigma_{1,f}$.= major principal stress at failure

$\sigma_{3,f}$.= minor principal stress at failure

The linear Mohr-Coulomb linear model expressed in principal stress can then be represented as follow:

$: \sigma_{1,f} = A.\sigma_3 + B$ (Equation 11)

Where:

$A = \frac{1+sin\phi}{1-sin\phi}$ and (Equation 12)

$B = 2C\frac{Cos\phi}{1-sin\phi}$ (Equation 13)

The graphical representation is given in Figure 2-24.

Resilient response

There have been several studies aimed at predicting the resilient behaviour of granular materials through the development of mathematical models. Computational modelling uses two approaches to describe the resilient response of granular materials. The first approach where the stress-strain behaviour is characterised by stress dependent resilient modulus and Poisson Ratio, and the second approach is the shear- volumetric approach that decomposes the stresses and strains behaviour into volumetric and shear components. In the latter approach, bulk and shear moduli replace the resilient modulus and Poisson Ratio (Lekarp *et al., 2000*). These models aim to develop an understanding of the stress dependence of the resilient modulus and Poisson Ratio according to the laboratory testing. The most common models that are based on the first approach are briefly introduced below:

σ_3 Model

Dunlap (1963) and Monismith *et al*. (1967) developed this model and the model postulates that the resilient modulus is a function of the confining stress (Lekarp *et al.*, 2000).

$M_r = k_1\sigma_3^{k2}$ (Equation 14)

Where M_r is the resilient modulus, σ_3 is the confining pressure, and k_1 and k_2 are experimental coefficients.

However, this model does not predict the resilient modulus of granular layer accurately since it does not take into consideration the deviator stresses that granular layer endures (Garg *et al.*, 2000).

K-Θ Model

This model aimed at improving the drawback of the first model by taking into consideration the effect of deviator stress to predict the material resilient modulus. In this model, the resilient modulus depends on the sum of principal stresses (Θ).

$$M_r = k_1 \Theta^{k2} \quad \text{(Equation 15)}$$

The simplicity of this model has made it the most widely used model to predict the resilient modulus of granular materials. However, it presents various drawbacks; it assumes a constant Poisson Ratio whereas this ratio is also stress dependent. The model also does not take into consideration the shear stresses. Molenaar (2005) indicated that this model is not fundamentally correct because it predicts an increase in resilient modulus when the material is closer to failure. Nevertheless, he indicated that this model could be used for practical purposes in a state of low stresses. Moreover, Cerni & Colagrande (2012) also indicated that this model predicts the resilient behaviour of granular materials well.

Uzan's Model

Uzan (1985) proposed a model for predicting the resilient behaviour of granular material. In his model, he improved the K-Θ model by incorporating the impact of shear strains in addition to the sum of the principal stresses. He indicated that the modulus prediction, based on both the sum of principal stresses and shear, has a good correlation with laboratory test results and with granular material behaviour.

$$M_r = k_1 \Theta^{k2} \sigma_d^{k4} \quad \text{(Equation 16)}$$

Where Θ is the sum of principal stress, σ_d is the deviator stress, and k_1, k_2 and k_4 are material parameters.

Despite the above-mentioned models, others studies have attempted to develop other mathematical models in order to improve the understanding of mechanical behaviour of granular materials. Even though some of them are likely to be sophisticated and difficult to understand but in most cases, they are physically sound. Some of these models are highlighted below:

Nataatmadja (1992) has developed models for both Constant Confining Pressure (CCP) and Variable Confining Pressure (VCP).

$M_r = \frac{\theta}{q}(A+Bq)$ for CCP and, (Equation 17)

$M_r = \frac{\theta}{\sigma 1}(C+Dq)$ for VCP (Equation 18)

Where Θ is the sum of the principal stresses; q is the repeated deviator stress; σ_1 is the major principal stress; and A, B, C and D are material parameters based on laboratory results.

Nataatmadja & Tan (2001) have used the model using CCP to predict the resilient modulus of recycled concrete road aggregates.

The AASTHO bulk stress model is also recommended to be used for unbound granular base and subbase materials. This model is expressed as follow:

$M_r = k_1 \Theta^{k2}$ (Equation 19)

With $\Theta = \sigma_d + 3\sigma_3$ and where Θ is the bulk stress; σ_d is the deviator stress; σ_3 is the confining pressure; and k_1, k_2 are material experimental parameters.

Furthermore, Jenkins (2000) established another successful model by modifying the Mr- σ_3-σ_1/ σ_{1f} model developed by Van Niekerk & Huurman (1995) in order to take into account deviator stress ratio rather than principal stress ratio. This model is fundamentally correct because it takes into account the damage or the reduction in resilient modulus as the material is close to failure. This is described by the second term $(1-k_3.(\sigma_d/\sigma_{df})^{k4})$ which is added to K-Θ Model. The k_3 define the decrease in stiffness as the material is loaded at the failure and the k_4 describes the shape of decrease.

$Mr = k_1(\Theta/\Theta_0)^{k2}.(1-k_3.(\sigma_d/\sigma_{df})^{k4})$ (Equation 20)

Where:

Mr = resilient modulus (MPa)

Θ = sum of principal stresses

σ_d = (cyclic) deviator stress

σ_{df} = deviator stress on the basis at failure

Θ_0 = reference principal stress = 1 kPa

k_1, k_2, k_3, k_4= model coefficients

The above-mentioned models from the simplest to sophisticated should be able to describe the stress dependency of the resilient modulus and should be reasonably understandable.

Van Niekerk (2002) stated that a good model that describes the Mr stress-dependency should be able to relate the resilient modulus to the stress parameters such as confining stresses and deviator stress. It must also provide a clear distinction on material stiffening at low deviator stress levels and softening as the stress increases closer to the failure.

In light of very accurate radial measuring devices required for the assessment of Poisson Ratio, which is practically difficult to obtain, limited studies has been carried out on resilient Poisson Ratio. For example, Morgan (1966) cited in Lekarp *et al.*(2000) has found values between 0.2 and 0.4 while Allen(1974) carrying a triaxial test at Variable Confining Pressure(VCP) and Constant Confining Pressure(CCP), has found for the same material, a range of 0.35 to 0.4 of Poisson Ratio for VCP and above 0.5 using a CCP . However, a value of 0.35 is commonly assumed for granular materials.

The resilient Poisson Ratio similar to the resilient modulus depends on materials intrinsic properties and extrinsic factors but primarily stresses in the material. The Poisson Ratio increases with the increase of the deviator stress and the decrease of confinement (Lekarp *et al*., 2000). From the study carried out by Karasahin (1993) on the resilient behaviour of granular material using both constant and variable confining pressures in a triaxial test, he proposed models to describe the stress dependency of the Poisson Ratio. He also indicated that the Poisson Ratio model is not as good as the resilient model due to less sensitivity of the radial measuring system. The equation below was suggested for a constant confining stress:

$$\nu = D\left(\frac{qm}{pu}\right)^{F}.\left(\frac{pm}{pu}\right)^{H}.\left(\frac{pu}{p}\right)^{L} \qquad \text{(Equation 21)}$$

Where:

q_m= mean value of deviator stress

q= deviator stress

pu= unit pressure(1kPa)

pm= mean value of mean normal stress

p= mean normal stress

D, F, H, L model coefficients.

Van Niekerk (2002) has established a series of Poisson Ratio models to understand the stress dependency of the Poisson Ratio. Some of them are presented below.

$\nu = n_1.(\frac{\sigma_d}{\sigma_{d,f}})^{n2}$ or $\nu = n_1.(\frac{\sigma_d}{\sigma_3})^{n2}$ (Equation 22)

$\nu = n_1.(\frac{\sigma_d}{\sigma_{d,f}})^{n2} .\sigma_3^{n3}$ or $\nu = n_1.(\frac{\sigma_d}{\sigma_3})^{n2}.\sigma_3^{n3}$ (Equation 23)

With:

ν = Poisson Ratio

σ_d = (cyclic) deviator stress

σ_{df} = deviator stress on the basis of the failure

σ_3= confining stress

n_1, n_2, n_3= model coefficients

Numerous researchers however, have assessed the mechanical behaviour of recycled materials. Van Niekerk *et al.* (2002) indicated that the shear properties of these materials are strongly dependent on the degree of compaction, composition and the curing time. They also indicated that the resilient response depends on stress, curing time and degree of compaction. They reported however that a significant effect was caused by the stress magnitude because at higher stress levels, limited influence of the degree of compaction and of curing time was observed. Moreover, a big influence of the moisture was also observed. Furthermore, the influence of composition, grading, moisture and especially compaction on the resilient modulus of recycled aggregates are also visible and are mentioned in different studies (Molenaar &van Niekerk, 2002; Nataatmadja & Tan, 2001; Groenendijk *et al*., 2000; Leite *et al.*, 2011; Arulrajah *et al.,* 2011).

Arulrajah *et al*. (2011) have found that the recycled materials exhibited good shear strength and resilient response comparable to that of fresh aggregates, even sometimes better. Cerni & Colagrande (2012) indicated that because the recycled materials stiffness depends strongly on confining pressure and this occurs in deep layers in the pavement, it is advisable to use recycled materials in these deep layers such as the subbase layer where the material is confined well and endures less wheel vertical stresses due the upper layers. Furthermore, Azam and Cameron (2013) have found that based on resilient modulus results, the blend of recycled concrete and clay bricks could meet the requirement of being used in base course. However, the results of the permanent deformation could not the meet the base course

requirement and hence the material was relegated to be used in subbase. Therefore, the stress ratio during testing and the final application in pavement layers must be of a great concern.

2.3.7 Saturation/ Moisture susceptibility

The performance response of granular bound and unbound materials in pavement depends on the material strength. The moisture present in the pavement materials however, influences the strength characteristic significantly (Emery, 1988). Section 2.3.4 of this study presents the prime importance of moisture as lubricant on the level of compaction. Nevertheless, when this compaction moisture is changed due to ingress of moisture caused by climate or capillary action associated with poor pavement drainage and material permeability, the performance of the material in the pavement is affected. Upon build-up of the moisture, the pavement material may develop excess pore water pressure, decreasing the effective stress thus reducing the material strength. This loss of material strength is manifested in the pavement by localised failures and deformation. High water pressure in the pavement caused by high degree of saturation and permeability of the pavement layer causes low effective stress in the material, which has a significant influence on the straining of the material. The material's internal stress reduces the stiffness and increases the permanent deformation (Thom & Brown, 1987). The moisture susceptibility can then be defined as a measure of the material weakening due the presence of moisture. This characterises the stability of the material over the change of moisture in the pavement.

However, research has an apparent information shortfall on the moisture susceptibility of recycled concrete and masonry materials. Only limited studies have tried to assess the RCM mechanical behaviour under different moisture changes. Poon & Chan (2005) in assessing the strength of the mix of recycled concrete and crushed clay brick have observed a negligible difference between unsoaked CBR and four days soaked CBR. Similarly, Blankenagel & Guthrie (2006) used tube suction test to assess the moisture susceptibility of recycled concrete materials. They have found that these materials are less susceptible on moisture. Moreover, Cerni & Colagrande (2012) have assessed the moisture susceptibility by testing the resilient modulus at the optimum moisture content and in saturation conditions. They have observed a "modest" decrease in resilient modulus with saturation, which is an indication of less susceptibility of the material to the moisture change.

The low moisture susceptibility characterises non-plastic granular materials, therefore according to the results of the studies mentioned above, it can be deduced that if RCM is well processed, it will behave as non-plastic material.

2.3.8 Mechanical Testing

After mixing and compaction, materials are subjected to testing in order to evaluate their performance under different factors. The aim of mix composition mechanical testing is assessing the performance behaviour that the materials exhibit under traffic loading and climate factors by trying to simulate the real situation in the field.

2.2.8.3 Triaxial testing

Triaxial testing is a mechanical test that is used to assess the material shear strength (shear parameters), stiffness (resilient and permanent deformation) in conditions closely similar to that the material endures in the pavement. The testing protocol (Mgangira & Jenkins, 2011) indicated that the shear strength is determined by applying a monotonic load on cylindrical specimen at a constant loading rate until the specimen fails. In pavement engineering, monotonic triaxial testing is often used to evaluate the shear parameters of materials and the results are expressed through Mohr-Coulomb model. The specimen is subjected to a vertical loading, and a confining pressure as illustrated in Figure 2-25. The friction angle (ϕ) is obtained from the slope of the tangent line (failure envelope) to the circles and the cohesion(C) is estimated on the intercept of the line to the shear stress axis. These parameters are determined by applying a linear regression analysis on the obtained stresses at failure.

Resilient modulus and permanent deformation consist of applying a specific repeated vertical load for a specified duration under constant confining pressure. This vertical loading is a haversine pulse consisting of loading and unloading period followed by a rest (Figure 2-26). It simulates a moving wheel on a pavement. The testing stress paths or the repeated axial load levels for a specified confining pressure are predetermined from the ratio of the shear strength. The resilient modulus is obtained from the resulting vertical strain due to the applied repeated vertical loads. The permanent deformation however, differs from resilient modulus by applying on the specimen at a large number of repeated axial loads at the same level.

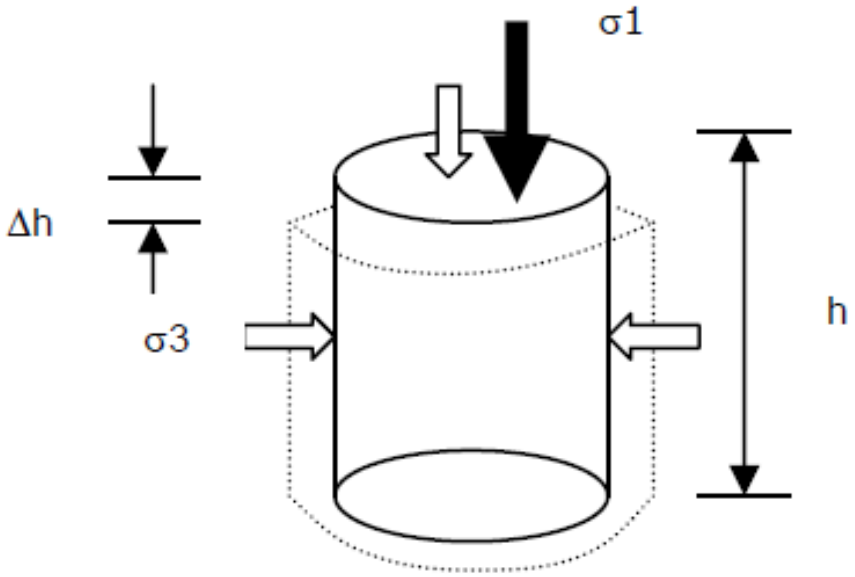

Figure 2- 25: Principle of Triaxial Testing (Molenaar, 2005)

Where σ_1 represent is the applied vertical axial stress and σ_3 is the confining pressure. The deviator stress σ_d is equivalent to $(\sigma_1 + \sigma_3) - \sigma_3 = \sigma_1$; and the vertical strain(ε_v) is equal $\Delta h/h$.

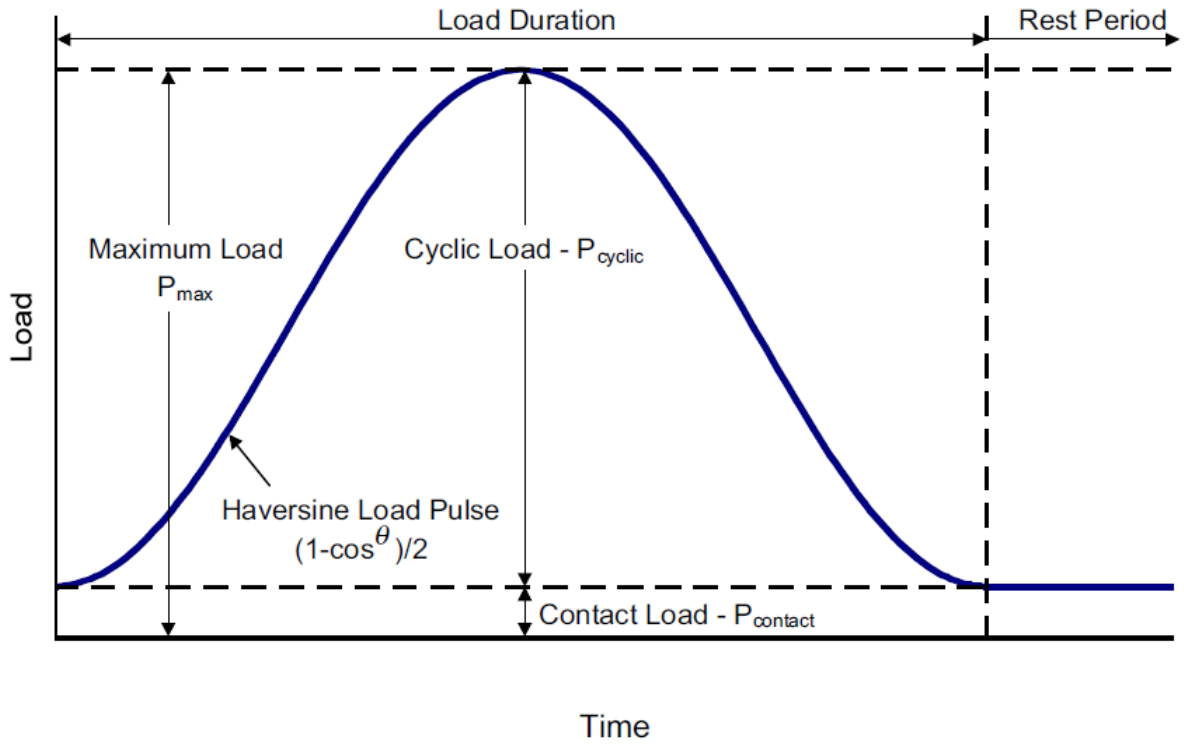

Figure 2- 26 : Definition of Resilient Modulus Terms (NCHRP 1-28a)

2.4 SYNTHESIS ON LITERATURE REVIEW

The priority placed on sustainable practices has made recycled concrete and masonry valuable material to consider for construction purposes. An increase in research and usage of these materials is noticeable worldwide. However, due to the lack of the historical performance information, the material is restricted in its application and it is not established in most of pavement material specifications especially in developing countries such as South Africa.

The major concern of these secondary materials starts with the demolition approaches and recycling methodologies used during processing. These aspects govern the quality and the properties of the recycled materials, which in return affect their mechanical performance in pavement layers.

Through synthesis of the literature, Figure 2-27 was developed to provide a graphical representation of the properties and the production method that affect the durability and performance. The predominant factors are red in colour and the level of influence decrease from red, orange to yellow. In other words, particle shape, contaminants (soluble salts for example), stress magnitude, saturation were mentioned in the literature to have a major influence on durability and mechanical performance behaviour when compared to other factors. The durability and mechanical characteristics are presented in a green colour in this figure. It was discussed that contaminants lead to less material stability while elongated aggregates are prone to crushing under wheel loading. Higher stresses generate pronounced rutting in unbound pavement layers while moisture softens the pavement layers leading to less bearing strength.

Secondary crushing during processing is important for the physical characteristics of recycled aggregates. The influence of aggregate strength on resistance to degradation (durability) was mentioned in various studies. Several researchers have also observed a noticeable effect of mix composition and the degree of compaction on RCM shear strength, resilient response and permanent deformation.

A number of studies have pointed out a non-negligible influence of grading, curing time and method (yellow in colour) on shear strength, resilient response and permanent deformation. Particularly, Curing contribute to strength gain for (cementitious) material such as RCM.

It was found that the characteristics of raw materials such as strength and water absorption have a remarkable influence on recycled aggregates performance especially the masonry constituent. In Figure 2-27, these inherent properties were summarised in aggregate strength.

Literature reviewed reiterated the paramount influence of the stress applied to the material on the performance characteristics. Therefore, mechanical behaviour such as shear behaviour, resilient modulus (Mr) and permanent deformation should be appropriately modelled taking into account of this important factor. Modelling however is not easy due the balance between complexity of granular material behaviour and the simplicity that is required for a model for easy understanding. The literature indicates that a good Mr model that describes the stress dependency of the material should be able to relate the resilient modulus model to important stress parameters such as confining stress σ_3, deviator stress σ_d differentiating the stiffening behaviour at low deviator stress and softening when the material is closer to failure. Several models are highlighted in the literature from Mr- σ_3 model to the well known simplistic Mr-Θ model, and to other sophisticated but sometimes physically real models.

This study however, focuses on processing, effect of aggregates physical and mechanical characteristics on RCM performance. It assesses also the effect of composition and compaction moisture and level on the shear strength and resilient response.

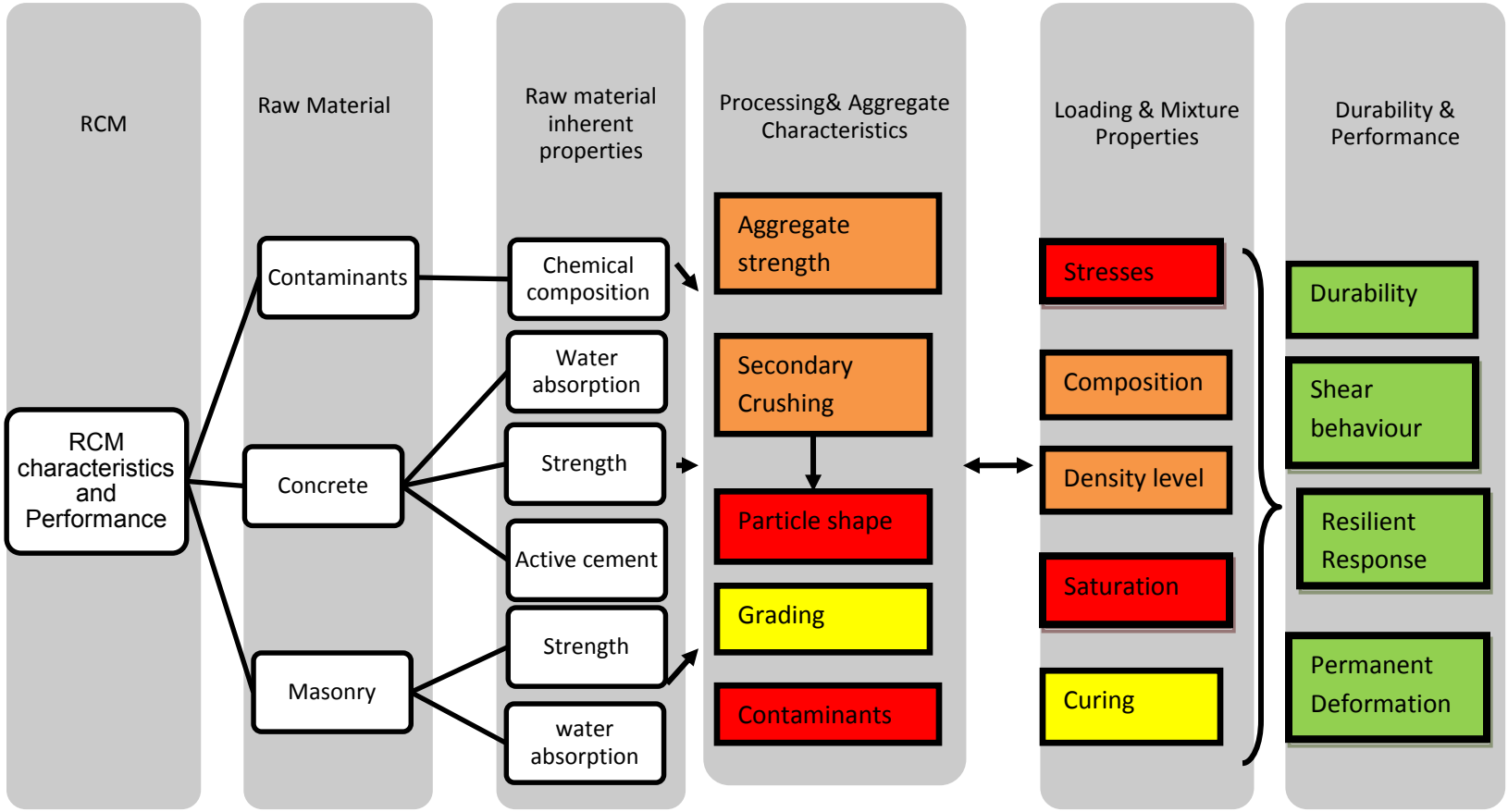

Figure 2- 27: Summary of Factors and their Level of Influence on Durability and Performance of RCM as Indicated in the Literature

CHAPTER 3

EXPERIMENTAL DESIGN AND METHODOLOGY

3.1 INTRODUCTION

The performance of granular materials in pavement layers depends on a variety of factors such as applied stresses, material properties, mix component characteristics, and preparation such as compaction and curing. There are various testing methods for evaluating the properties and mechanical performance of these materials as discussed in Chapter 2 of this study.

To evaluate the influence of the mix composition, degree of compaction and compaction moisture on mechanical performance, an experimental program was developed. This was based on factorial design at two levels 2^3 (Box *et al*., 1978). According to this method, two levels of each of three independent variables (investigated factors) were selected.

In essence, the following methodology procedure was followed in this research:

- Acquisition of the raw materials: collecting demolition waste and stocking
- Processing of the demolition waste: quality measures employed at preventing contamination of raw materials, crushing and sizing
- Material characterisation: assess the physical and the mechanical characteristics of the aggregates
- Compaction characterisation: validating previous studies (Louw, 2013) on compaction procedures for RCM and assessing the resulting particle break down
- Curing criterion: establishing a rational curing procedure for the target saturation
- Specimen preparation: prepare specimen according to the experimental design
- Mechanical performance testing: This step consisted of testing the failure monotonic and the resilient behaviour of RCM
- Performance understanding: fitting models on the obtained test results in order to develop an understanding of the mechanical performance response.

This chapter details the methodology of the tests that have been undertaken in this research. It provides a detailed research methodology developed for material processing, aggregates properties assessment and material mechanical experimental testing. It also gives information and motivation on the adopted experimental program.

3.2 MATERIALS

The concrete rubbles, i.e reinforced concrete were collected from a demolished site of the concrete laboratory at the Engineering Faculty of Stellenbosch University. The masonry rubbles, i.e clay bricks with the attached mortar were obtained from the demolished partition walls. Concrete and masonry rubbles were collected and stocked separately. As can be seen in Figure 3-1 and Figure 3-2, quality control measures were undertaken in order to remove undesired objects such as gypsum, steel bars, woods, etc.

Figure 3- 1: Demolition Rubbles

Figure 3- 2: Masonry Rubbles (left) and Concrete Rubbles (right) Storages

Due to the large stone size of the rubbles, crushing of rubbles using the laboratory jaw crusher were considered. The crushing was executed in two steps i.e primary crushing and secondary crushing as shown in Figure 3-3 to Figure 3-5. This crushing was done with the aim to obtain desirable aggregates sizes and reduce flakier aggregates and generates fines. The primary crushing was carried out using a large jaw-opening while, with secondary crushing the jaw opening was reduced.

Figure 3- 3: SU Laboratory Jaw Crusher and Crushing Process

Figure 3- 4: Concrete Primary Crushing (left) and Secondary Crushing (right)

Figure 3- 5: Masonry Primary Crushing (left) and Secondary Crushing (right)

3.2.1 Material properties characterisation

Grading

After crushing the concrete and masonry, sieving of the obtained material was carried out separately into five fractions (<19-13.2mm, <13.2-6.7mm, < 6.7- 4.75 mm, <4.75 – 0.425 mm, < 0.425- 0.075 mm, < 0.075 mm). The aim of this exercise was to facilitate accurate and consistent blending during specimen preparation. Figure 3-6 shows the used sieving machine.

Figure 3- 6: SU Sieve Machine

A grading for both mix compositions was selected based on the Fuller curve, which has proven to provide a denser packing. Additionally a reasonable grading that can be achieved at the commercial recycling plant was taken into consideration. This comparison was made based on two grading from two different recycling companies; one in Cape Town and another in Durban as presented in Figure 3-7.

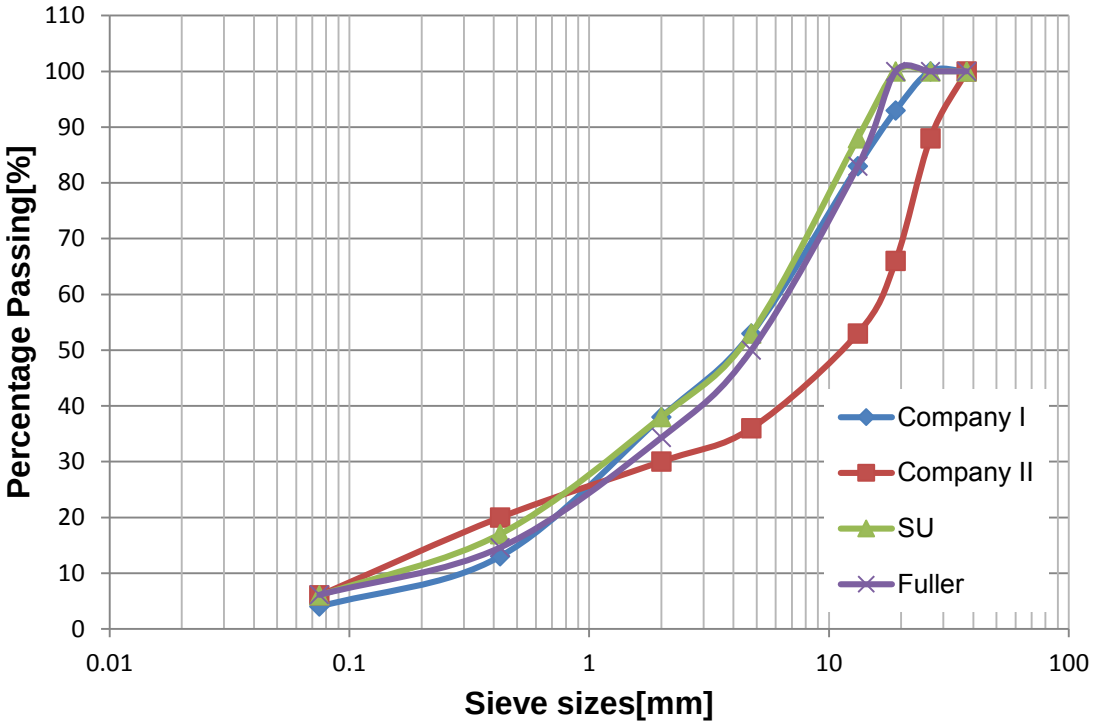

Figure 3- 7: Grading Characteristic

Particle shape (Flakiness index)

The Flakiness index was carried out according to TMH 1 Method B 3 and the apparatus used is shown in Figure 3-8.

Figure 3- 8 : Flakiness Index Test Apparatus

Particles Bulk Relative Density (BRD), Apparent Relative Density(ARD) and Water Absorption(WA)

The determination of BRD, ARD and WA was done using the Rice Method (Botha and Semmelink, 2004). This method measures the BRD based on the aggregate dry to surface wet conditions with a wetting period comprising of 1.5 minutes as it is shown on Figure 3-9. The ARD and WA are obtained after 24 hours sample immersion in a Rice flask or after 30 minutes of applying a vacuum pump.

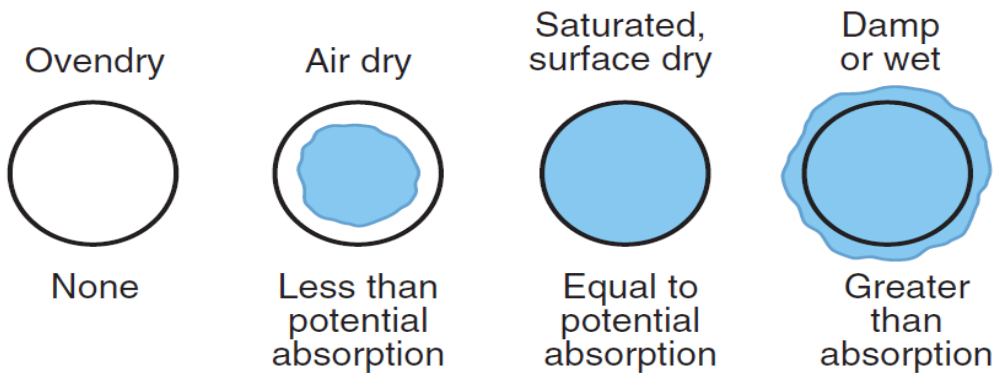

Figure 3- 9: Moisture Condition on Aggregate (Suvash, 2011)

The test consists of weighing the mass of the empty Rice flask with watch glass (M1), recording the mass when full of water (M2) and then adding the material (M3). When the flash contains material and filled at its capacity with no bubbles after 1.5 minutes the mass recorded is (M4). The sample is allowed to stand for 27 minutes after which new developed bubbles are removed by stirring then the mass is recorded (M5). When the vacuum pump is used for 30 minutes or the sample is allowed to stand for 24 hours in the laboratory after which also new developed bubbles are removed, the mass of the sample (M6) is recorded. The test apparatus is presented in Figure 3-10.

$BRD_{1.5\ min} = (M3-M1)/[(M2-M1)-(M4-M3)]$ (Equation 24)

$ARD_{30\ min} = (M3-M1)/[(M2-M1)-(M5-M3)]$ (Equation 25)

$ARD_{24\ hour} = (M3-M1)/[(M2-M1)-(M6-M3)]$ (Equation 26)

$WA_{24\ hour} = (1/BRD_{1.5\ min} - 1/ARD_{24\ hour}) \times 100\%$ (Equation 27)

For this research, this method was used for both > 4.75mm and < 4.75mm fractions, and no vacuum pump was used, thus the sample was allowed to stand for 24 hours in the laboratory. A duplicate sample for both fractions was tested.

Figure 3- 10 : Determination of BRD, ARD and WA by Rice Method

Material Density

The density of the mix compositions were assessed using Modified AASHTO compaction test; this determines the maximum dry density and optimum moisture content of gravel, soil and sand, Method A7 TMH1(1986). Two types of mix compositions were prepared and tested; 70%Concrete 30% Masonry denoted 70C:30M and 30% Concrete 70% Masonry (denoted 30C:70M). However, this percentage applies only on medium and fine particles (4.75mm to < 0.075mm). The composition of coarse particles (≥ 6.7mm) was selected to be 70% concrete 30% masonry for both mix compositions. The reason for this composition results from the experimental information obtained from Louw (2013). Louw showed that when these coarse aggregates are not strong enough, they are prone to crushing.

The compaction protocol included 55 blows per layer using a 4.536 kg hammer. A mould of 152mm diameter and 152 mm height including the collar (i.e 127 mm effective height) was utilised and the material was compacted in five layers.

10% Fine Aggregate Crushing Test (10% FACT)

The 10% FACT test indicates the strength and durability of the aggregates. The Method B2 of the TMH1 (1986) provides the test protocol that determines the force required to crush a

material sample (<13.2mm retained on 9.5 mm sieves) in order to produce 10% of the total sample that passes the 2.36 mm sieve. The test was undertaken in both dry and wet conditions.

The tests were conducted for three specimens corresponding to three different forces that can generate <7.5%, 7.5- 12.5%, and > 12.5% fines (passing the 2.36 mm sieve). The sample was placed in crushing cylinder in three layers by applying 25 light strokes with a tamping rod for each layer as presented in Figure 3-11. The aggregates surface was levelled and the plunger was inserted, and then the material was subjected to crushing in a compression machine. After compression, the force was recorded and the material was sieved through 2.36 mm sieve and the mass was recorded in order to check the percentage passing. However, for the wet test, the material was oven dried at 105-110 ^{0} C for 24 hours before sieving it.

A curve of percentage fines against the applied forces was plotted and the value of 10% fines was obtained from this graph.

Figure 3- 11: 10% FACT Testing

3.3 EXPERIMENTAL PROGRAM

Three factors influencing the mechanical behaviour of RCM materials were investigated. These factors were the mix composition, i.e ratio in mass of concrete to masonry, the degree of compaction and the compaction moisture. At each independent variable (factor), two levels were selected; mix composition with 70C:30M and 30C:70M, compaction moisture with 80% OMC and 70% OMC, and the degree of compaction varying from 100% Modified AASTHO to 102% Modified AASTHO. To this end, a method of factorial experimental design at two levels 2^3

(Box et al., 1978) was used. Each independent variable was coded; the minus (–) sign indicates the low level and the plus (+) sign indicates the high level. This is given in the design matrix provided in Table 3-1. A duplicate sample was prepared for each variable in order to assess the standard error.

Table 3- 1: 2^3 Factorial Design Matrix

Test run	M	DOC	CM	Mr(ν)
1	-	-	-	
2	+	-	-	
3	-	+	-	
4	+	+	-	
5	-	-	+	
6	+	-	+	
7	-	+	+	
8	+	+	+	

Note:

- M: the mix composition composed by (-)= 30% C and (+) denoting 70% C
- DOC indicating the degree of compaction with (-) corresponding to 100% Modified AASTHO and (+) denoting 102% Modified AASTHO
- CM indicates the compaction moisture which varies from 70% OMC(-) to 80% OMC (+)
- Mr is the yielded resilient modulus and ν is the yielded Poisson Ratio

This experimental design has a good number of advantages:

- It requires relatively few test runs and can reasonably provide major insights of the study parameters
- It can be used as building blocks so that the complexity of the study can be matched by the final constructed design
- It is relatively easy to interpret and it is preferable at an early stage of investigation where a large number of parameters need to be assessed.

3.4 SPECIMEN PREPARATION

3.4.1 Material blend

The choice of the material was based on the experimental design. Two types of mix composition were selected, i.e 70C:30M and 30C:70M. Bear in mind that this percentage content is only applied to the ≤ 4.75mm fractions of the sample since the coarser fractions (> 4.75mm to < 19mm) are composed for both mix compositions with 70C:30M.

3.4.2 Mixing and compaction moisture

The compaction moisture was determined based on the Optimum Moisture Content (OMC) determined from the Modified AASTHO compaction test. Based on the experimental design, two compaction moistures; 70% OMC and 80% OMC were selected. These were selected after a trial on three compaction moistures (90%, 80% and 70% OMC) which showed that 90% OMC generated a pronounce pumping of fines. The hygroscopic moisture of each sample was recorded and therefore, the real moisture to add for compaction was determined accordingly.

Mixing of the material in the presence of moisture was undertaken using the laboratory mixer shown in Figure 3-12. Material was mixed until consistency was observed.

Figure 3- 12 : Laboratory Mixer

3.4.3 Specimen Compaction

The specimens were compacted using a vibratory hammer in a spilt mould measuring 150mm internal diameter and 300mm height. Two different compaction efforts, i.e 100% and 102% densities were targeted according to the maximum dry density obtained by standard Modified AASTHO compaction test.

The compaction efforts, i.e 100% and 102%, were designed using Equation (28).

$$D_{designed}=\frac{DE\ x\ Dmod}{100} \quad \text{(Equation 28)}$$

Where $D_{designed}$ is the designed density corresponding to the designed compaction effort, DE is the designed compaction effort or the degree of compaction and D_{mod} represents the reference maximum density from Modified AASTHO test.

The designed density and compaction moisture governed the amount of material per layer in order to achieve a 60mm-compacted height of the layer. The cylindrical triaxial specimen (150x300mm) was then compacted in five-60mm layers. To ensure an interlock between layers, the surface of the layer was lightly scarified using a scarifying tool and a driller before compacting another layer. The compaction height per layer was clearly marked on measuring tape mounted on the frame of the vibratory hammer. To this end, initially the vibratory hammer is lowered into the empty mould and then the starting position is marked (zero line). Form the zero line, the five layers of 60mm each are marked until 300mm height of the specimen is reached as shown in Figure 3-13.

Figure 3- 13: Vibratory Compaction

3.4.4 Curing

The aim of curing was to homogenise the moisture in the entire specimen and allow the specimen to dry back to the target saturation moisture of 65% OMC. This saturation corresponds to reasonable equilibrium moisture in pavement base course for the Western Cape region based on moisture indices.

The curing protocol for this type of material is not yet established. In this regard, a specimen mass monitoring approach has been used to determine the specimen mass corresponding to the above mentioned selected saturation moisture at testing. Based on this approach, the specimen was initially allowed to dry back and then sealed in a plastic bag at room temperature of 25^{0}C for a period of four days before testing. Figure 3-14 shows the specimen under curing process.

Figure 3- 14 : Curing of Specimens

3.5 MATERIAL BREAK DOWN

From Chapter 2, it was discussed that the recycled materials are prone to crushing during compaction due to the inertness of the particles comprised in the mix, i.e soft materials such as mortar and masonry. The more crushable the material is the less durable and consequently poorer performance. To evaluate this, wet sieving was done after compaction and the grading was compared to the initial designed grading. To achieve this, the entire compacted specimen was broken and dried in the oven for 24hours at 110 ^{0}C and the mass of the sample was recorded. The material was then soaked for 24 hours and wet sieved through 0.075mm sieve. Material retained on 0.075mm sieve was oven dried for 24hours and sieved to assess the grading.

3.6 TRIAXIAL TESTING

Triaxial testing was conducted to assess the shear strength characteristics of RCM materials and characterise their response under cyclic loading while simulating field conditions.

The two triaxial tests conducted are the monotonic triaxial compression test to characterise the shear strength, and the repeated load triaxial testing to assess the resilient response. The machine used during this testing program was the Material Testing System (MTS) 2703 (Figure 3-15). The applied load was measured using a load cell of with a capacity of 100 kN (10 metric ton) installed inside the triaxial cell. Air pressure was used to apply confinement.

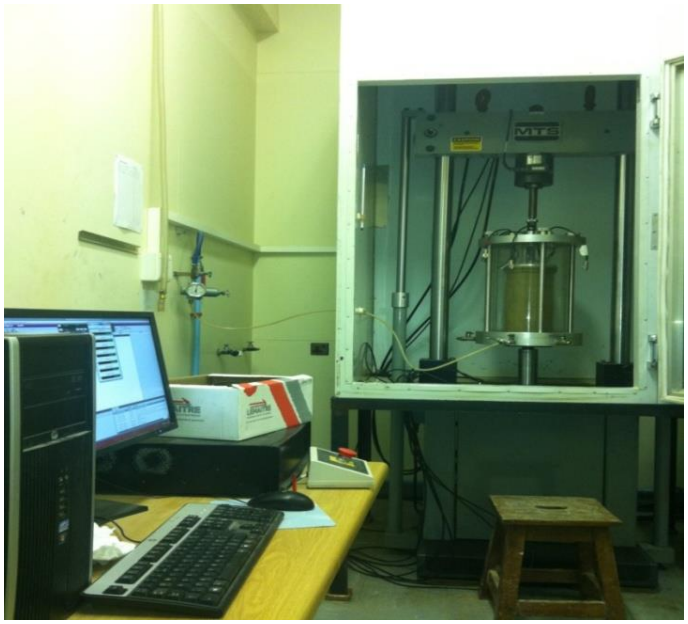

Figure 3- 15 : Triaxial Apparatus and Data Capturing

3.6.1 Triaxial Monotonic Test

The pavement structure is characterised by its failure parameter (shear properties) and response parameters (resilient and permanent deformation), loading rate, etc. Since not all pavements fail by shear, the response properties are the most representative characteristics of the pavement materials. Nevertheless, shear properties provide valuable information on strength of pavement materials and the materials safe stress states are usually related to their ultimate shear strength.

The monotonic triaxial test was performed to obtain the shear properties (C, ϕ) of the RCM material after four days specimens curing time. The test was carried out at three different confining pressures: 50 kPa, 100 kPa and 200 kPa at strain rate of 3mm/min. The stress at failure of the specimen at each confinement was recorded. The combination of three stresses at failure corresponding to three different confinements was fitted into the Mohr-Coulomb model using a linear regression analysis in order to obtain the shear parameters (C, ϕ). It is well known that in order to obtain good reliability on the results of the shears parameters, three combinations of confining pressures are required. Monotonic triaxial test on preloaded cyclic samples were performed however on a combination of only two confining pressures (200 kPa and 50 kPa). The reason for this is that only two specimens, i.e initial and duplicate, were available after cyclic resilient test.

3.6.2 Repeated load Triaxial testing

The resilient test was conducted to assess the influence of mix composition, compaction moisture and degree of compaction on the mechanical performance response of RCM materials under repeated cyclic loading.

3.6.2.1 Specimen assembly in triaxial cell

After four days of specimen curing, the specimen was subjected to testing. The testing protocol for resilient and permanent deformation testing (Mgangira &Jenkins, 2011) was followed. Figure 3-16 presents the procedure used.

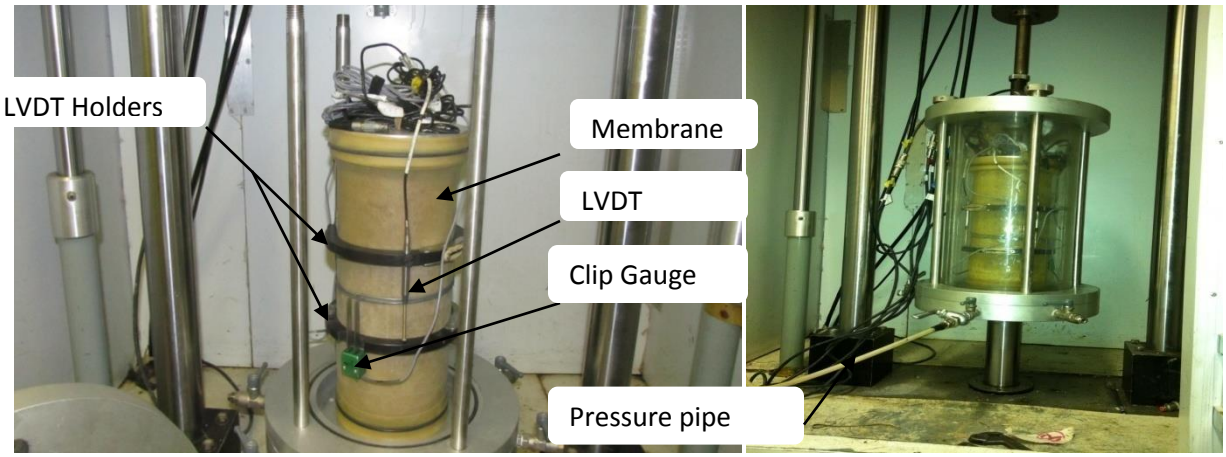

Figure 3- 16 : Sample Assembly in Triaxial Cell

3.6.2.2 Testing

The resilient modulus tests were conducted in accordance with the protocol for resilient modulus and permanent deformation characteristics of unbound and bound granular materials (Mgangira & Jenkins, 2011). During testing, a haversine-shaped load purse was applied as stipulated in the protocol. Load pulse of 0.1 sec loading duration and 0.9 sec rest period was adopted as illustrated in Figure 3-17.

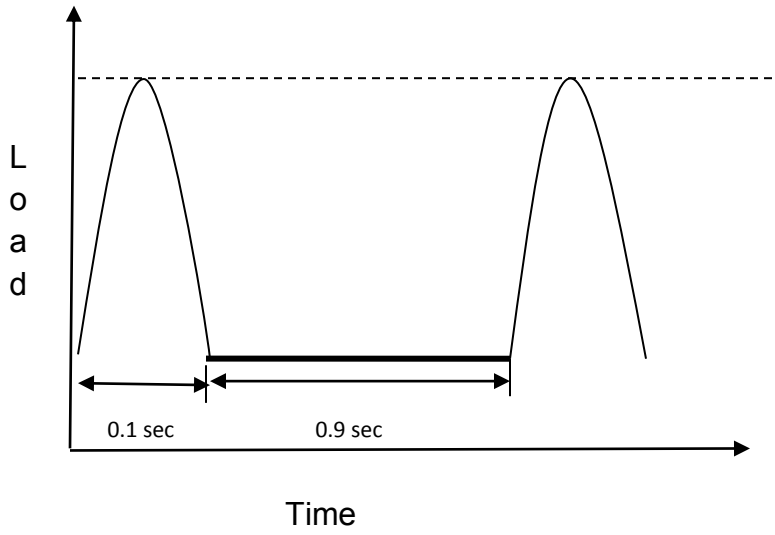

Figure 3- 17: Harvesine Load Pulse

The test consists of a conditioning period in order to eliminate the initial permanent deformation that can develop during the resilient test. After conditioning, the loading sequences followed by

varying the confining pressure as well as the deviator stresses. The stress ratios used in this cyclic test were determined as a ratio of the deviator stress at failure (σ_{df}) obtained during monotonic testing. Table 3-2 presents the load sequences used in this study. The stress ratios used in this study are ≤ 0.55 σ_{df}. This is qualified to mild stress regime compared to severe stress regime with stress ratios >0.60 σ_{df}.

During testing, axial and radial deformations were recorded by means of three Linear Variable Transducers (LVDTs) and two clip gauges. The resilient modulus Mr at each confinement and stress ratio was calculated as follow:

$$Mr=\frac{\sigma\ cyclic(N)}{\varepsilon a(N)} \quad \text{(Equation 29)}$$

Where $\varepsilon a(N)$ is the resilient axial strain per load cycle N, and $\sigma_{cyclic(N)}$ is the cyclic deviator stress for each cycle N.

$$\varepsilon_{a(N)}=\frac{\Delta\delta a(N)}{Lg} \quad \text{(Equation 30)}$$

With: - $\Delta\delta_{a(N)}$, the average vertical resilient deformation recorded by the LVDTs and L_g is the gauge length(100mm in this study).

$$\sigma_{cyclic(N)}=\sigma_{max(N)}=\sigma_{max(N)}-\sigma_{contact(N)} \quad \text{(Equation 31)}$$

The resilient Poisson Ratio ν was calculated using the following formula:

$$\nu=\frac{\varepsilon\ rad(N)}{\varepsilon a(N)} \quad \text{(Equation 32)}$$

Where $\varepsilon_{rad(N)}$ is the resilient radial strain measured using clip gauge, and $\varepsilon_{a(N)}$ is the resilient axial strain.

$$\varepsilon_{r(N)}=\frac{\Delta\delta rad(N)}{R} \quad \text{(Equation 33)}$$

With: - $\Delta\delta_{rad(N)}$, the average radial resilient deformation recorded by the clip gauges and R is the specimen radius.

The first five and the last five cycles were captured during testing but only the last five cycles where the loading is stable were reported. The consistency of reading for LVDTs (Figure 3-18) was checked and the average of three or two reading closely the same was taken into

consideration. A reasonable range of 0.8 to 1.2 LVDT/LVDT $_{(Avg)}$ was considered as previous research has shown this to be practical limits.

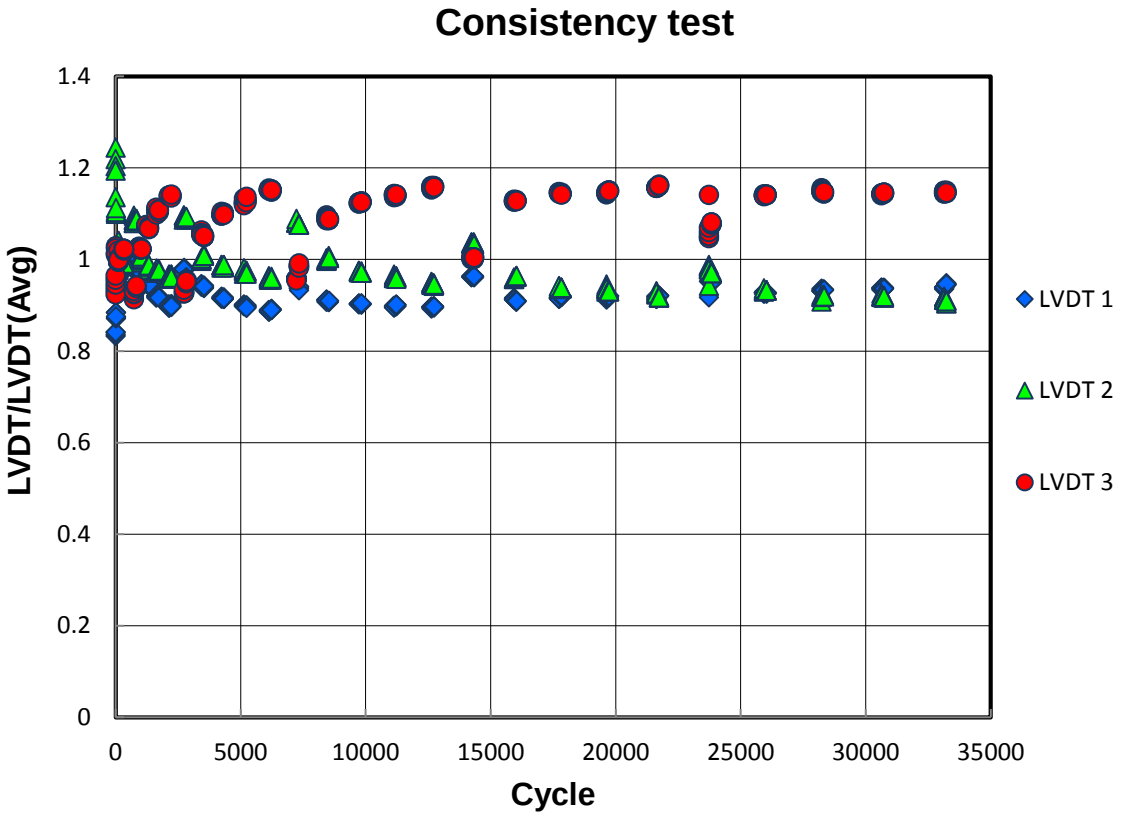

Figure 3- 18 : LVDT Reading Consistency Test

To understand the stress dependency of RCM, the Mohr-Coulomb model (Equation 11) was used to model the failure behaviour. The resilient response behaviour for each tested sample, was modelled by the Mr-Θ (Equation 15) and Mr-Θ-σ_d/ σ_{df} (Equation 20) models for resilient modulus and "Exponential" ν-σ_d/σ_3 model (Equation 22) and ν-σ_d/σ_3- σ_3 model (Equation 23) for resilient Poisson Ratio. The resilient models were fitted to the data by means of non-linear regression using Solver (Excel). The regression analysis is discussed in Appendix F.

Table 3- 2 : Loading Sequences

Loading sequence	Confining pressure(kPa)	Contact stress(kPa)	Cyclic stress(kPa)	Load repetitions(Cycles)
Conditioning	200	22.6 kPa	$0.1\sigma_{df}$	100
			$0.2\sigma_{df}$	100
			$0.3\sigma_{df}$	100
			$0.4\sigma_{df}$	200
			$0.55\sigma_{df}$	200
1	200	22.6 kPa	$0.1\sigma_{df}$	100
			$0.2\sigma_{df}$	100
			$0.3\sigma_{df}$	100
			$0.4\sigma_{df}$	100
			$0.55\sigma_{df}$	100
2	150	22.6 kPa	$0.1\sigma_{df}$	100
			$0.2\sigma_{df}$	100
			$0.3\sigma_{df}$	100
			$0.4\sigma_{df}$	100
			$0.55\sigma_{df}$	100
3	100	22.6 kPa	$0.1\sigma_{df}$	100
			$0.2\sigma_{df}$	100
			$0.3\sigma_{df}$	100
			$0.4\sigma_{df}$	100
			$0.55\sigma_{df}$	100
4	50	22.6 kPa	$0.1\sigma_{df}$	100
			$0.2\sigma_{df}$	100
			$0.3\sigma_{df}$	100
			$0.4\sigma_{df}$	100
			$0.55\sigma_{df}$	100
5	25	22.6 kPa	$0.1\sigma_{df}$	100
			$0.2\sigma_{df}$	100
			$0.3\sigma_{df}$	100
			$0.4\sigma_{df}$	100
			$0.55\sigma_{df}$	100

CHAPTER 4

TEST RESULTS AND DISCUSSION

4.1 INTRODUCTION

This chapter presents the results of the laboratory experimental testing program conducted to characterise the RCM materials properties in order to understand and model their performance behaviour within pavement layers.

4.2 MATERIAL PROCESSING

4.2.1 Crusher characteristics

4.2.1.1 Gradation

Figure 4-1 presents the material grading after crushing from wet sieving test. The crushing was carried out using a jaw crusher in two phases, i.e primary crushing and secondary crushing. The jaws of the crusher were set to provide coarse aggregates as well as fine aggregates. Respectively the recycled concrete generated limited fines compared to recycled masonry. Observation showed that a significant proportion of fines could be generated if the jaws opening of the laboratory crusher are narrowed during secondary crushing. However, this operation resulted in less coarse particles in the material.

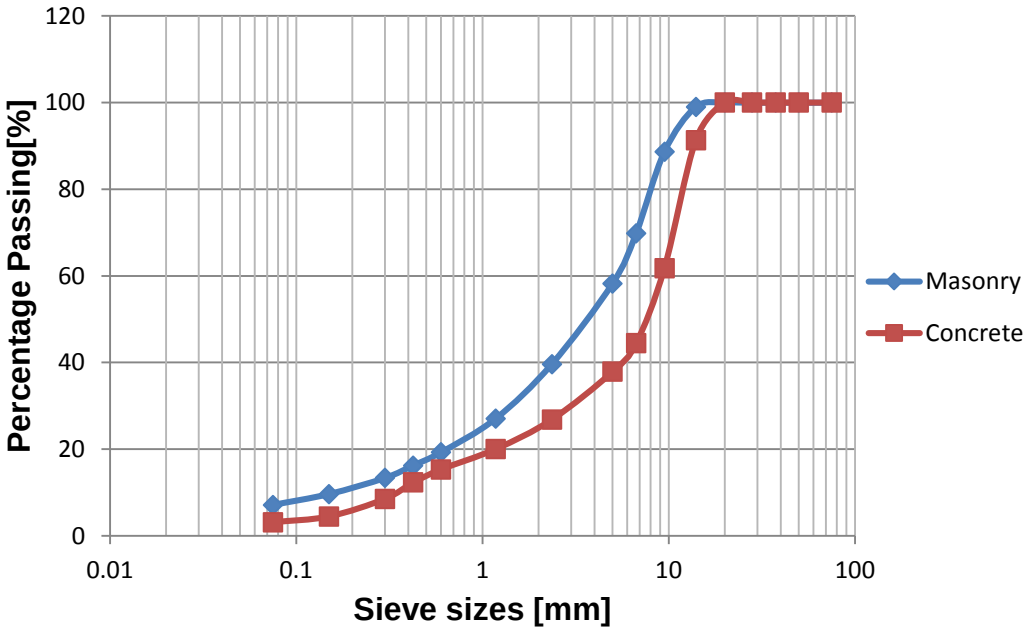

Figure 4- 1 : Crusher Grading

It is possible to conclude that recycled material, in particular the recycled concrete generates less fines during the crushing process than recycled masonry. This is in good agreement with the results obtained from the crushing of concrete rubbles in the commercial recycling plant (Company I) as presented in Figure 3-7. In contrast, the crushing of the masonry easily generates fines.

4.2.1.2 Particle shape

The crusher produced two different aggregate characteristics from the two stages of crushing. Figure 3-4 and Figure 3-5 show that the primary crushing resulted predominantly in larger flat aggregates with low fine content compared to secondary crushing which generated cubical aggregates with more fines. The secondary crushing reduced the flat particles in both crushed masonry and concrete materials. However, based on visual assessment, a slight amount of flat aggregates is contained in medium sized particles (≤ 4.75mm) for both crushed concrete and masonry. These particles in the crushed concrete were predominantly from the mortar attached to the aggregates in the concrete rubble. However, the general trend for the aggregate shape of the crushed material used in this study is cubical. From this, one can notice the importance of secondary crushing for recycled materials.

4.3 AGGREGATES CHARACTERISATION TESTS RESULTS

The aim of selecting the grading of the material was to obtain a denser packing. TRH14 (1985) provides grading envelopes for crushed rock granular materials (G1 up G3) and natural gravel (G4). However, it does not specify grading envelopes for recycled materials. Therefore, the grading (Figure 4-2) of the material used in this study was selected based on the Fuller curve with an exponent of 0.45 and the aggregate maximum size of 19mm as indicated in Section 3.2.1. In addition, practical aspects have been taken into consideration by assessing the gradation achieved by local recycling industries. The grading modulus was used to assess the grain distribution of the target grading. The value of 2.36 presented in Table 4-1 was obtained and this value compares to a good grading for soil and gravel as indicated in SAPEM (2013).

Table 4-1 and Figure 4-3 present the results of the flakiness index test. It is illustrated in Figure 4-3 that recycled masonry has more flaky particles than concrete. These particles were predominantly found with the large aggregates sizes (< 19mm-13.2mm). However, all the aggregates types and mix compositions meet the COLTO (1998) and TRH 14 (1985) specifications (maximum of 35%) and the TRH 8 (1987) (maximum of 20%) for base course

materials. Bear in mind that the flakiness index is similar for both mixes on larger aggregates since this fraction is composed exclusively by 70C:30M as discussed in Section 3.4.1.

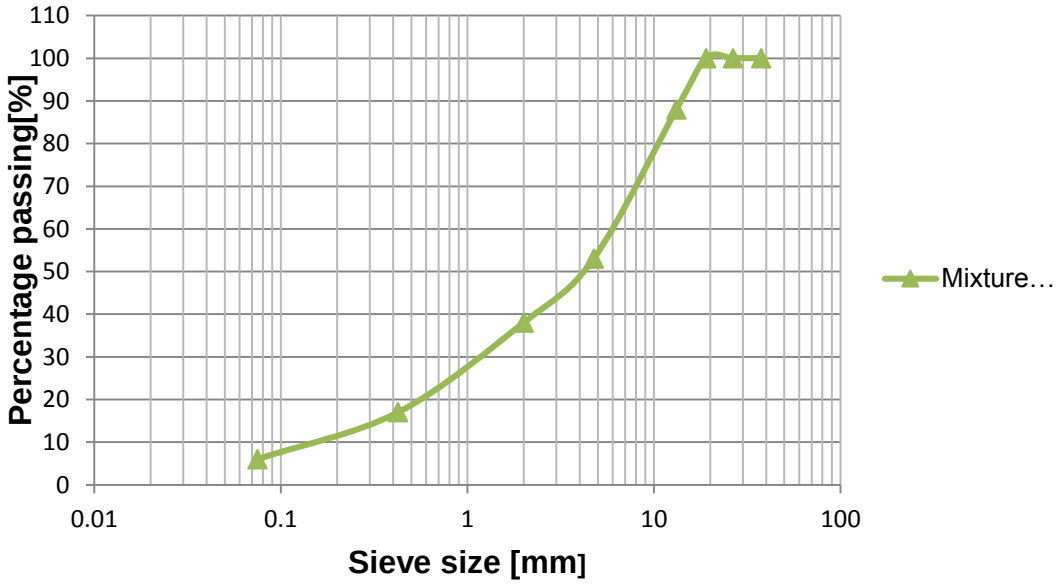

Figure 4- 2 : RCM Target Grading

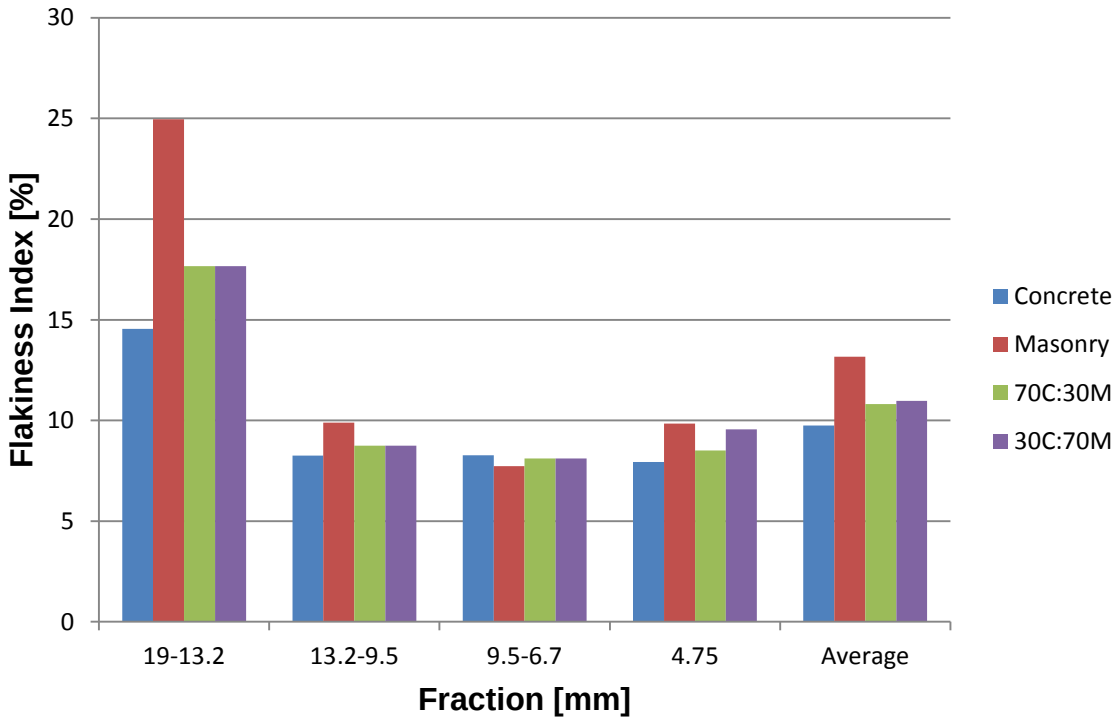

Figure 4- 3 : Flakiness Index

Table 4- 1 : Summary of the Aggregates Physical and Mechanical Properties

Physical properties				
	70 C:30M		30C:70M	
	>4.75mm	<4.75 mm	>4.75mm	<4.75 mm
GM	2.39		2.39	
Flakiness Index (%)	10.8		11.02	
Atterberg Limit	None plastic		None plastic	
BRD(-)	2.52	2.51	2.51	2.49
ARD(-)	2.55	2.57	2.54	2.56
Water Absorption (%)	1.22	1.40	1.32	1.92
Mechanical Properties				
Moisture-Density	γ=1829 (kg/m^3) w= 14.1 (%)		γ=1807 (kg/m^3) w= 15.45 (%)	
10% FACT (kN)	Dry	131	131	
	Wet	89	89	
	Ratio	68%	68%	

Figure 4-4 presents the specific gravity (Bulk Relative Density) and Water Absorption of different mix types used in this study. Mix compositions containing high concrete exhibited high Bulk Relative Density (BRD) and lower Water Absorption (WA) than mix compositions with high masonry content; this was observed for both material fractions. This can be explained by the composition of recycled concrete that comprises of denser, strong and less porous granulates in comparison to the masonry granulates. The BRD of the mix composition is lowered by the content of less dense granulates such as clay bricks granulates (clay minerals and some quarts) and mortar granulates (porous aggregates). Also, note that the densities for the fraction larger than 4.75 mm has the same result as the blend is similar for both compositions. This mix composition characteristic was selected to optimising the usage of strong aggregate as well as valuing the less strong aggregates.

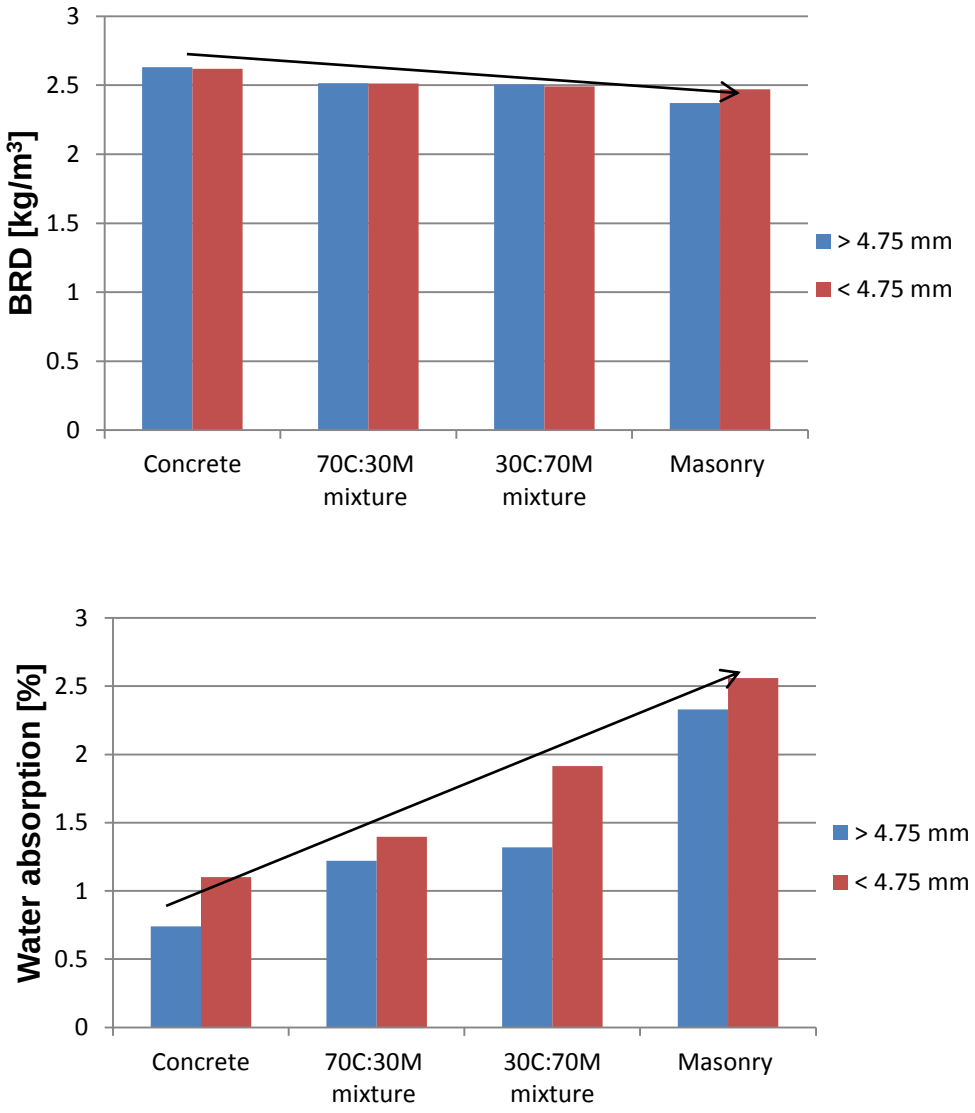

Figure 4- 4 : Bulk Relative Density (BRD) and Water Absorption (WA)

The water absorption increases with the increase of fine particles. This is due to the high surface area that absorbs more water. In light of this characteristic, the water absorption was found to be high for the <4. 75 mm fraction than that of > 4.75 mm fraction. However, a remarkable difference in absorption is observed between the two different mix compositions, i.e 70C:30M and 30C:70M especially for the < 4.75 mm fraction.

The evaluation of the aggregates water absorption provided a range of 1.22% to 1.92% and these are slightly higher than 1% recommended by TRH 8(1987). However, the South African Pavement Engineering Manual SAPEM (2013) does not prioritise water absorption among aggregate properties as a requirement for base course application.

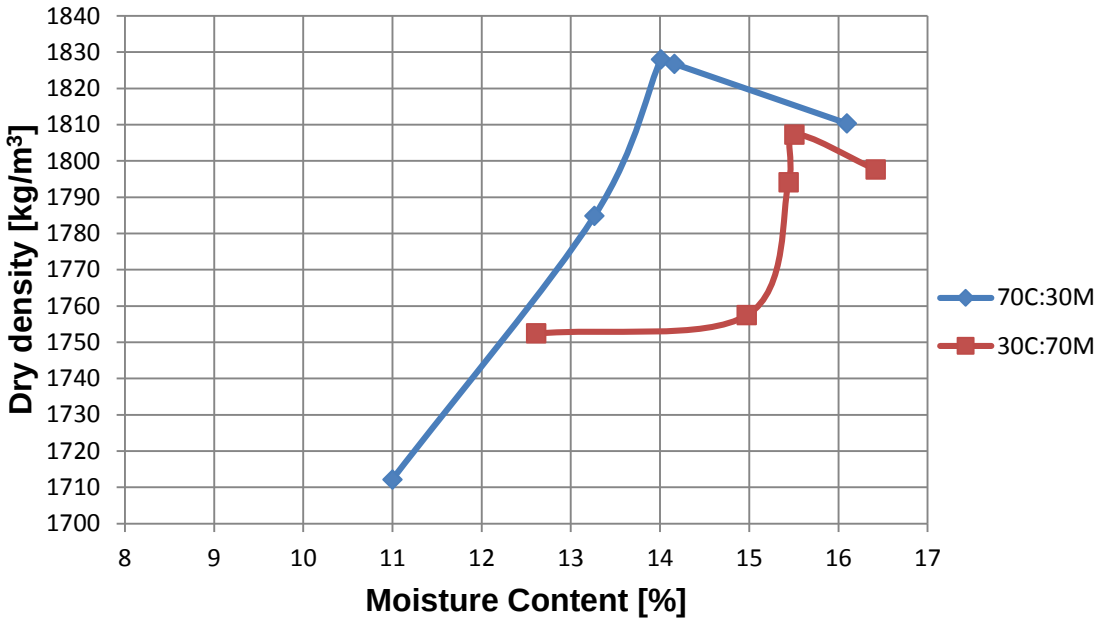

Figure 4- 5 : Moisture–Density Relationships for two Mix Compositions

Figure 4-5 shows the moisture –density relationships obtained from the Modified AASTHO compaction test for the two mix compositions. It was observed that the mix composition with high concrete content, i.e 70C:30M yielded high density and low optimum moisture than the mix composition containing a high fraction of masonry, i.e 30C:70M. The density range from 1807kg/m^3 to 1829 kg/m^3 and the optimum moisture from 14.1% to 15.45 % as summarised in Table 4-1.

Furthermore, Table 4-1 presents the results of the aggregates mechanical test, i.e-crushing resistance obtained from the 10% FACT test. It can be seen from this table that the results are the same for both mix compositions since the aggregate fraction (<13.2mm - >9.5mm) specified for this test is the same for both mix compositions. The results of 131 kN for dry 10% FACT test and 89 kN for wet conditions were obtained. This indicates that the material exhibits good resistance to crushing in dry condition because the result obtained is higher than the required (110 kN) for base course material as specified in TRH 14 (1985), COLTO (1998) and SAPEM (2013). However, the obtained dry–wet ratio of 68% failed to meet the minimum of 75% specified in the above-mentioned manuals and specification. This can be explained by the fact that when these aggregates are soaked, the water softens the mortar attached to the aggregates and weakens the clay bricks granulate. When these soft constituents are crushed

during 10% FACT test, they generate more fines at low forces. Gabr & Cameron (2012) have also observed this low crushing resistance of RCM in wet conditions. This reiterates the benefits of the secondary crushing, which in addition to the role of improving the aggregate physical properties reduces the amount of mortar attached to the aggregates.

4.4 MATERIAL BREAK DOWN DURING COMPACTION

The crushing of particles is likely to occur during handling, compaction in the field and during in-service life due to the dynamic loading of the vehicles. The crushing changes the gradation of the material that contributes to better material densification and hence good performance (Leite *et al.*, 2011, Boudlal & Melbouci, 2009). Nevertheless, this should happen during compaction not in service. When this happens at a significant rate during in service due to the cyclic traffic loading, increased pore water pressure could result in pronounced permanent deformation (Nataatmadja & Tan, 2001).

Figure 4-6 and Figure 4-7 present the results of the difference in percentage passing for various aggregate sizes before and after compaction. This is the difference between the target grading of the material and the obtained grain size distribution in the material after compaction expressed in terms of the percentage passing on the sieve series. From the figures, no predominant effect of any variable among the mix composition, compaction moisture or degree of compaction was observed regarding the aggregates break down. However, one can see a non-negligible impact of compaction moisture especially with 70C:30M mix composition (Figure 4-6) whereby 70% OMC corresponds to less moisture added for compaction than the 70% OMC of the 30C:70M(Figure 4-7) due to different respective OMC's. A notable increase of 9.5mm aggregates size in the material is observed as illustrated in Figure 4.6 and Figure 4.7 by a negative difference. This could be attributed to the crushing of the coarse fraction i.e 19mm-13.2 characterised by a high content of flaky aggregates as shown by the flakiness index test and presented in Figure 4-3. Appendix A gives the grading before and after compaction.

In conclusion, trend of influence of compaction moisture on material break down after compaction is visible but no distinctive effect of any of the investigated factors was discerned. However, even though crushing has occurred during compaction for the material used in this study but this crushing was not excessive when compared to the results obtained by Leite *et al.* (2011).

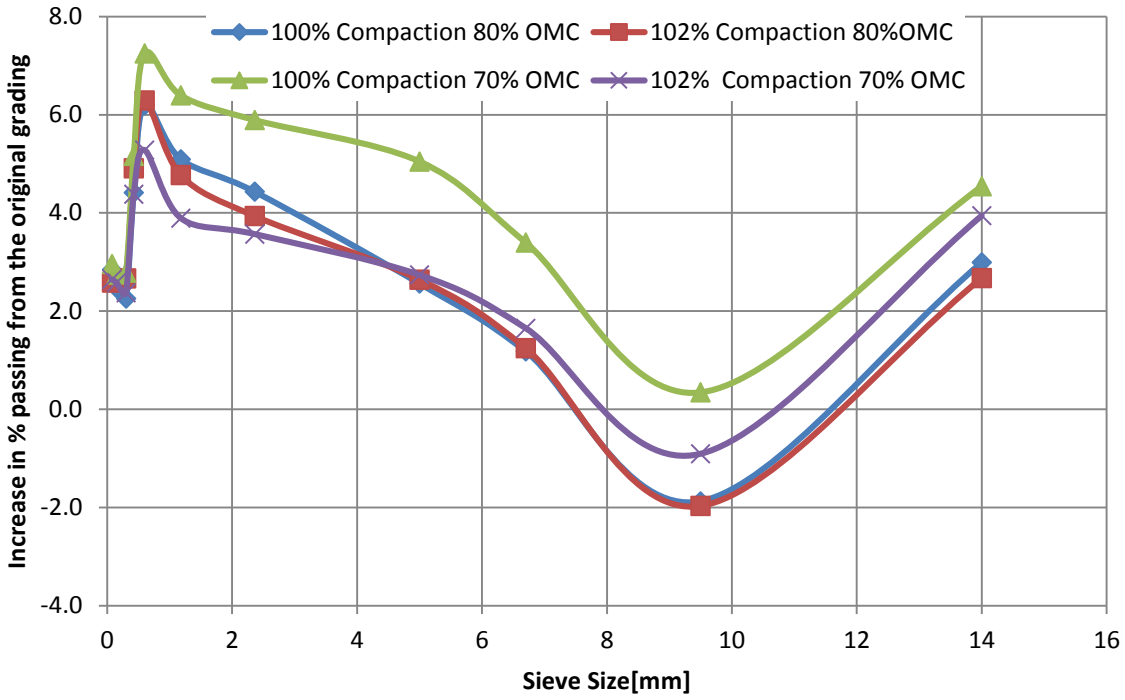

Figure 4- 6: Particle Break Down for the 70C:30M Mix Composition

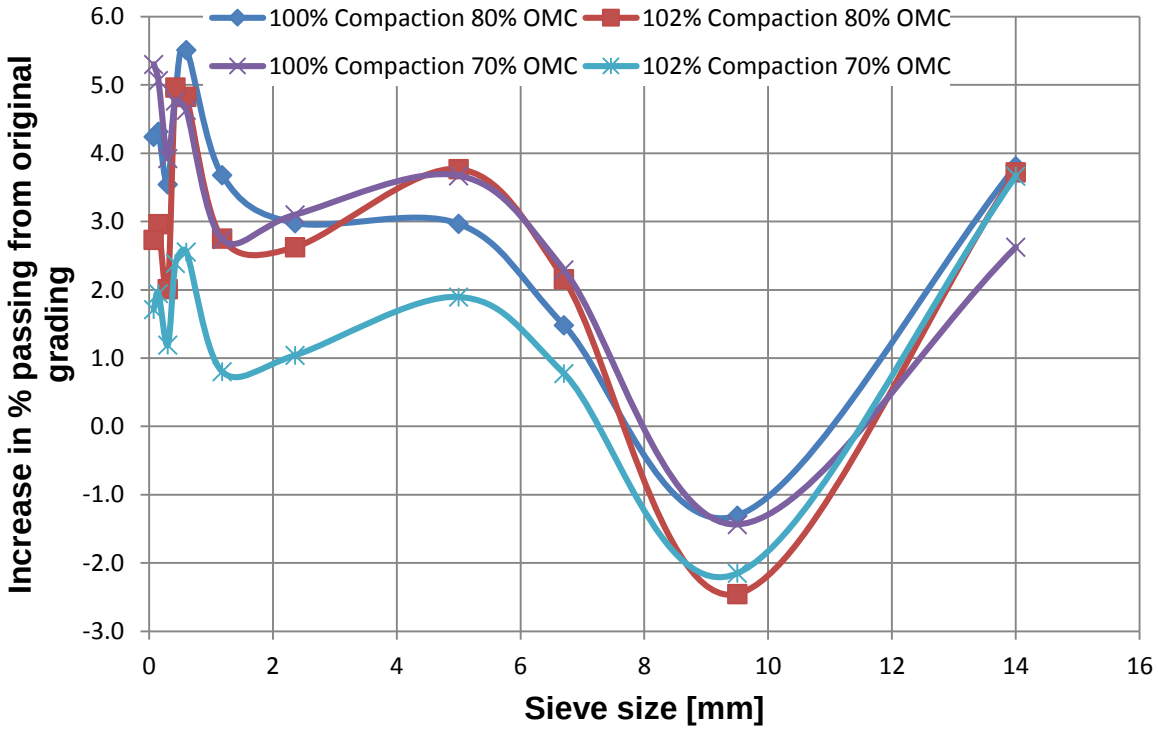

Figure 4- 7: Particle Break Down for the 30C:70M Mix Composition

4.5 MONOTONIC FAILURE TEST RESULTS

Two sets of monotonic triaxial tests were carried out on virgin samples, i.e samples not previously tested, and samples subjected to resilient triaxial testing. This section presents the results of these monotonic tests and the influence of the study variables such as mix composition, compaction moisture and degree of compaction. Furthermore, the results of the impact of stress history on the failure behaviour as obtained by monotonic testing after cyclic loading of the resilient modulus test are also presented. To understand the failure behaviour of RCM, the Mohr-Coulomb failure criterion was considered. This failure model characterises material through failure parameters C and ϕ. The results of shear or failure parameters for each investigated variable is summarised in Table 4-2 and Table 4-3.

Table 4- 2: Monotonic Test Results for Virgin Samples

Mix composition	Compaction Moisture (%)	Degree of Compaction (%)	Curing time (days)	Testing Moisture (% OMC)	C(kPa) Φ (^{0})	Model R^2
70C:30M	70[1] *68.1-73.1*[2]	100 *100.2-100.6*	4	65 *65-66*	223 45.4	0.997
	80 *79.6-81.3*	100 *100.2-100.8*	4	65 *64-70*	266 48.72	0.993
	70 *70.3-74*	102 *101.9-102.2*	4	65 *64-68*	314 48.4	0.919
	80 82-84.6	102 102-102.3	4	65 64-67	313 51.26	0.992
30C:70M	70 *68.3-71*	100 *100.4-100.8*	4	65 *64-65*	285.9 42.5	0.97
	80 *80.1-84.6*	100 *100-100.5*	4	65 64-68	171.5 50.3	0.956
	70 *70.6-73.1*	102 *101.9-102.5*	4	65 *63-65*	257 48.36	0.998
	80 *80.6-85*	102 *101.7-102.3*	4	65 *63-65*	203 53.61	0.992
Average R^2						0.977

[1]: Target

[2]: Actual range for three samples

The results in Table 4-2 show that the Mohr-Coulomb model can adequately describe the stress dependency of the RCM failure behaviour. This is indicated by the coefficient of determination R^2 averaging 0.977 or 97.7%.

Figure 4-8 gives the stress-strain relationship obtained during the monotonic triaxial test. The curves in this figure as well as the figures included in Appendix B show that the strain corresponding to the ultimate stress ranges from 1% to 3%. This seems to be in good agreement with the results obtained by Jenkins (2000) for granular materials.

Figure 4-8 shows that as the strain increases before failure, the shear strength increases. This indicates that RCM exhibits *strain-hardening* behaviour. Moreover, it can be seen from this figure that the slope of the curve increases as the confinement increases; this shows the *stress stiffening* behaviour of RCM.

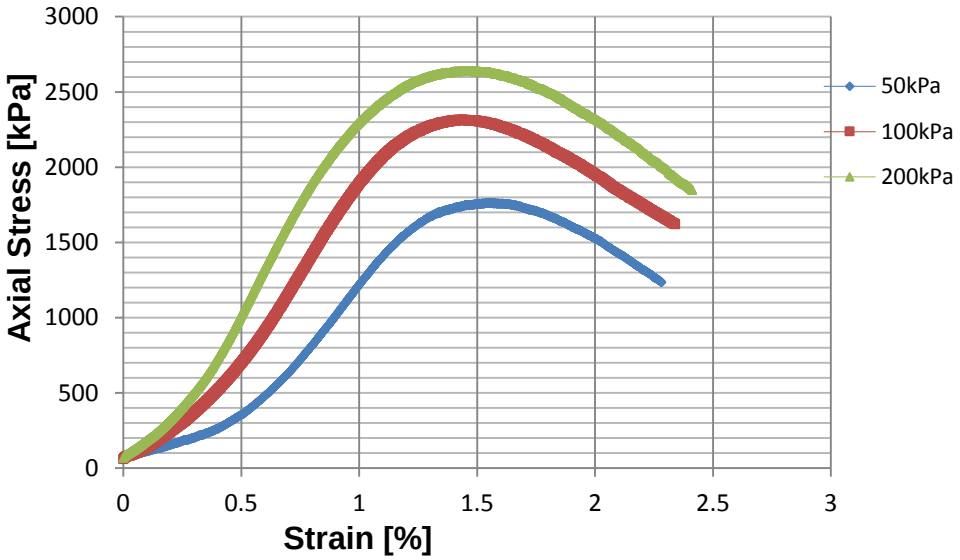

Figure 4- 8: Stress-Strain Relationship for 70C:30M -102%DOC-70%CM

Figure 4-9 provides a stress-strain relationship as a function of the degree of compaction and mix composition. From this figure, the following observations were made:

- The shear strength increases(represented by ultimate axial stress at failure) with an increase of the degree of compaction
- A visible trend in the increase in shear strength by increasing the concrete granulates in the mix composition
- Increase of stiffness (as denoted by the slope of the curve) related to the increase of concrete in the mix composition (70C:30M). However, no clear distinction is provided by this figure on the influence of the degree of compaction on the stiffness. In Section 4-6, this parameter will be discussed in further details.

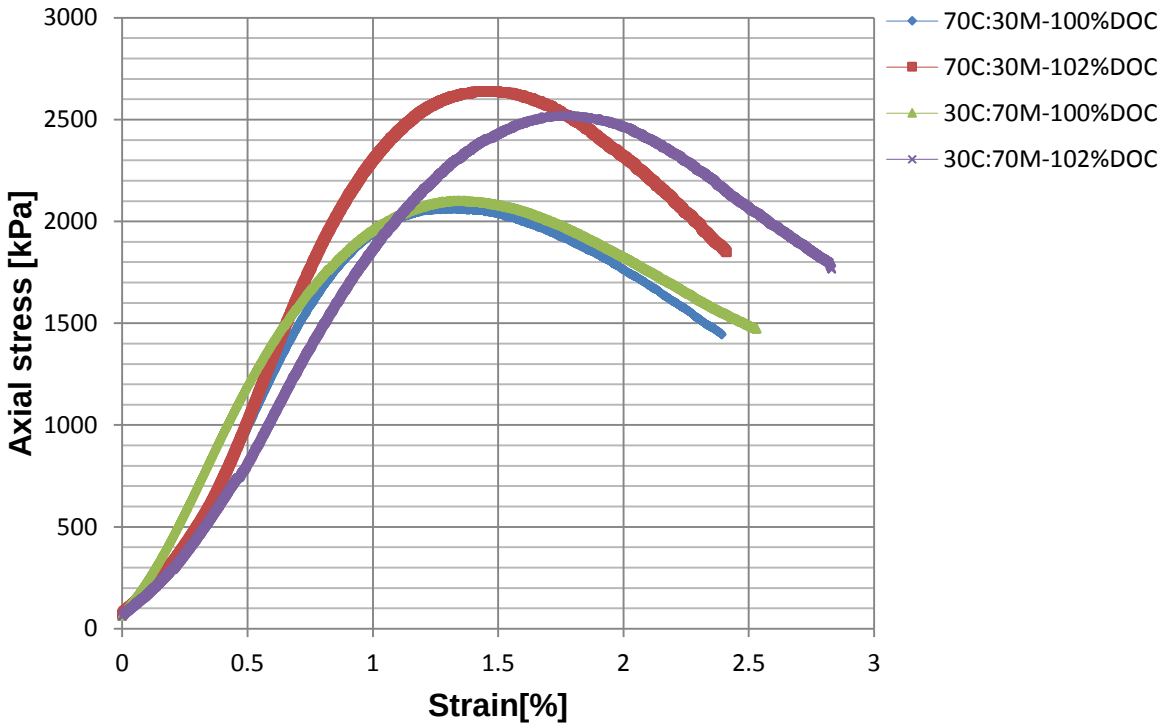

Figure 4- 9 : Stress-Strain Behaviour as a Function of DOC and Mix Composition at 200 kPa Confinement and 70% CM

Figure 4-10 shows a trend in the increase of the cohesion(C) as the degree of compaction increases from 100% DOC to 102%DOC. According to the analysis of the shear failure based on the Mohr-coulomb failure criterion represented geometrically in Appendix C and summarised in Table 2, the following observations were made:

- The shear strength increases with the increase of the degree of compaction. The degree of compaction increases the cohesion of the material by enhancing the interparticle contact.
- The 70C:30M mix exhibits higher shear strength than 30C:70M. This results from the increase of cementitious material in the mix that are likely to generate bonds upon hydration. This enhances the particle interlock and increase the cohesion. The shear strength of 70C:30M also results from the strong aggregate skeleton compared to that of 30C:70M mix.
- No significant difference was observed in shear strength between 70% CM and 80% CM.

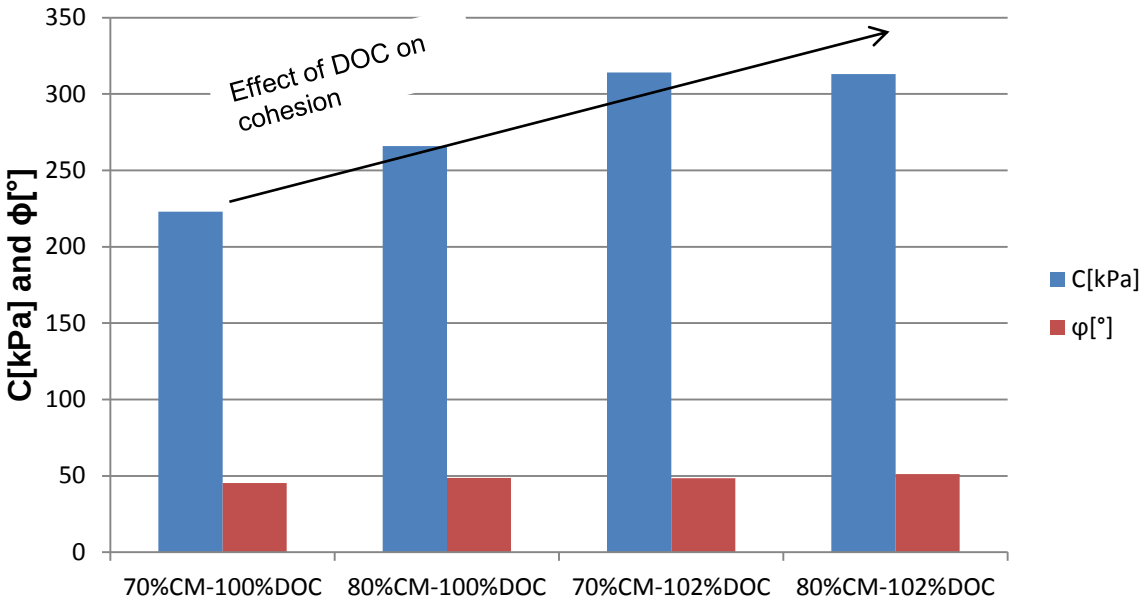

Figure 4- 10 : C and ϕ as a Function of DOC for 70C:30M at 70% CM and 80%CM for Virgin Samples

Table 4- 3 : Monotonic Test Results after Resilient Modulus Test

Mix composition	Compaction Moisture (%)	Degree of Compaction (%)	Curing time (days)	Testing Moisture (% OMC)	C(kPa) Φ (^{0})	Model R^2
70C:30M	70[1] *71.1-72.1*[2]	100 *99.5-100.2*	4	65 *64-67*	236 51.84	-
	80 *80.9-83.7*	100 *100.1-100.5*	4	65 *65-67*	324.5 46.85	-
	70 *69.7-72*	102 *102.2-102.5*	4	65 *62-67*	321.2 52.5	-
	80 81-84.6	102 101.8-102.2	4	65 63-65	443.3 45.77	-
30C:70M	70 *72.6-73*	100 *100.1-100.2*	4	65 *63-66*	342.1 45.2	-
	80 *81.4-83.1*	100 *100-100.3*	4	65 64-68	292.7 45.2	-
	70 *70.6-72.3*	102 *102.1-102.1*	4	65 *64-66*	385.2 48.28	-
	80 *80.8-82*	102 *101.8-102.3*	4	65 *63-64*	509.56 41.48	-

[1]: Target

[2]: Actual range for three samples

The influence of stress history on failure behaviour was assessed in this study by carrying out the monotonic tests on specimens used for cyclic (Mr) testing. The results are summarised in Table 4-3. The regression analysis to obtain shear parameters has been carried out on two points for preloaded specimens. In this case, the R^2 was not reported in Table 4-3, as it would yield a value of one. Appendix D presents The Mohr-Coulomb model for the preloaded specimens.

Figure 4-11 and Figure 4-12 illustrate a significant increase of the cohesion(C) whilst the friction angles range in the same order of magnitude between virgin specimens and specimens tested after the Mr test. This substantiates the results obtained by Van Niekerk (2002) for recycled materials in these two different specimen conditions. An explanation given by Van Niekerk (2002) is that the increase in shear strength results from post compaction or consolidation due to cyclic loading which increases the interparticle contact. The limited load cycles during the Mr test further compact the specimen but with low risk of damaging the entire specimen or waning out the aggregates surface as shown by the low difference in friction angle presented in Table 2 compared to Table 3. Therefore, the specimen will strengthen without failing during these cyclic loadings.

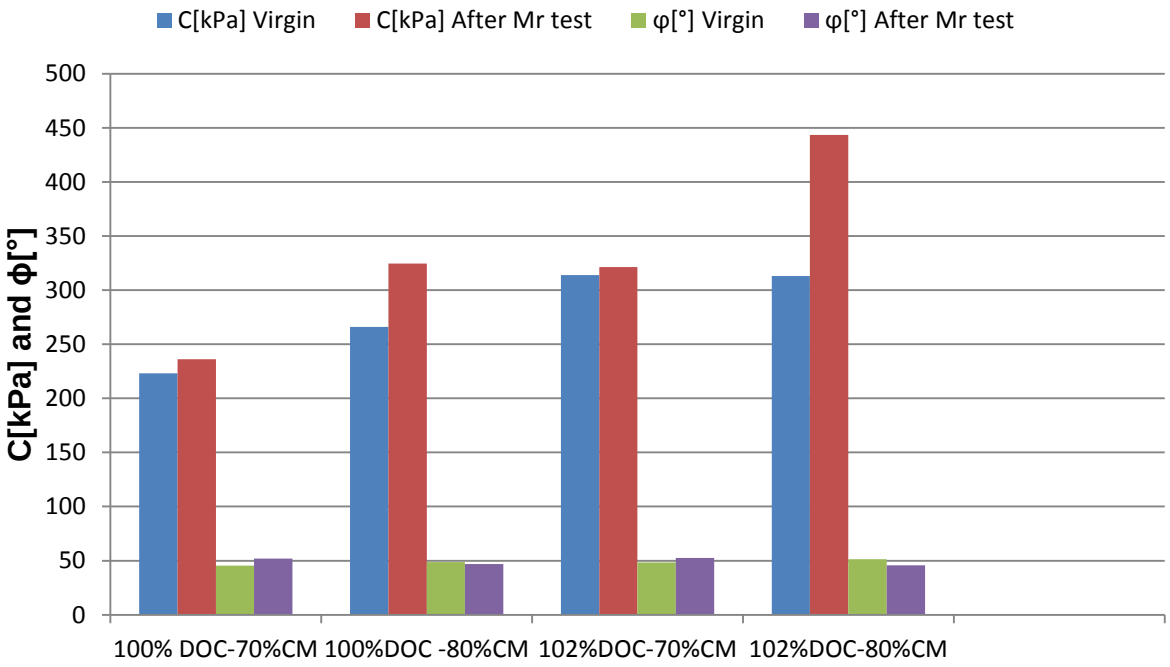

Figure 4- 11: Shear Parameters for Virgin Samples and after Mr Test for 70C:30M Mix Composition

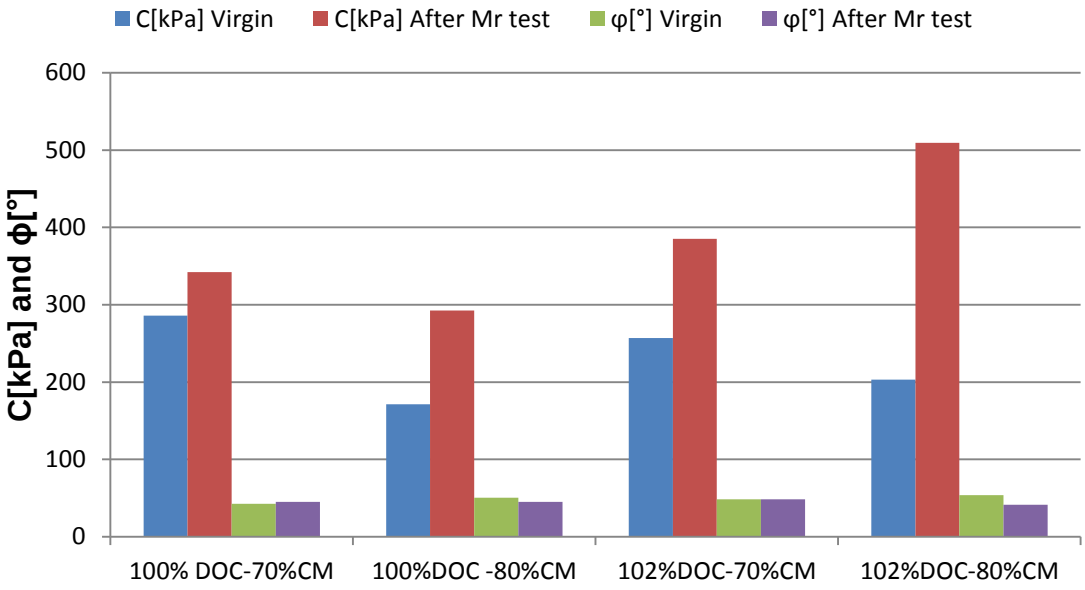

Figure 4- 12: Shear Parameters for Virgin Samples and after Mr Test for 30C:70M Mix Composition

Figure 4-12 shows a significant increase (more than 100%) of the cohesion after cyclic test for 30C:70M-102% DOC- 80% CM specimen. One can imagine based on the slight pumping of water that occurred during compaction that high moisture availability during compaction caused a certain degree of floating of particles. This floating resulted in some water-filled voids in the compacted sample. These voids were reduced through further compaction due to cyclic loading that resulted in higher cohesion. This trend is also observed for both mix compositions and degrees of compaction when a comparison is made on the average increase in cohesion for virgin and preloaded samples for the two compaction moistures (70% and 80%). Figure 4-11 and Figure 4-12 show these trends; however, a remarkable difference in cohesion is observed for the 30C:70M mix composition.

4.6 RESILIENT TRIAXIAL TEST RESULTS

The resilient modulus and the Poisson Ratio describe the resilient response of granular material. Resilient triaxial test was carried out to investigate the influence of the study variables, i.e mix composition, compaction moisture and the degree of compaction on the resilient deformation. Section 2.3.6.2.1 discussed two approaches that are used in computational modelling of the resilient response of granular materials. In this study, the approach which defines the resilient response by means of resilient modulus and Poisson Ratio was used since it is the well known approach in South Africa. This section comprises of two main parts:

- The first part consists of calibrating the four constitutive models discussed in Section 3.6.2.2 to the obtained resilient response test results and deriving the model parameters and R^2. In this part comprehensive discussions are also provided
- The second part presents the results and discusses the effect of each study factor on the resilient modulus and Poisson Ratio. It also provides the relative magnitude effects of the mix composition, compaction moisture and degree of compaction on the resilient modulus and Poisson Ratio.

4.6.1 Models calibration results

The literature reviewed provides a number of mathematical models for describing the stress dependence of the resilient response of granular materials. However, an important aspect is to select an appropriate model that exhibits a good correlation with the testing regime and material behaviour. To this end, four models, i.e two for resilient modulus and two for Poisson Ratio were selected to fit the obtained results of the resilient response testing. The Mr-Θ model (Equation 15) and the Mr-Θ-σ_d/ σ_{df} model (Equation 20) were calibrated to the test results for the resilient modulus. The Poisson Ratio data have been fitted with two models; the "exponential" ν-σ_d/σ_3 model (Equation 22) and ν-σ_d/σ_3-σ_3 model (Equation 23). These models were fitted to the data by means of non-linear regression analysis. Appendix F discusses this method.

Table 3-2 presents the loading sequences used in this test. The highest stress level used during resilient testing was 55% of the failure level of the material ($0.55\sigma_{df}$). This testing regime, which is qualified as "mild" since it is well below the failure stress, was selected with the aim of avoiding damage of the bonds developed due to probable self-cementing.

This section compares the best fitting of the above-mentioned models and discusses the stress dependency of the RCM material. The representative figures are given in the text but the comprehensive figures on all tests are given in Appendix E. However, to avoid that the representation becomes laborious, models were combined in one figure for each test results and the summary of the models coefficients and the coefficient of determination R^2 for all test results based on "homogenous" series(mix composition for example) are presented in Table 4-4 through Table 4-11. The models coefficients are indication of the material stiffness (K_1), the rate of increase in stiffness as bulk stress increases (K_2) for Mr-Θ model or the decrease of Mr as the material is loaded at failure (K_3) and the shape of that decrease (K_4) for the extended Mr-Θ.

For example, the characteristic of the material, i.e stiffness represented by K_1 and rate of stiffening given by K_2 as presented in Table 4-4 to 4-11 for different mix composition,

compaction and degree of compaction for Mr-Θ model, can be discerned through model lines changes in Figure 4.21 to Figure 4.23 in Section 4.6.2.

70C:30M resilient response testing (test series 1)

Figure 4-13 shows the plot for test results (data), fitted Mr-Θ and Mr-Θ-σ_d/ σ_{df} models for 70C:30M-102%DOC-70%CM sample. It can be seen that both models fit the measured resilient modulus data but with better fitting provided by Mr-Θ-σ_d/ σ_{df} (R^2= 0.964) than that of the Mr-Θ model with a R^2= 0.899. Figure 4-13 shows also that the Mr increases with the confinement and stress ratio. This is in good agreement with stress dependency of granular materials. However, with the use of the Mr-Θ-σ_d/ σ_{df} model, it was not possible to distinguish the stiffening to softening behaviour because the material was tested at the "mild" stress regime. It is believed that in this stress regime, the material experiences only stiffening. Therefore, the simple Mr-Θ as well as the extended Mr-Θ-σ_d/ σ_{df} describe almost perfectly the observed stress dependency of Mr.

The best fitting for both models is also observed for the full testing series1 as presented in Table 4-4. This is indicated by the R^2 averaging 0.935 for Mr-Θ and 0.971 for Mr-Θ-σ_d/ σ_{df} for four different tested samples of the 70C:30M mix composition.

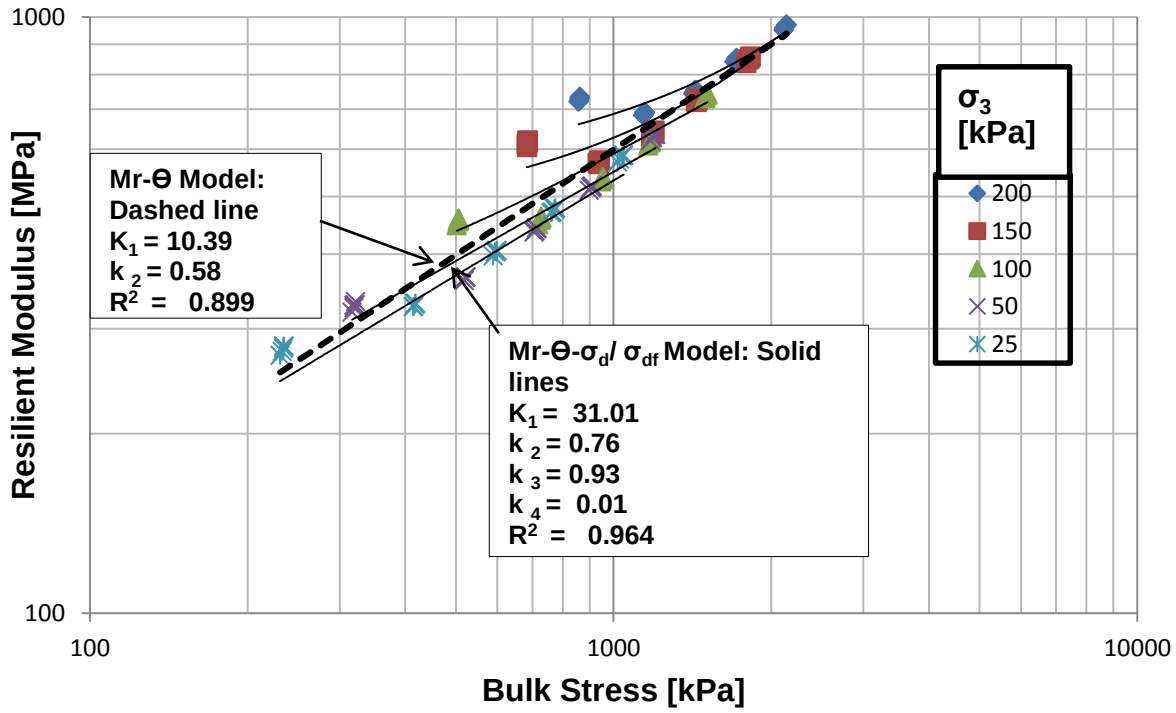

Figure 4- 13 : Data, Mr-Θ and Mr-Θ-σ_d/ σ_{df} Models for 70C:30M- 102%DOC- 70%CM

Table 4- 4 : Model Parameters and R^2 for Mr- Θ Model and Mr- Θ-σ_d/σ_{df} Model for 70C:30M Mix Composition

CM (%)	DOC (%)	Curing (days)	T M (% OMC)	**Mr- Θ**			**Mr- Θ -σ_d/σ_{df}**				
				k_1	K_2	R^2	K_1	K_2	K_3	K_4	R^2
70[1] *72.1*[2]	100 *100.2*	4	65 *64*	8.96	0.61	0.897	24.19	0.77	0.90	0.02	0.973
80 *80.9*	100 *100.5*	4	65 *67*	7.52	0.60	0.971	16.23	0.63	0.63	0.01	0.973
70 *72*	102 *102.2*	4	65 *67*	10.39	0.58	0.899	36.01	0.76	0.93	0.01	0.964
80 *81*	102 *102.2*	4	65 *65*	5.86	0.64	0.974	18.81	0.68	0.787	0.01	0.977
Average R^2						**0.935**	Average R^2				**0.971**

[1]: Target

[2]: Actual

Figure 4-14 gives the ν- σ_d/σ_3 plot, obtained test results and fitted "Exponential" ν-σ_d/σ_3 model and "Exponential" ν-σ_d/σ_3- σ_3 model for 70C:30M-102%DOC-70%CM. The figure shows that the resilient Poisson Ratio is also stress dependent. It decreases as the confinement increases and stress ratio σ_d/σ_3 decreases. One can also note a low value of Poisson Ratio for 70C:30M mix (averaging 0.17) in comparison with 30C:70M. The results are however low compared to that obtained by Van Niekerk (2002). This disparity as well as other seldom agreement in research findings for Poisson Ratio as mentioned in Section 2.3.6.2.1 of this study result from the practical complexity related to the required sophisticated instruments to measure consistently the radial strain compared to axial strain.

It is noteworthy to show that the "Exponential" ν-σ_d/σ_3-σ_3 model which takes into consideration the confinement, fits perfectly the observed data (R^2= 0.959) than the "Exponential" ν-σ_d/σ_3 model. However, the latter model also fits the obtained stress dependency of the Poisson Ratio (R^2=0.870) well.

This general trend of best fitting of the "Exponential" ν-σ_d/σ_3- σ_3 model in comparison with "Exponential" ν-σ_d/σ_3 model is observed for all tests of series 1 as presented in Table 4-5. However, the simple "Exponential" ν-σ_d/σ_3 still fit the observed data better with relatively no significant difference observed between these two models, i.e the average coefficient of determination R^2 that is 0.848 and 0.876 respectively for "Exponential" ν-σ_d/σ_3 model" and Exponential" ν-σ_d/σ_3- σ_3 model.

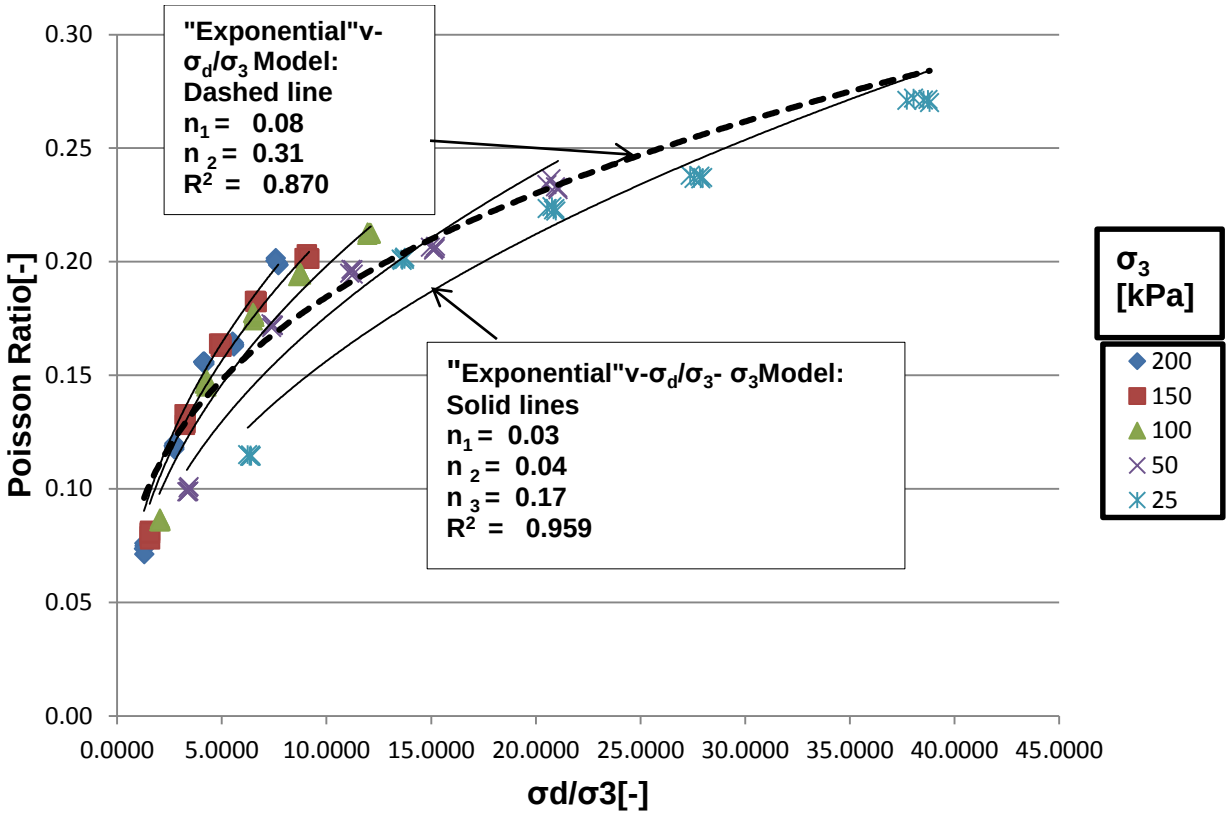

Figure 4- 14 : Data, "Exponential" v-σ_d/σ_3 and "Exponential" v-σ_d/σ_3- σ_3 Models for 70C:30M- 102%DOC- 70%C

Table 4- 5 : Model Parameters and R^2 for "Exponential" v-σ_d/σ_3model and "Exponential" v-σ_d/σ_3- σ_3 model for 70C:30M Mix Composition

CM (%)	DOC (%)	Curing (days)	T M (% OMC)	"Exponential" v-σ_d/σ_3			"Exponential" v-σ_d/σ_3- σ_3			
				n_1	n_2	R^2	n_1	n_2	n_3	R^2
70[1] *72.1[2]*	100 *100.2*	4	65 *64*	0.07	0.41	0.724	0.08	0.40	-0.01	0.724
80 *80.9*	100 *100.5*	4	65 *67*	0.08	0.43	0.896	0.05	0.48	0.06	0.903
70 *72*	102 *102.2*	4	65 *67*	0.08	0.31	0.870	0.03	0.04	0.17	0.959
80 *81*	102 *102.2*	4	65 *65*	0.18	0.21	0.905	0.23	0.18	-0.04	0.921
Average R^2						**0.848**	Average R^2			**0.876**

[1]: Target

[2]: Actual

The results have shown that the resilient modulus was better fitted through mathematical models when compared to the resilient Poisson Ratio. This is shown by the average coefficients of determination R^2 ranging 0.935 to 0.971 for the resilient modulus models compared to R^2 ranging 0.848 to 0.876 for the Poisson Ratio. In addition, for all curves fitting, lower R^2 was yielded on Poisson Ratio model with a value of 0.724. The reason could be attributed to the difficult measurement of radial resilient deformation compared to resilient modulus using normal devices especially at low stresses. This can lead to less agreement between obtained data and model predicted results and hence a lower R^2.

70C:30 M resilient response testing: Duplicate

Figure 4.15 shows the plot for test results (data) and fitted Mr-Θ and Mr-Θ-σ_d/ σ_{df} models for the 70C:30M-102%DOC-70%CM duplicate specimen. By comparing Figure 4-15 to Figure 4-13, good repeatability is observed between stress dependencies of the resilient modulus. This repeatability is also observed for good fitting of models as well as the average coefficient of determination obtained for all four tests as presented in Table 4-6. The Mr-Θ model yielded an average R^2 of 0.935 for the initial test and an average R^2 of 0.921 for duplicate samples.

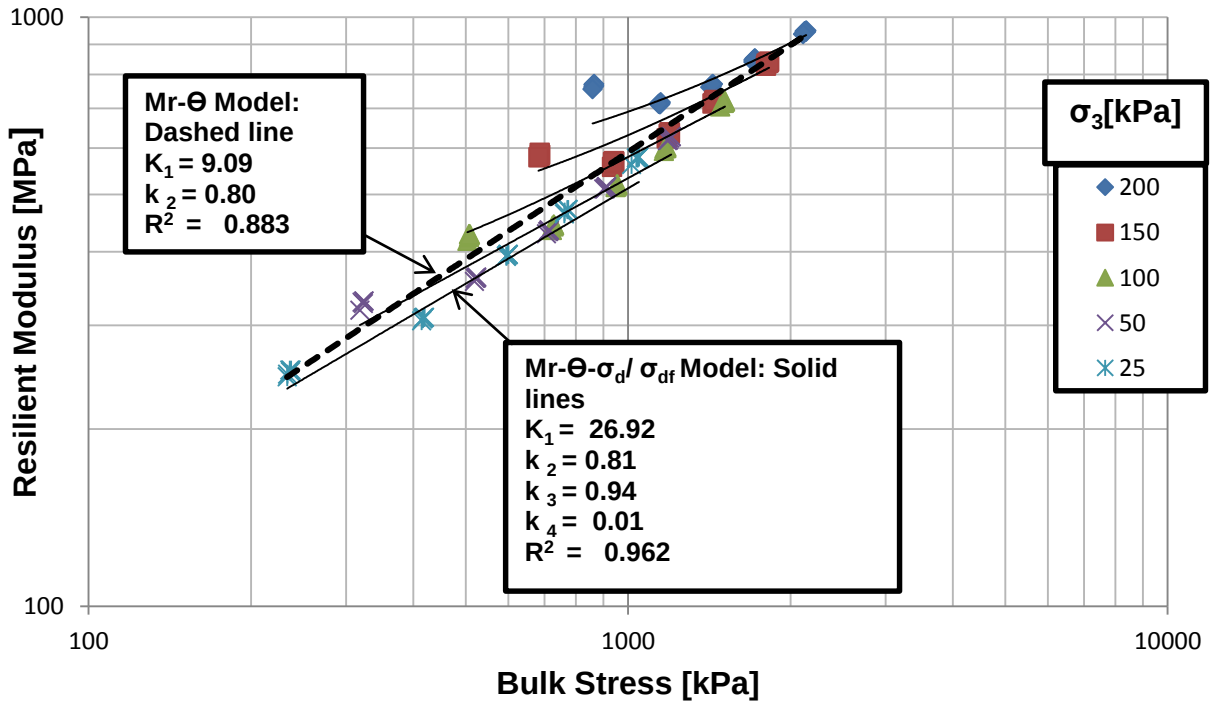

Figure 4- 15 : Data, Mr-Θ and Mr-Θ-σ_d/ σ_{df} Models for 70:C30M-102%DOC - 70%CM Duplicate Sample

Table 4- 6 : Model Parameters and R^2 for Mr-Θ model and Mr-Θ-σ_d/σ_{df} model for 70C:30M Mix Composition Duplicate Sample

CM (%)	DOC (%)	Curing (days)	T M (% OMC)	Mr-Θ			Mr-Θ-σ_d/σ_{df}				
				k_1	K_2	R^2	K_1	K_2	K_3	K_4	R^2
70[1] *71.1*[2]	100 *99.5*	4	65 *67*	9.67	0.58	0.873	31.61	0.74	0.92	0.02	0.958
80 *83.7*	100 *100.1*	4	65 *65*	6.36	0.62	0.954	18.06	0.70	0.81	0.02	0.969
70 *69.7*	102 *102.5*	4	65 *62*	9.09	0.80	0.883	26.92	0.81	0.94	0.01	0.962
80 *84.8*	102 *101.8*	4	65 *63*	6.95	0.62	0.979	28.25	0.66	0.82	0.01	0.983
Average R^2						**0.921**	Average R^2				**0.968**

[1]: Target

[2]: Actual

Figure 4-16 gives the ν- σ_d/σ_3 plot, obtained test results and fitted "Exponential" ν-σ_d/σ_3 model and "Exponential" ν-σ_d/σ_3- σ_3 model for the duplicate sample 70C:30M-102%DOC-70%CM. A similar trend of repeatability for resilient Poisson Ratio stress dependency is also notable.

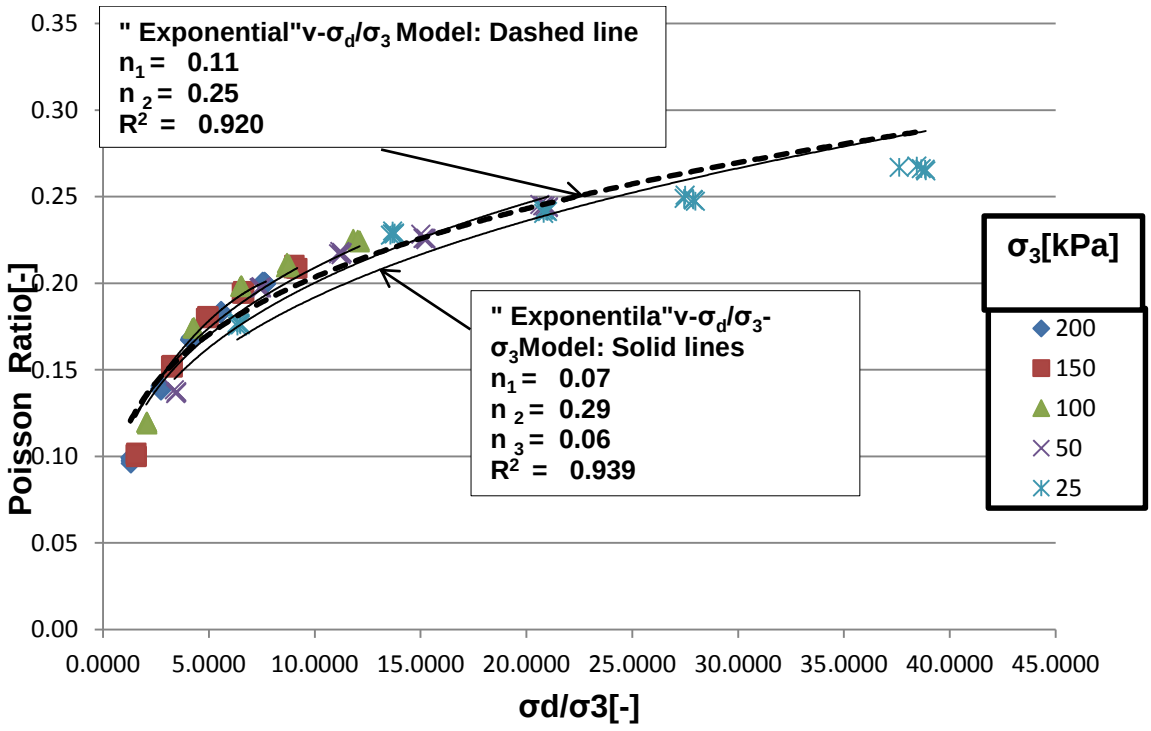

Figure 4- 16 : Data, ν-σ_d/σ_3 and ν-σ_d/σ_3- σ_3 Models for 70C:30M-102%DOC- 70%CM Duplicate Sample

Table 4-7 shows the repeatability trends for all four tests of the duplicate specimens. However, the magnitude of repeatability for the resilient modulus is higher compared to the Poisson Ratio as indicated by the R^2's obtained for the initial and duplicate specimens. This can still be attributed to the difficulty related to radial deformation recording devices.

Table 4- 7 : Model Parameters and R^2 for "Exponential" ν-σ_d/σ_3model and "Exponential" ν-σ_d/σ_3- $\sigma_3$model for 70C:30M Mix Composition Duplicate Sample

CM (%)	DOC (%)	Curing (days)	T M (% OMC)	"Exponential" ν-σ_d/σ_3			"Exponential" ν-σ_d/σ_3- σ_3			
				n_1	n_2	R^2	n_1	n_2	n_3	R^2
70[1] *71.1*[2]	100 *99.5*	4	65 *67*	0.02	0.79	0.646	0.57	0.33	-0.59	0.781
80 *83.7*	100 *100.1*	4	65 *65*	0.14	0.21	0.933	0.12	0.23	0.02	0.936
70 *69.7*	102 *102.5*	4	65 *62*	0.11	0.25	0.920	0.07	0.29	0.06	0.939
80 *84.8*	102 *101.8*	4	65 *63*	0.03	0.52	0.815	0.04	0.8	0.34	0.927
Average R^2						**0.828**	Average R^2			**0.895**

[1]: Target

[2]: Actual

Briefly, it was observed that the two resilient models Mr-Θ and Mr-Θ-σ_d/ σ_{df} could closely fit the observed resilient modulus stress dependency as shown by initial test samples and their respective duplicates coefficients of determination. This good fitting applies also for the resilient Poisson Ratio test data. However, better repeatability was observed for the resilient modulus than for the Poisson Ratio due to the reason mentioned above.

30C:70 M resilient response testing (test series 2)

Figure 4-17 presents the plot for data and fitted Mr-Θ and Mr-Θ-σ_d/ σ_{df} models for 30C:70M-100%DOC-80% CM sample. Both these models almost fit perfectly the observed stress dependency of the resilient modulus with R^2= 0.966 for the simple Mr-Θ and R^2= 0.978 for the extended Mr-Θ-σ_d/ σ_{df}. Table 4-8 shows also the consistency in best fitting of these resilient modulus models on the observed stress dependency of Mr. This is indicated by the average R^2 values for the overall tests of series 2 that are 0.926 for Mr-Θ model and 0.942 for Mr-Θ-σ_d/ σ_{df} model.

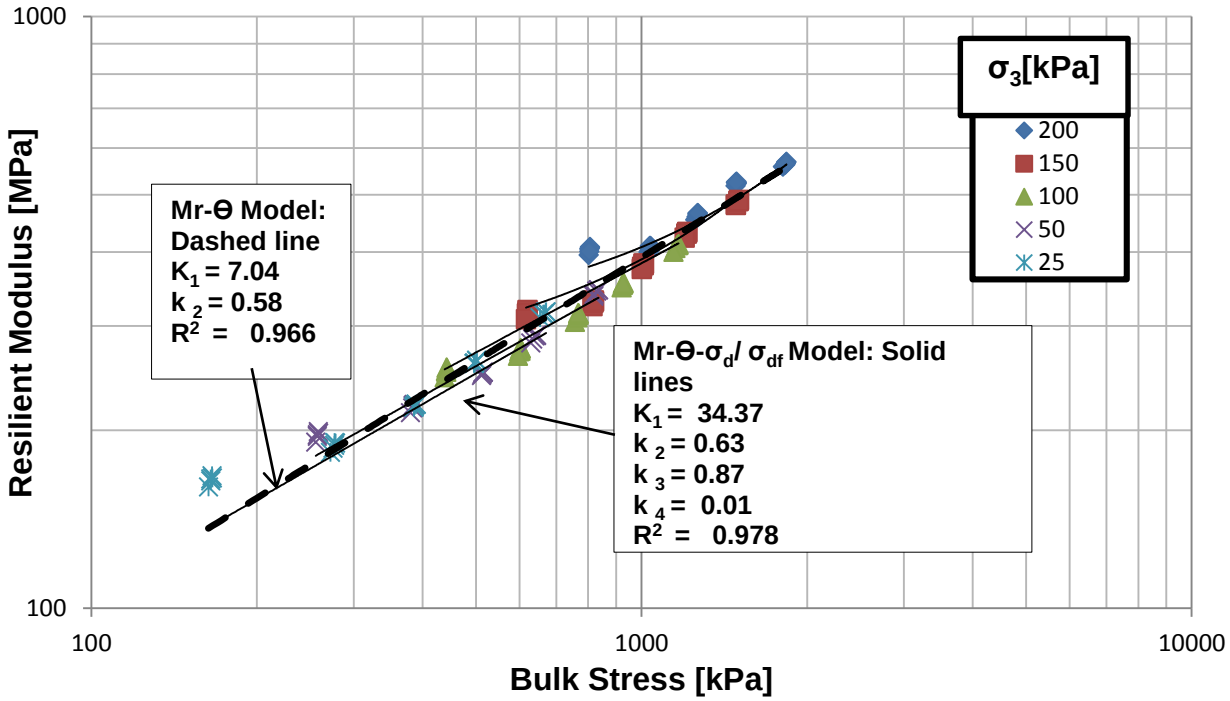

Figure 4- 17: Data, Mr-Θ and Mr-Θ-σ_d/ σ_{df} models for 30C:70M- 100%DOC- 80%CM

Table 4- 8 : Model parameters and R^2 for Mr-Θ Model and Mr-Θ-σ_d/σ_{df} Model for 30C:70M Mix Composition

CM (%)	DOC (%)	Curing (days)	T M (% OMC)	**Mr-Θ**			**Mr-Θ-σ_d/σ_{df}**				
				k_1	K_2	R^2	K_1	K_2	K_3	K_4	R^2
70[1] *72.6*[2]	100 *100.2*	4	65 *66*	16.26	0.48	0.818	35.27	0.62	0.86	0.03	0.908
80 *81.4*	100 *100.3*	4	65 *68*	7.04	0.58	0.966	34.37	0.63	0.87	0.01	0.978
70 *72.3*	102 *102.1*	4	65 *66*	6.70	0.60	0.956	33.48	0.67	0.88	0.01	0.968
80 *82*	102 *101.8*	4	65 *64*	5.12	0.62	0.967	8.23	0.54	-0.77	2.43	0.986
Average R^2						**0.926**	Average R^2				**0.942**

[1]: Target

[2]: Actual

Figure 4-18 gives the ν- σ_d/σ_3 plot, the obtained test results and fitted "Exponential" ν-σ_d/σ_3 model and "Exponential" ν-σ_d/σ_3- σ_3 model for the 30C:70M-100%DOC-80%CM sample. The models fitted well the observed stress dependency of the Poisson ratio. The R^2 = 0.860 for the simple "exponential" ν- σ_d/σ_3 and R^2= 0.892 for the "exponential" ν-σ_d/σ_3- σ_3 model were

obtained. An increase of the Poisson Ratio is notable for the 30C:70M mix composition compared to the 70C:30M mix composition. It can be argued that higher compaction (102%DOC) for the 70C:30M mix composition contributed to reduce the radial deformation by enhancing interparticle contact compared to lower compaction (100%DOC) for 30C:70M mix composition. In addition, radial deformation reduces due to addition of strong aggregate in the mix, which has an influence on aggregates matrix. Self-cementing is likely to happen for 70C:30M mix composition that could have residual active concrete fines. When these active fines hydrate, they generate bonds due to self-cementing which in return prevent dilation when the material is loaded. This can explain the observed low values of Poisson Ratio for the 70C:30M mix.

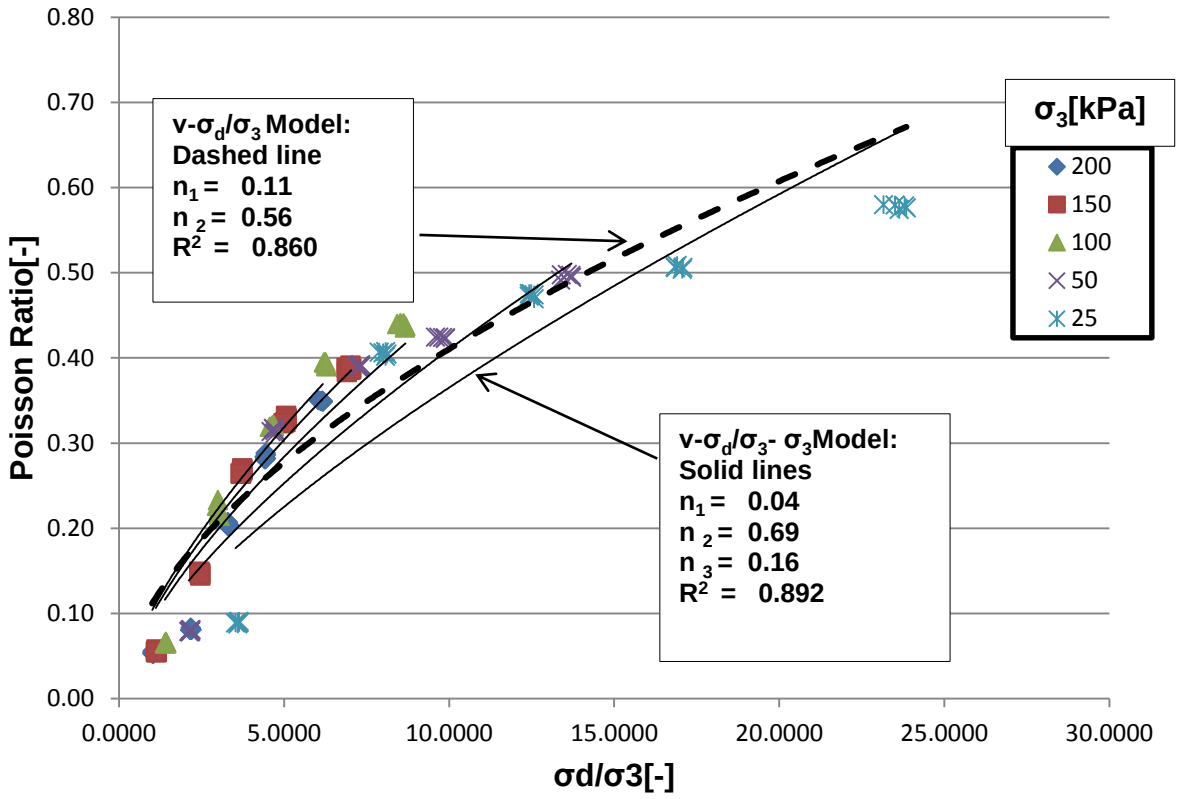

Figure 4- 18 : Data, v-σ_d/σ_3 and v-σ_d/σ_3- σ_3 Models for 30C:70M-100%DOC- 80%CM

Table 4-9 presents individual and the average R^2 values of test series 2 for the resilient Poisson Ratio. The average coefficient of determination R^2= 0.916 for "exponential" ν- σ_d/σ_3 and R^2= 0.926 for "exponential" σ_d/σ_3- σ_3 model were obtained for this test series.

Table 4- 9 : Model Parameters and R^2 for "Exponential" v-σ_d/σ_3 Model and "Exponential" v-σ_d/σ_3- σ_3 Model for 30C:70M Mix Composition

CM (%)	DOC (%)	Curing (days)	T M (% OMC)	"Exponential" v-σ_d/σ_3			"Exponential" v-σ_d/σ_3- σ_3			
				n_1	n_2	R^2	n_1	n_2	n_3	R^2
70[1] *72.6*[2]	100 *100.2*	4	65 *66*	0.08	0.43	0.989	0.12	0.37	-0.07	0.982
80 *81.4*	100 *100.3*	4	65 *68*	0.11	0.56	0.860	0.04	0.69	0.16	0.892
70 *72.3*	102 *102.1*	4	65 *66*	0.10	0.32	0.982	0.09	0.33	0.01	0.983
80 *82*	102 *101.8*	4	65 *64*	0.08	0.58	0.835	o.16	0.49	-0.11	0.850
Average R^2						**0.916**	Average R^2			**0.926**

[1]: Target

[2]: Actual

30C:70 M resilient response testing: duplicate

Figure 4-19 shows the plot for data and fitted Mr-Θ and Mr-Θ-σ_d/ σ_{df} models for 30C:70M-100%DOC-80% CM duplicate sample. The models fitted the observed stress dependency of the Mr well. This is shown by the R^2= 0.951 for the simple Mr-Θ model and R^2= 0.965 for the extended Mr-Θ-σ_d/ σ_{df} model. Table 4-10 shows that the best fitting is repeatable by comparing the average R^2 values obtained for the first round with the duplicate samples, i.e R^2= 0.926 and R^2= 0.942 for Mr-Θ model respectively. Mr-Θ-σ_d/ σ_{df} also yielded R^2= 0.944 and R^2= 0.967 for initial and duplicate specimens.

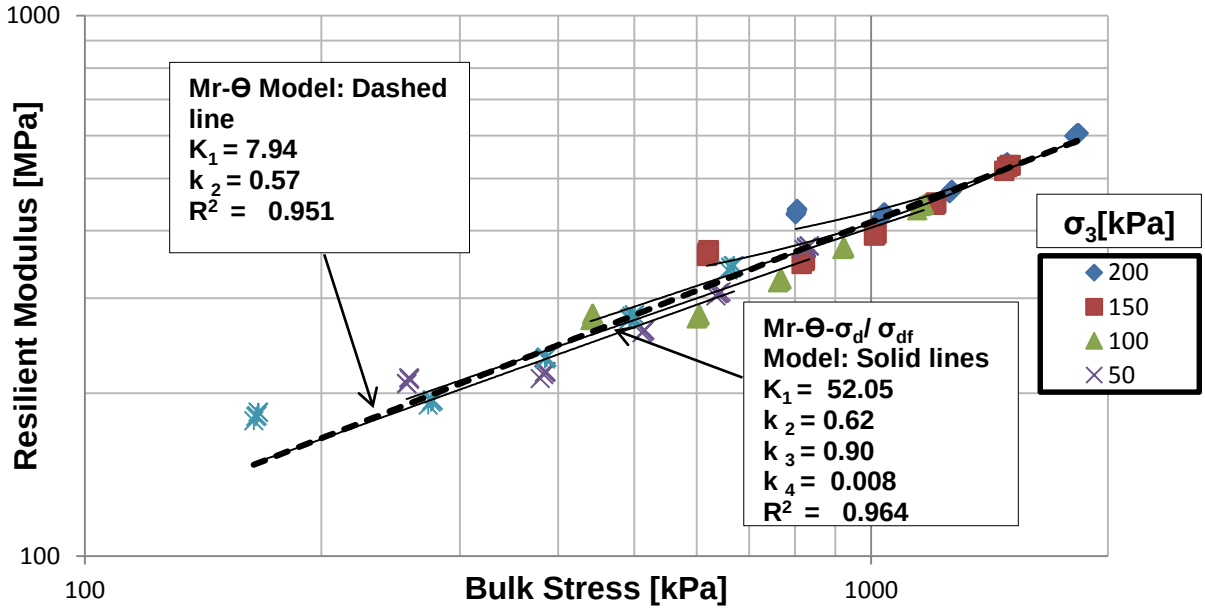

Figure 4- 19 : Data, Mr-Θ and Mr-Θ-σ_d/ σ_{df} Models for 30C:70M- 100%DOC-80%CM Duplicate Sample

Table 4- 10 : Model Parameters and R^2 for Mr-Θ Model and Mr-Θ-σ_d/σ_{df} Model for 30C:70M Mix Composition Duplicate Sample

CM (%)	DOC (%)	Curing (days)	T M (% OMC)	**Mr-Θ**			**Mr-Θ-σ_d/σ_{df}**				
				k_1	K_2	R^2	K_1	K_2	K_3	K_4	R^2
70[1] *73*[2]	100 *100.1*	4	65 *63*	6.53	0.58	0.931	44.69	0.67	0.93	0.008	0.953
80 *83.1*	100 *100*	4	65 *64*	7.94	0.57	0.951	52.05	0.62	0.90	0.008	0.964
70 *70.6*	102 *102.1*	4	65 *64*	7.20	0.61	0.933	46.64	0.75	0.95	0.01	0.976
80 *80.8*	102 *102.3*	4	65 *63*	5.34	0.63	0.962	34.06	0.70	0.91	0.009	0.975
Average R^2						**0.944**	Average R^2				**0.967**

[1]: Intended

[2]: obtained

Figure 4-20 gives the ν- σ_d/σ_3 plot, obtained test results and fitted "Exponential" ν-σ_d/σ_3 model and ν-σ_d/σ_3- σ_3 model for the 30C:70M-100%DOC-80%CM duplicate sample. The models poorly fitted the observed data, which has resulted in low R^2= 0.736 for the simple "exponential" ν- σ_d/σ_3 model and R^2= 0.750 for the "exponential" ν-σ_d/σ_3- σ_3 model. Results presented in Table 4-11 shows variability in average R^2 compared to initial test. The average R^2 of the first round

equals to 0.916 for "exponential" ν- σ_d/σ_3 and 0.926 for "exponential" ν-σ_d/σ_3- σ_3 model whereas for duplicate samples, R^2 were 0.789 for "exponential" ν- σ_d/σ_3 and 0.793 for "exponential" ν-σ_d/σ_3- σ_3 model.

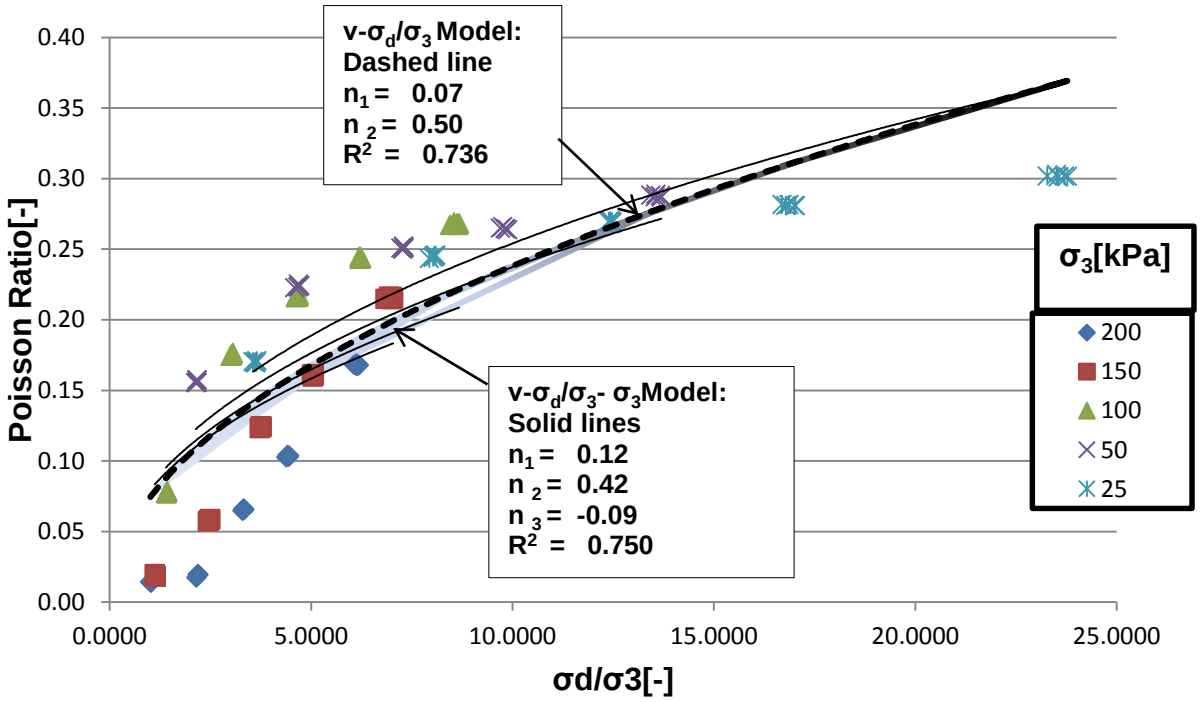

Figure 4- 20 : Data, ν-σ_d/σ_3 and ν-σ_d/σ_3- σ_3 Models for 30C:70M-100%DOC-80%CM Duplicate Sample

Table 4- 11 : Model Parameters and R^2 for "Exponential" ν-σ_d/σ_3model and "Exponential" ν-σ_d/σ_3- $\sigma_3$model for 30C:70M Mix Composition Duplicate Sample

CM (%)	DOC (%)	Curing (days)	T M (% OMC)	"Exponential" ν-σ_d/σ_3			"Exponential" ν-σ_d/σ_3- σ_3			
				n_1	n_2	R^2	n_1	n_2	n_3	R^2
70[1] *73[2]*	100 *100.1*	4	65 *63*	0.05	0.47	0.767	0.07	0.42	-0.068	0.772
80 *83.1*	100 *100*	4	65 *64*	0.07	0.50	0.736	0.12	0.42	-0.09	0.750
70 *70.6*	102 *102.1*	4	65 *64*	0.07	0.36	0.769	0.05	0.40	0.05	0.745
80 *80.8*	102 *102.3*	4	65 *63*	0.14	0.24	0.884	0.10	0.2	0.05	0.908
Average R^2						**0.789**	Average R^2			**0.793**

[1]: Target

[2]: Actual

In general, the results of the test series 2 corresponding to the first round and duplicate resilient response tests for 30C:70M mix composition showed that the two resilient modulus models fitted the data well. The two resilient Poisson Ratio models used in this study also exhibited better fitting for the first round but with poor fitting for duplicate samples. This mix composition exhibited also low range for resilient modulus and a higher range of Poisson Ratio compared with the 70C:30M mix composition in tests series 1 as explained previously. Moreover, tests series 2 were characterised by notable variability between initial and duplicate specimens in Poisson Ratio modelling and results. However, it is possible to deduce that despite the variability, the models fitted the observed stress dependency of the resilient modulus and the Poisson Ratio well.

4.6.2 Influence of investigated factors on the resilient response

Section 4.6.1 highlighted the significant stress dependency of the resilient response of RCM. This was observed through the resilient modulus that increased as the confinement and sum of principal stresses increased. The Poisson Ratio decreased as the confinement increased and the ratio of the deviator stress and the minor principal stresses decreased. Studies seem to agree on the dependency of resilient response of granular material on stress and material saturation. However, literature reviewed showed seldom agreement on the influences of other factors such as density, composition, grading, particle shape, etc on the resilient response (Lekarp *et al.*, 2000).

This section presents the results of the assessed influence of composition or Mix composition (M) characteristics, Degree of Compaction (DOC) and Compaction Moisture (CM) on the resilient response. The trends and magnitudes of the effect of each of the study variables mentioned above are also discussed. Values for resilient modulus and Poisson ratio for each variable is analysed at 300 kPa, 900 kPa and 1500 kPa bulk stress respectively for Mr and 1, 10 and 23 σ_d/σ_3 for Poisson Ratio. These stresses were selected since they represent more or less the minimum, medium and high stress ranges that the materials in this study were subjected to.

Resilient modulus

Figure 4-21 through Figure 4-23 show the trend for the variation in resilient modulus with the change of the degree of compaction, compaction moisture and mix composition as indicated by the shift of the model lines and the arrows.

Figure 4-21 shows the increase of resilient modulus as the composition increases relatively from 30% concrete content to 70% concrete content and the compaction moisture decreases from 80% Modified AASTHO OMC compaction moisture for both 100% and 102% Modified AASTHO MDD degree of compaction. This results in an upward shift of the model lines.

Figure 4-22 shows an increase of the resilient modulus with the increase in concrete content and the change of the degree of compaction from 100% to 102% for both 70% and 80% compaction moisture. From the same figure, one can discern a large influence of mix composition on the resilient modulus. It can be seen from this figure that for the same composition, the degree of compaction does not have a notable impact. These observations are indicated by two separate sets of model lines where a clear gap is observed between the set of model lines illustrating that the 70% concrete mix composition is positioned clearly above the set of the 30% concrete mix composition irrespective of degree of compaction and compaction moisture. This shows a significant increase in the resilient modulus for a 70% concrete content mix composition. The second observation, which indicates that the degree of compaction has lesser influence, is shown by model lines of the same composition which are closer to each other. This is observed for the two different degrees of compaction at both 70% and 80% compaction moisture. This trend can also be observed in Figure 4-21 when comparing the two graphs.

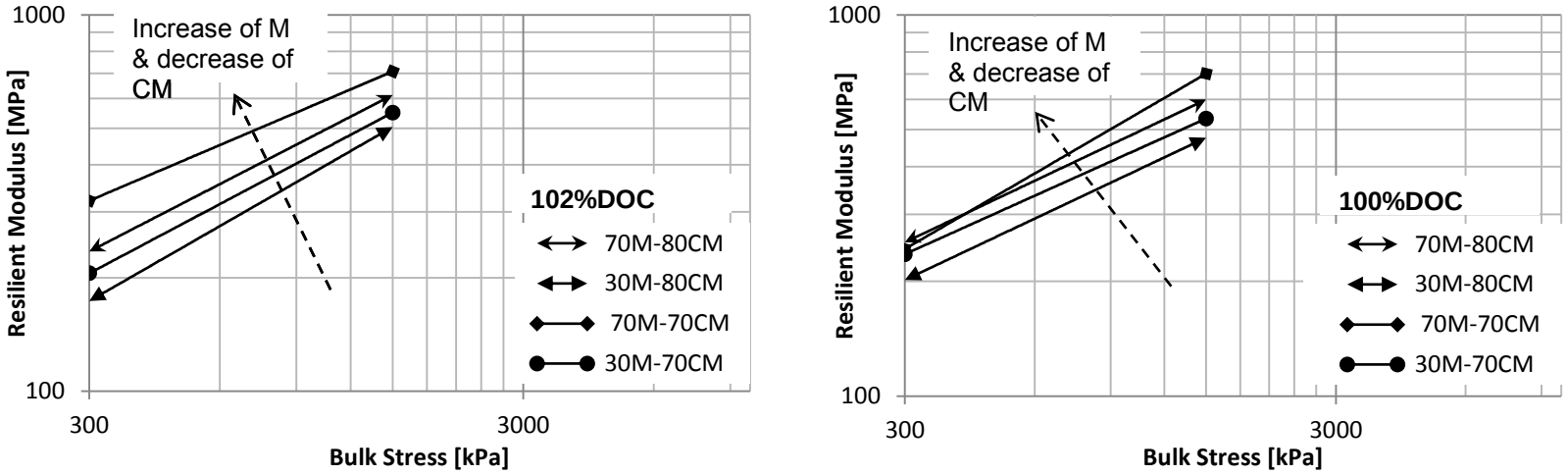

Figure 4- 21 : Variation in Resilient Modulus due to Change in Mix Composition (M) and Compaction Moisture (CM) for 102%DOC (left) and 100%DOC (right)

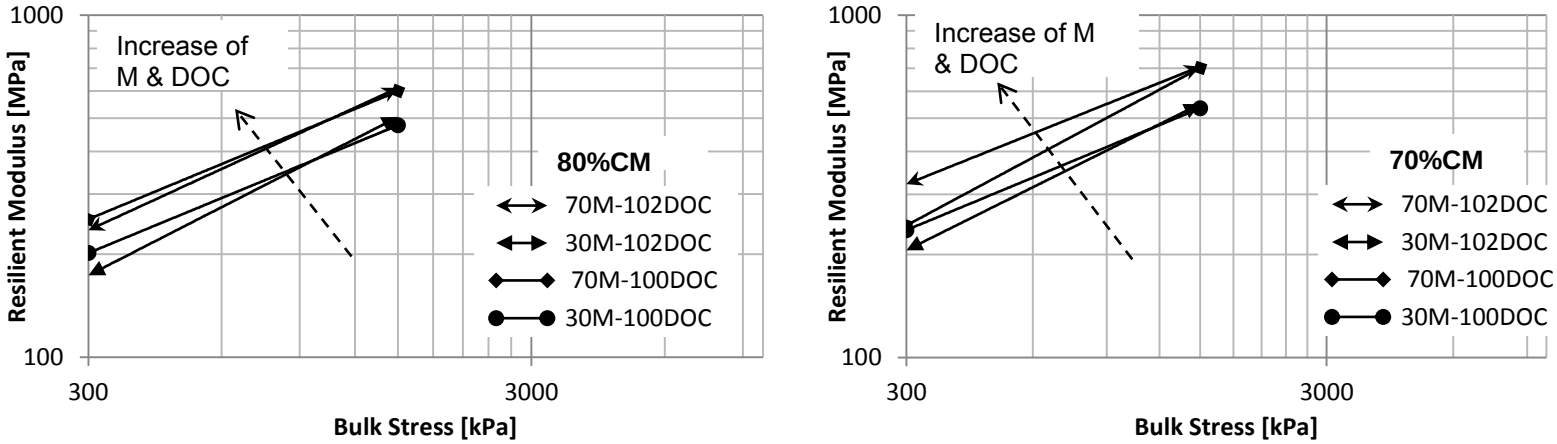

Figure 4- 22 : Variation in Resilient Modulus due to Change in Mix composition (M) and Degree of Compaction (DOC) for 80 % CM (left) and 70%CM (right)

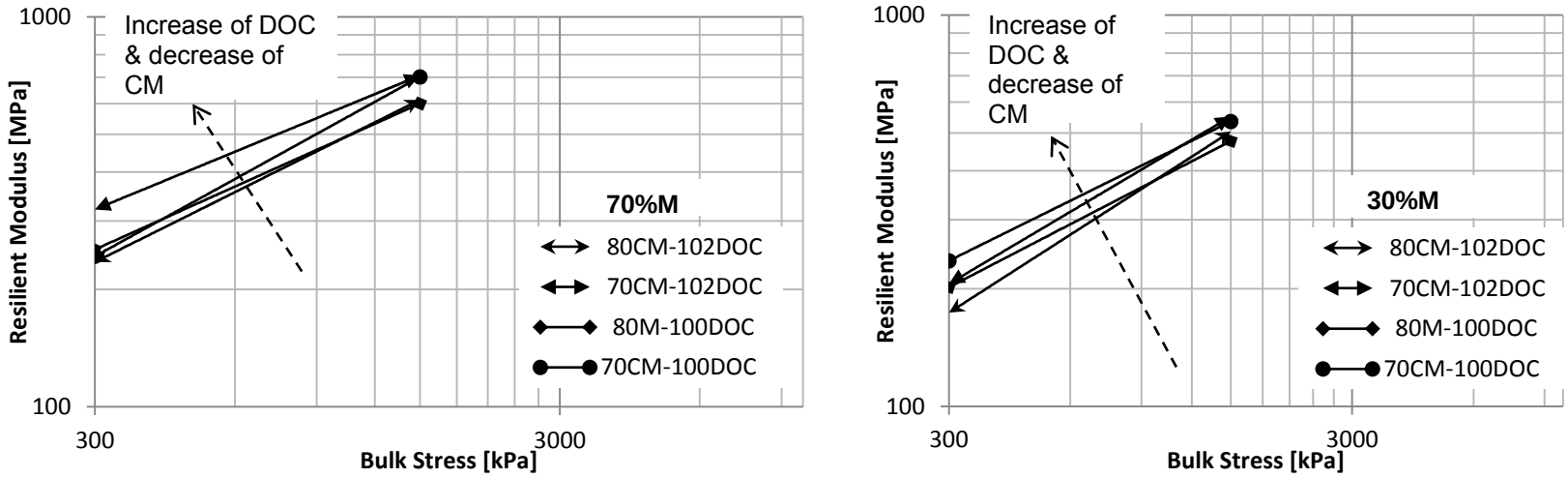

Figure 4- 23 : Variation in Resilient Modulus due to Change in Compaction Moisture (CM) and Degree of Compaction (DOC) for 70 % M (left) and 30% M (right)

Table 4- 12 : Factorial Experimental Design Analysis for the Resilient Modulus

Test run	Mix composition (M)	Compaction Moisture (CM)	Degree of Compaction (DOC)	Average Mr (MPa)	Parameter	effect	Standard error
1	70	80	102	434.68			
2	30	80	102	347.01	M	101.5	
3	70	70	102	527.69	CM	-56.7	
4	30	70	102	387.92	DOC	8.6	± 15.2
5	70	80	100	437.78	DOC x CM	-10,3	
6	30	80	100	347.39	M x CM	-7.2	
7	70	70	100	482.95	M x DOC	-3.3	
8	30	70	100	394.95	DOC x CM x M	-13.6	

Figure 4-23 indicates a noteworthy upward shift of the model lines with a decrease in compaction moisture. However, a less pronounced upward shift of the model lines due to change in the degree of compaction for the same compaction moisture and both mix compositions occurred. Bear in mind that the upward shift in model lines indicates an increase in resilient modulus as a variable change. Moreover, one can also observe from this figure that a mix composition with a relative concrete content of 70% yielded higher resilient modulus than a mix composition with a relative percentage concrete content of 30% when comparing the two diagrams.

The magnitude of the average relative change in Mr resulting from the changing of the composition, compaction moisture and degree of compaction was assessed based on a method of factorial experimental design at two level 2^3 (Box *et al.,* 1978). The details of the calculations are provided in Appendix F and the results are summarised in Table 4-14. The average resilient modulus presented in this table corresponds to the average of the three resilient modulus obtained at the three bulk stresses used for the assessment of the magnitude of the effects.

Table 4-12 shows the average magnitude of the main effects, i.e Mix composition (M), Compaction Moisture (CM) and Degree of Compaction (DOC). It provides also the two-factor interactions, i.e DOC x CM, M x CM and M x DOC and the three-factor interaction effect, i.e DOC x CM x M. It can be observed that changing the mix composition from 30% concrete content to 70% concrete increases relatively 101.5 MPa to the Mr or an increase of closely 30%. This is in good agreement with results obtained by Azam & Cameron (2013) that observed a decrease of 7 to 33% on resilient modulus by replacing 20% recycled concrete with recycled clay bricks. An increase of compaction moisture from 70% to 80% decreases relatively 56.7 MPa to the Mr or a decrease of roughly 13%.

Table 4-12 also indicates that an increase in the degree of compaction from 100% to 102% increases the Mr with only 8.6 MPa corresponding to an average relative increase of 2%. To confirm this interpretation and to assess variables that are worthy to be included in the model, correlation tests, which show a linear relationship between variables, were carried out between the independent variables themselves (M, DOC and CM) and with the dependent variable (Mr). The results of the correlation test are summarised in Table 4-13. The correlation ρ between two variables X and Y named ρ_{XY} varies between -1 and 1($-1 \leq \rho_{XY} \leq 1$). Variables that are strongly correlated have a correlation value that is closer or equal to 1 or -1. In contrast, variables that

are not correlated have a value of the correlation that is zero or close to zero (Montgomery & Runger, 2007).

It is clear from Table 4-13 that the independent variables are less correlated to each other and hence it is possible to deduce that no interaction between independent variables can affect the Mr. Accordingly, all of these independent variables can be interpreted separately and be included in the model because there is a low risk of a multicollinearity effect. However, the same Table 4-13 shows that apart from the degree of compaction, other independent variables have strong correlations with the dependent variable (Mr). Therefore, the degree of compaction should not be included in the Mr model.

Table 4- 13: Correlation Test for Dependent and Independent Variables

	Mr	DOC	M	CM
Mr	1	0.147	0.852	-0.527
DOC	0.147	1	0.094	0.014
M	0.852	0.094	1	-0.0631
CM	-0.527	0.014	-0.0631	1

The observations on the above-mentioned effects were further used during regression analysis on the test results. Several attempts on regression models were carried out in order to describe the relationship between the investigated factors and the resilient modulus. The significance of the overall model was evaluated by the coefficient of determination R^2 and F statistic, and the significance of investigated factors were tested based on P values. Table 4-14 presents the R^2 and P values. However, the description of regression analysis is provided in Appendix F.

Table 4- 14 : R^2 and p values for Mr Regression models

Model	R^2	P values
Mr-M-CM-DOC	0.974	P<0.05 except P(DOC)= 0.476
Mr-M-CM	0.970	P<0.05
Mr-M-DOC	0.748	P(M)=0.01,P(DOC)=0.813
Mr-CM-DOC	0.298	P(CM)=0.21,P(DOC)=0.721

The model selected was the one that describes the resilient modulus in relation with mix composition and compaction moisture. Although this model yielded slightly less coefficient of correlation R^2 (0.970) compared to Mr-M-CM-DOC model with R^2 of 0.974, the values of the P test for the degree of compaction obtained for the latter model was greater than the level of significance α(0.05) taken in this study. This resulted in discarding the degree of compaction

from the model. This confirms the results obtained during the correlation test, which indicated that the degree of compaction had less correlation with the resilient modulus. Moreover, the T test displayed by the regression analysis substantiated the interpretation provided earlier on the magnitude of the effects where the mix composition showed significance followed by the compaction moisture and less distinctively the degree of compaction. Note that discarding the degree of compaction among the parameters that has influence on the resilient modulus does not mean that this parameter does not affect the Mr. However, according to the compaction range (100% to 102%) used in this study no distinctive relative effect was observed compared to the other investigated variables. Therefore, further study is required with a larger compaction window for clearly assessing the influence of compaction on the resilient modulus.
The final relationship of the resilient modulus is given in Equation 34 below:

$$Ln(Mr) = 9.84 + 0.27Ln(M) - 1.12\,Ln(CM) \quad \text{(Equation 34)}$$

Resilient Poisson Ratio

Figure 4-24 to Figure 4-26 show the trend for the variation in resilient Poisson Ratio as the degree of compaction, compaction moisture and mix composition change. This variation is indicated by the relative upward shift of the model lines.

Figure 4-24 shows the trend in variation of the resilient Poisson Ratio as the concrete content decreases and the compaction moisture increases for both 102% and 100% degrees of compaction. One can note a trend in the decrease of the resilient Poisson Ratio as the composition increases relatively from 30% concrete content to 70% concrete content. A decrease is also notable when compaction moisture decreases from 80% to 70 % Modified AASTHO OMC compaction moisture for both 102% and 100% degrees of compaction. This is shown by the downward shift of the model lines. The decrease of the Poisson Ratio indicates less radial deformation of particles during sample loading.

Figure 4-25 shows a trend in the decrease of the resilient Poisson Ratio as the composition increases in concrete content and the degree of compaction increases from 100% to 102% Modified AASHTO MDD for both 70% and 80% compaction moisture. From this figure, it can be argued that compaction does not manifest a distinctive impact when compared to the composition. The less distinctive effect of the degree of compaction on the resilient Poisson Ratio can also be seen in Figure 4-24 when comparing the two diagrams of 102% DOC and 100% DOC.

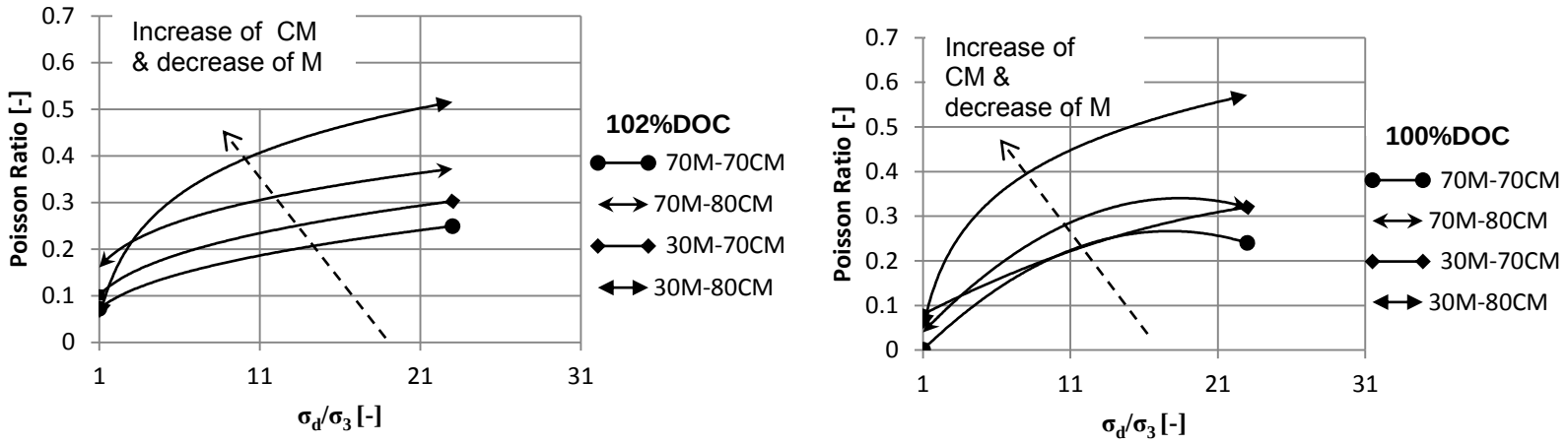

Figure 4- 24 : Variation in Resilient Poisson Ratio due to Change in Mix Composition (M) and Compaction Moisture (CM) for 102%DOC (left) and 100%DOC (right)

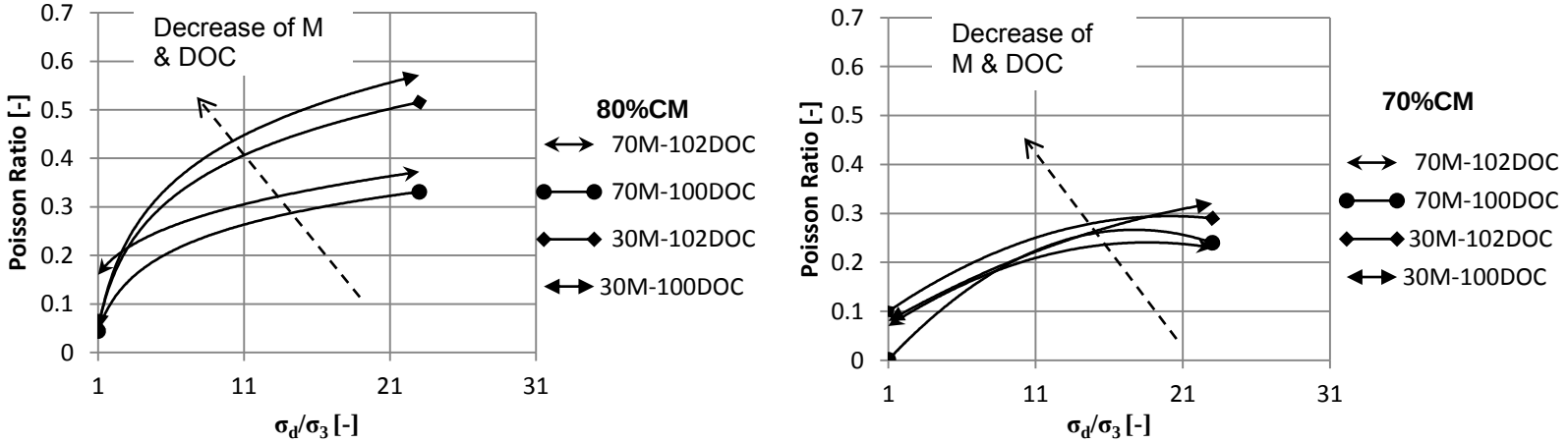

Figure 4- 25 : Variation in Resilient Poisson Ratio due to Change in Mix Composition (M) and Degree of Compaction (DOC) for 80 % CM (left) and 70%CM (right)

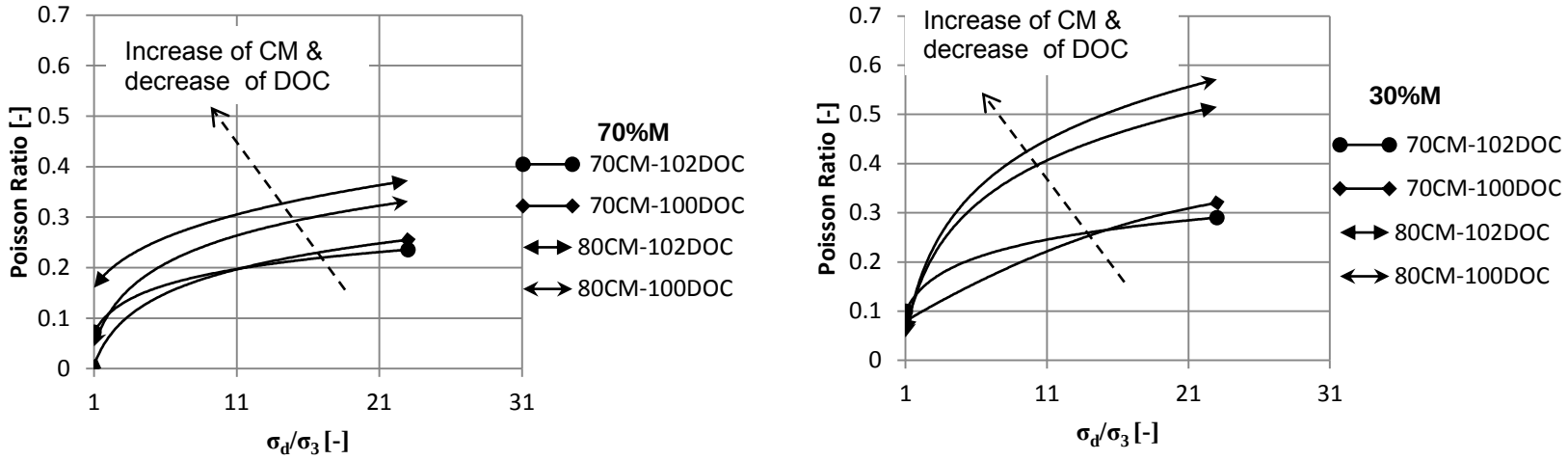

Figure 4- 26 : Variation in resilient Poisson Ratio due to Change in Compaction Moisture (CM) and Degree of Compaction (DOC) for 70 % M (left) and 30% M (right)

Table 4- 15 : Factorial Experimental Design Analysis for the Resilient Poisson Ratio

Test run	Mix composition (M)	Compaction Moisture (CM)	Degree of Compaction (DOC)	Average ν (-)	Parameter	effect	Standard error
1	70	80	102	0.28			
2	30	80	102	0.32	M	-0.07	
3	70	70	102	0.17	CM	0.106	
4	30	70	102	0.21	DOC	0.015	
5	70	80	100	0.21	DOC x CM	0.003	± 0.030
6	30	80	100	0.35	M x CM	-0.021	
7	70	70	100	0.15	M x DOC	0.026	
8	30	70	100	0.20	DOC x CM x M	0.021	

Figure 4-26 presents a trend in the increase of the resilient Poisson Ratio as compaction moisture increases from 70% OMC to 80% Modified AASTHO OMC and the degree of compaction decreases from 102% Modified AASHTO dry density to 102% for both 70% and 30% concrete content mix compositions. An influence of the compaction moisture on the resilient Poisson Ratio is distinctive. This is indicated by two separate sets of model lines where a clear gap is observed between the set of model lines composed by 70% compaction moisture which is positioned clearly below the set of 80% compacted material irrespective of the composition. From this figure also, one can observe low values of Poisson Ratio for the mix composition containing 70% concrete than mix composition with 30% concrete

The relative magnitude of the effect of each of the study variables were assessed using the same approach as mentioned for the resilient modulus. The summary of the results is presented in Table 4-15. Note that the average resilient Poisson Ratio indicated in this table is the average of the three resilient Poisson Ratio corresponding to the three stress σ_d/σ_3 ratios that were used in this study for the evaluation of the investigated factors effects.

Table 4-15 shows the average magnitude of the main effects, i.e mix composition (M), compaction moisture (CM) and degree of compaction (DOC). It provides also the two-factor interactions, i.e DOC x CM, M x CM and M x DOC and the three-factor interaction effect, i.e DOC x CM x M. It can be seen that changing the mix composition from 30% concrete content to 70% concrete decreases the Poisson Ratio value with 0.07 or 25%. An increase of compaction moisture from 70% to 80% increases relatively 0.106 to the ν corresponding approximately to an average relative increase of 60%. Table 4-15 shows also that when the degree of compaction increases from 100% to 102%, ν is increased with 0.015, which corresponds to an average relative increase of 7%. This increase of Poisson Ratio as the degree of compaction increases does not however seem sound according to some theory. To interpret and also to evaluate variables that should be included in the model, correlation tests were carried out between independent variables, i.e M, DOC and CM, and with the dependent variable (ν). The results of the test are summarised in Table 4-16.

It can be observed in Table 4-16 that the independent variables demonstrate less correlation against each other and thus their effect can be interpreted separately. Furthermore, it is important to note that apart from the degree of compaction, other independent variables manifest a strong correlation with the dependent variable (ν). Therefore, the degree of compaction should be discarded from the model.

Table 4- 16 : Correlation Test for Dependent and Independent Variables

	ν	DOC	M	CM
ν	1	0.0705	-0.519	0.822
DOC	0.0705	1	0.094	0.014
M	-0.519	0.094	1	-0.0631
CM	0.822	0.014	-0.063	1

Linear regression analysis was carried out on the investigated factors in order to provide their relationship with the resilient Poisson Ratio. A number of attempts were carried out to obtain the model that can describe the relationship between the dependent variable (ν) and the independent variables (DOC, M and CM). The results of the regression model confirmed the results obtained from the correlation tests, i.e that the degree of compaction should not be part of the relationship model between ν and the independent variables. This is indicated by the P value of the independent variables compared to the level of significance (α) used in this study which is 0,05. The characteristics of these models are summarised in Table 4-17. Moreover, the T test of the regression analysis supported the significant effect of compaction moisture followed by the mix composition on the resilient Poisson Ratio as discussed in the section of the magnitude of the effects early above.

Table 4- 17: R^2 and p values for v Regression models

Model	R^2	P values
ν-M-CM-DOC	0.938	P<0.05 except P(DOC)= 0.308
ν -M-CM	0.918	P<0.05
ν -M-DOC	0.304	P>0.05
ν -CM-DOC	0.699	P(CM)=0.019,P(DOC)=0.705

The final Poisson Ratio relation model is then given by the Equation 35:

$$Ln(\nu) = 3.80Ln(CM) - 0.30\,Ln(M) - 16.78 \quad \text{(Equation35)}$$

Discussion on the observed trends and magnitude of effects

Following the observed trends on the variation of the resilient modulus and Poisson Ratio, the following conclusions are made:

- Increasing the concrete relatively to masonry from 30% to 70% in the mix composition enhances the aggregate skeleton due to the addition of relative strong aggregates. It increases also the likeliness of development of bonds from residual cementitious elements that are comprised in the concrete. This strong skeleton and bonds increase the resilient modulus. In addition, the developed bonds prevent pronounced dilation when the material is loaded and hence decreases the Poisson Ratio.
- Increasing the compaction moisture from 70%OMC to 80%OMC decreases the resilient modulus and increases the Poisson Ratio. This can be explained by the hypothetical role of lubricant that moisture plays on particles. When moisture is increased, the localised pore suctions is reduced and this leads to less interparticle contact forces that reduces the stiffness (Mr) of the material and increases radial dilation due to particles rearrangement when loaded.
- Increasing the degree of compaction from 100% DOC to 102% DOC increases the resilient modulus and reduces the Poisson Ratio. When the degree of compaction is increased, it enhances the particles packing that in return improve the aggregates skeleton. This strong aggregate skeleton exhibits high stiffness (Mr) and can withstand to a certain extent the tension caused by particles rearrangement when loaded thus reduce the radial deformation or the Poisson Ratio.

The analysis of the magnitude of the effects has shown that the resilient modulus was more sensitive to change in mix composition as increasing concrete content increased the resilient modulus with 30%. However, the resilient Poisson Ratio showed high sensitivity to compaction moisture when compared to other variables. This is shown by the fact that increasing the compaction moisture from 70% OMC to 80% OMC increased the Poisson ratio to 60%. The explanation on this behaviour is similar with the ones provided early above on trends.

Note that in the introduction of Section 4.6.2, it was discussed that the resilient response is significantly influenced by stress and saturation. Since the curing protocol adopted has shown slight variability in testing moisture, it was important to assess the possible influence that this variability could have on the resilient response results. Therefore, this parameter was added in the regression analysis with other study parameters. However, no evident influence was

obtained and the parameter was discarded from the final resilient modulus relation model and Poisson Ratio model.

The performance behaviour of secondary materials is quite often compared with natural granular materials that are taken as a reference in order to obtain the relative performance. In this study, RCM was compared with granular crushed stone G1 hornfels (Araya, 2011) in order to gain insight into the performance of RCM compared to high quality natural crushed stones.

G1 material was compacted at 102% DOC at "moderate" compaction moisture of 4%. The testing moisture was performed at 3.9% (Araya, 2011). This G1 material was compared with 30C:70M-100%DOC-80%CM (less stiffer) and 70C:30M-102%DOC-70%CM (stiffer) materials of this research. The comparison was made at four bulk stresses 100 kPa, 300 kPa, 900 kPa and 1500kPa based on the Mr-Θ models as given in Table 4-18.

Table 4- 18 : Mr-Θ Model Parameters and Shear Properties of RCM and G1 (Hornfels)

	K1	K2	C and ϕ
70C:30M-102%DOC-70%CM	10.39	0.58	314 48.4
30C:70M-100%DOC-80%CM	7.04	0.58	171 50.3
G1(Hornfels)	10.66	0.604	130.9 58.6

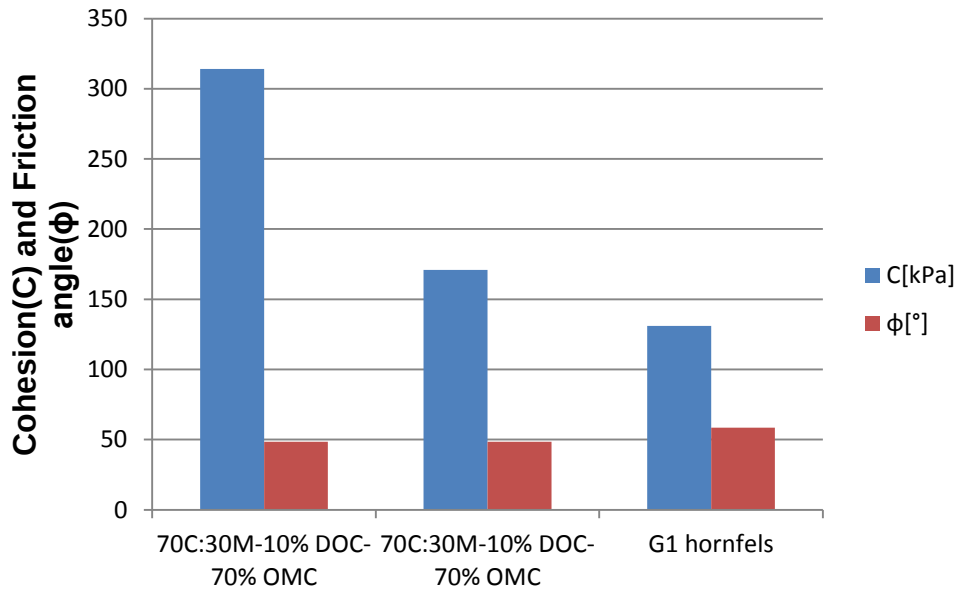

Figure 4- 27 : Shear Parameters of RCM and G1 Hornfels

Figure 4-27 gives the shear parameters of the two RCM mixes and the G1 hornfels. It can be seen that G1 (hornfels) has a higher friction angle which enables it to resist at higher confinement, particularly closely under contact with the wheel load. In contrast, RCM materials exhibit higher cohesion and consequently good shear strength at low lateral confinement which occurs deep in the pavement layers.

It can be observed from Figure 4-28 that the high quality G1 (hornfels) exhibits higher stiffness followed by 70C:30M-102%DOC-70%CM and 30C:70M-100%DOC-80%CM. Figure 4-28 shows that at low stress levels (low bulk stress) the well-compacted RCM demonstrates the same stiffness as the high quality G1 material due to its cohesive nature. However, the natural aggregate shows a notable difference in stiffness as stresses increases from 100 kPa to 1500 kPa creating a gap with RCM materials. This increase results from high G1 friction angle as discussed earlier above.

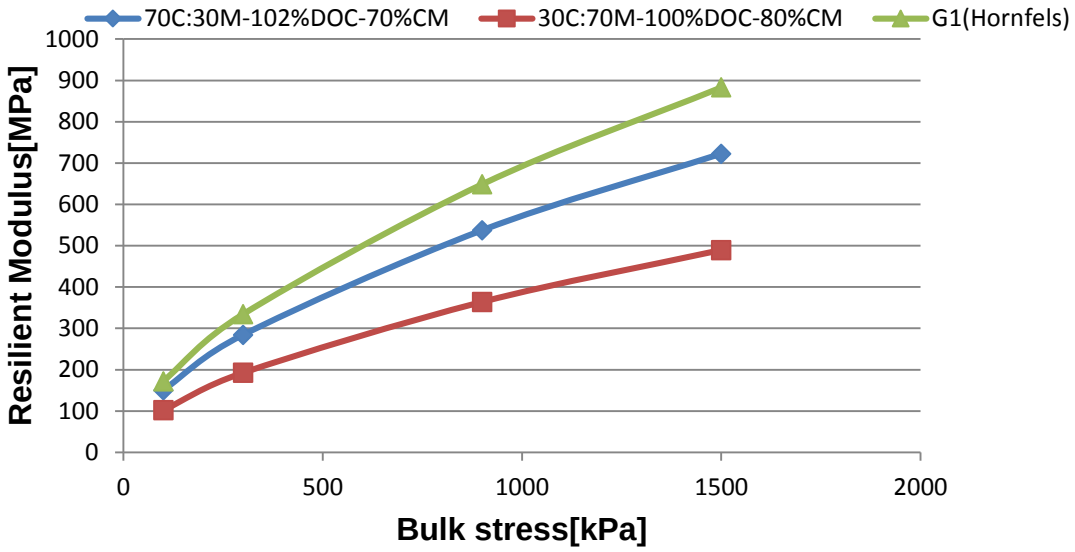

Figure 4- 28: Resilient Modulus of RCM and G1 Hornfels

It can be concluded based on shear properties, and resilient modulus that 70C:30M-102%DOC-70%CM mix behaviour is nearly similar to G1 (hornfels) at low stress levels. Therefore, this shows that these secondary materials, if blended correctly and compacted sufficiently can perform well in pavement layers that experience low stress levels. In other words, they can satisfactorily be used in the structure of pavements with less heavy vehicles or be protected with a thick top layer if used in heavily trafficked pavements.

CHAPTER 5

APPLICATION OF THE RESULTS

5.1 INTRODUCTION

The pavement is a system composed of different layers in which various materials types and quality are used depending on the traffic that the pavement is required to carry and the strength of the subgrade. In developing countries as shown in Figure 2-1, the flexible pavement system comprises of:

- A thin wearing course composed either by asphalt or seals
- A base course composed by cement bound granular material but predominantly high quality unbound granular material
- A subbase made of lightly cemented or purely unbound granular material, and
- A subgrade composed of unbound granular material.

The material used in these pavement layers must meet performance requirements. Aggregates physical and mechanical properties such as grading, aggregate shape, specific gravity, resistance to crushing, etc, are able to provide insight into the material performance but they do not measure this directly. Therefore, mechanical performance testing such as shear test, resilient response and permanent deformation tests are the appropriate measures of the material failure behaviour and the response and damage behaviour under cyclic loading of moving vehicles.

The application of material mechanical properties such as strength properties (C, ϕ) and the resilient properties (Mr and ν) is integral in flexible pavement modelling and mechanistic design as can be seen in Figure 5-1. These material characteristics are among the variable inputs during the analysis of the structural capacity of granular pavement layers. The shear properties provide the ultimate failure strength of the material whereas the resilient modulus and the Poisson Ratio provide the response of granular material under loading. The ultimate shear strength of the material characterises the highest stress that it can withstand. However, in real life, granular materials in pavements experience dynamic loading from the moving wheel, and this generates shear stress in the material. The magnitude of generated shear stress depends on the stiffness or specifically on the resilient modulus of granular material, which is an indication of the load spreading capacity. During the evaluation of the structural capacity of

granular pavement layers, the material ultimate shear strength is compared to the developed shear stresses in order to derive the number of load repetitions at failure thus the layer life.

For pavement modelling, multi-layer linear-elastic or non-linear-elastic software can be used. The Mr-Θ material model can be used satisfactorily in multi-layer linear elastic pavement modelling but due to its drawback of predicting a continuous increase of the resilient modulus as the stress increases, this restricts its effective usage in non-linear pavement modelling such as using finite elements. To this end, the Mr-Θ-σ_d/ σ_{df} model or simply the Mr-Θ-σ_1/ σ_{1f} model is therefore used. However, since multi-layer linear-elastic software is used during pavement analysis in this study, only the Mr-Θ model is considered.

This chapter aims at providing a good understanding and the practicality of material mechanical characterisation and modelling. It provides a link between the material properties and pavement response (modelling). This is achieved by carrying out stress-strain analysis through pavement layers that comprise of some of the materials investigated in this study.

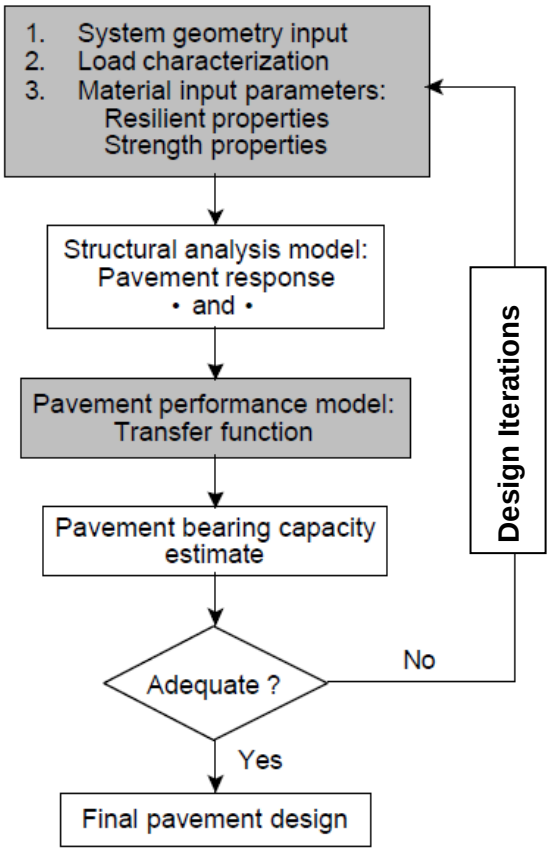

Figure 5- 1 : Schematic Diagram of a Mechanistic-Empirical Design Procedure (Theyse & Muthen, 2000)

5.2 DESIGN OF TYPICAL PAVEMENT STRUCTURES COMPOSED BY RCM OR NATURAL AGGREGATES AS UNBOUND GRANULAR LAYERS

The performance of the RCM materials compared to natural granular crushed aggregates is evaluated through the analysis of virtual pavement structures comprising of these materials in granular pavement layers. The stresses and strains in pavement layers were determined with a linear-elastic multi-layer computer program BISAR.

The first selected pavement for analysis is a second order South African road named Category B. It should be able to accommodate between 1 to $3x10^6$ standard axle (80kN) repetitions over 20 years with a design reliability of 90%. The second analysis is on a South African rural road (category C) capable of carrying 0.3 to $10x10^4$ over 15 years with a design reliability of 80%.

5.2.1 Loading Characteristics

The standard design load for South Africa is a 40 kN dual wheel load at 350 mm spacing between centres and a contact pressure of 520 kPa (Theyse & Muthen, 2000). However, there is a remarkable increase in technology in the tyre industry and truck manufacturing by which tyres can perform at higher pressures and trucks can support increased loads on their axles. In this regard, the study conducted by Morton *et al.* (2004) indicated that axle loading up to 9.45 tonnes and above with tyre pressures ranging from 700 kPa to 825 kPa were recorded on one of the South African National roads namely the N3.

To take into account this change in loading, the author has used a 50kN dual wheel load and a tyre pressure of 700 kPa in the analysis and design.

5.2.2 Material properties for pavement analysis

The analysis was carried out on two different pavement types as given in Figure 5-2. The materials used in this analysis are:

- A thin continuously graded asphalt layer (40mm) for the wearing course with the materials properties assumed from the results obtained by Freeme (1983) as presented in Theyse & Muthen(2000). This layer was modelled as linear-elastic
- A seal for pavement type B. This is not modelled since a conservative assumption is made that seals do not contribute structurally to the pavement. This is accepted practice in South Africa.
- Base course composed by three different types of materials: RCM materials, i.e 70C:30M-102%DOC-70%CM and 30C:70M-100%DOC-80%CM, and one natural crushed granular

materials G1 hornfels (Araya, 2011). Because these materials are the centre of this analysis, the base layer is modelled by sub-dividing the layer into three sub-layers and carry out manual iterative calculations of the stiffness. The iterations are performed up to when convergence or the difference between the input stiffness value and the BISAR computer program stiffness output is negligible. The thickness used during the analysis is 200mm for Pavement A and 125mm for Pavement B.

- A subbase composed of cement stabilised material C4 or RCM. This layer is modelled as linear-elastic for Pavement A or modelled sub-divided for Pavement B. The thickness of the layer is 200mm for Pavement A and 125mm for Pavement B.
- A subgrade consisting of gravel-Soil G7 and modelled as linear-elastic.

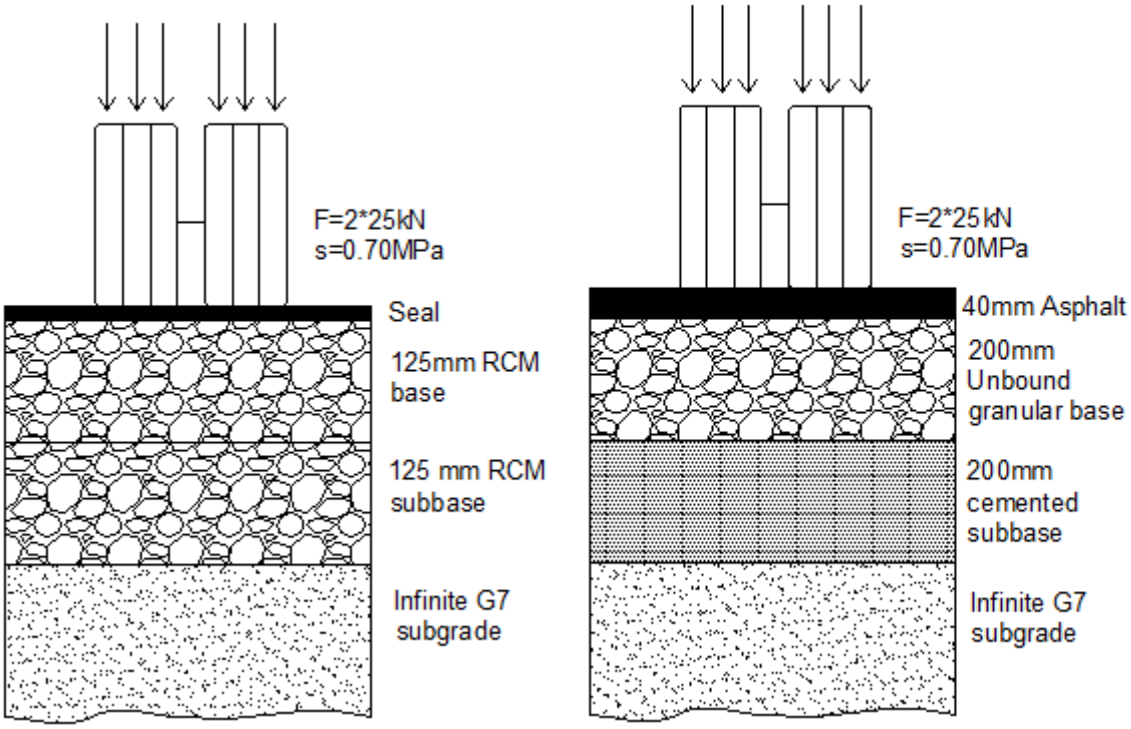

Figure 5- 2: Pavement Structures: Type (B) left and A (right)

The mechanical characteristics of the material used in the analysis are summarised in Table 5-1 to Table 5-5. The thickness selected represents the common pavement layer thicknesses used in Southern Africa as provided in the design catalogue provided in TRH 4(1996). The material characteristics except unbound materials are hypothetical since they are based on assumption. However, the assumptions are related to pavement conditions and values presented in Theyse & Muthen (2000).

Table 5- 1: Shear Parameters of Stress Dependent Granular Materials

Material Type	C[kPa]	$\phi(^0)$
RCM: 70C:30M-102%DOC-70% CM	314	48.4
RCM: 30C:70M-100%DOC-80% CM	171.5	50.3
G1	130.9	58.6

Table 5- 2: Resilient Modulus Model for Stress- Dependent Granular Materials

Material Type	Model	K_1	K_2	R^2
70C:30M-102%DOC-70% CM	Mr-Θ	10.39	0.58	0.899
30C:70M-100%DOC-80% CM	Mr-Θ	7.04	0.58	0.966
G1(Hornfels)	Mr-Θ	10.66	0.604	0.916

Table 5- 3: Resilient Response for Materials used in the Analysis

Pavement layer	Analysis	Mr[MPa]	ν
Asphalt surfacing	Linear-elastic	2500	0.45
Seal	-	-	-
Base course	Non-linear-elastic	Variable	Variable
Cemented Subbase	Linear-elastic	1000	0.35
Granular subbase	Non-linear-elastic	Variable	Variable
Subgrade	Linear-elastic	150	0.35

Table 5- 4 : Material Stiffness and Resilient Modulus of the Base Course Materials Predicted by the Software (BISAR) for Pavement A

Layer	Material	Thickness (mm)	Stiffness[MPa]		
			70C:30M-102%DOC-70%CM	30C:70M-100%DOC-80%CM	G1 Hornfels
Layer 1	Asphalt	40	2500	2500	2500
Layer 2	Granular Base	67	373	275	686
Layer 3		67	284	213	508
Layer 4		66	216	199	459
Layer 5	Subbase (C4)	200	1000	1000	1000
Layer 6	Subgrade(G7)	Infinite	150	150	150

Table 5- 5: Material Stiffness and Resilient Modulus of the Base and Subbase Materials Predicted by the Software (BISAR) for Pavement B

Layer	Material	Thickness (mm)	Stiffness[MPa]	
			70C:30M-102%DOC-70%CM	30C:70M-100%DOC-80%CM
Layer 1	Seal	-	-	-
Layer 2	RCM for Base and Subbase	62.5	668	477
Layer 3		62.5	356	256
Layer 4		62.5	289	189
Layer 5		62.5	243	149
Layer 6	Subgrade(G7)	Infinite	150	150

5.2.3 Pavement modelling and bearing capacity for type A

5.2.3.1 Stresses and Strains in pavement layers

The stresses and strains in the pavement were modelled using BISAR. The convention signs used in BISAR computer program is "-" for compression and "+" for tension. However, in this study, these convention signs were not followed, instead, they were converted and the compression stresses are denoted "+" whereas tensile stresses are designated by "-"sign. The base course was sub-divided into three sub-layers, and other pavement layers were modelled undivided.

Figure 5-3 shows the variation of stresses in the pavement structure as the thickness increases toward the bottom of the pavement. It can be seen that the applied vertical stress reduce towards the bottom of the pavement due to load spreading capacity of the pavement layers. It can also be observed that horizontal stress decreases as the depth increases and the G1 (hornfels) seems to exhibit higher lateral stress compared to RCM materials. These two characteristics can explain the observed reduction of the resilient modulus of the modelled stress dependent base sub-layers (Table 5.4) toward the bottom of the layer, and the higher resilient modulus values exhibited by the G1 material.

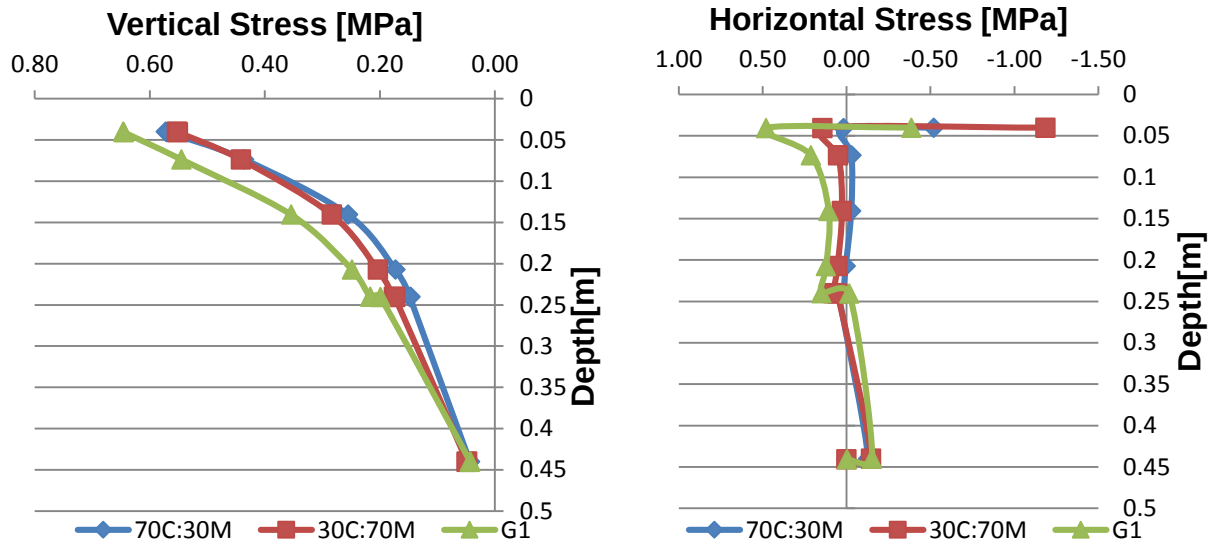

Figure 5- 3 : Horizontal and Vertical Stresses in Type A Pavement layers

It is noteworthy from Figure 5-4, that the strain reduces also with depth and the G1 material in the base layer exhibits less vertical strain.

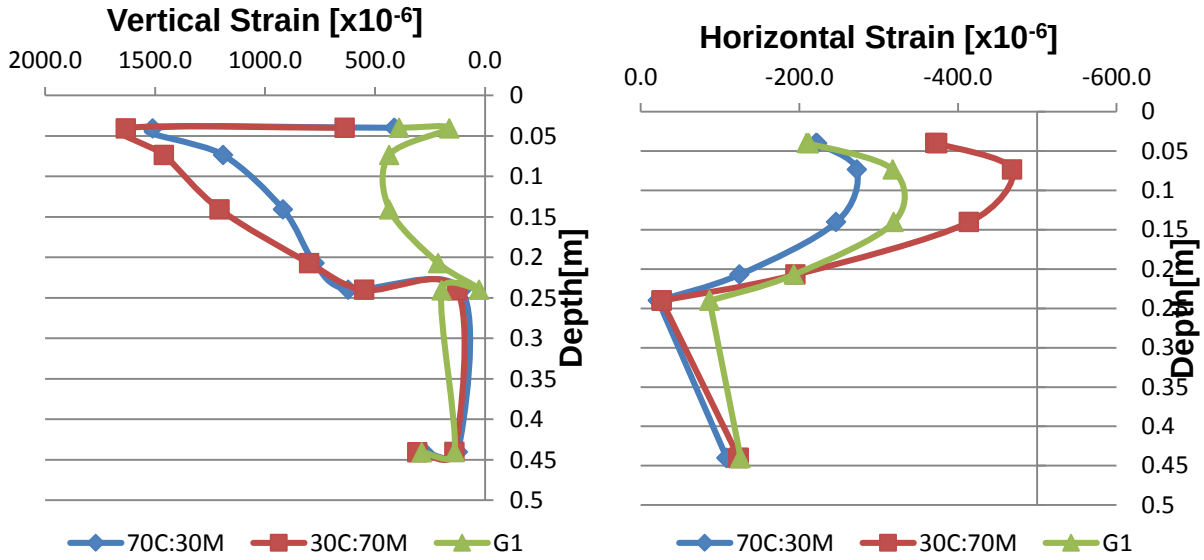

Figure 5- 4 : Vertical and Horizontal Strains in Type A Pavement Structure

5.2.3.2 Structural analysis and transfer functions

The structural analysis thus the stresses and strains are determined at the following critical points as indicated in South African Mechanistic Pavement Design Method (SAMDM) and presented in Figure 5-5:

- The maximum horizontal strain at the bottom of the asphalt layer which results in asphalt fatigue
- The principal stresses in the middle of unbound granular base which cause the deformation of the base layer
- The vertical stresses causing the crushing on top, and the horizontal strains resulting in effective fatigue at the bottom of the cemented subbase layer
- The vertical strain causing deformation on top of the subgrade layer

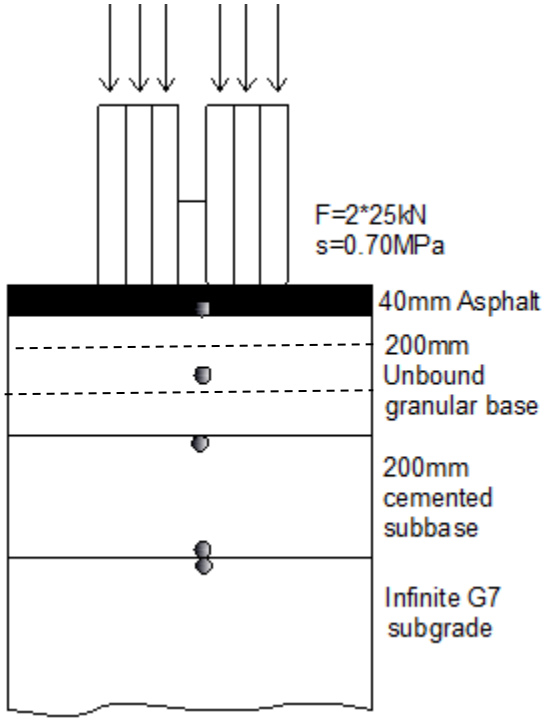

Figure 5- 5 : Analysis Points in Pavement A

The transfer function indicates "the relationship between the value of the critical parameter and the number of load repetitions that can be sustained at that value of the critical parameter, before the particular material type fails in a specific mode of failure" (Theyse *et al*., 1996). To this end, the following formulas as provided by the latter authors were used to calculate the transfer functions for pavement layers:

$$N_f = 10^{17.46\left(1-\frac{log\ \varepsilon t}{3.41}\right)} \qquad \text{(Equation 36)}$$

Where N_f is the transfer function for the asphalt wearing course for road category B, and ε_t is the strains in asphalt layer.

$N_{eff}=10^{6.84(1-\frac{\varepsilon t}{7.63\varepsilon b})}.SF$ (Equation 37)

With:

- N_{eff} = transfer function due to the effective fatigue at the bottom of cemented subbase
- ε_b = strain at break
- SF = the shift factor in order that the effective fatigue takes into account the layer thickness (d).

$SF= 10^{(0.00285d-0.293)}$ (Equation 38)

The Equation 39 gives the advanced crushing of cemented subbase.

$N_{Ca}=10^{(8.1841-\frac{\sigma v}{1.2\ UCS})}$ (Equation 39)

Where: σ_v is the vertical stress at the top of the subbase layer.

The transfer function due to the deformation of the subgrade is given by;

$N= 10^{(A\ -\ 10\ log\ \varepsilon v)}$ (Equation 40)

With:

- A = the regression coefficient for subgrade deformation transfer function; 33.38 for category B road
- ε_v = vertical strain at the top of the layer

The transfer function for the unbound base course is base on safety factor (F) and is calculated as follow:

$F=\frac{\sigma 3\left[K\left(tan^2\left(45+\frac{\Phi}{2}\right)-1\right)\right]+2KCtan(45+\frac{\Phi}{2})}{(\sigma 1-\sigma 3)}$ (Equation 41)

Then the number of load repetitions at failure for a road Category B is:

$N_B= 10^{(2.605122F+3.707667)}$ (Equation 42)

Note:

- C = the cohesion
- σ_1 ,σ_3=the major and minor principal stresses

- ϕ = friction angle
- K= constant of moisture condition, 0.8 taken in this example for moderate moisture

Table 5- 6 : Results of the Analysis

Depth(mm)	Design Criteria	Critical Factor	70C:30M-102%DOC-70%CM[1]	30C:70M-100%DOC-80%CM[2]	G1(Hornfels)
40	Fatigue (asphalt)	max ε_t[μstrain]	221.3	371.4	209.4
140	Deformation (Base)	σ_1[kPa]	257	285	356
		σ_3[kPa]	-29	28	107
240	Crushing (Subbase)	max σ_v[kPa]	142	168	194.2
440	Fatigue (Subbase)	max ε_t[μstrain]	117.5	134.7	136.7
440.5	Deformation (Subgrade)	max ε_v[μstrain]	302.8	339.5	313.2

[1]: Referred to as 70C:30M

[2]: Referred to as 30C:70M

5.3.2.2.1 Effect of horizontal strains at the bottom of the asphalt

The horizontal strains at the bottom of the asphalt layer result in the fatigue of the layer, which influences the layer life. Table 5-6 shows that higher strains are likely to occur at the bottom of the asphalt when 30C:70M is used in the base course because of the relative low stiffness. Even though the difference in horizontal strains at the bottom of asphalt when supported by a well blended and compacted 70C:30M or a G1 may seem to be low, it has a significant effect on the asphalt layer life when transfer function (Equation 36) is used. The asphalt over a G1 base material will support $3.77x10^5$ load repetitions at failure whereas the asphalt supported with 70C:30M will bear $2.84x10^5$ load repetitions before failure. This corresponds to a decrease of approximately 32% in asphalt layer life.

The asphalt layer life with the lowest number of load repetitions was with 30C:70M as base material supporting $2x\ 10^4$ load repetitions at failure. This value is however unrealistically low. The lower asphalt layer life when supported with 30C:70M can be attributed to thin asphalt layer and the higher modular ratio (approximately 11) between the asphalt and the 30C:70M base. Higher modular ratio is an indication of a poorly balanced/unbalanced pavement structure where there is no smooth reduction in material strength and stiffness with increasing depth. The

consequence of an unbalanced pavement structure could be the premature failure as observed by the results obtained above.

In general, the values of the strains at the bottom of asphalt layer were higher in this example. Although it is a hypothetical example, it does show insight into the difficulty of predicting thin asphalt layer life using the transfer function presented in Equation 36, and the benefit of using a strong base layer for protecting thin asphalt layers.

5.3.2.2.2 Effect of principal stresses on granular base layer

The principal stresses, i.e vertical stress (major principal stress σ_1) and horizontal stress (minor principal stress σ_3) are the critical aspects that result in the deformation of the unbound granular layer. To model the behaviour of the granular layer, the deviator stress, i.e the difference of principle stresses is compared with the ultimate shear strength of the material referred to as the deviator stress at failure. The deviator stress at failure is the difference of the principal stress at failure (σ_{1f}) to the minor principal stress at failure (σ_{3f}).

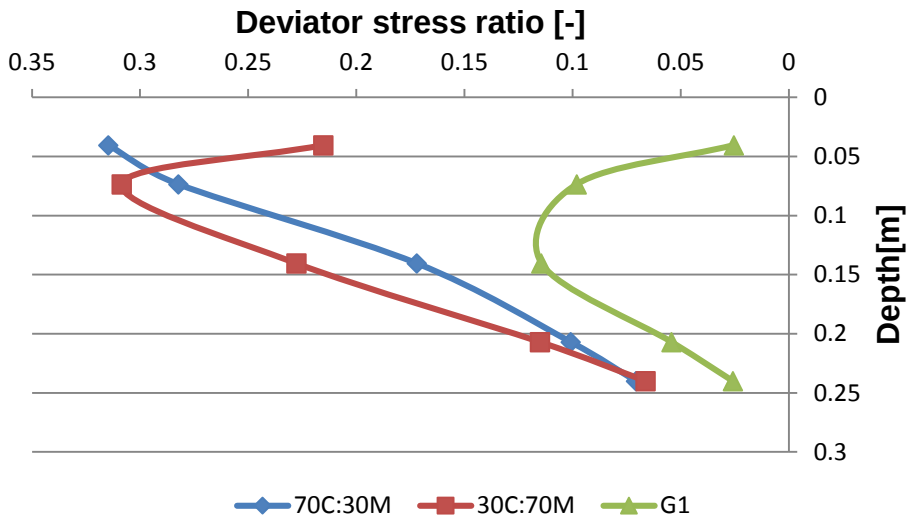

Figure 5- 6 : Deviator Stress Ratio in the Base Course Sub-layers

Figure 5-6 shows the deviator stress distribution in the base course sub-layers over a depth of 200 mm. It can be seen that the G1 (Hornfels) exhibits a lower deviator stress ratio than the 70C:30M and 30C:70M materials. This figure also shows that the critical deviator stress ratio for G1 (Hornfels) which is stiffer in this example occurs below the critical deviator stress ratio of the less stiff material 30C:70M. However, the location of the critical deviator stress ratio for 70C:30M cannot be discerned. This is attributed to the shifting of principal stresses due to the

development of tensile stress which is theoretically not correct but applicable during calculations when these tensile stresses occur. During shifting, the minor principal stress σ_3 is set to zero while maintaining the deviator stress. The consequences of shifting the principal stress are the increase in the deviator stress while the deviator stress at failure reduces. This occurs since the first term of the Equation 11 becomes zero and the second term (B) is not stress dependent because it does not take into account of the horizontal stress or the minor principal stress.

Using Equations 41 and 42, the safety factors and the life or the number of load repetitions at failure were calculated. The safety factory calculated are 6.91 for G1, 4.64 for 70C:30M and 3.48 for the 30C:70M. The calculation of base life for G1(hornfels) yielded $4.98x10^{21}$ while the 70C:30M and the 30C:70M yielded $6.09x10^{15}$ and $5.98x10^{12}$ load repetitions respectively. Although these values are practically unrealistic, they show that a change in the material stiffness of the base layer has a significant influence on log scale during layer life calculation based on the transfer function.

The experience gained in this study has shown that there is a possible crushing of the RCM material, therefore crushing on the top of the unbound granular layers in which RCM is used should also be evaluated.

5.3.2.2.3 Subbase fatigue analysis

The subbase is analysed for fatigue at the bottom of the layer since it was found in the worked example that the crushing was not the critical aspect in the subbase layer. The fatigue at the bottom of the cemented subbase layer is generated by the horizontal strains in the layer.

Following the calculation of the subbase layer life due to fatigue, the numbers of load repetitions at failure are $1.87x10^6$ for G1, $2.46x10^6$ for 70C:30M and $1.92x10^6$ for 30C:70M. It can be deducted that the layer life of the C4 cemented subbase underneath a G1, 70C:30M or 30C:70M is in the same range of load repetitions at failure.

5.3.2.2.4 Deformation of the subgrade

The deformation of the subgrade results from the vertical stress at the top of the layer. It can be seen from Figure 5-4 and Table 5-6 that the vertical strains at the top of the subgrade when the base is constructed of 70C:30M material or natural granular material is closely identical.

The transfer function based on Equation 40 was used to assess the subgrade layer life with three different base materials. The subgrade below a 70C:30M layer yielded $3.7x10^8$ load repetitions while subgrade below a G1 material exhibited $2.64x10^8$ load repetitions at failure.

The subgrade layer life reduced when is protected in the base by a 30C:70M material, where $1.18x10^8$ load repetitions at failure was calculated.

Table 5- 7: Life Prediction of Pavement A layers

Pavement layers lives			
Layer	70C:30M-102%DOC-70%CM	30C:70M-100%DOC-80%CM	G1(Hornfels)
Asphalt	$2.84 x10^5$	$2 x10^4$	$3.77 x10^5$
Base	$6.09 x10^{15}$	$5.98 x10^{12}$	$4.98x10^{21}$
Subbase	$2.46x10^6$	$1.92x10^6$	$1.87x10^6$
Subgrade	$3.7x10^8$	$1.18x10^8$	$2.64x10^8$

Following the results summarised in Table 5-7, it can be deduced that 70C:30M and G1 (Hornfels) in this example have shown nearly identical load spreadability.

5.2.4 Pavement modelling and bearing capacity for type B

5.2.4.1 Stresses and strains

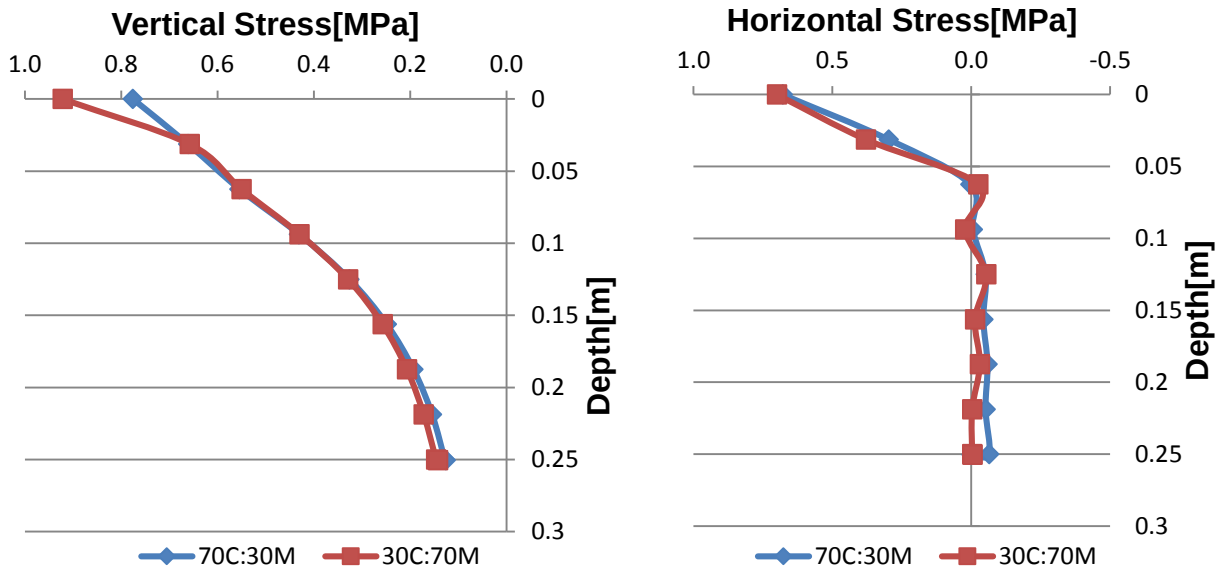

Figure 5- 7 : Vertical and Horizontal Stresses in Type B Pavement Layers

Figure 5-7 and Figure 5-8 give the stresses and strains distribution in the Pavement B layers. Comparing these figures with Figure 5-3 and Figure 5-4, it can be seen that the stresses and strains at the top of the base layer as well as in underneath layers are higher in Pavement B compared to that of Pavement A. This is attributed to the wearing layer that has only a functional role to the pavement. This difference results also from the material characteristics in different layers, and the layers thicknesses.

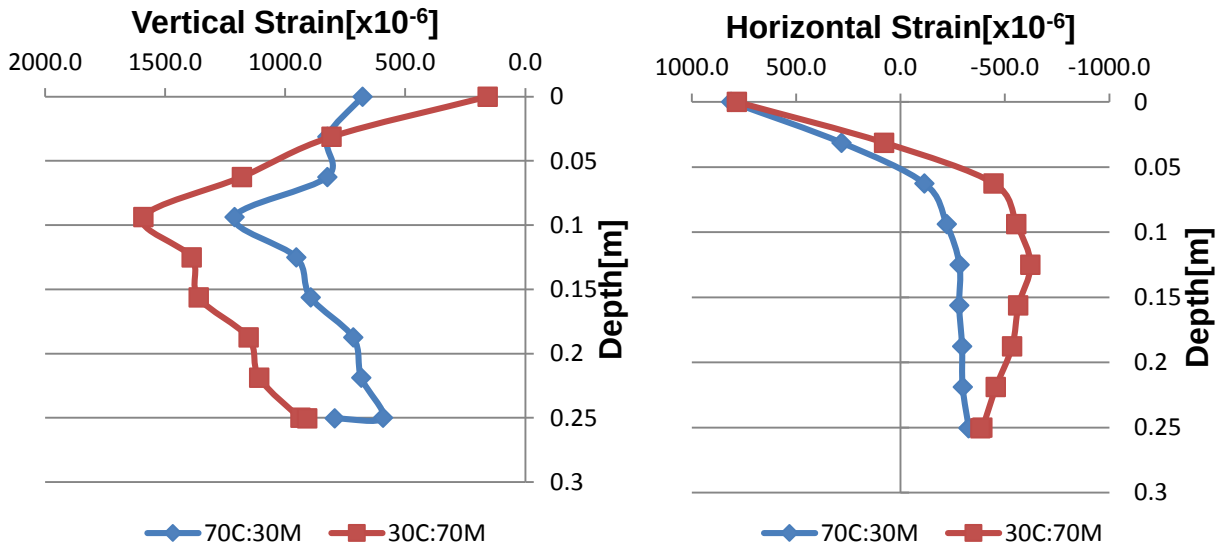

Figure 5- 8 : Vertical and Horizontal Strains in Pavement B layers

5.2.4.2. Structural analysis and transfer function

For structural analysis, the stresses and strains are determined at the following critical points as presented in Figure 5-9:

- The principal stresses in the middle of the unbound granular base which cause the deformation of the base layer
- The principal stresses in the middle of unbound granular subbase which cause the deformation of the subbase layer
- The vertical strain at top of the subgrade resulting in the deformation of the subgrade layer

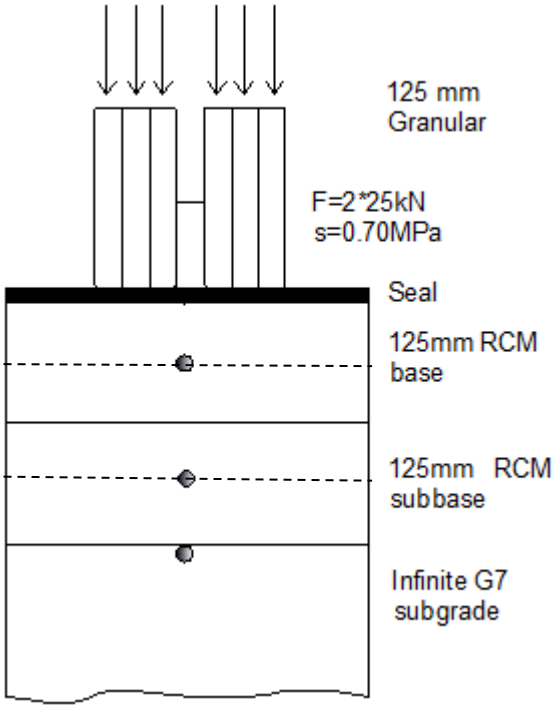

Figure 5- 9: Analysis Points for Pavement B

For road category C, the granular layer life is calculated as follow:

$$N_C = 10^{(2.605122F+3.93324)} \quad \text{(Equation 43)}$$

With F, the safety factor which is given in Equation 41.

Equation 40 is used for the transfer function of the subgrade and the A constant in this equation is 33.47 for road Category C.

Table 5- 8: Results of the Analysis of the Pavement B

Depth(mm)	Design Criteria	Critical Factor	70C:30M-102%DOC-70%CM	30C:70M-100%DOC-80%CM
62.5	Deformation(Base)	σ_1[kPa]	550	550
		σ_3[kPa]	3	-20
187.5	Deformation (Subbase)	σ_1[kPa]	190	210
		σ_3[kPa]	-60	-30
250.5	Deformation(Subgrade)	max ε_v[μstrain]	793.9	908.7

5.2.4.2.1 Effect of principal stresses on granular base and subbase

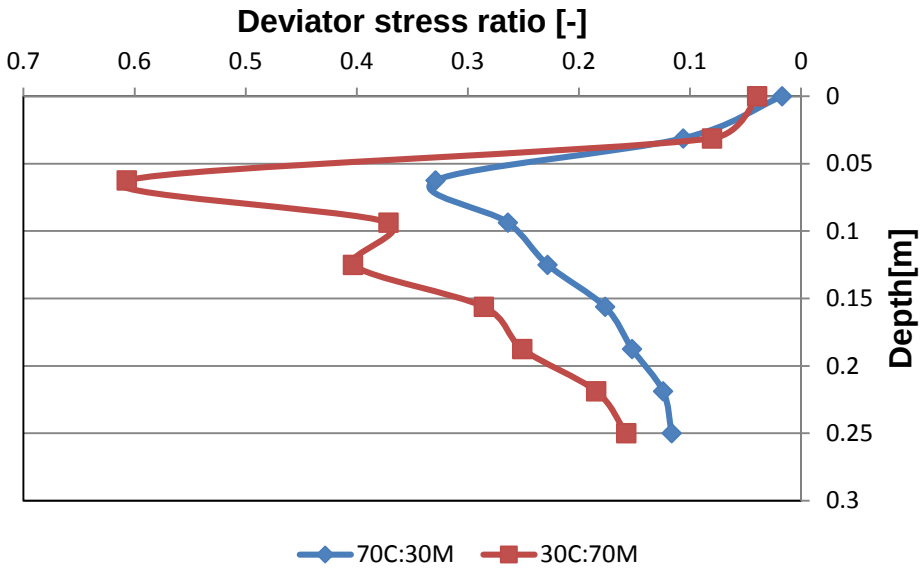

Figure 5- 10 : Deviator stress Ratio in Granular Base and Subbase of the Pavement B

Figure 5-10 shows the deviator stress ratio at different points in the granular base and subbase. It can be observed that the critical deviator stress occurs approximately in the middle of the base layer where the minor principal stress (horizontal stress) is zero. In other words, it corresponds to the point where tensile stress tends to develop in the granular material. This figure also shows that the critical deviator stress of the 30C:70M is relative upper in layer depth compared to the 70C:30M mix. It can also be seen that the deviator stress ratios are relatively higher in Pavement B compared to Pavement A in this example.

The safety factors calculated are 1.31 and 3.19 for the base and the subbase for the 30C:70M material. These safety factors correspond to 2.67×10^{7} and 2.05×10^{12} load repetitions at failure for the base and subbase layers. The base life of 2.67×10^{7} load repetitions is however unrealistically high for a deviator stress ratio of 0.605. This will be discussed later. The calculated 70C:30M safety factors were 2.4 and 5.25 for base and subbase layers. These correspond to 2.5×10^{10} and 4.83×10^{17} load repetitions at failure for the base and the subbase layers.

It can be concluded from the results that RCM materials perform quite well in the bottom layers of the pavement as indicated by the difference in layer life between the base and the subbase.

5.2.4.2.2 Deformation of the subgrade

Following the strain conditions in the Pavement B layers, it was argued in Section 5.2.4.1 that the combination of the loading condition and the structure of the pavement have resulted in higher strains compared to Pavement A. Table 5-8 shows that the vertical strains at the top of the subgrade are considerably high and this reduces the subgrade layer life. The calculated subgrade layer lives are $3x10^4$ and $7.69x10^3$ load repetitions at failure respectively for 70C:30M and 30C:70M.

Table 5- 9: Life Prediction of Pavement B layers

Pavement layers lives		
Layer	70C:30M-102%DOC-70%CM	30C:70M-100%DOC-80%CM
Base	$2.5 x10^{10}$	$2.67 x10^7$
Subbase	$4.83 x10^{17}$	$2.05 x10^{12}$
Subgrade	$3 x10^4$	$7.69x10^3$

Following the results in Table 5-9 and the design catalogue provided in TRH 4(1996) for low trafficked road Category C, the base and subbase thickness of 125mm each, beside of being less practical, it results also in higher vertical strains at the top of the subgrade layer. These pronounced strains reduce considerably the subgrade layer life as can be observed for the results presented in Table 5-9.

Van Niekerk (2002) has carried out a number finite element analysis in granular base layer to assess the development of rutting due to wheel loading and various base materials characteristics. From his extensive study, he developed a number of design charts for granular materials at various grading and degrees of compaction. Following the results, he has found that for base materials experiencing the stress ratios σ_1/ σ_{1f} of ≤ 0.3-0.35, rutting hardly occurs for large number of load repetitions whereas excessive rutting is likely to occur under low number of load repetitions for base materials experiencing the stress ratios σ_1/ σ_{1f} of ≥ 0.6-0.7. From design charts, he developed a log-log type relationship; for example for a mix composition of Lower Limit (LL) grading and compacted at 100% DOC, Equation 44 was derived for the development of 20mm rutting in the base layer:

$$\text{Log } N = 2.301 - 10.667 \log \sigma_d/ \sigma_{df} \qquad \text{(Equation 44)}$$

The number of load repetitions at failure predicted by SAMDM through transfer functions is 2.67 x10^7 while Equation 44 predicts approximately 10^5 load repetitions at failure for 30C:70M-100%DOC-80%CM for the same deviator stress ratio of 0.605. This shows more than 100% difference in predicted base layer life for these two approaches. Since the results of Van Niekerk (2002) were obtained based on permanent deformation tests carried out at a significant number of load repetitions(1 million) compared to that of SAMDM (20000 load repetitions), it can be concluded that the base layer life predicted by the SAMDM is an over-estimation therefore, the results should be analysed with care. It is accordingly recommended to revisit transfer functions as provided by SAMDM, as this is a shortcoming in the method.

5.3 CONCLUSION

The objective of this chapter was to demonstrate the application of material mechanical characterisation and modelling as discussed in Chapter 4 of this study. This was done through pavement modelling to assess the material response due to the applied load, and design to predict the layer performance.

Following the results, the subsequent conclusions can be drawn:

- The stiffness of the base layer influences the stresses and strains in the overlying and underlying layers but particularly at the bottom of the wearing course
- The stiffness and thickness of the layers overlying the subgrade influence the vertical strains on top of the subgrade layer. Based on the two worked out examples, it is possible to deduce that the thickness has a larger influence on the yielded vertical strains on top of the subgrade layer
- Following the pavement design through transfer functions, it was found that G1(hornfels) performs better than the RCM materials but satisfactory performance can be provided by 70C:30M at low stresses much deeper in the pavement
- It is very important to use a correct material model to assess the material response under loading rather than assumed values since it was found that this results in disparity in predicted stresses and strains in pavement layers but particularly in layer life prediction. The results of this study will provide assistance
- The prediction of the pavement layer life using transfer functions as given in the SAMDM design should be used with care, as it does not allow realistic calculation at higher stress ratios.

Briefly, despite the fact that this chapter was merely aimed at showing the application of the factors and parameters investigated in this research, it has also provided an insight into where RCM materials can be successfully used and the care that is required during pavement analysis and design. This is good foundation for further research on different alternatives to improve RCM materials and provide specific applications.

CHAPTER 6

SYNTHESIS

6.1 INTRODUCTION

The objective of the research was to characterise RCM materials and evaluate their performance behaviour. To this end, an extensive testing was carried out and the results are presented in Chapter 4 of this study. The RCM materials behaviour was modelled and factors that influence the strength and resilient modulus were evaluated.

RCM should exhibit behaviour and performance similar to other natural granular materials. In this regard, RCM performance results were compared with natural granular crushed stone G1 (Hornfels). The performance results of RCM and G1 (Hornfels) were further applied in a typical pavement structure analysis and design (Chapter 5) in order to highlight the role of material mechanical behaviour evaluation and modelling.

This chapter provides a summary of the findings from visual assessment, characterisation and mechanical tests results. It summarises also the observed behaviour of recycled concrete and masonry and a typical natural crushed stone in the pavement structure. In order to reduce the repeatability in this chapter, links to tables, figures in Chapter 4 and 5, and to the literature in Chapter 2 are frequently referenced.

The investigated factors were the material properties such as aggregate shape, specific gravity, grading, crushing resistance, material compaction behaviour, composition, and the material condition such as the degree of compaction and the compaction moisture.

6.2 MATERIAL PROCESSING

The material was collected from the provisional dumping place of the construction site. This material was a mix composition of concrete rubbles, masonry rubbles, steel bars, woods, etc. From the processing methodology undertaken in this study, the following were found:

- Separation of demolition rubbles is very important; this reduces the risk of contamination and enables to the potential to control the quality of the desired recycled aggregates
- Crushing in more than one stage plays a key role in the quality of recycled aggregates; it was observed that the secondary crushing reduces the flakier aggregates in the material and the attached mortar on the aggregates. It increases also the amount of fines in the material. Moreover, it was observed that cubical and sufficient fines can be generated with

the laboratory jaw crusher when the size of the rubble feed to the crusher is small, in other words when the crusher operated at low "reduction ratio". However, this reduced the amount of coarse aggregates in the material

- The general trend was that recycled concrete generated slightly less fines compared to masonry.

6.3 AGGREGATE PHYSICAL AND MECHANICAL PROPERTIES

From the flakiness index test, grain size distribution, specific gravity and water absorption test, and the 10% FACT, the following was observed:

- The grain size distribution was selected to provide denser packing and thus a well graded grading was used. The fraction passing 19mm and retained on 6.7mm was composed exclusively with 70% concrete and 30% masonry whereas the fraction ≤ 4.75 mm was varied according the experimental design. The aim was to obtain a strong mix composition while valuing the recycled clay bricks
- The flakier materials increase with the increase of masonry content and it is predominant in the coarser fraction. However, the material used in this study met the TRH 14 (1985) and TRH 8(1987) recommendations for granular base materials
- Concrete aggregates are characterised by higher specific gravity and low water absorption relative to masonry granulates. It was observed that the specific gravity decreased and the water absorption increased as the masonry content increased in the mix composition. Generally, the material used in this study did not have higher water absorption (1.22% to 1.92%) even though it was slightly higher than the maximum 1% recommended in the above mentioned guidelines
- The recycled concrete and masonry resisted to disintegration due to crushing in the dry conditions as indicated by the results of the 10% FACT (131 kN). However, the ratio of dry to wet (68%) could not meet the 75% recommended in SAPEM (2013).

The results are summarised in Table 4-1 and graphically presented in Figure 4-2 trough Figure 4-4.

6.4 COMPACTION BEHAVIOUR

The compaction using the Modified AASTHO proctor test was carried out to evaluate the moisture-density relationship. This was also the reference compaction for vibratory compaction during specimen preparation. Furthermore, material break down due to compaction was assessed after vibratory compaction. From results, the following findings were made:

- The mix composition containing higher amount of recycled concrete which is characterised by aggregates with higher specific gravity and low moisture absorption relative to recycled masonry, exhibited higher dry density and low optimum moisture content
- The values of the dry density of RCM are lower than natural crushed granular materials as mentioned in various studies. In addition, the values of the Optimum Moisture Content of RCM are higher than natural crushed granular materials. This depends on the mix composition of RCM which comprises of less dense and porous aggregates compared to natural granular materials
- The evaluation of grading before and after compaction showed an insight on particles crushing of RCM when this material is compacted at low compaction moisture and high compaction energy. The rate of breakage was also dependent on the mix composition. However, less pronounced crushing was observed in this study since it was the target during mix and grading design after experience gained from the study carried out by Louw (2013).

Graphical representations are given in Figure 4-5 to Figure 4-7 and in Appendix A.

6.5 MATERIAL MECHANICAL BEHAVIOUR

This section summarises the findings from the triaxial tests results. The triaxial test results carried out in this study were the monotonic test to assess the failure shear strength of RCM, and the dynamic triaxial test to evaluate the resilient response of the RCM materials.

The specimens for mechanical testing were prepared, and compacted using the vibratory hammer according to three selected investigated factors, i.e mix composition (70C:30M and 30C:70M), compaction moisture (80% and 70% Modified AASTHO OMC) and the degree of compaction (100% and 102% Modified AASTHO MDD).

6.5.1 Monotonic test results

Monotonic tests were carried out on virgin specimens; specimens prepared only for monotonic testing, and preloaded specimens (after the dynamic triaxial test). From the tests results, the following were found:

- The strain-stress relationship of the RCM showed that the shear strength increases up to failure as the strain increases. Therefore, RCM material exhibited a *strain-hardening* behaviour

- Shear strength increased as the degree of compaction increases from 100% to 102% DOC and the concrete content in the mix composition increases from 30% to 70%. Higher compaction effort enhances the particles matrix while an increase of the concrete material in the mix results in the development of bonds and/or in strong aggregates skeleton. The bonds increase the particles interlock while strong concrete aggregates in the mix enhance the strength of the aggregate skeleton
- Shear strength slightly increased with the increase in compaction moisture from 70% to 80% OMC. However, this was less distinctive compared to other investigated factors
- The shear parameters c and ϕ obtained in this study for RCM varied between 171.5 to 314 kPa for cohesion and 42.5°-53.61° for friction angle. On the other hand the shear parameters of quality natural granular material (G_1- G_4) used in South African base course in both dry and wet conditions varies between 65-35 kPa for cohesion and 55°- 48° for friction angle(Maree & Freeme 1981 cited in Jenkins, 2013). This shows that the RCM exhibits similar even better shear strength than some of the South African natural crushed stones.
- The shear properties particularly the cohesion was found to be affected significantly by the stress history. This was observed comparing the shear properties of the virgin specimens and the cyclic preloaded specimens. A special case was observed where the cohesion increased more than 100%. This was attributed to further compaction of the specimen due to cyclic loading of the Mr test
- The Mohr-Coulomb failure condition model has modelled well the failure behaviour of the RCM materials.

Figure 4-11 and Figure 4-12 show these results, and show the variation in shear parameters for virgin and preloaded specimens. Figure 6-1 summarises the variation of the cohesion in light of the stress history and the increase of the degree of compaction.

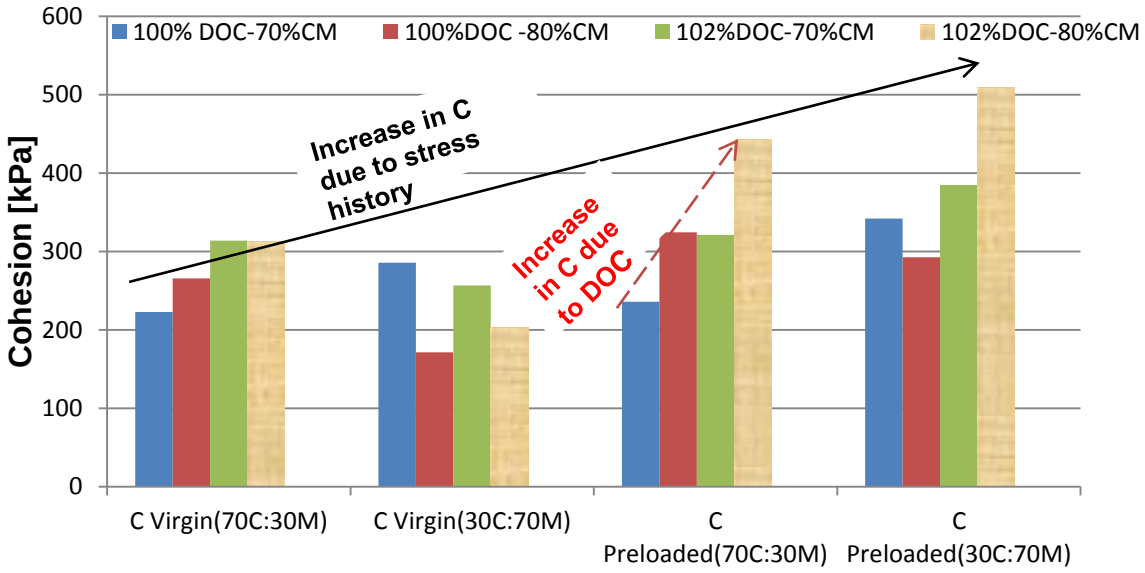

Figure 6- 1 : Variation in Cohesion due to DOC and Stress History

6.5.2 Resilient response

6.5.2.1 Testing and Modelling

There is a strong agreement in studies on the significant impact of stress and saturation on the resilient response of granular materials. The effect of stress has a pronounced influence on material containing residual cement since there is a risk of damaging the bonds that are developed due to self cementing. Therefore, testing in this study was carried out in *mild* stress regime ($\leq 0.5\sigma_{df}$) and at a target testing saturation of 65% OMC.

The stress dependency of the resilient response (Mr and ν) was observed during testing for the resilient modulus and the Poisson Ratio as illustrated in Figure 6-2 to Figure 6-3. From these figures, it was found that:

- The resilient modulus increases as the confinement and the normal stress level increase. This behaviour is named *stress stiffening*
- The resilient Poisson Ratio decreases as the confinement increases and slightly increases as normal stress increases
- The resilient modulus is affected by both normal stress and lateral stress. However, the Poisson Ratio showed a higher dependency on lateral stress than the vertical stress.

This stress dependency of the resilient response is clearly seen in different modelling figures plotted in Chapter 4 and in Appendix E.

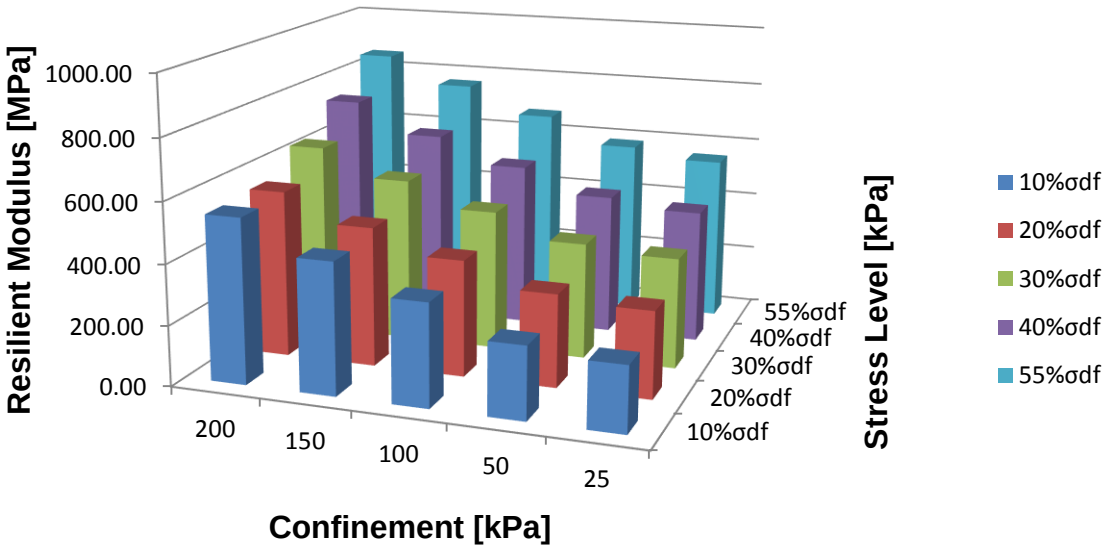

Figure 6- 2: Stress Dependency of the Resilient Modulus for 70C:30M-102%DOC-80% CM

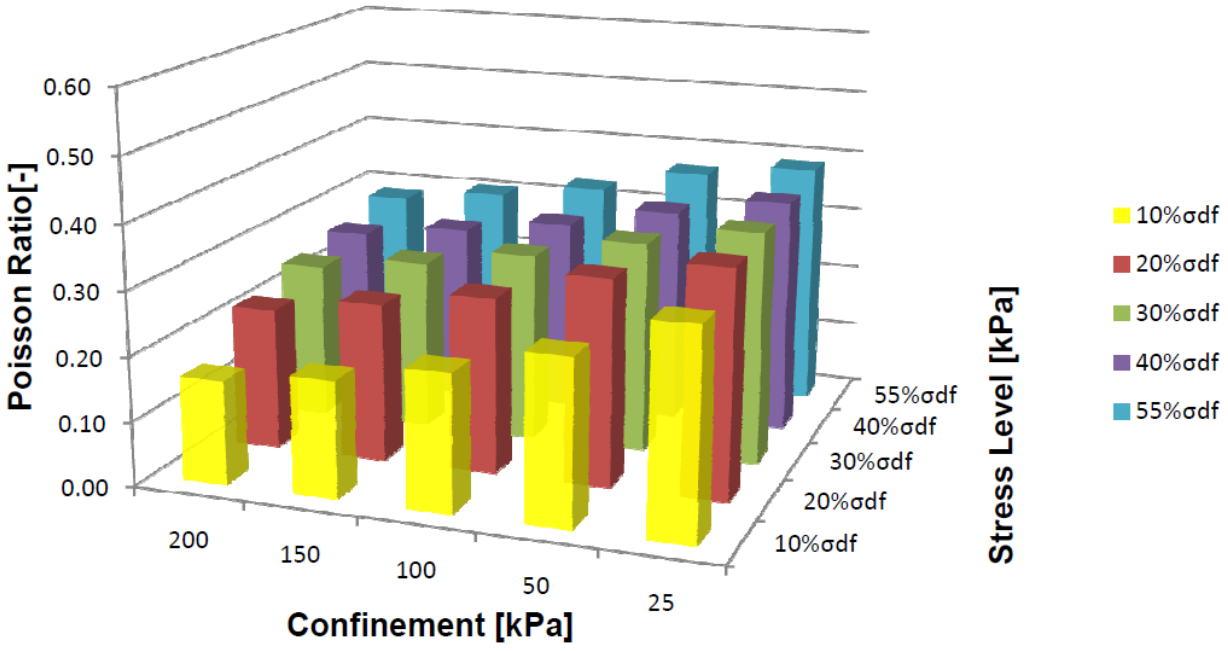

Figure 6- 3 : Stress Dependency of Poisson Ratio for 70C:30M-102%DOC-80% CM

A number of models that describe the stress dependency of the resilient modulus and the resilient Poisson Ratio are found in the literature and were discussed in Chapter 2. In this study the stress dependency of the resilient modulus were described by means of simple Mr-Θ model

and the extended Mr-Θ-σ_d/ σ_{df}. The "exponential" ν- σ_d/σ_3 model and "exponential" ν-σ_d/σ_3- σ_3 model were used to describe the stress dependency of the resilient Poisson Ratio.

Following the model fitting by means of non-linear regression on the data, it was found that:

- The resilient response stress dependency has been well described by the Mr-Θ and Mr-Θ-σ_d/ σ_{df} models for the resilient modulus, and the "exponential" ν- σ_d/σ_3 and "exponential" ν-σ_d/σ_3- σ_3 for Poisson Ratio. However, the Mr-Θ-σ_d/ σ_{df} model was not able to distinguish the stress stiffening from stress softening since the tests were carried out in mild stress regime where it is believed that the material experiences only the stiffening
- The fitting of the resilient Poisson ratio exhibited higher variability than resilient modulus. It was found also that low agreement between the model prediction and the test data that results in low R^2 was predominant for the Poisson Ratio. This is in agreement with literature as indicated in Section 2.3.6.2.1 highlighting the problem related to radial strain measuring devices that leads to less agreement in research findings, and in limited research on this aspect
- The best fitting on RCM data of the mathematical models initially developed for granular materials showed that these materials perform similarly to normal granular material. Therefore, these models can be used successfully for RCM materials.

6.5.2.2 Influence of the investigated factors on the resilient response

This study endeavoured to evaluate the effect of material properties such as composition, and the material condition such as the compaction moisture and the degree of compaction on the resilient response.

The effects were presented graphically by means of model lines and the average relative magnitude of the effect was calculated using the factorial experimental design method (Box et., 1978). Mathematical relationships (models) between the investigated factors and the resilient response (Mr and ν) were drawn. Figure 6-4 and Figure 6-5 summarise the obtained effects. The bars represent the average ± the standard deviation, and the lines show full range of the data in accordance with all stress levels used in this study as presented in Table 3-2. The value of bulk stress in this study ranged between 163 kPa and 2141 kPa.

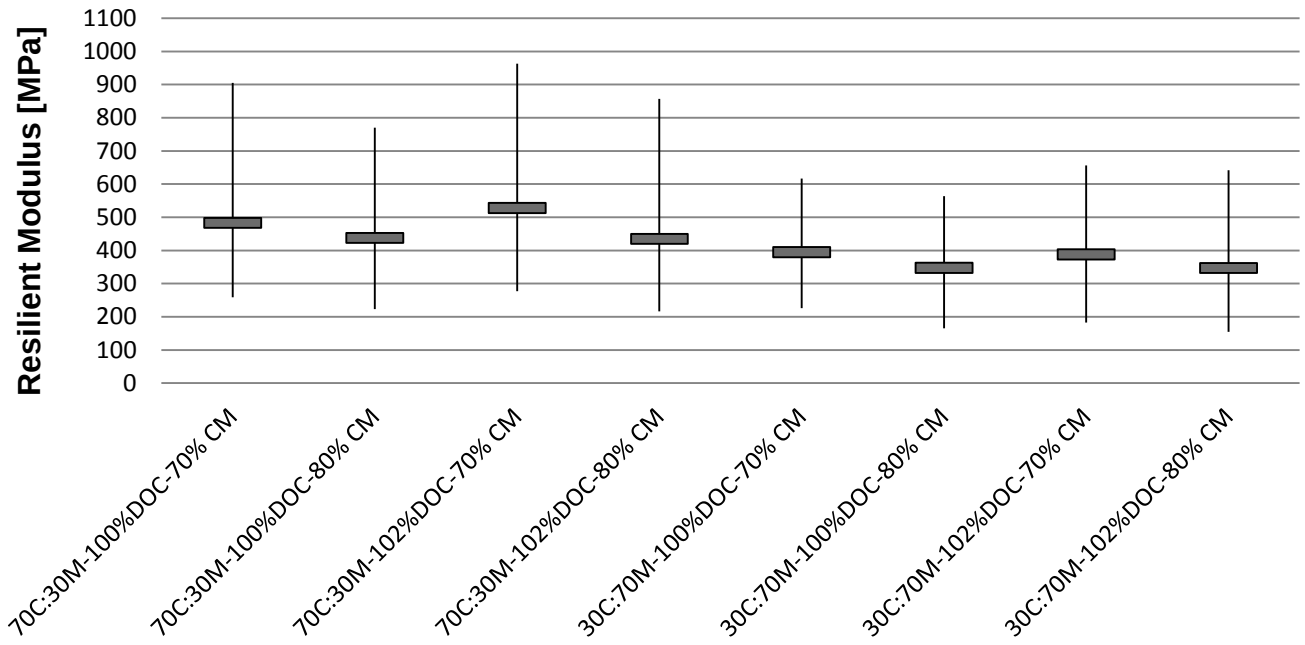

Figure 6- 4 : Resilient Modulus Ranges and the Effects of Investigated Factors

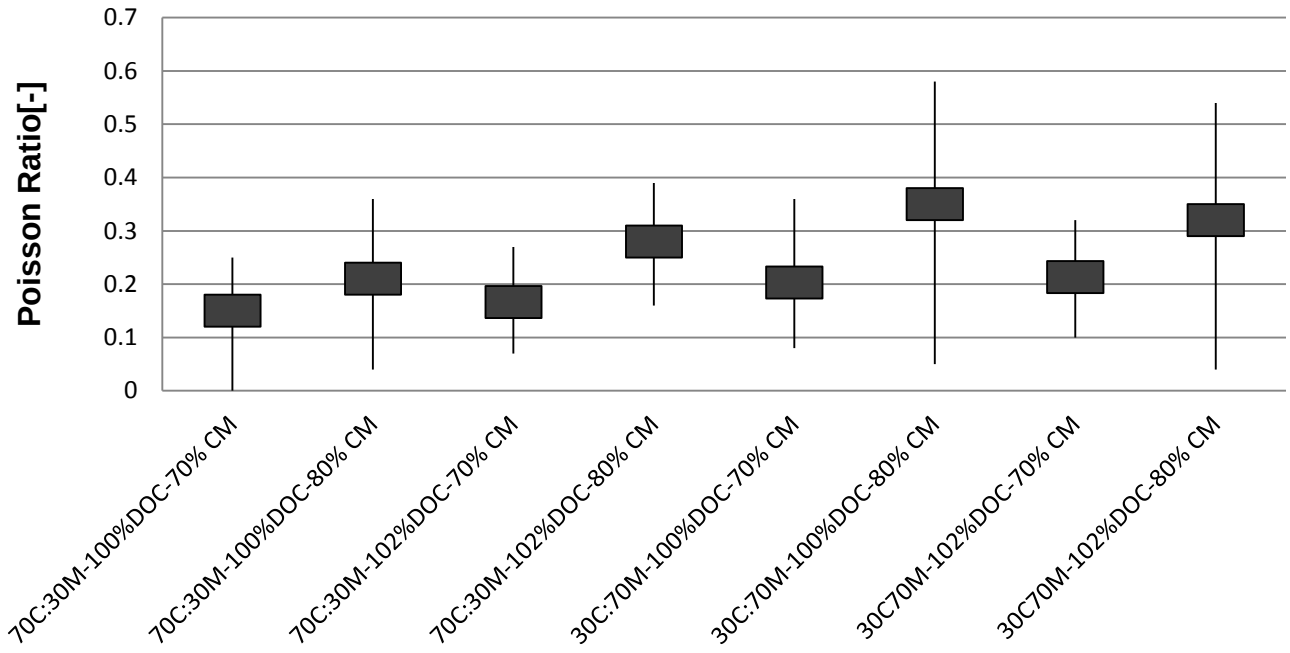

Figure 6- 5 : Resilient Poisson Ratio Ranges and the Effects of Investigated Factors

To facilitate a direct comparison, the average taken is the average of the three resilient responses obtained at three stresses (bulk stresses of 300 kPa, 900 kPa and 1500 kPa) for the

resilient modulus and (σ_d/σ_3 of 1, 10 and 23) for the Poisson Ratio. Therefore, for these figures, the reader can observe the effect of each parameter by means of bars and can see the full range of data of resilient response obtained during the test for each combination of factors by means of lines.

The following findings were made from the results:

- The resilient modulus increases and the resilient Poisson ratio decreases as the concrete content increases relative to masonry in the mix composition. The development of a strong aggregate skeleton due to strong concrete aggregates results in this behaviour. It results also from the probable development of bonds due to self-cementing when increasing the cementitious materials in the mix composition that enhance the particle interlock
- Decreasing the compaction moisture from 80% OMC to 70% OMC increases the resilient modulus and decreases the Poisson Ratio. The reason being is that when higher moisture is available in the material, it lubricates the material that in return reduces the interparticle contacts thus resulting in low resilient modulus and an increase in radial deformation when the material is loaded
- Increasing the degree of compaction from 100% to 102% increases the resilient modulus and decreases the Poisson Ratio. The compaction enhances the packing of the material and this increases the interparticle contacts that improve the aggregate skeleton. Strong aggregate skeleton exhibits higher resilient modulus and reduce pronounced radial deformation
- From the thickness of the bars, it can be seen that the Poisson Ratio is characterised by higher variability than the resilient modulus. This is also in good agreement with the model fitting as discussed in Section 6.5.2.1. This is attributed to good repeatability in axial strain measuring compared to radial strain
- It was observed in this study that the degree of compaction exhibited less distinctive effect than other investigated factors. This was confirmed by the correlation test, and the P test of the linear regression
- It was concluded that in this study, the predominant factors to the resilient response were the mix composition composition and the compaction moisture. Therefore, the final model of the resilient response and the investigated parameters related only the mix composition and the compaction moisture to the Mr and ν
- From the comparison of the RCM material with the natural crushed granular material G1 (Hornfels) investigated by Araya (2011), it was found that 70C:30M-102%DOC-70% OMC

could perform well at low stress levels (low bulk stress) when comparison is made to the high quality G1.

6.6 APPLICATION OF MATERIAL MECHANICAL PROPERTIES IN PAVEMENT STRUCTURE DESIGN

The investigated RCM mechanical properties and response models were applied in a typical pavement structure design to demonstrate the application of the results. From the worked examples, it was found that:

- It is very important to study and model the material mechanical behaviour since this comprises of inputs during pavement modelling and design; slight changes in these inputs has a significant influence in the calculated stresses and strains but particularly in the pavement layers performance prediction. Therefore, care should be taken to use the correct values of the material mechanical properties. The results of this study will assist
- Loading characteristics and the base layer stiffness influences the strains at the bottom of asphalt. The thickness and stiffness, particularly the thickness of layers protecting the subgrade, in addition to the loading characteristics contributes significantly to vertical strains occurring at top of the subgrade
- RCM material, particularly with good mix composition and well compacted has shown to perform successfully in pavement layers under low stresses.

CHAPTER 7

CONCLUSIONS AND RECOMMENDATIONS

7.1 CONCLUSIONS

To meet the objective of this study, different methodologies and analysis were undertaken, and these are detailed in Chapter 3 to Chapter 5 with a summary provided in Chapter 6. Material processing was monitored and tests were carried out following the methodology given in Chapter 3 of this study. Chapter 4 provides the results of the experimental program undertaken to characterise aggregates properties and evaluate the material mechanical performance under various material properties and conditions. Since it is essential to model the material behaviour in order to understand better its performance, this was performed and the results are presented in Chapter 4 as well. In order to illustrate the benefit of this research, Chapter 5 was dedicated to the practical applications of the obtained results. The discussions, conclusions and recommendations from findings were given in these chapters, and the important aspects to consider were summarised in Chapter 6.

This chapter provides general conclusions and recommendations since specific details are given in the above-mentioned chapters. Therefore, based on the results of this study, the following conclusions can be drawn concerning the properties of RCM materials and their performance response:

- The jaw crusher was able to produce cubical aggregates but less fines for concrete compared to masonry
- To achieve the good quality material, it was observed that separation and secondary crushing are very important
- The flakiness, the specific gravity and the water absorption depends largely on the type of material. The results showed that flakier materials resulted from soft aggregates such as clay bricks and concrete mortar attached to the aggregates. However, the mix compositions used in this study met all South African pavement materials guidelines for base course for flakiness index. The results for water absorption showed to be higher than specified in South African Pavement material specifications even though this property is not emphasised in these specifications
- The crushing strength of RCM showed satisfactory results in dry conditions but reduces below acceptable limits in the wet conditions

- The compaction methodology undertaken in this study has shown a moderate change in material grain-size distribution after compaction. This assessment has provided good insight on the importance of a good mix design and adjustment of compaction methodology
- The failure behaviour, i.e the shear strength showed to be dependent on composition and degree of compaction but less with compaction moisture. Moreover, the stress history affected the shear behaviour particularly the cohesion of RCM. This was shown by the difference in the obtained results for the shear parameters on "virgin" samples and samples preloaded by the cyclic loading of the resilient test
- The comparative study on shear parameters of RCM and South African high quality granular materials given in Jenkins (2013) has shown that RCM material performance in terms of the shear strength is within the range, even better to some of the specified good quality South African granular materials
- The resilient modulus for RCM is stress dependent. This stress dependency is modelled well by the Mr-Θ model as well as the Mr-Θ-σ_d/ σ_{df} model. The resilient Poisson Ratio was satisfactorily modelled by both "exponential" ν- σ_d/σ_3 and "exponential" ν-σ_d/σ_3- σ_3 model but the latter model for Poisson Ratio described better the stress dependency
- The material composition and compaction moisture were found to have a relative distinctive effect on the resilient response. However, a trend in the increase of the resilient modulus as the degree of compaction increases was also observed but the magnitude was less remarkable compared to the other investigated factors
- Theyse (2007) indicates that the compaction moisture for better performance for crushed material is between 80% and 90% saturation, and 70% and 80% saturation for gravel. The results showed that in this study, the RCM material performed better at 70% saturation compaction moisture
- Comparative studies carried out between RCM and fresh quarry aggregates G1 hornfels showed that RCM exhibited nearly similar stiffness with this natural aggregate at low stress levels. Furthermore, results of practical application showed that RCM could perform satisfactorily in the pavement layers that bear low stresses
- The empirical related tests showed that the RCM material in some conditions was not able to meet specifications but the performance related behaviour showed that this material could perform satisfactory in unbound pavement layers. Therefore, performance related material characterisation could be more realistic than material selection based on

empirical tests. These tests are sometimes restrictive even though they provide good indications.

In summary, it can be concluded that the mix composition selection and compaction procedure contribute significantly to the performance of the RCM material and hence should be well controlled. Results of this study also showed that RCM materials are valuable materials that can perform well in pavement layers.

7.2 RECOMMENDATIONS

The performance of the material requires a large spectrum analysis of parameters and factors. Based also on the observations encountered in this study, the following recommendations for further research are made:

- Recycled concrete has shown to generate smaller amount of fines. The author recommends that further research on the use of masonry as fine particles in the mix and/or importing fines(mechanical stabilisation) be carried out
- Assessing the performance of other material mixes to provide information on various mixes characteristics and mechanical behaviour
- Evaluate the influence of compaction on the performance of RCM at various degree of compaction or for a large compaction window in order to assess qualitatively and quantitatively its effect on RCM break down and mechanical performance
- Establish curing protocol for RCM materials as this contributes to the performance of these 'cementitious' materials
- Carry out a study on the permanent deformation behaviour of RCM since the performance of the material is not only characterised by its resilient response but also by its damage response
- Further study on the influence of crushing of RCM on the mechanical performance
- Field trials to validate the material suitability and field performance criterion with related durability
- Comparative performance studies carried out in the same conditions are required between RCM material and natural granular materials so that direct performance comparison can be made
- Further study on life cycle cost analysis with cognisance of sustainability and cost saving on project
- Further quantitative and qualitative studies on potential self-cementing of the RCM materials

- Further study on different types of stabilisation in order to improve the performance of RCM materials with cognisance of boundary between fatigue and permanent deformation
- Development of test protocols and specifications for RCM aimed as alternative material type for use in pavements. The reason for this is that specifications developed for natural materials can be sometimes restrictive to these secondary materials while they can perform well in pavement layers.

.

COMPREHENSIVE REFERENCES

AASHTO T 85. 1999. **Standard test method for the specific gravity and absorption of coarse aggregate**. AASHTO Standard Specifications for Transportation Materials, Part II, Washington, D.C.

Allan,J.J. 1974. **Resilient response of granular materials subjected to time-dependent lateral stresses**. *Transport Research Record 510*: 1-13.

Araya, A.A. 2011. **Characterisation of Unbound Granular Materials for Pavements**. PHD dissertation at Delft University of Technology. The Netherlands.

Arulrajah, A., Piratheepan, Aatheesan, Bo. M. W,M. ASCE. 2011. **Geotechnical properties of recycled crushed brick in pavement applications**. *Journal of Materials in Civil Engineering* 23(10):1444-1452.

Aurstrad J.& Uthus N.S. 2000. **Use of stockpiled asphalt and demolition debris in road construction in Norway**. In Dawson R. Andrew (Ed). *Proceeding of the 5th International symposium on unbound aggregates in roads/UNBAR5*. Nottingham: 87-92.

Azam, A.M & Cameron, D.A. 2013. **Geotechnical properties of blends of recycled clay masonry and recycled concrete aggregates in unbound pavement construction**. *Journal of Materials in Civil Engineering* 25(6): 788-798.

Barbudo A., Agrela F., Ayuso J., Jiménez J.R, Poon C.S. 2011. **Statistical analysis of recycled aggregates derived from different sources for sub-base applications**. *Construction and Building Material* 28(1): 129-138.

Barksdale D. R. (ed). 1991. ***The aggregate handbook***. United States of America: Braun-Brumfield, Inc.

Bester J.J, Kruger D., Hinks A. 2004. **Construction and demolition waste in South Africa**. In John Roberts, Mukesh C Limbadiya(eds). *Proceedings of the international conference organised by the concrete and masonry research group*, London: Thomas Telford publishing :63-67.

Bjarnason G., Petursson, Erlingson S. 2000. **Aggregates resistance to fragmentation, weathering and abrasion**. In Dawson R. Andrew (ed). *Proceeding of the 5th International symposium on unbound aggregates in roads/UNBAR5*. Nottingham: 3-11.

Blankenagel, J.B & Guthrie, W.S. 2007. **Laboratory characterisation of recycled concrete for use as pavement base material.** *Transportation Research Record 1952*, Transportation Research Board, Washington, DC: 21-27.

Botha P.B and Semmelink C.J. 2004. **Determination of the Bulk Relative Density (BRD) and Apparent Relative Density(ARD) of granular materials in one test by means of the rice method(suitable for all types of material for both≥ 4.75 mm and < 4.75 mm fractions)**. Proceedings of the 8th conference on asphalt pavements for Southern Africa (CAPSA'04). Sun city, South Africa.

Boudlal, O & Melbouci, B. 2009. **Study of the behaviour of aggregates demolition by proctor and CBR tests**. GeoHunan International conference . *American Society of Civil Engineers* : 75-80

Box E. P.G, Hunter W.G, Hunter J.S. 1978. ***Statistics for Experimenters: An introduction to design, data analysis, and model building***. USA: John Wiley& Sons.

Brandon J. Blankenagel& W. Spencer Guthrie. 2006. **Laboratory characterisation of recycled concrete for use as pavement base material**. *Transport Research Record 1952*: 21-26.

Cerni G & Colagrande S. 2012. **Resilient modulus of recycled aggregates obtained by means of dynamic tests in triaxial apparatus.** Procedia-Social and Behavioural Science 53(1): 475-484.

Cho G.C, Dodds J., Santamarina J.C. 2006. **Particle shape effects on packing density, stiffness, and strength: natural and crushed sands**. *Journal of Geotechnical and Geoenvironmental Engineering* 132(5): 591-602

Clay Brick Association. 2002. ***Clay brick manufacture technical guide in South Africa***. South Africa: Clay Brick Association.

Committee of Land Transport Officials (COLTO). 1998. **Standard specifications for road and bridge works for state road authorities**. South African Institute of Civil Engineers. South Africa.

Cultrone G., Sebastián E., Elert K., Maria José de la Torre. 2004. **Influence of mineralogy and firing temperature on the porosity of bricks**. Journal of European Ceramic Society 24(3): 547-564.

Department of Environmental Affairs. 2012. ***National waste information baseline report***. Department of Environmental Affairs. Pretoria, South Africa.

Dix William. 2013. Personal Interview. 30 January, Cape Town.

Dukatz, E.L. 1989. **Aggregate properties related to pavement performance**. *Proceedings of Association of Asphalt Paving Technologist*, Nashville, Tennessee 58: 492-502.

Emery, C.J. 1988. ***The prediction of moisture content in untreated pavement layers and an application to design in Southern Africa***. CSIR research report 644. Pretoria.

Environment Council of Concrete Organizations. 1999. ***Recycling concrete and masonry***. Information, Illinois, USA: Environment Council of Concrete Organizations.

European Standard EN 13286-7. 2002. ***Unbound and hydraulically bound mix compositions. Part 7: Cyclic load triaxial test for unbound mix compositions***. Brussels: European Committee of standardisation.

Federal Highway Administration (FHWA). 2004. ***Transportation application of Recycled aggregate concrete.*** US department of transportation. USA.

Gabr, A.R. & Cameron, D.A. 2012. **Properties of recycled concrete for unbound pavement** construction. *Journal of Materials in Civil Engineering* 24(6): 754-764.

Garg N., Thompson M.R., Gomez-Ramirez M.F. 2000. **Unbound granular base modelling-effects on conventional flexible pavement critical responses**. In Dawson R. Andrew (ed). *Proceeding of the 5th International symposium on unbound aggregates in roads/UNBAR5*. Nottingham: 271-277.

Gauteng Department of Agriculture, Conservation and Environment 2009. ***Gauteng provincial building and demolition waste guidelines***. Pretoria, South Africa.

Groenendijk, K., Van Haasteren, C.R., Van Niekerk, A.A. 2000. **Comparison of stiffness moduli of secondary road base materials under laboratory and in situ conditions**. In Dawson R. Andrew (ed). *Proceeding of the 5th International symposium on unbound aggregates in roads/UNBAR5*. Nottingham: 201-208.

Hamzah O.M., Puzi A. A.M, Azizli M.A.K. 2010**. Properties of geometrically cubical aggregates and its mix composition design**. *IJRRAS* 3(3): 249-256.

Hansen T.C. (Ed.). 1992. ***Recycling of demolished concrete and masonry***. RILEM report 6. USA, Taylor & Francis.

Houston, W.N., Houston, S. L. and Anderson, T. W., 1993. **Stress state considerations for resilient modulus testing of pavement subgrade**. *Transportation Research Record* 1406, Washington, D.C:124-132.

Jenkins J. K. 2000. ***Mix design considerations for cold and half-warm bituminous mixes with emphasis on foam bitumen***. PHD dissertation. South Africa : Stellenbosch University.

Jenkins, J. K. 2010. **South African hot mix asphalt design**. Pavement material II lecture notes presented at Stellenbosch University. South Africa. Unpublished.

Jenkins, J. K. 2013. **Hitchhiker's guide to pavement engineering**. Pavement material I lecture notes presented at Stellenbosch University. South Africa. Unpublished.

Karaman S., Ersahin S., Funal H. 2005. **Firing temperature and firing time influence on mechanical and physical properties of clay bricks**. *Journal of Scientific & Industrial Research* 65(02): 153-159.

Karasahin Mustafa. 1993. ***Resilient behaviour of granular materials analysis of highways pavements***. PHD dissertation. UK : University of Nottingham.

Kelfkens R.W.C, 2008. **Vibratory Hammer Compaction of Bitumen Stabilized Material**. Master Thesis of Science in Engineering, University of Stellenbosch. South Africa.

Khogali, E.I.W & Zeghal, M. 2000. **On the resilient behaviour of unbound material**. In Dawson R. Andrew (Ed). *Proceeding of the 5th International symposium on unbound aggregates in roads/UNBAR5*. Nottingham: 29-34

Leek Colin. 2008. **Use of recycled crushed demolition materials as base and subbase in road construction**. Personal communication. Canning, Australia.

Leite D.C., Motta R.S., Vasconcelos L.K., Bernucci L. 2011**. Laboratory evaluation of recycled construction and demolition waste for pavements**. *Construction and Building Materials* 25(6): 2972-2979.

Lekarp F., Isacsson U., Dawson A. 2000. **State of art: resilient response of unbound aggregates**. *Journal of Transportation Engineering 126(1):* 66-75.

Linglin X., Wei G., Tao W., Nanru Y. 2004. **Study on fired bricks with replacing clay ash in high volume ratio**. *Construction and Building Materials* 19(3): 243-247.

Little D.N, Males H.E, Prusinski R.J, Stewart B. 2001. **Cementitious stabilisation**. *Transportation in the New Millennium*. Transport Research Board. Washington: 1-7.

Louw Kristin. 2013. **Compaction of recycled concrete and crushed clay brick aggregate blends using the modified and vibratory hammer**. Bachelor degree thesis. Stellenbosch Univeristy. Unpublished.

Marradi A.& Lancieri F. 2008. **Performance of Cement Stabilised Recycled Crushed Concrete**. *First International Conference on Transport Infrastructure ICTI*, Beijing, China,vol. CD: 1-10.

Metso. 2007. ***Crushing and screening handbook***. Finland: Kirjapaino Hermes.

Mgangira, M.B & Jenkins, J.K. 2011. ***Proposed protocol for resilient modulus and permanent deformation characteristics of unbound and bound granular materials***, Report No SANRAL/SAPDM/B1-c/2011-01, CSIR& university of Stellenbosch, RSA.

Michigan Department of Transportation (MDOT). 2011. ***Using recycled concrete in MDOT's transportation infrastructure – manual of practice.*** Final Report Nº RC-1544. Michigan.

Mitchell, J.K. 1993. ***Fundamentals of soil behaviour, 2nd edition***, USA :John Wiley & sons, inc.

Molenaar A.A. A. & van Niekerk A.A. 2002. **Effects of gradation, composition, and degree of compaction on the mechanical characteristics of recycled materials**. *Transportation Research Record* 1787. Transportation Research Board, Washington, DC: 73-82.

Molenaar, A.A.A. 2005. **Cohesive and non-cohesive soils and unbound granular materials for bases and sub-bases in roads**. Road materials Part I lecture notes. Delft University of Technology.

Morton, B.S, Lutting, E., Horak, E., Visser, A.T. 2004. **The effect of axle load spectra and tyre inflation pressures on standard pavement design methods**. *Proceedings of the 8th conference on asphalt pavement for Southern Africa (CAPSA'04)*. Sun City. Unpublished: 1-15

Nataatmadja A.& Tan Y.L. 2000. **The performance of recycled crushed concrete aggregates**. In Dawson R. Andrew (ed). *Proceeding of the 5th International symposium on unbound aggregates in roads/UNBAR5*. Nottingham: 109-115.

Nataatmadja A.& Tan Y.L. 2001. **Resilient response of recycled concrete road aggregates**. *Journal of Transportation Engineering* 127(5): 450-453.

Novoa-Martinez Brenda. 2003. ***Strength properties of granular materials***. Master's thesis. Louisiana State University and Agricultural and Mechanical College. Louisiana.

Paige-Green P. 2010. **A preliminary evaluation of the reuse of cementitious materials**. *Proceedings of the 29th Southern African Transport Conference (SATC 2010).* Pretoria: 520-529.

Paige-Green, P. 2010b. **Relationship between climatic variables (temperature and rainfall), temperature, and moisture in pavements**. Report SANRAL/SAPDM/E-1/2010-01draft 1. CSIR, Pretoria, South Africa.

Park Taesoon. 2003. **Application of construction and building debris as base and subbase materials in rigid pavement**. *Journal of Materials in Civil Engineering* 129(5): 558-563.

Poon, C.S. & Chan, D. 2005. **Feasible use of recycled concrete aggregates and crushed clay brick as unbound road base**. *Construction and Building Materials* 20(8): 578-585.

Republic of South Africa . 2010. ***National Environmental Management Strategy***. Gauteng: Draft. Pretoria, South Africa.

Roberts, L.F, Kandhal, S.P, Brown, E.Ray, Lee, Y.D, Kennedy, W. T. 1996. ***Hot mix asphalt materials, mix composition design, and construction 2nd ed***. Maryland: NAPA Research and education foundation.

Rodriguez A.R. del Castillo H & Sowers G.F., 1988. ***Soil Mechanics in Highway Engineering*.** Republic of Germany:Trans Tech Publications.

Sánchez de Juan, M.& Gutiérez, A. P. 2008. **Study on the influence of attached mortar content on the properties of recycled concrete aggregate**. *Construction and Building Materials* 23(3): 872-877.

Scott Wilson. 2007. **Development of durability tests for hydraulically bound mix compositions**. Report AGG 79-005, UK: Waste & Resources Action Program.

Scrivinet L.Karen & Nonat André. 2011. **Hydration of cementitious materials, present and future**. *Cement and Concrete Research* 41(7): 651-665.

Siswosoebrotho B.I., Widodo P. , Augusta E. 2005. **The influence of fines and plasticity on the strength and permeability of Aggregate for base course material.** *Proceedings of the Eastern Asia Society for Transportation Studies 5: 845-856.*

Sivakugan N. (2000). **Soil classification**. James cook University geongineering lecture handout. USA. Unpublished.

Slim J.A & Wakefield R.W. 1991. **The utilisation of sewage sludge in the manufacture of clay bricks**. *Water SA* 17(3): 197-202.

South African Pavement Engineering Manual (SAPEM). 2013. ***South African Pavement Engineering Manual 1st edition***. Republic of South Africa.

Suvash Paul CHANDRA. 2011. **Mechanical behavior and durability performance of concrete containing recycled concrete aggregate**. Master's thesis at Stellenbosch University. South Africa.

Technical Methods for Highways (TMH1). ***Standard methods of testing road construction materials*. 2nd edition**. Department of Transport, Pretoria, South Africa.

Technical Recommendations for Highways (TRH 14). 1985. ***Guidelines for road construction materials***. Department of Transport, Pretoria, South Africa.

Technical Recommendations for Highways (TRH4).1996. ***Structural design of flexible pavements for interurban and rural roads***. Department of Transport, Pretoria, South Africa.

Technical Recommendations for Highways (TRH8).1987. ***Design and use of hot-mix in pavements***. Department of Transport, Pretoria, South Africa.

Theyse H., & Muthen M., 2000. **Pavement analysis and design software (PADS) based on the South African mechanistic-empirical design method.** *South African transport conference 'Action in transport for the millennium'*. South Africa.

Theyse, H.L, De Beer, M., Rust, F.C. 1996. **Overview of South African mechanistic pavement design method**. *Transportation Research Record 1539*. Transportation Research Board. Washington: 6-16.

Theyse, H.L. 2007. ***A mechanical-empirical design model for unbound granular pavement layers***. Dissertation for Doctor Ingeneriae, University of Johannesburg, South Africa.

Thom, N. H., & Brown, S. F. 1987. **Effect of moisture on the structural performance of a crushed-limestone road base**. *Transportation Research Record. 1121*, Transportation Research Board, Washington, D.C., 50–56.

Thornthwaite, C. W. 1948. **An approach toward a rational classification of climate**. *Geographical Review,* 38(1):55-94.

Twagira E. Mathaniya. 2010. ***Influence of durability properties on performance of bitumen stabilised materials***. PHD dissertation. University of Stellenbosch, South Africa.

Uzan, J. 1985. **Characterisation of granular material.** *Transportation Research Record 1022*, Transportation Research Board, Washington, D.C: 52–59.

Van Niekerk, A.A, Huurman, M. 1995. **Establishing complex behaviour of unbound road building materials from simple material testing**. Report 7-95-200-16, Delft University of Technology. The Netherlands.

Van Niekerk, A.A. 2002. ***Mechanical behaviour and performance of granular bases and sub-bases in pavements***. PHD dissertation at the Delft University of Technology. The Netherlands.

Van Niekerk, A.A., Molenaar, A.A.A., Houben, L.J.M. 2002. **Effect of quality and compaction on the mechanical behaviour of base course materials and pavement performance**. *In 6th International conference on the bearing capacity of roads and airfields*. Lisbon. Portugal. 1071-1081.

Vegas I., Ibanez J.A, Lisbona A., Sáez de Cortazar A., Frías M. 2010. **Pre-normative research on the use of mixed recycled aggregates in unbound road sections**. *Waste management* 25(5): 2674-2682.

Vegas I., Ibanez J.A, San José J.T, Urzelai A. 2008. **Construction demolition waste, waelz slag and MSWI bottom ash: a comparative technical analysis as material for road construction**. *Waste management* 28(3): 565-574.

Weinert H.H. 1980. ***The natural road construction materials of Southern Africa***. Academia. CapeTown.

Weng C.H, Lin D.F, Chiang P.C. 2003**. Utilisation of sludge as brick materials**. *Advances in Environmental Research* 7(3): 679-685.

Williamson Gregory S. 2005. ***Investigation of testing methods to determine long-term durability of Wisconsin aggregate resources including natural materials, industrialby-products, and recycled/reclaimed materials***. Master's Thesis at Virginia Polytechnic Institute and State University. Virginia.

Wilson Scott. 2007. **Development of durability tests for hydraulically bound mix compositions**. AGG79-005 report. Waste & Resources Action Programme. UK.

Xing Weihong. 2004. ***Quality improvement of granular secondary raw building materials by separation and cleansing techniques***. Master's thesis at Delft University of Technology. The Netherlands.

Xuan Dongxing, Molenaar, A.A.A, Houben, J.M.L, Shui, Z. 2011. **Prediction of the mechanical properties of cement treated mix granulates with recycled masonry and concrete**. *Transport Research Board annual meeting*. Washington,D.C.

APPENDIX A : MATERIAL BREAKAGE DURING COMPACTION

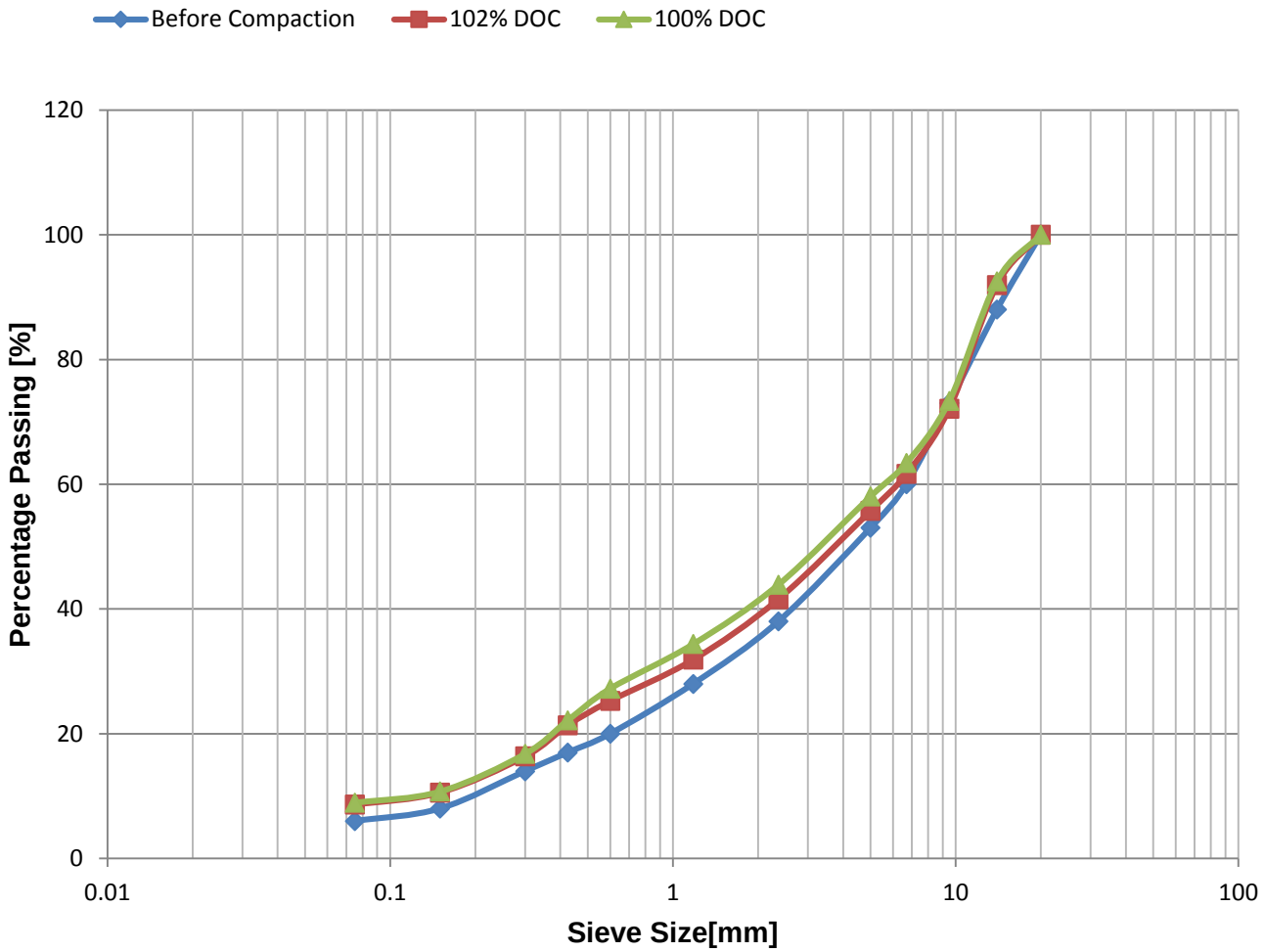

Figure A- 1 : Grading before and after Compaction for 70C:30M - 70% CM

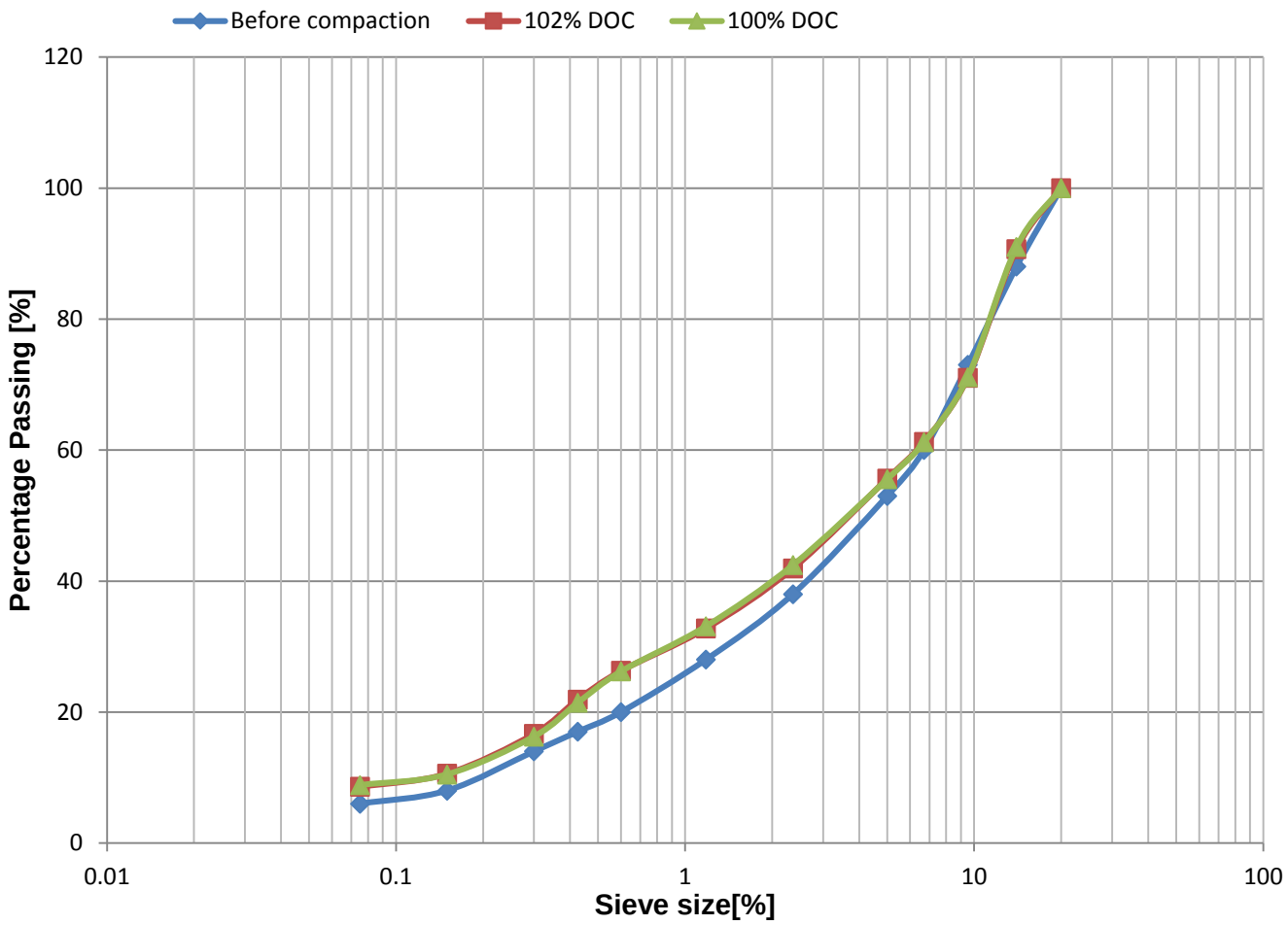

Figure A- 2 : Grading before and after Compaction for 70C:30M - 80% CM

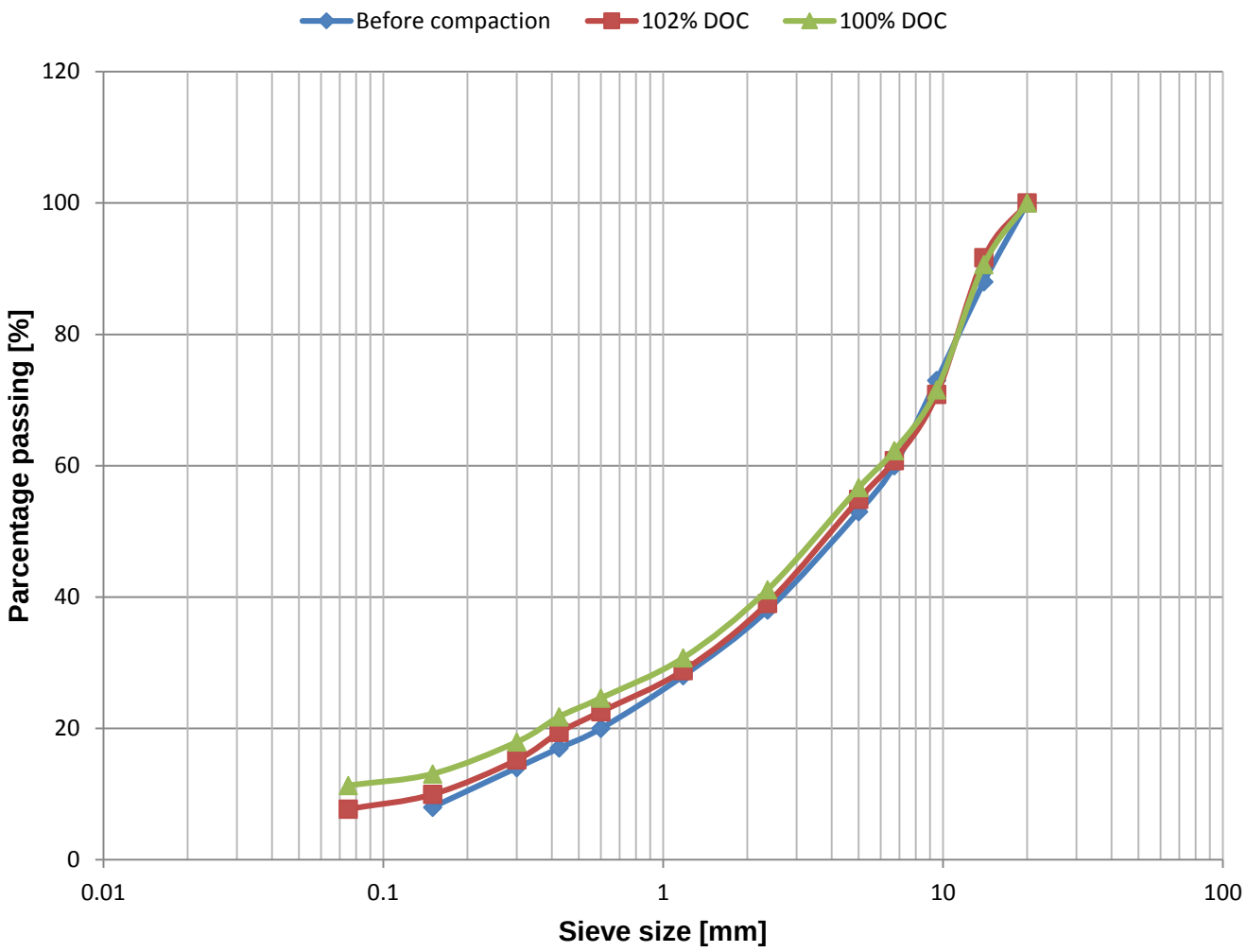

Figure A- 3 : Grading before and after Compaction for 30C:70M - 70% CM

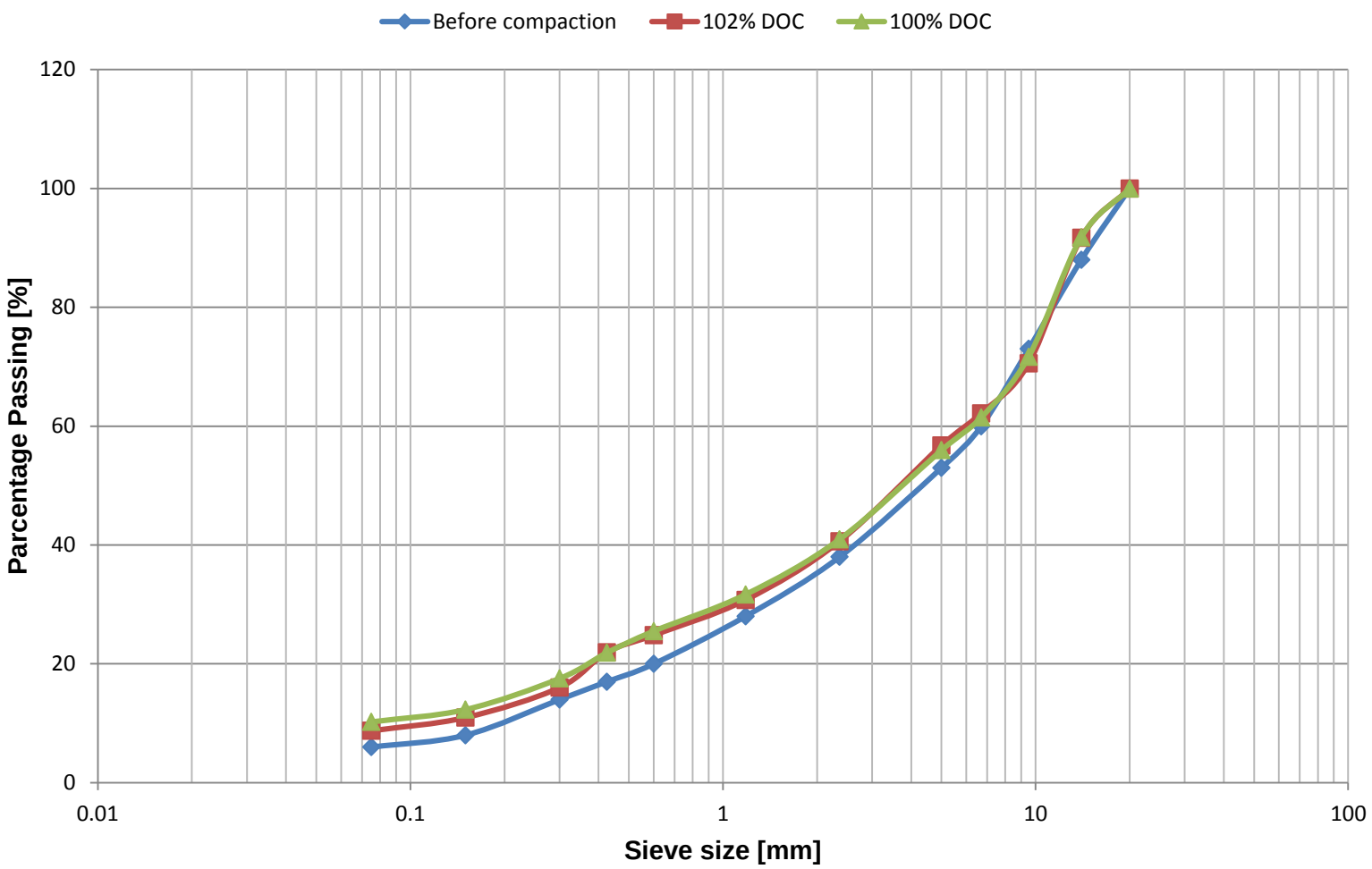

Figure A- 4 : Grading before and after Compaction for 30C:70M - 80% CM

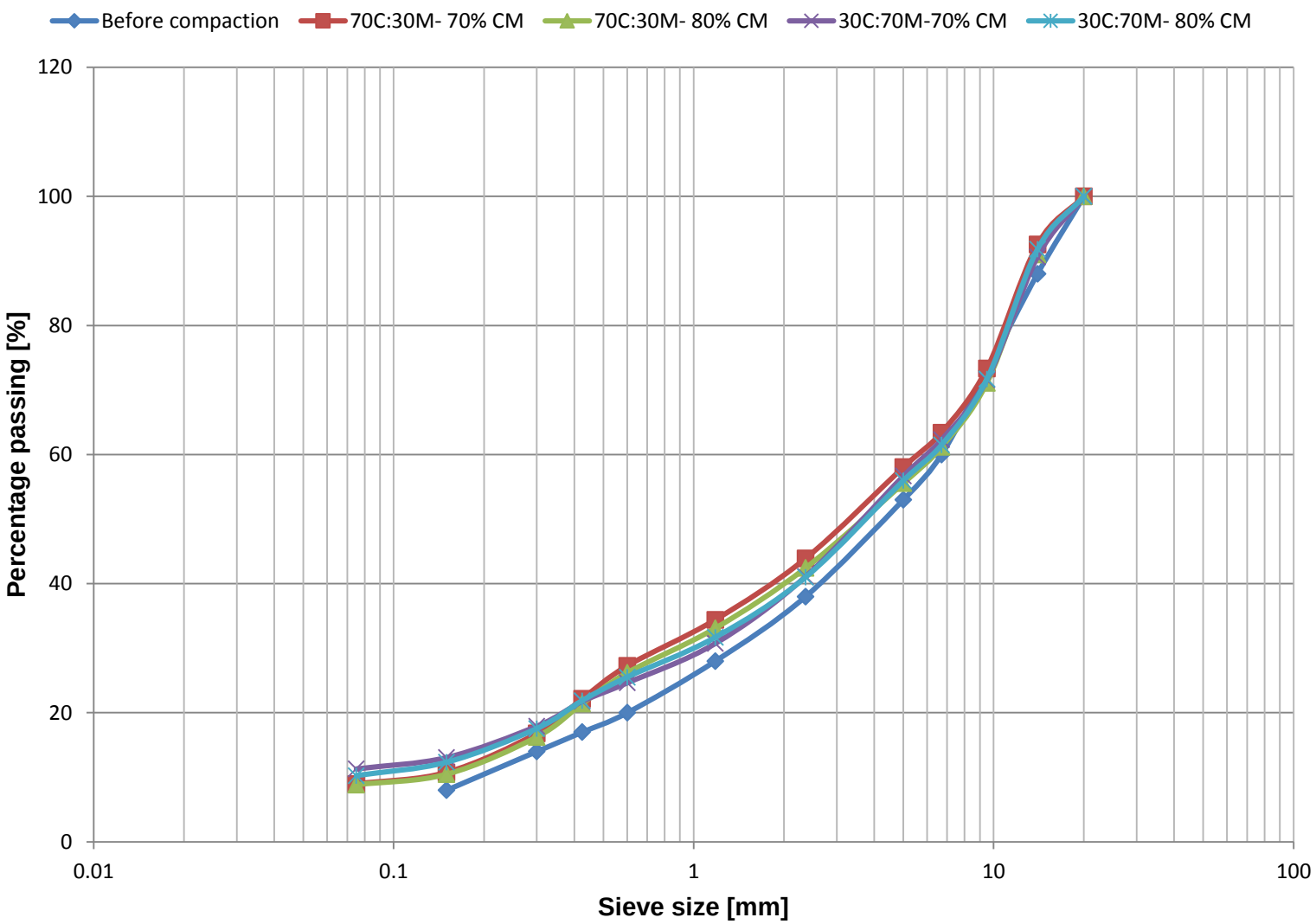

Figure A- 5 : Grading before and after Compaction for 100% DOC – all Mix Compositions

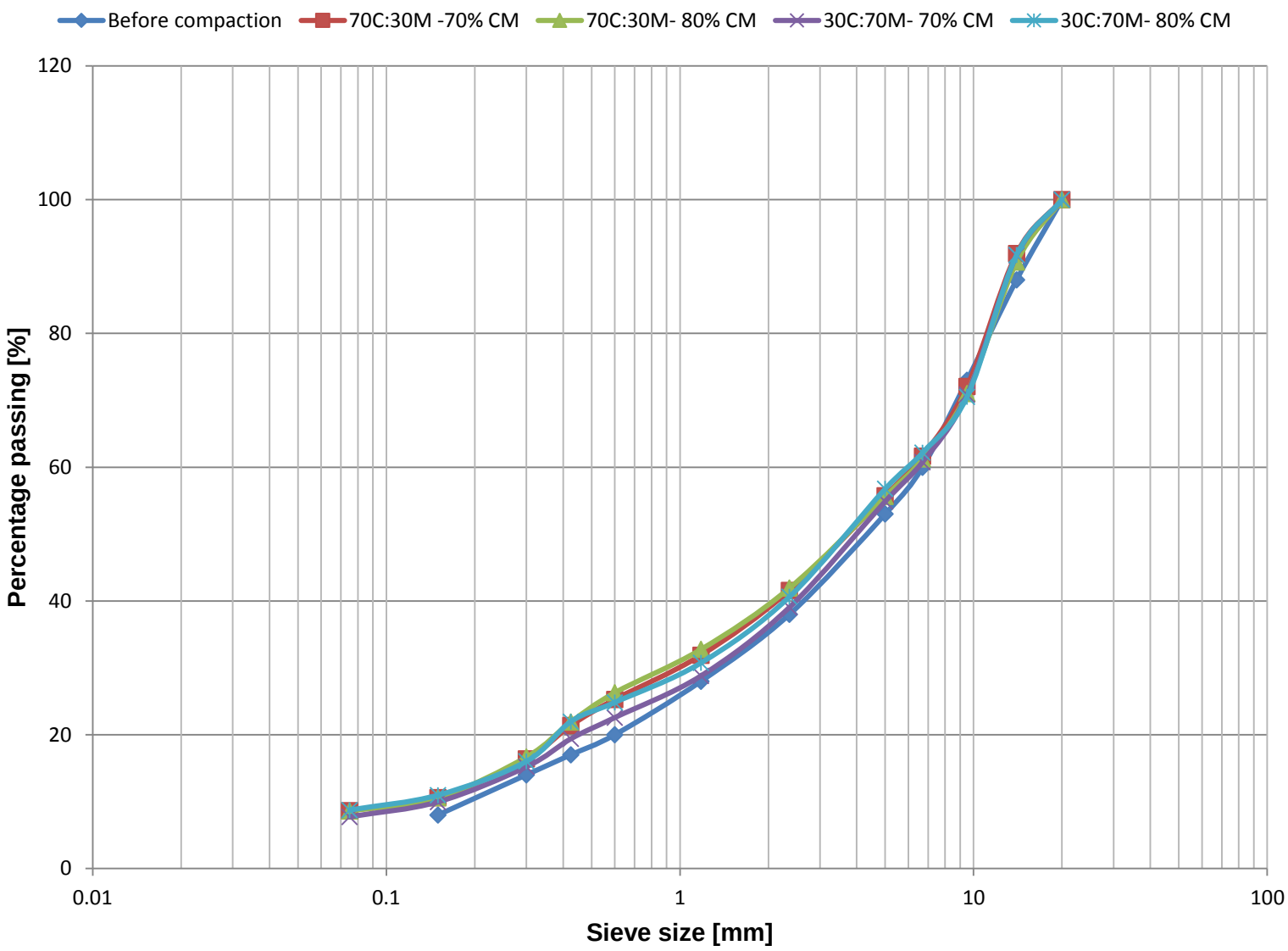

Figure A- 6 : Grading before and after Compaction for 102% DOC – all Mix Compositions

APPENDIX B: STRESS- STRAIN BEHAVIOUR FOR MONOTONIC TEST

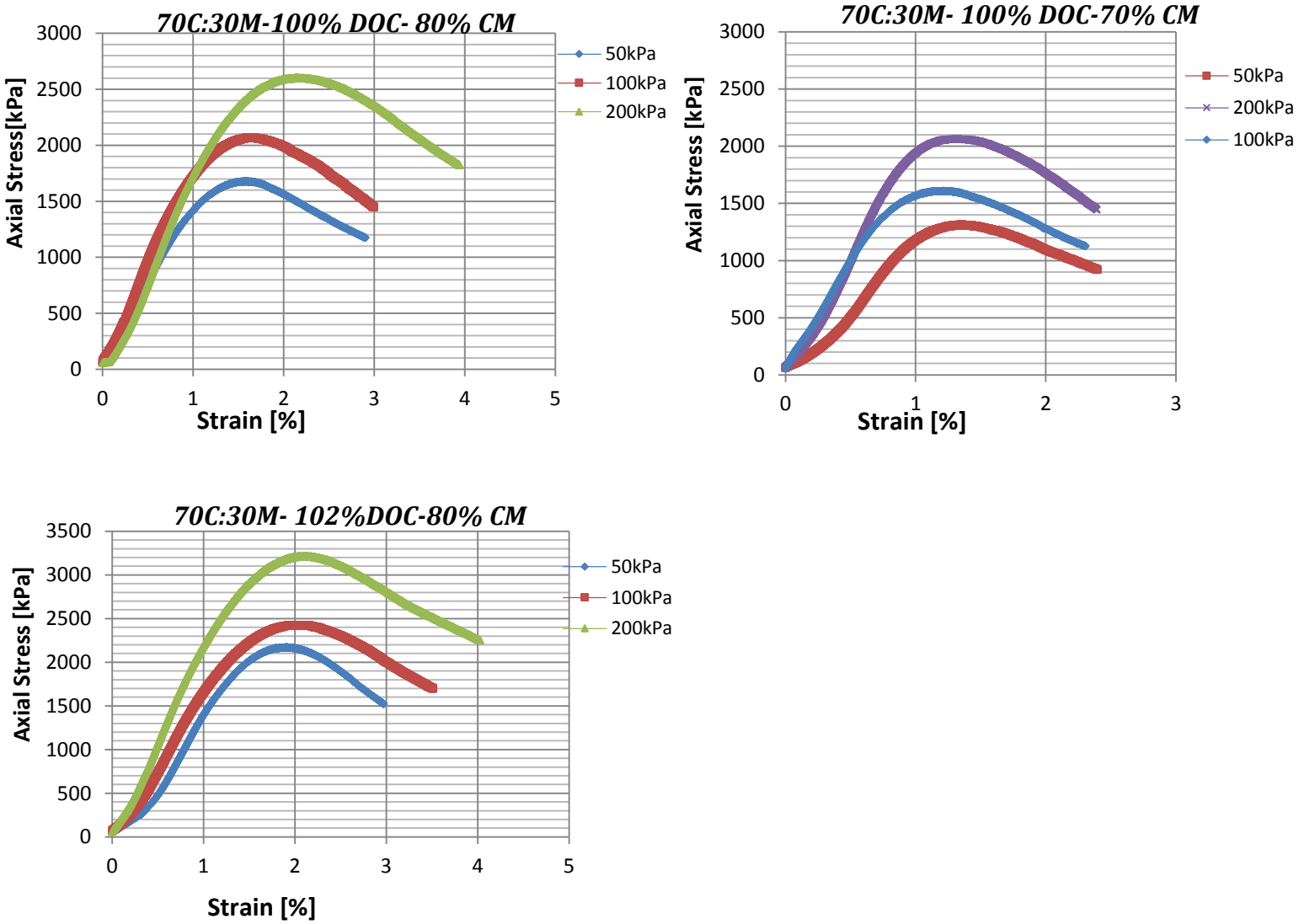

Figure B- 1 : Stress-Strain Behaviour for 70C:30M Mix Composition

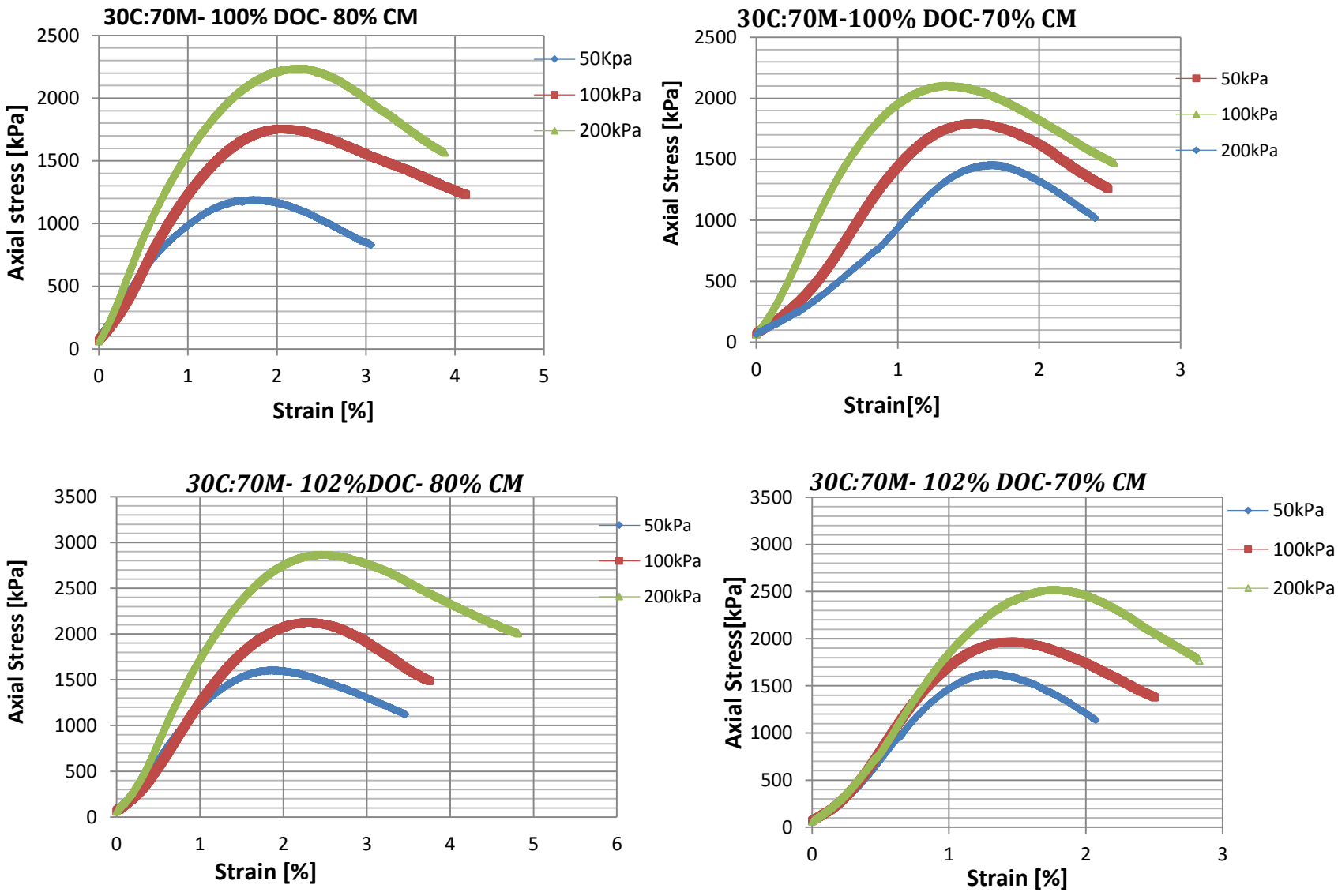

Figure B- 2: Stress-Strain Behaviour for 30C:70M Mix Composition

APPENDIX C: MOHR-COULOMB MODEL FOR VIRGIN SPECIMENS

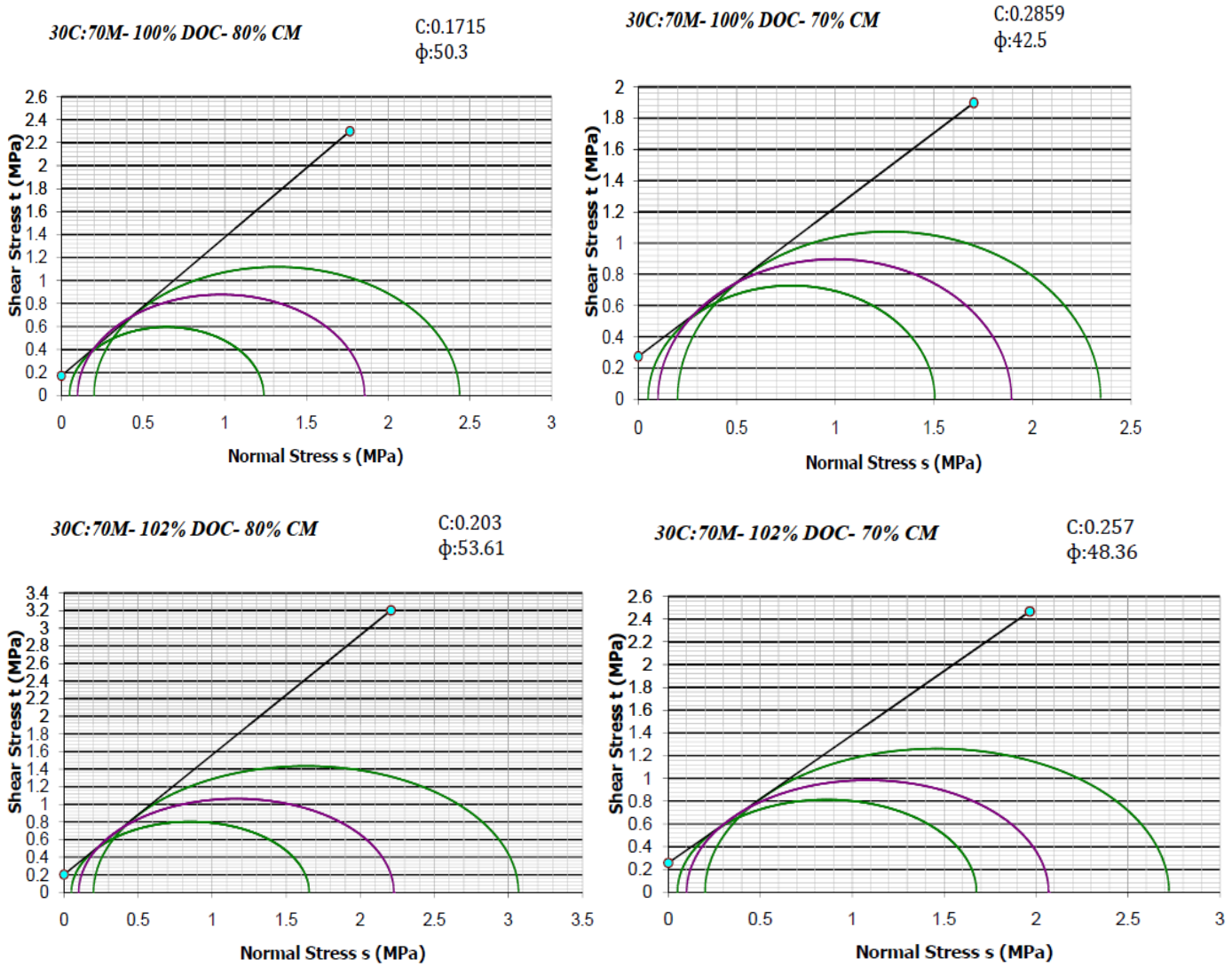

Figure C- 1 : Mohr-Coulomb Model for 30C:70M Virgin Samples

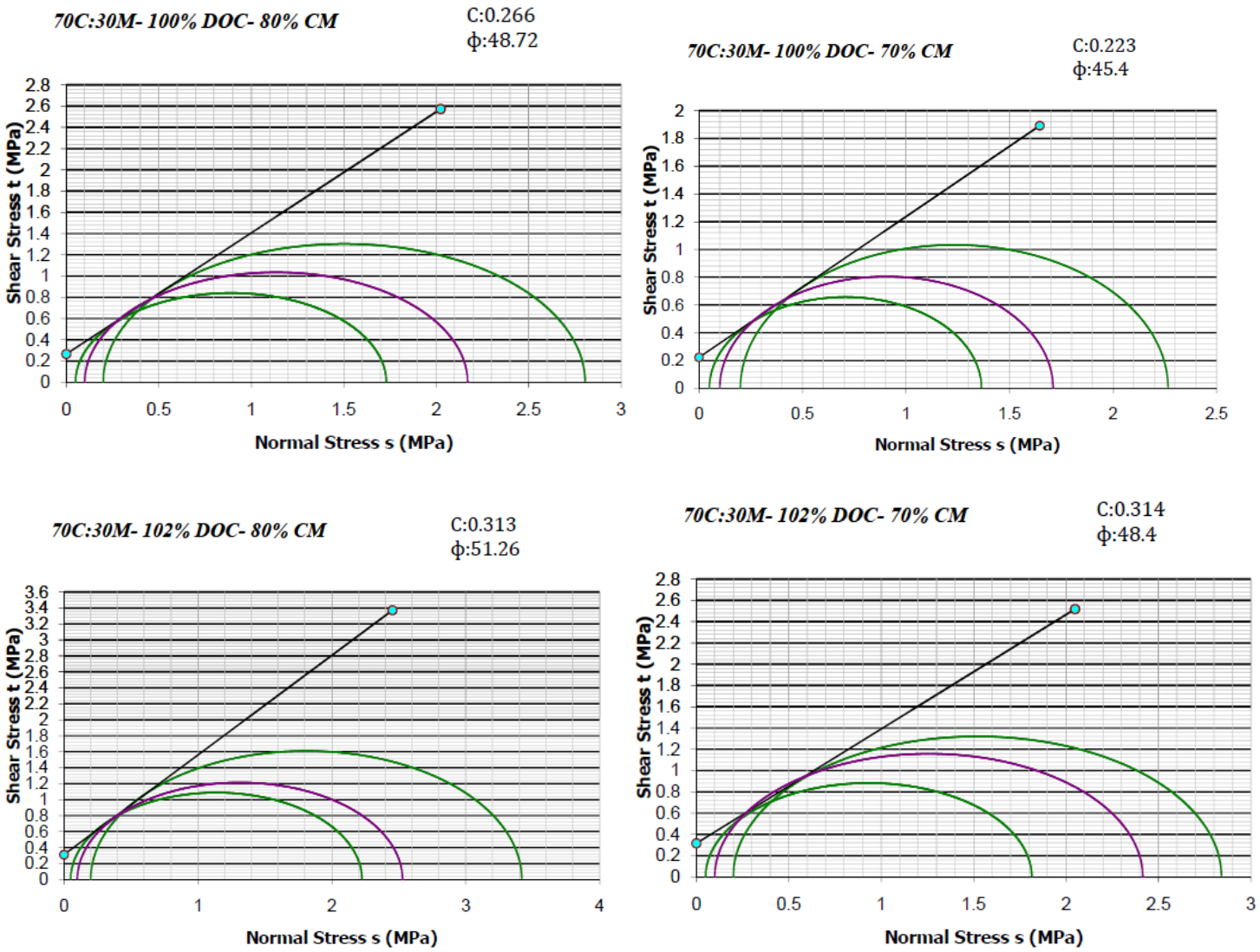

Figure C- 2 : Mohr-Coulomb Model for 70C:30M Virgin Samples

APPENDIX D: MOHR-COULOMB MODEL FOR PRELOADED SAMPLES

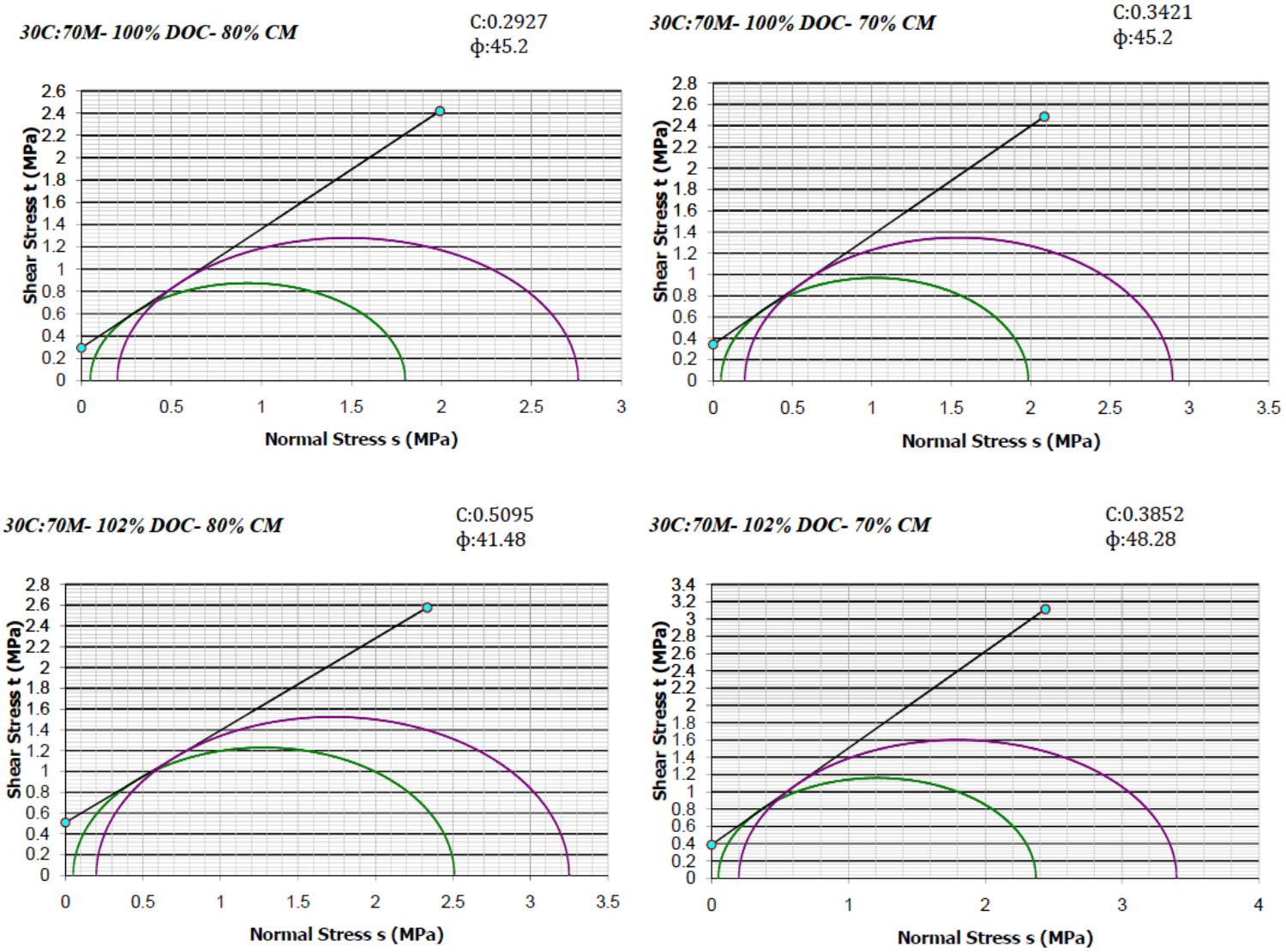

Figure D- 1 : Mohr-Coulomb Model for 30C:70M Preloaded Samples

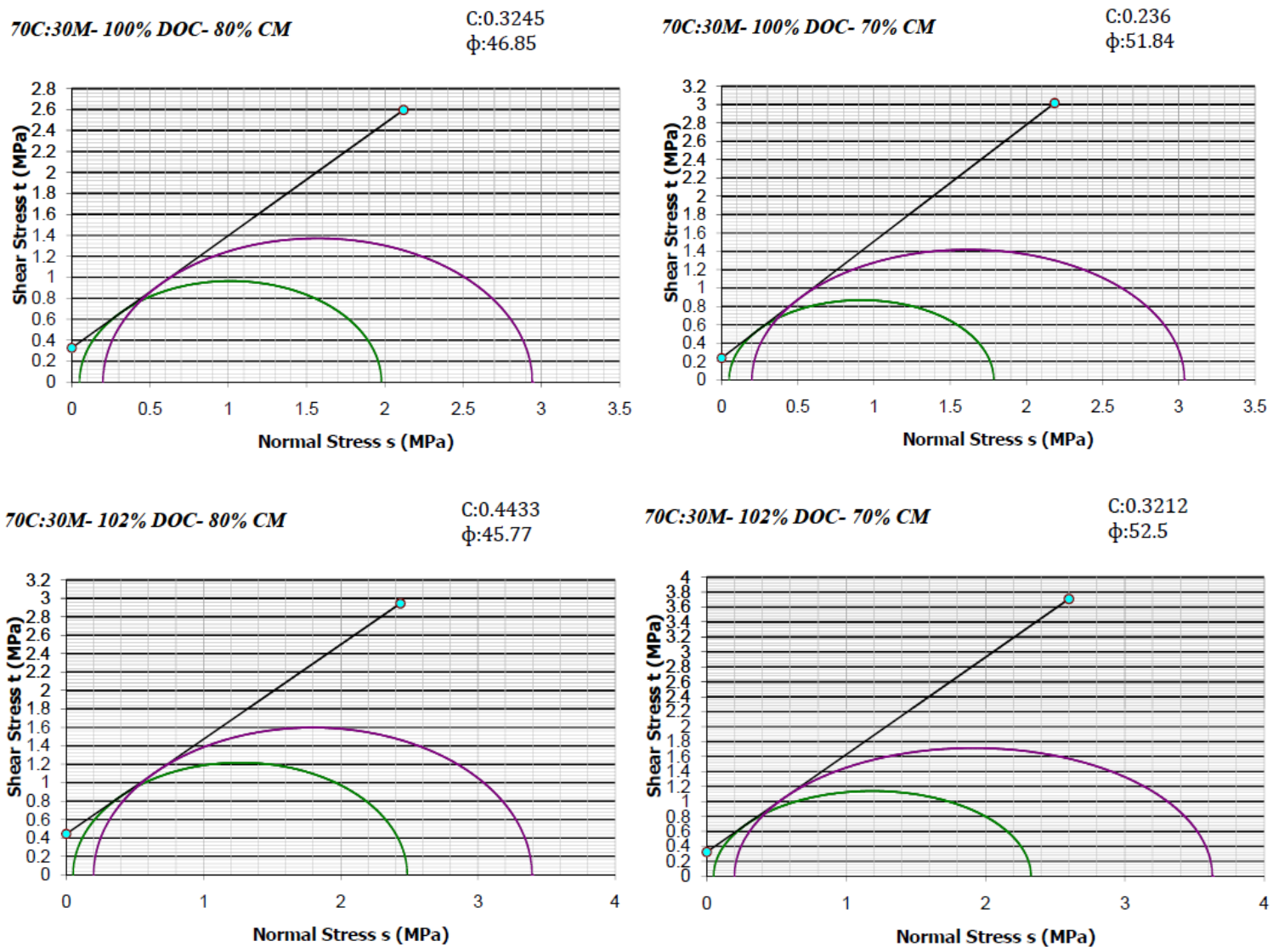

Figure D- 2 : Mohr-Coulomb Model for 70C:30M Preloaded Samples

APPENDIX E: RESILIENT RESPONSE MODELLING

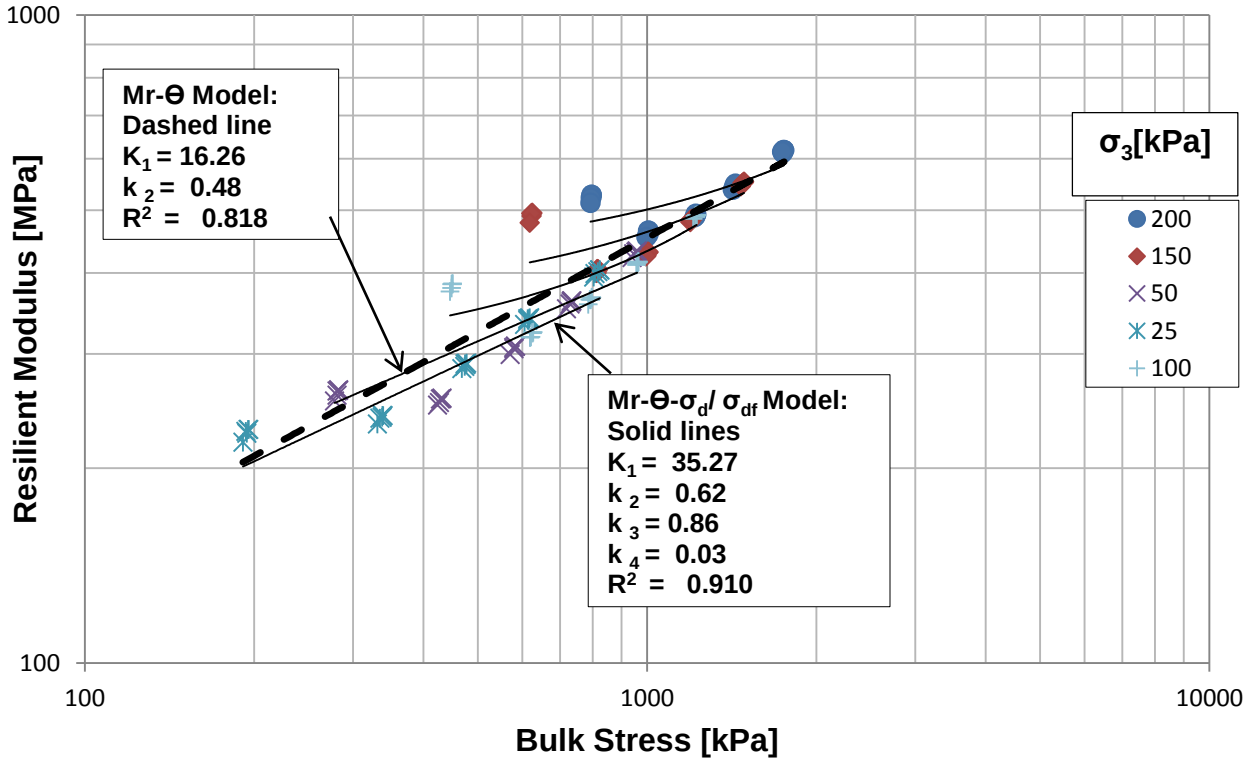

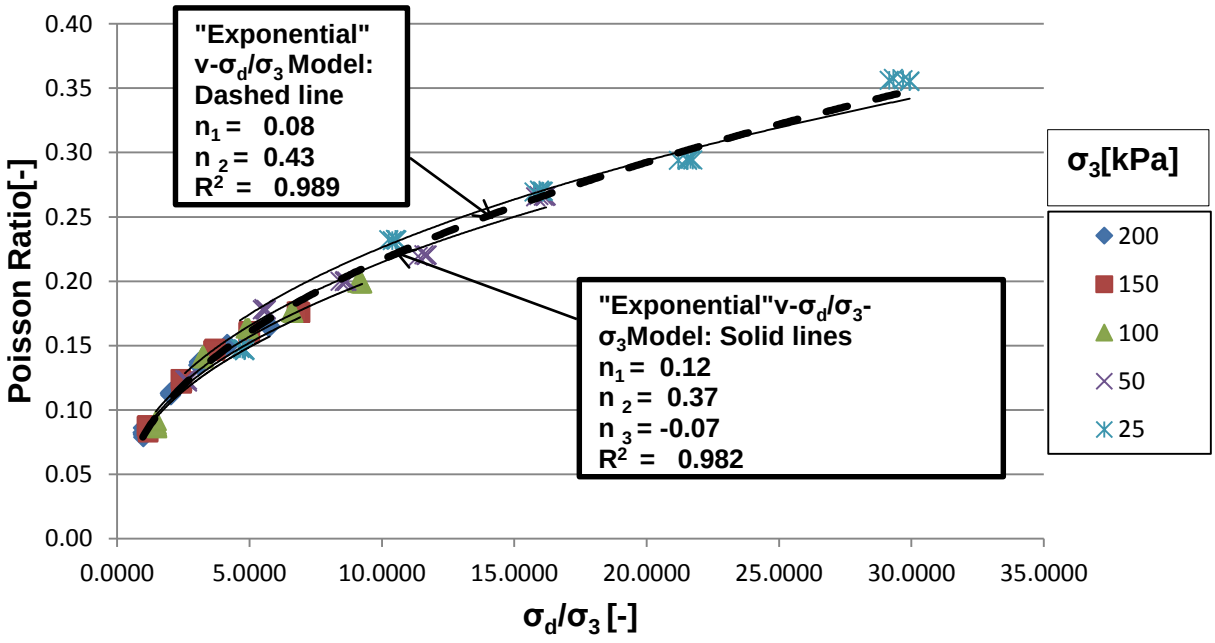

Figure E- 1 : Resilient Modulus and Poisson Ratio Modelling for 30C:70M-100%DOC-70%CM

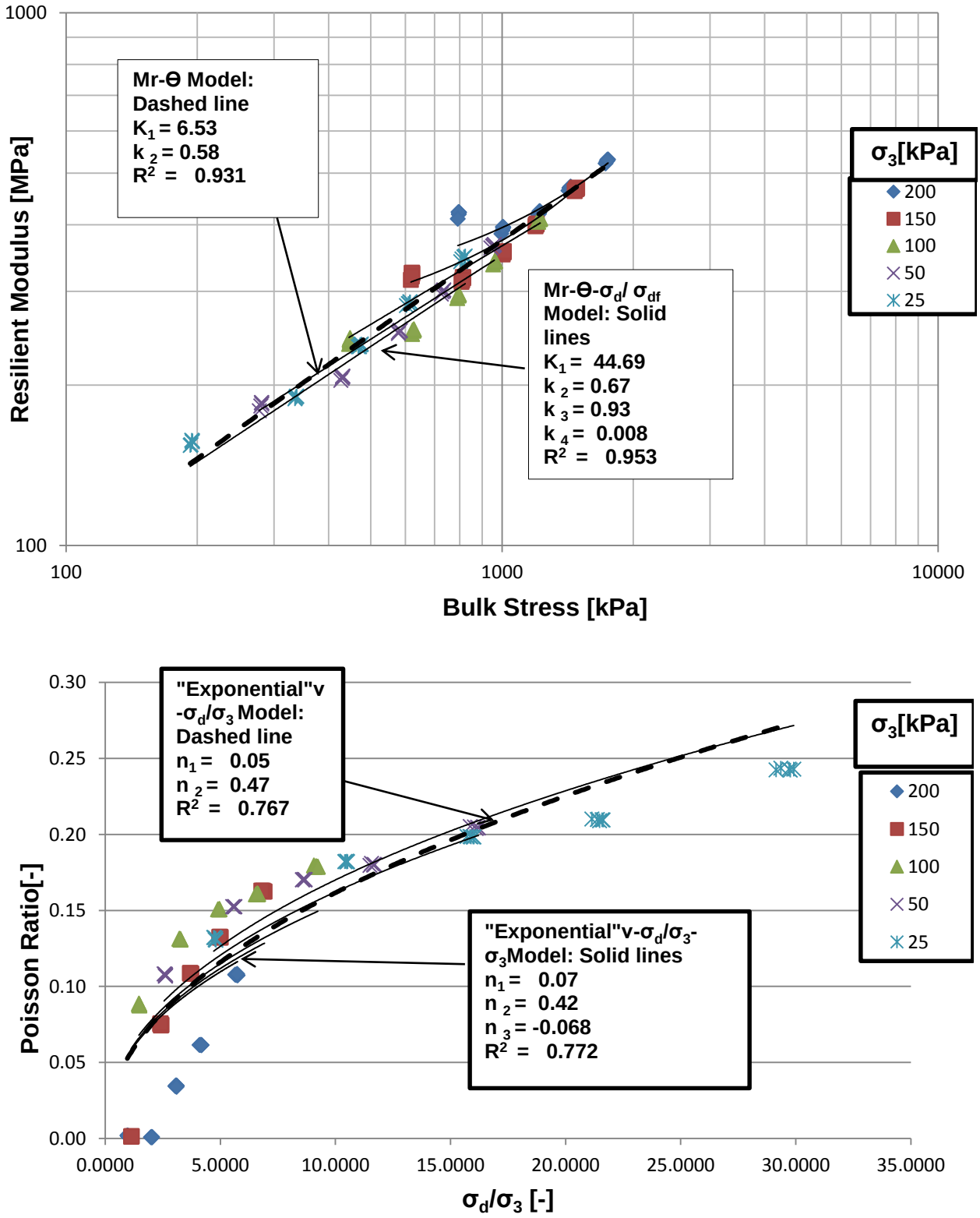

Figure E- 2 : Resilient Modulus and Poisson Ratio Modelling for 30C:70M-100%DOC-70%CM Duplicate Sample

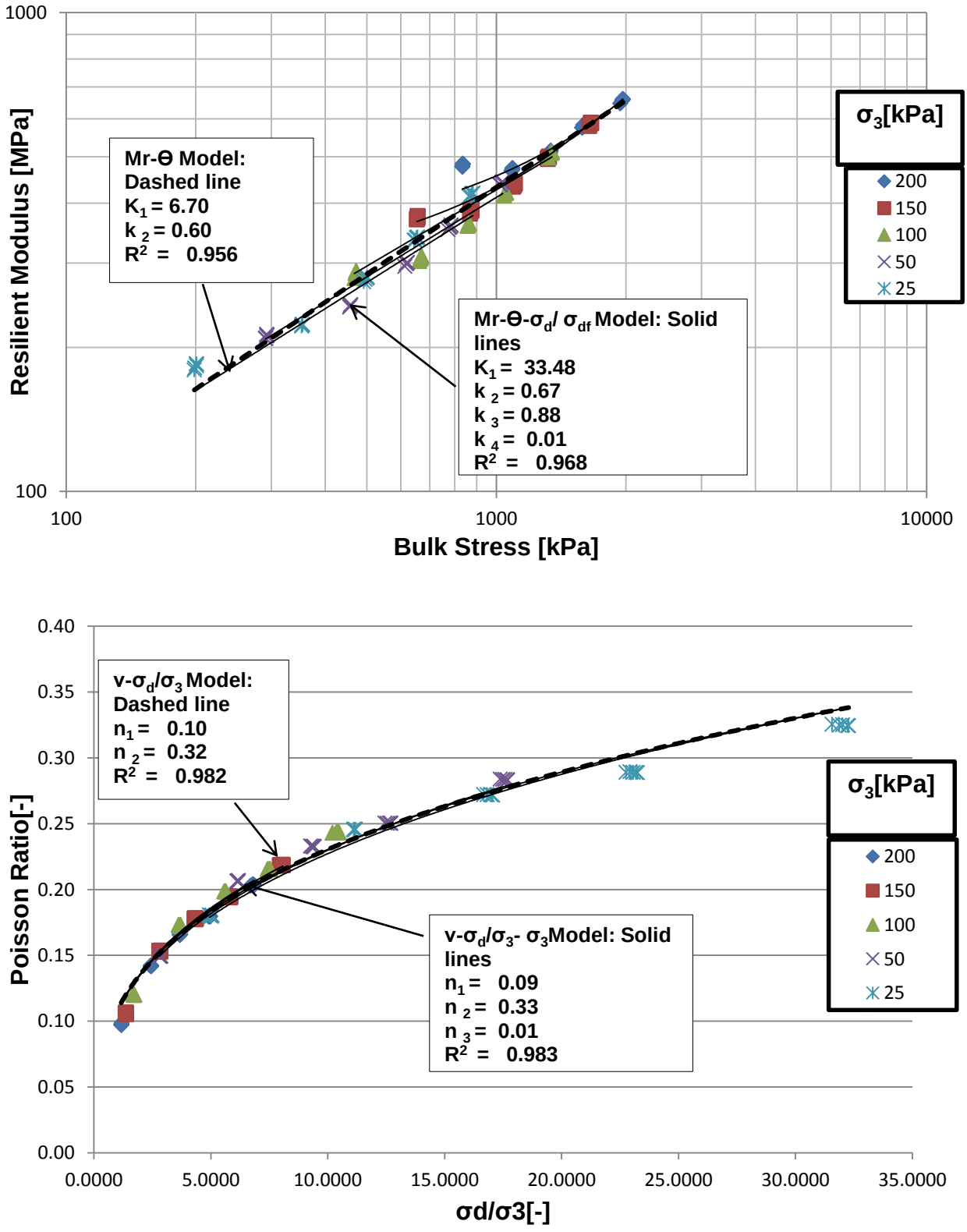

Figure E- 3 : Resilient Modulus and Poisson Ratio Modelling for 30C:70M-102%DOC-70%CM

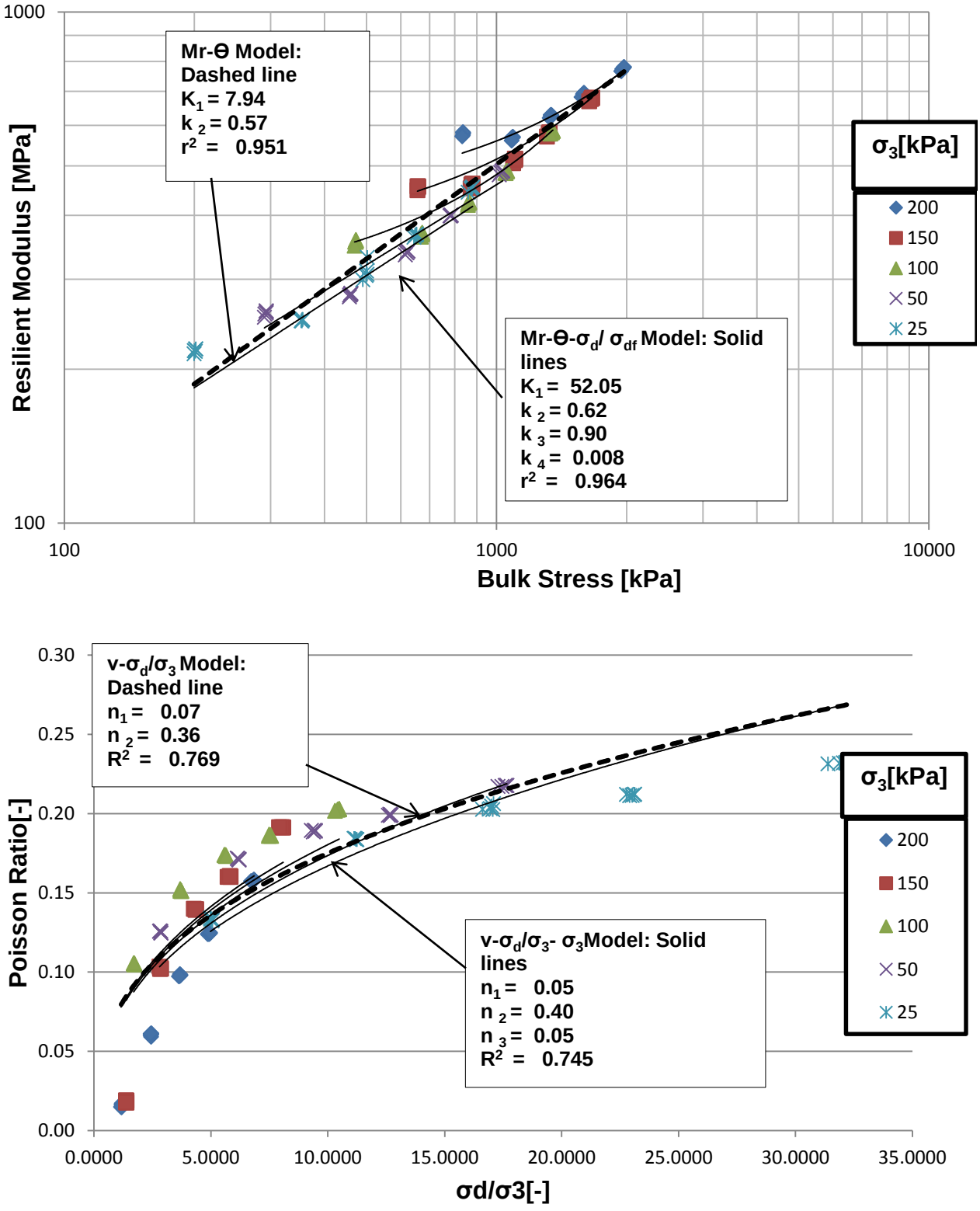

Figure E- 4 : Resilient Modulus and Poisson Ratio Modelling for 30C:70M-102%DOC-70%CM Duplicate Sample

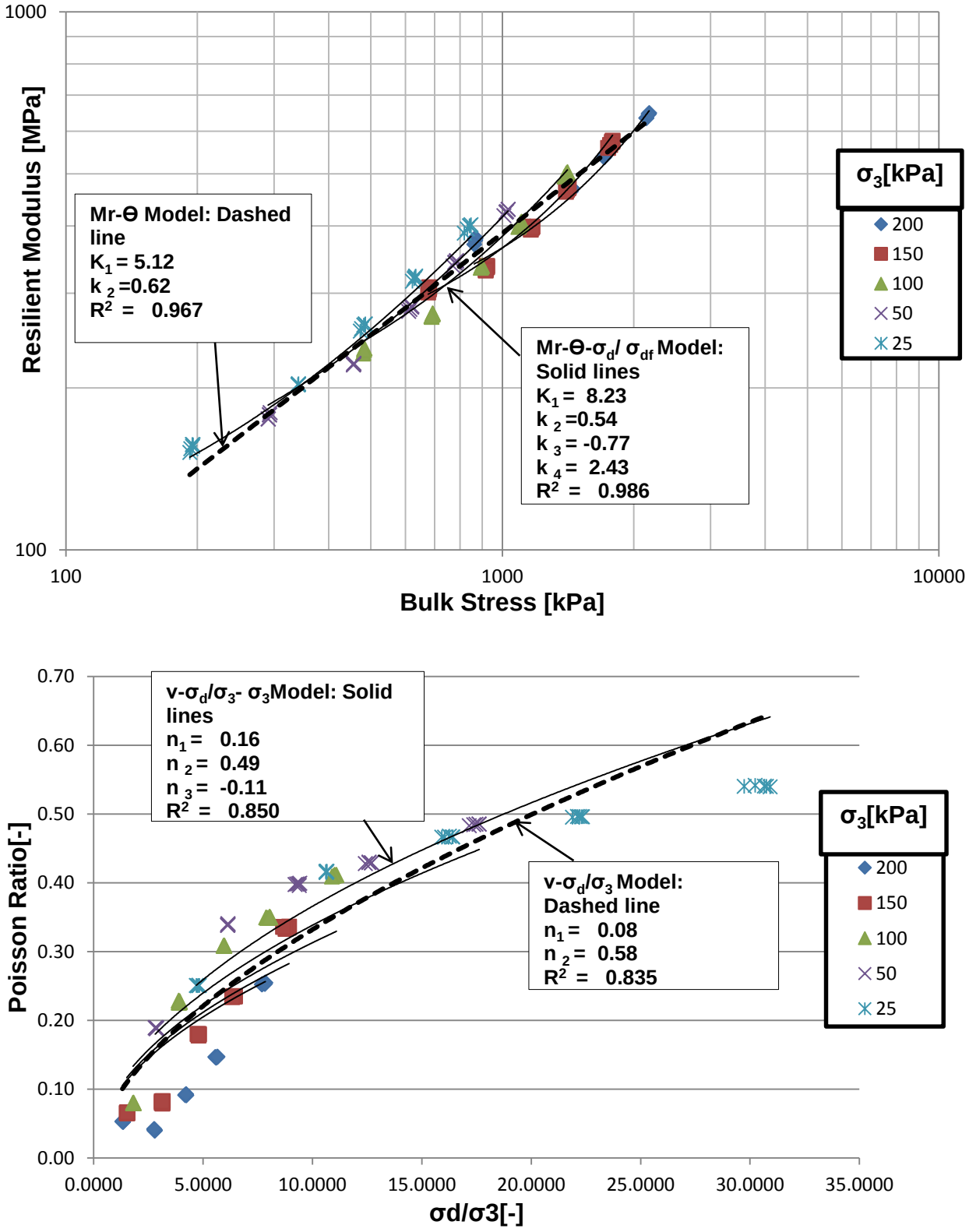

Figure E- 5 : Resilient Modulus and Poisson Ratio Modelling for 30C:70M-102%DOC-80%CM

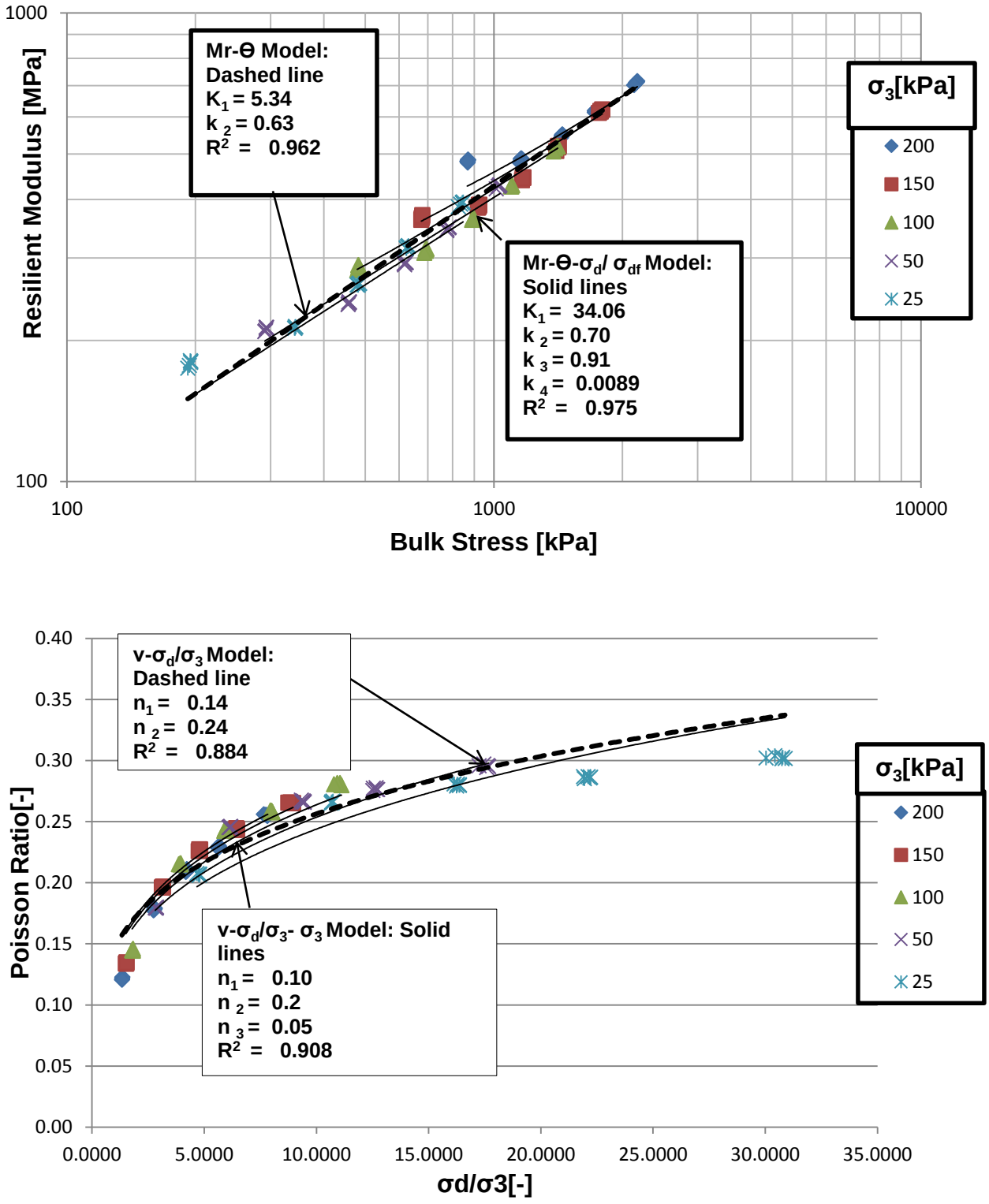

Figure E- 6: Resilient Modulus and Poisson Ratio Modelling for 30C:70M-102%DOC-80%CM Duplicate Sample

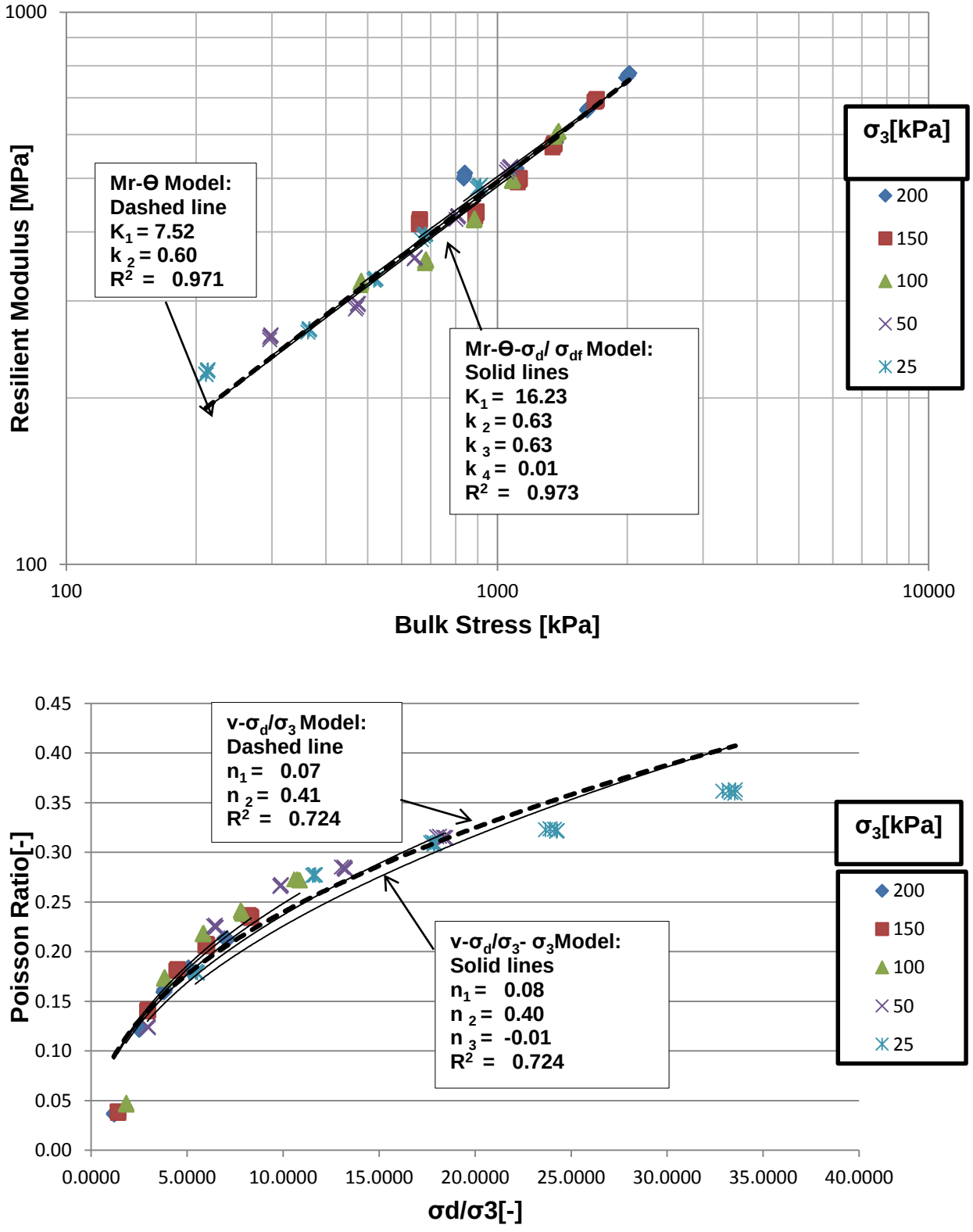

Figure E- 7: Resilient Modulus and Poisson Ratio Modelling for 70C:30M-100% DOC-80%CM

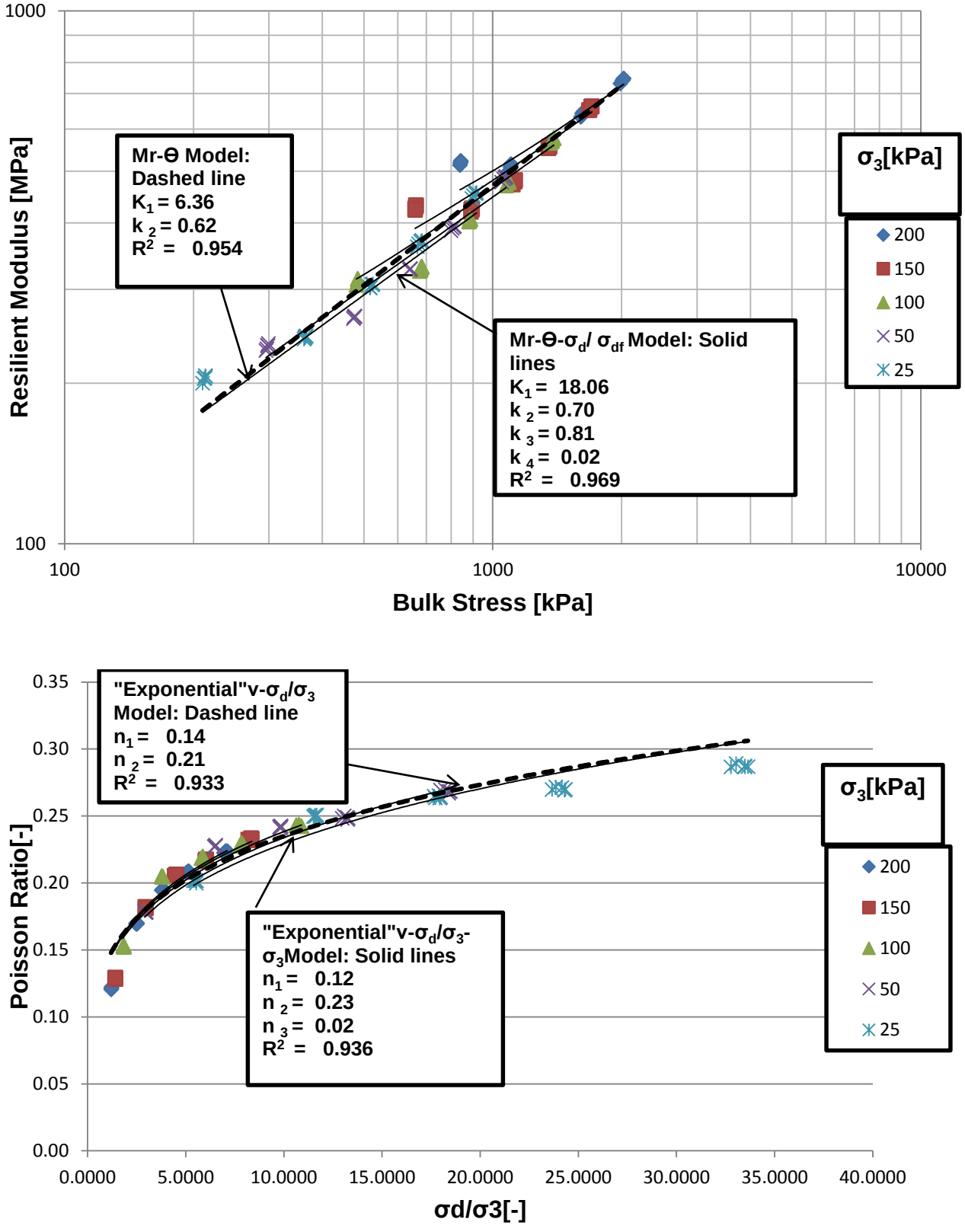

Figure E- 8 : Resilient Modulus and Poisson Ratio Modelling for 70C:30M-100%DOC-80%CM Duplicate Sample

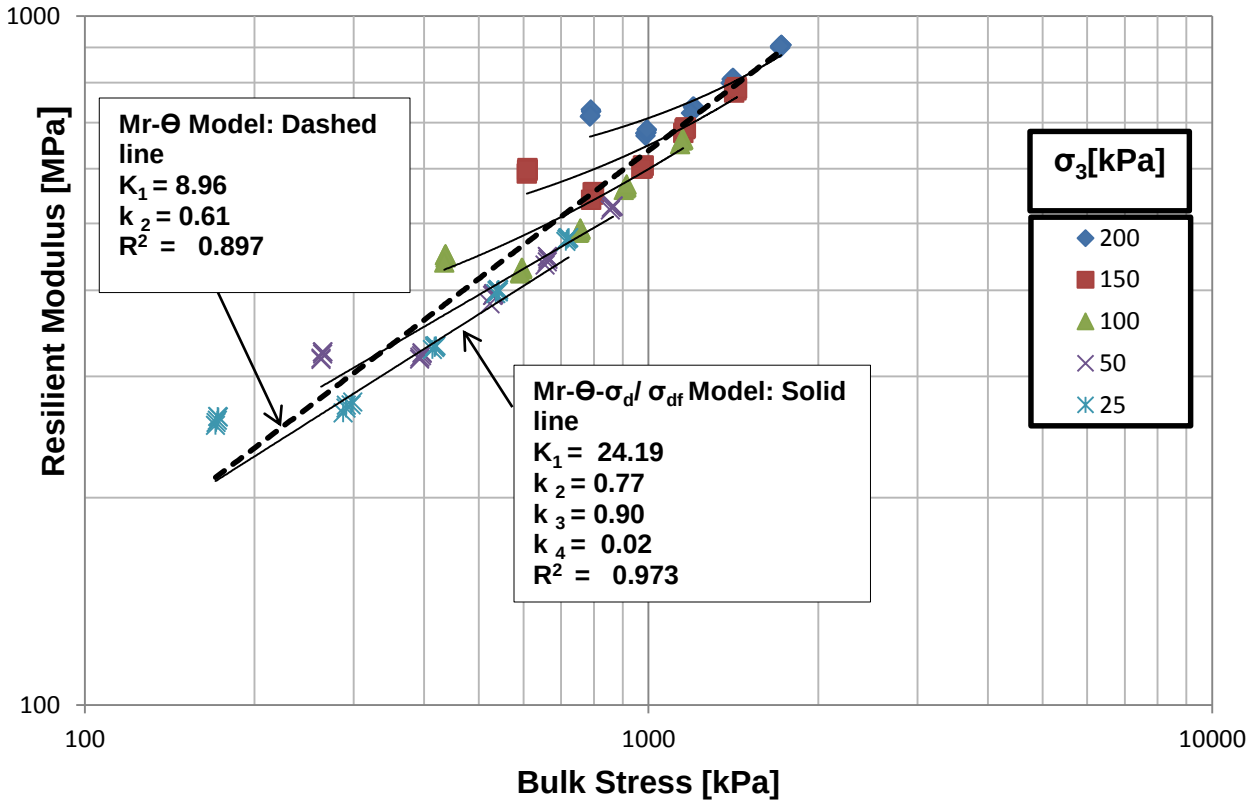

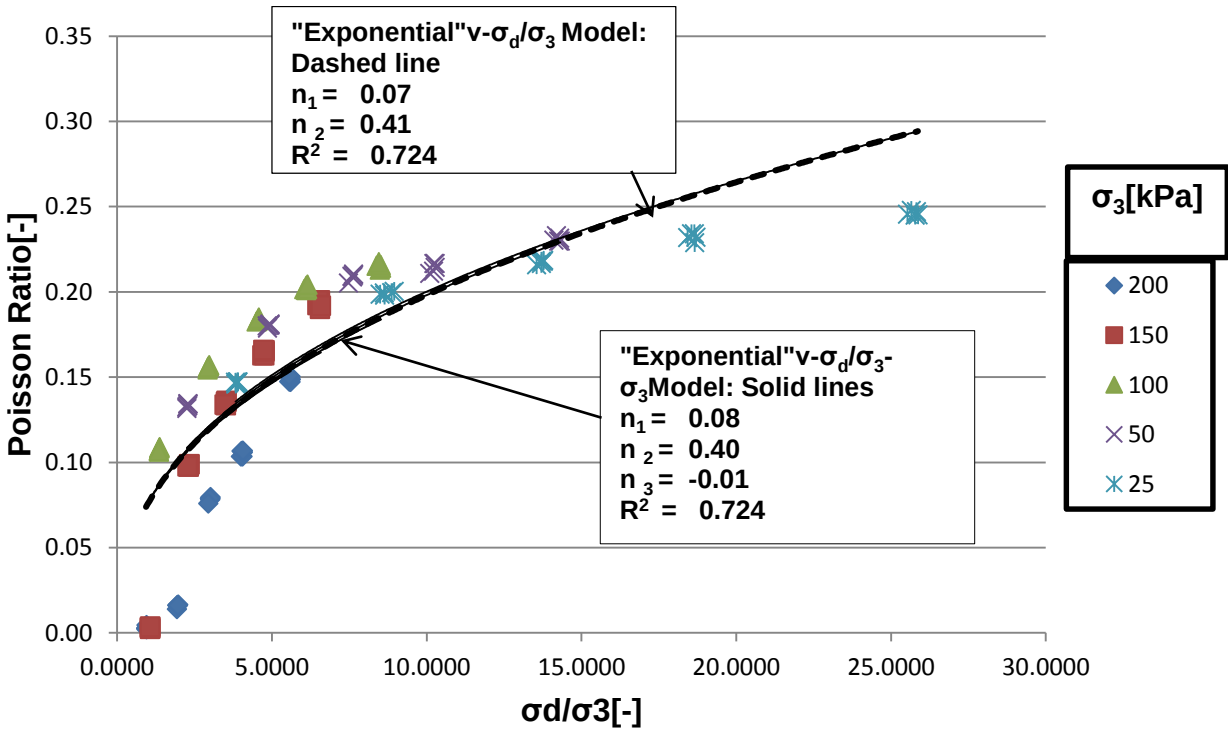

Figure E- 9: Resilient Modulus and Poisson Ratio Modelling for 70:C30M-100%DOC-70%CM

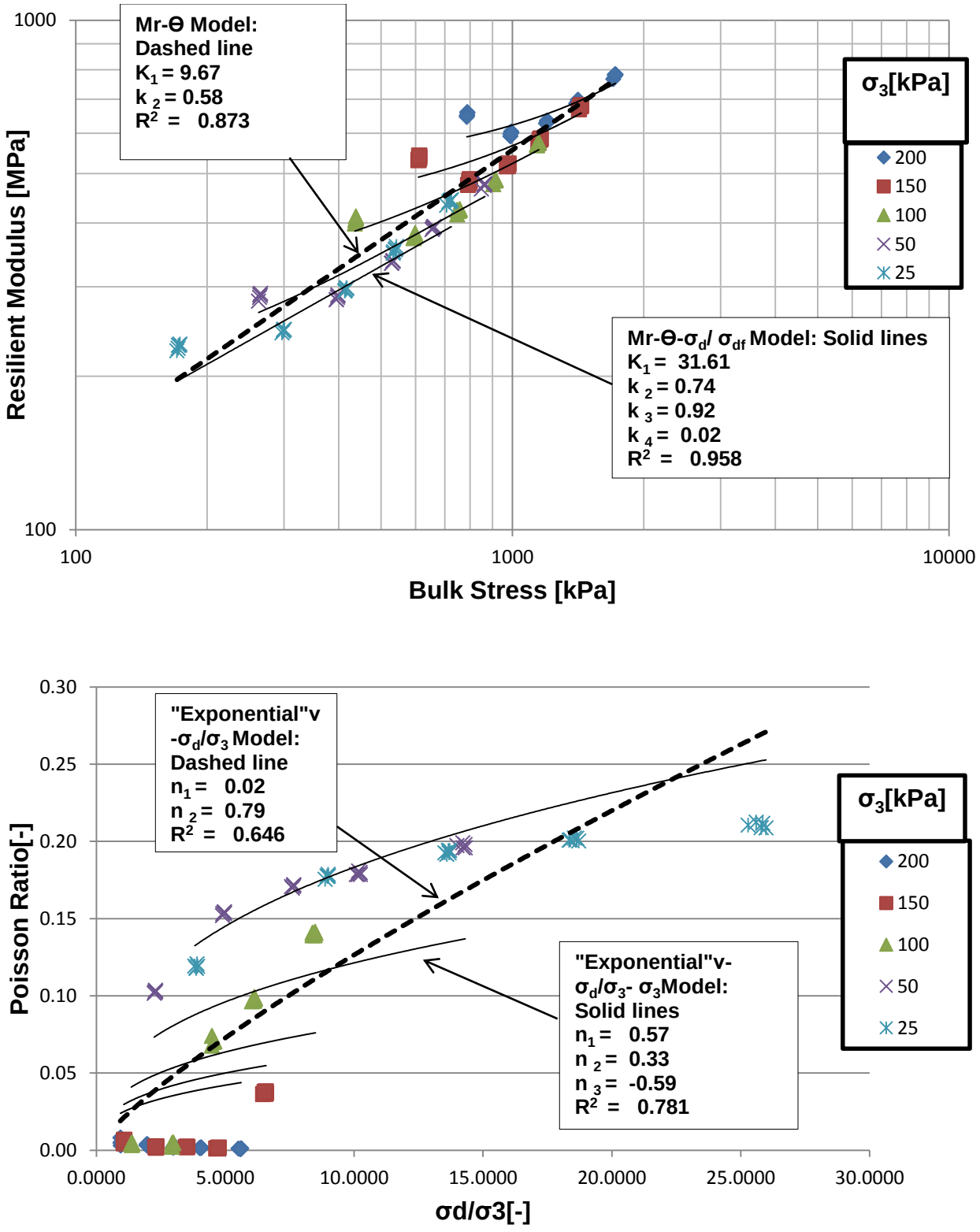

Figure E- 10 : Resilient Modulus and Poisson Ratio Modelling for 70C:30M-100%DOC-70%CM Duplicate Sample

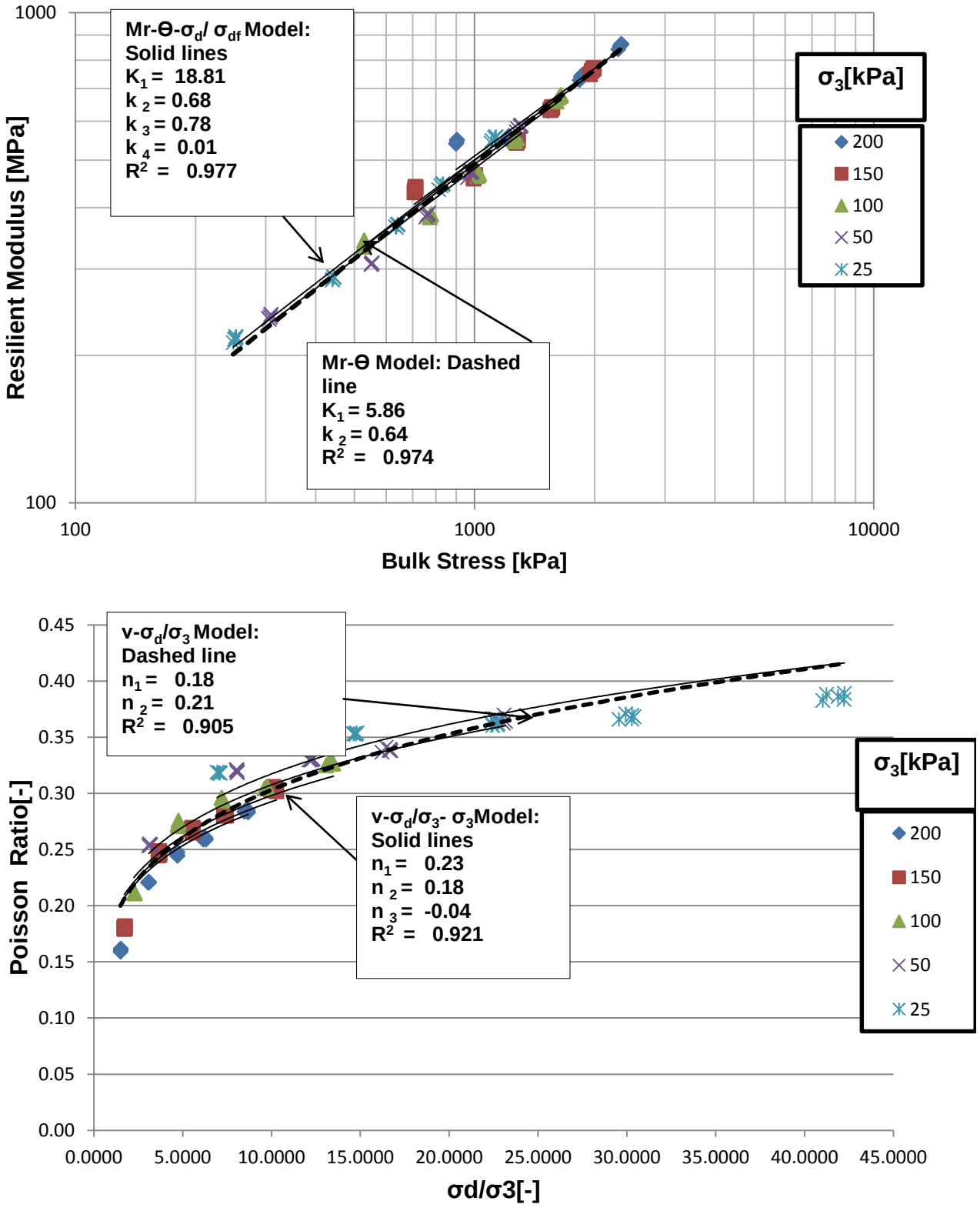

Figure E- 11 : Resilient Modulus and Poisson Ratio Modelling for 70C:30M-102%DOC-80%CM

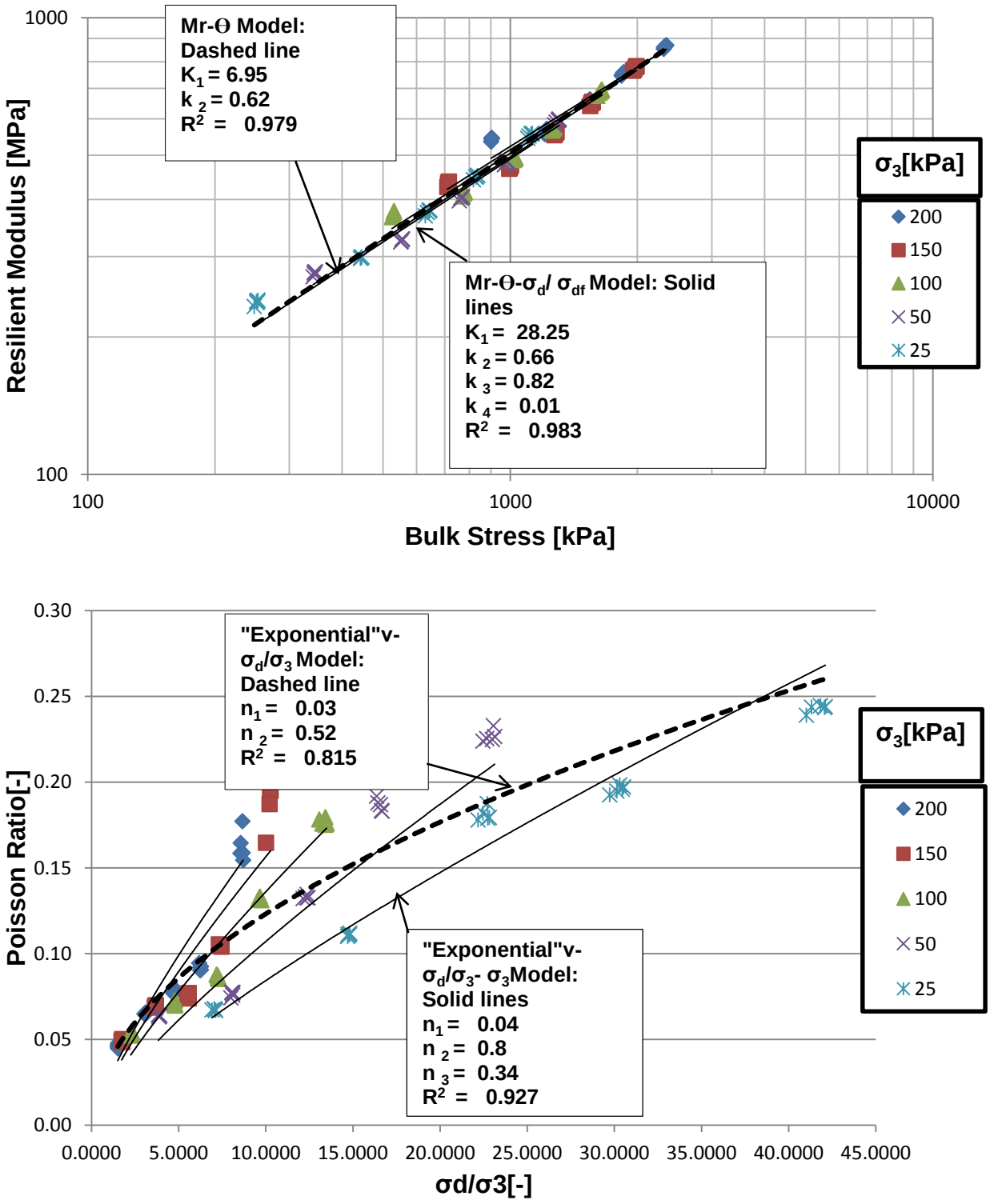

Figure E- 12 : Resilient Modulus and Poisson Ratio Modelling for 70C:30M-102%DOC-80%CM Duplicate Sample

APPENDIX F: CALCULATIONS OF EFFECTS AND REGRESSION ANALYSIS

The average magnitude of the effect for each of the three variables(factors) investigated is assessed using the table of contrast method (Box *et al.*, 1978) at three bulk stresses for resilient modulus and three σ_d/σ_3 ratios for Poisson Ratio. The "effect" means the change in response as we move from the low to high level of the factor. For example, it represents the change in obtained resilient modulus as variable Compaction Moisture (CM) changes from 70% OMC compaction moisture to 80%OMC compaction moisture. Table F-1 provides the obtained values of the resilient modulus for primary and duplicate samples corresponding to each level of the study variables on the above mentioned bulk stresses.

For illustration, the average effect named *main effect* of the compaction moisture at 1500 kPa bulk stress is calculated as follow:

Effect (CM) = [(637.7-738.26) + (527.7-579.35) + (626.8-718.9) + (485.67-550.16)]/4= -77.2

This measures the average effect of compaction moisture over all conditions of other variables such as degree of compaction and mix composition. The effect means that the resilient modulus reduces of 77.2 MPa as the compaction moisture is increased from 70% OMC to 80% OMC. The same procedure is used to calculate the other main effects for different bulk stress levels.

However, it can be seen for example in Figure 4-21 that variable Mix composition(M) has a big effect at the low level of the compaction moisture thus they do not behave additively but they interact. This interaction is measured by the difference between the average mix composition effect at 80% compaction moisture and the average mix composition effect at 70% compaction moisture. Then the interaction factor is half of this difference. For illustration, at the same bulk stress of 1500 kPa, the M x CM effect is calculated as follow:

MxCM={ [(637.7-527.7)+(626.8-485.67)]/2-[(738.26-579.35)+(718.9-550.16)]/2}/2= -19.3

Moreover, at a certain combination of two variables, Mr results are obtained at each of the two levels of the remaining one, therefore the three factor interaction noted M x CM x DOC should also be assessed.

MxDOCxCM={[(637.7-527.7)-(626.8-485.67)]/2-[(738.26-579.35)-(718.9-550.16)]/2}/2

= -5.32

After calculation of the effects, standard error for effects is calculated using replicated runs. When *g* of experiments are "genuinely" replicated with n_i the replicate runs at i^{th} set, it yields an estimated pooled variance of:

$$S^2=\frac{\nu_1 s_1^2+\nu_2 s_2^2+\cdots\ldots+\nu_g s_g^2}{\nu_1+\nu_2+\cdots\ldots+\nu_g} \quad \text{(Equation 45)}$$

With $\nu=\nu_1+\nu_1+\ldots\ldots+\nu_g$ = degree of freedom.

When only two replicates are carried out, the pooled estimate of run variance is:

$$S^2=\sum\frac{d_i^2}{2g} \quad \text{(Equation 46)}$$

Where, d_i is the difference between duplicate observations.

The estimated variance for effect while conducting a two-level factorial design is:

$$V\ (effect)=\frac{4}{N}\sigma^2 \quad \text{(Equation 47)}$$

Where, N is the number of runs made during two-level factorial design.

Replacing σ^2 by s^2, the estimated variance (effect) is obtained. The square route of this variance gives the estimated standard error. The effects as well as the standard error for the resilient modulus are presented in Table F-2.

This overall procedure is also applicable for the calculation of effects and standard error for the Poisson Ratio and the results are presented in Table F-3 to F-4.

Table F- 1: Resilient Modulus at Θ=1500 kPa, 900 kPa and 300 kPa for initial and Duplicate Samples

	Variables			Θ= 1500 kPa		Θ= 900 kPa		Θ= 300 kPa	
Test run	M	CM	DOC	Mr	Mr duplicate	Mr	Mr duplicate	Mr	Mr duplicate
1	70	80	102	637.7	658.4	426.79	451.5	239.54	275.3
2	30	80	102	527.7	540.6	335.97	364.56	177.37	211.47
3	70	70	102	738.26	737.09	517.5	513.29	327.31	326.32
4	30	70	102	579.35	631.2	373.6	435.9	210.8	257
5	70	80	100	626.8	599.3	428	411	258.53	237.16
6	30	80	100	485.67	535	353	371.74	203.5	201.7
7	70	70	100	718.9	837.6	484	564.6	245.94	271.14
8	30	70	100	550.16	482.3	395.9	323.9	238.8	189

Table F- 2 : Effects of Variables at Θ=1500 kPa, 900 kPa and 300 kPa and the Average

	Θ= 1500 kPa		Θ= 900 kPa		Θ= 300 kPa		**Average**	
Effect	Estimate	σ^2	Estimate	σ^2	Estimate	σ^2	Estimate	σ^2
Main effects								
M	144.7	± 14	99.5	± 11.7	60.2	± 7.9	**101.5**	**± 15.2**
CM	-77.2	± 14	-56.8	± 11.7	-36.0	± 7.9	**-56.7**	**± 15.2**
DOC	25.4	± 14	-1.8	± 11.7	2.1	± 7.9	**8.6**	**± 15.2**
Two- factor Interactions								
DOCxCM	1.1	± 14	-7.4	± 11.7	-24.6	± 7.9	**-10.3**	**± 15.2**
MxCM	-19.1	± 14	-48.0	± 11.7	-1.6	± 7.9	**-7.2**	**± 15.2**
MxDOC	-10.2	± 14	-28.9	± 11.7	29.1	± 7.9	**-3.3**	**± 15.2**
Three- factor Interactions								
DOCxCMxM	-5.3	± 14	-10.0	± 11.7	-25.6	± 7.9	**-13.6**	**± 15.2**

Table F- 3 : Poisson Ratio at σ_d/σ_3=23, σ_d/σ_3=10and σ_d/σ_3=1 for Initial and Duplicate Samples

	Variables			σ_d/σ_3=23		σ_d/σ_3=10		σ_d/σ_3=1	
Test run	M	CM	DOC	ν	ν duplicate	ν	ν duplicate	ν	ν duplicate
1	70	80	102	0.37	0.23	0.31	0.19	0.16	0.05
2	30	80	102	0.51	0.29	0.40	0.27	0.05	0.12
3	70	70	102	0.23	0.24	0.20	0.21	0.07	0.1
4	30	70	102	0.29	0.21	0.25	0.20	0.1	0.02
5	70	80	100	0.32	0.27	0.27	0.24	0.04	0.12
6	30	80	100	0.58	0.3	0.42	0.26	0.05	0.01
7	70	70	100	0.24	0.12	0.21	0.18	0.001	0.01
8	30	70	100	0.32	0.32	0.21	0.18	0.08	0.001

Table F- 4 : Effects of variables at Θ=1500 kPa, 900 kPa and 300 kPa and the Average

	σ_d/σ_3=23		σ_d/σ_3=10		σ_d/σ_3=1		**Average**	
Effect	Estimate	σ^2	Estimate	σ^2	Estimate	σ^2	Estimate	σ^2
Main effects								
M	-0.135	± 0.037	-0.0725	± 0.021	-0.0025	± 0.017	**-0.07**	**± 0.030**
CM	0.175	± 0.037	0.1325	± 0.021	0.0125	± 0.017	**0.106**	**± 0.030**
DOC	-0.015	± 0.037	0.0075	± 0.021	0.0525	± 0.017	**0.015**	**± 0.030**
Two- factor Interactions								
DOCxCM	0.005	± 0.037	-0.0025	± 0.021	0.0075	± 0.017	**0.003**	**± 0.030**
MxCM	-0.065	± 0.037	-0.0525	± 0.021	0.0525	± 0.017	**-0.021**	**± 0.030**
MxDOC	0.035	± 0.037	0.0025	± 0.021	0.0425	± 0.017	**0.026**	**± 0.030**
Three- factor Interactions								
DOCxCMxM	0.025	± 0.037	0.0225	± 0.021	0.0175	± 0.017	**0.021**	**± 0.030**

Regression Analysis

"Data have no meaning in themselves; they are meaningful only in relation to a conceptual model of the phenomenon studied" (Box *et al*, 1978). In this regard, linear and non-linear regression was carried out on obtained data in order to develop explanatory models or to fit the existing models to the test results. Regression analysis is a statistical procedure, which is used to determine a relationship between phenomena. The dependent phenomenon is categorised as the *dependent variable* and the parameters that this dependent variable lays on are called *independent variables*. This statistical technique reduces the sum of the squares of the deviations of scatted points to the y-axis of the least-squares line of best fit (Joseph, 2007).

Linear regression

The linear regression is divided into two main parts; simple linear regression and multiple linear regressions. The first explores the relationship between one independent variable and one dependent variable. The second part establishes the relationship between more than one independent variable and one dependent variable. These linear regressions have in common that they are both used in empirical models where an investigator needs to establish a mathematical relation of the study factors based on the obtained experimental results. In this study however, only multiple linear regression was used to explore the relationship between the resilient modulus or the Poisson Ratio with the independent variables such as the degree of compaction, mix composition and the compaction moisture.

The form of linear regression is as follow:

$$Y=\beta_0+\beta_1x_1+\beta_2x_2+\beta_3x_3+\epsilon \qquad \text{(Equation 48)}$$

Where Y is the dependent variable, X_1, X_2, X_3 represent the independent variables, β_0 is the intercept and β_1, β_2, β_3 are partial regression coefficients (Montgomery & Runger, 2007). Moreover, this equation can be extended to include interactions between independent parameters. A computer program is used to perform regression analysis. However, the user should understand well the model parameters in order evaluate the adequacy of the model. In this study, Microsoft excel (Solver) was used to fit multiple regression models.

The most important step before fitting the model is to check the dependency of the so-called independent variables. When these dependencies are strong, it can lead to what is defined as *multicollinearity*. This multicollinearity affects the estimation of model parameters and can

reduce the adequacy of the general model (Montgomery & Runger, 2007). In this study, the correlation test was carried out between independent variables themselves and with the dependent variable. The results were presented in the table before the introduction of regression modelling.

Best fitting of the model is tested through several hypothesis testing. This testing is carried out on the significance of the overall model and on the adequacy of the individual model variables. One can cite test statistic for ANOVA (F test), and the coefficient of multiple determination R^2 for the regression model, and the t-statistic test and p value for model parameters. In this study, R^2 and p value were used to test the adequacy of the overall model and the model parameters. Moreover, because this study aimed to assess the magnitude of the independent variable, t-statistic test also was carried out.

The R^2 varies from one to zero. One means perfect correlation and zero means no correlation (Joseph, 2007). In this study, R^2 was the scaling factor for the best fitting of the models.

p value is " the smallest level of significance that would lead to rejection of the null hypothesis H_0 with the given data" (Montgomery & Runger, 2007). It can be seen that p value is based on a specific level of confidence α to judge whether the null hypothesis can or cannot be rejected. A variable is significant when the null hypothesis H_0 is rejected. This corresponds to a p value smaller than the level of confidence α, and the investigator can have confidence that the investigated parameter is significant. The confidence interval α selected in this study is 0.05 because it is the commonly used. This means for example that there is 95% probability that an independent variable has in effect on the dependent variable. Note that the p value does not provide the magnitude of significance of independent variable towards the dependent variable, but the T-statistic test is required to assess the level of significance.

T-statistic test is used to evaluate the level of significance of the individual independent valuable to the dependent variable. The value of the T-statistic displayed by the computer is compared to the T critical value corresponding to a confidence interval and a degree of freedom. This value can be obtained from tables provided in any statistics book. When T-statistic is greater than the T-critical, the null hypothesis that the independent variable significantly affects the dependent variable is rejected; therefore, this independent variable has a strong influence and can be included in the model. The level of significance increases as the value of T-statistic increases.

Non-linear regression

The linear regression is characterised by linearity in parameters, which is in contrast with non-linear regression where the model parameters are not linear. However, both these regression analysis use the least squares to fit the model (Box *et al*, 1978).

The non-linear regression on the contrary to the linear regression does not require many analytical expressions and hypothetical testing but it is a trial and error method. It consists of finding the model coefficients that can minimise the sum of squares of the deference between model predicted values and the observed values (Joseph, 2007). There is a variety of computer software that can be used for non-linear- regression, in this study non-linear regression model fitting using Excel Solver was performed.

In this regression method, the user starts with guessing the model parameters and then runs the regression. The computer proposes to keep the solver solution or to display the guessed values. At this stage, the judgement of the user is very important since the tendency of the computer is to minimise the difference between the observed and the predicted results. The user should judge whether the model parameters are practically meaningful.

Solver is an optimisation package that can detect the minimum, the maximum or a specific value from a target cell. This method can perform both linear and non-linear least squares curve fittings. The author has used this method for fitting the resilient response models to the obtained test results in order explore the stress dependency of the resilient modulus and the Poisson Ratio.